Palacký University in Olomouc
Faculty of Sciences
Department of Biophysics

DOCTORAL THESIS

The Sodium-Potassium ATPase – Expression, Purification and its Interactions with Small Molecules

Author: **Mgr. Jaroslava Šeflová**
Program: Biophysics
Supervisor: doc. RNDr. Martin Kubala, Ph.D.

Declaration

"I declare that, except where explicit reference is made to the contribution of others, that this dissertation is the result of my own work and has not been submitted for any other degree at the Palacký University in Olomouc or any other institution."

Signed: .....

In Olomouc, September 19, 2017

.....
Mgr. Jaroslava Šeflová

Bibliografická identifikace

Jméno a příjmení autora	Mgr. Jaroslava Šeflová
Název práce	Sodno-draselná ATPasa – exprese, purifikace a její interakce s malými molekulami
Typ práce	Dizertační práce
Pracoviště	Katedra biofyziky
Vedoucí práce	doc. RNDr. Martin Kubala, Ph.D.
Rok obhajoby práce	2017
Abstrakt	Dizertační práce se zaměřuje na studium významného membránového proteinu, sodno-draselné pumpy. Tento enzym svou funkcí vytváří elektrochemický gradient, který je významný pro celou řadu buněčných procesů. V případě nesprávné funkce sodno-draselné ATPasy dochází ke vzniku patologických stavů, poruch a nemocí. Cílem této práce bylo studovat souvislosti mezi strukturou a funkcí toho proteinu s využitím dostupných experimentálních postupů. Příprava celé sodno-draselné pumpy byla provedena dvěma metodami – přímou izolací z tkáně a heterologní expresí v kvasinkách. Enzym izolovaný z prasečích ledvin byl použit pro zkoumání inhibice sodno-draselné pumpy po interakci s flavonolignany, halogenovanými chinolony a platinovými cytostatiky. Změna aktivity enzymu byla detekována pomocí modifikované Baginského metody, která určuje koncentraci fosfátu z hydrolýzy ATP. Dále byly heterologní expresí v bakteriích připraveny izolované cytoplasmatické segmenty proteinu (C45 a C23 kličky). Tyto kličky umožňují zkoumat interakci sodno-draselné pumpy a biologicky významných látek rozpustných ve vodných pufrech. Vybrané aktivní látky byly cílem dalšího výzkumu zaměřeného na odhalení vazebného místa a mechanismu inhibice enzymu.
Klíčová slova	sodno-draselná ATPasa, exprese v bakteriích, exprese v kvasinkách, C45 klička, C23 klička, Baginského metoda určení ATPasové aktivity, flavonolignany, halogenované chinolony, cisplatina
Počet stran	145
Počet stran příloh	32
Jazyk	anglický

Bibliographical identification

Autor's first name and surname	Mgr. Jaroslava Šeflová
Title	The Sodium-Potassium ATPase – Expression, Purification and its Interactions with Small Molecules
Type of thesis	Doctoral
Department	Department of Biohysics
Supervisor	doc. RNDr. Martin Kubala, Ph.D.
The year of presentation	2017
Abstract	The Na^+/K^+-ATPase (NKA) is an essential membrane protein establishing electrochemical gradient used in cell processes. Dysfunction of NKA leads to pathological states and diseases. This thesis is focused on the relations between structure and function using available experimental approaches. Whole protein was prepared by two methods – direct isolation from porcine kidney and by heterologous expression in yeast. NKA isolated from porcine kidney was used for testing of biologically active molecules such as potential drugs (flavonolignans, halogenated hydroquinolones and platinum-based complexes). Furthermore, we studied the interactions of promising molecules inhibiting NKA activity using the modified Baginsky assay. Isolated cytoplasmic parts of the enzyme, represented by C23 and C45 loops, were used for determination of their binding site and for study of inhibitory mechanism.
Keywords	sodium-potassium ATPase, heterologous expression in bacteria, heterologous expression in yeast, C45 loop, C23 loop, Baginsky assay, flavonolignans, halogenated quinolones, cisplatin
Number of pages	145
Number of pages of appendices	32
Language	English

Contents

Acknowledgements

I would like to thank to my supervisor doc. RNDr. Martin Kubala Ph.D. for leading my research as in the laboratory as during writing all publications and this thesis. I am especially grateful for his scientific suggestions and relevant discussions.

I am really grateful for the collaboration with Professor Poul Nissen from Department of Molecular Biology and Genetics (Aarhus University, Denmark), Professor Per Amstrup Pedersen from Department of Cell Biology (University of Copenhagen, Denmark), Dr. Natalya Fedosova from Department of Physiology and Biophysics (Aarhus University, Denmark). I also would like to thank to their excellent co-workers, namely Joseph Lyons (expert on flipases and ATPase-expressing genius), David Sorensen (technician with expertise in yeast transformation), Oleg Sitsel and Alya Sitsel (for many advices, trouble shooting, trouble solving, motivating, ...), Ingrid Dach (for all kind help during my stay in Denmark), Sigrid Thirup Larsen (for yeast expression consultations and honest friendship), Peter Aasted Paulsen (for introduction into yeast expression), Florian Hilbers (for his great experience with β subunit and FXYD proteins), Hanne Poulsen (for advising me about disease-linked mutations in the NKA genes), Azadeh Shahsavar (for being excellent researcher without loosing her stamina), Cristine Betzer (for letting me to use the compact FPLC instrument), Marie Rose Ash (for being motivating and enthusiastic), Kaituo Wang (for discussing the stabilization of proteins after elution), Pontus Gordon (for showing me how to face the challenges),... They all always helped me with struggles of my challenging projects and kindly supported my attempts.

I would like to thank to my collaborators from Palacký University: Petra Čechová (who does the best figures of the NKA structure, for doing the most language corrections of my texts and for showing unlimited mental support), Miroslav Huličiak (who helped me to start expressing C45 loops and developed protocol for Baginsky assay), Tibor Stolárik (who helped me to optimize Western Blots and has been an amazing colleague), Karolina Machalová Šišková (an excellent Raman spectroscopist with broad knowledge of everything), Martina Kopečná and David Kopečný (who helped me to optimize the heterologous expressions in *E. coli*, they led my first steps in cloning and they were very supportive at any time), Petr Nádvorník (who helped me to optimize PCR and shared with me his scientific enthusiasms), Radka Končitíková (who was my great colleague), Tomáš Fürst (who is well-skilled mathematician with astonishing knowledge of Matlab), Ursula Ferretti (fantastic user of HPLC), Lenka Kuchařová (who is a very brave biophysicist), Lukáš Nosek (who elevated PAGE to state-of-art analysis), Marek Šebela (who helped me with mass spectrometry), Jitka Prachařová (who did HEK293 transfections for me and who discussed with me the experimen-

tal setting for experiments with cisplatin), Michal Biler (for long-term friendship and competition), and many other.

I really appreciate my husband's support, patience and help with Matlab and Python programming. Without him and my family I would be never able to finish my studies.

This work was supported by the grant L1204 from the National Program of Sustainability I of the Ministry of Education, Youth and Sports of the Czech Republic and the Institutional Fund of Palacký University.

Finally, I would like to express my gratitude to EMBO and Endowment Fund of Palacký University for supporting my research.

List of Publications

I **Šeflová, J.**, Biler, M., Hradil, P., Kubala, M., and Čechová, P. (2017). Inhibition of Na^+/K^+-ATPase by 5,6,7,8-tetrafluoro-3-hydroxy-2-phenylquinolin-4(1H)-one. *Biochemie*, 4: 30104 – 30109.

II **Šeflová, J.**, Čechová, P., Šišková, K. M., Kapitán, J., Kubala, M., Šebela, M. and Mojzeš, P. (2017) Cisplatin Interacting with Cytoplasmic Loop (C45) of the Na^+/K^+-ATPase: Role of Cysteine Residues. [Manuscript in preparation].

III Kubala, M., Čechová, P., **Geletičová, J.**, Biler, M., Štenclová, T., Trouillas, P., and Biedermann, D. (2016). Flavonolignans as a Novel Class of Sodium Pump Inhibitors. *Frontiers in Physiology*, 7: 1 – 10.

IV Vacek, J., Zatloukalová, M., **Geletičová, J.**, Kubala, M., Modrianský, M., Fekete, L., Mašek, J., Hubatka, F., and Turánek, J. (2016) Electrochemical Platform for the Detection of Transmembrane Proteins Reconstituted into Liposomes. *Analytical Chemistry* 88: 4548 – 4556.

V Kubala, M., **Geletičová, J.**, Huličiak, M., Zatloukalová, M., Vacek, J., and Šebela, M. (2014). Na^+/K^+-ATPase inhibition by cisplatin and consequences for cisplatin nephrotoxicity. *Biomedical Papers*, 158: 194 – 200.

List of Abbrevations

Amino acids

A	Ala	alanine	I	Ile	isoleucine	R	Arg	arginine
C	Cys	cysteine	K	Lys	lysine	S	Ser	serine
D	Asp	aspartic acid	L	Leu	leucine	T	Thr	threonine
E	Glu	glutamic acid	M	Met	methionine	V	Val	valine
F	Phe	phenylalanine	N	Asn	asparagine	W	Trp	tryptophan
G	Gly	glycine	P	Pro	proline	Y	Tyr	tyrosine
H	His	histidine	Q	Gln	glutamine			

α DDM	n-dodecyl-α-D-maltoside
β DDM	n-dodecyl-β-D-maltoside
ABC transporter	ATP-binding cassette transporter
ACN	acetonitrile
ADE2	selection marker encoding auxtrophy to adenine
ADP	adenosinediphosphate
AHC	Alternating Hemiplegia of Childhood
AMP	ampiciline
ATP	adenosinetriphosphate
ATP1A1	gene encoding α_1 isoform of NKA
ATP1A2	gene encoding α_2 isoform of NKA
ATP1A3	gene encoding α_3 isoform of NKA
ATP2A3	gene encoding SERCA3 isoform
BKH	baby hamster kidney cell line

BSA	bovine serum abumin
cAMP	cyclic adenosinemonophosphate
CAP	catabolite activator protein
CAPOS	Cerebellar Ataxia, Areflexia, Pes Cavus, Optic Atrophy, Sensorineural Hearing Loss Syndrome
CF	chromatofocusing
CHAPS	3-(3-cholamidopropyl)diethyl-amino-1-propane
CHO	Chinese hamster ovary cell line
CHS	cholesterylhemisuccinate
CMC	critical micelle concetration
COS-1	green monkey kidney cell line
CTAB	cetyltrimethylamonium bromide
CTS	cardiotonic steroids or cardiotonic glycosides
$C_{12}E_8$	octoethyleneglycolmonodecylether
C23	loop connecting transmembrane helices M2 and M3
C45	large cytoplasmic loop connecting transmembrane helices M4 and M5
DHSB	dehydrosilybin
DHSCH	dehydrosilychristin
DHSD	dehydrosilydianin
DM	n-decyl-β-D-maltopyranoside
DMSO	dimethylsulfoxide
DOPS	1,2-dioleoyl-*sn*-glycero-3-phospho-L-serine
DTT	dithiotreitol
EDTA	ethylenediamintetraacetic acid
EGTA	egtazic acid or ethylene-bis(oxoethylenenitrilo)tetraacetic acid

ER	endoplasmic reticulum
FHM2	Familial Hemiplegic Migraine 2
FPLC	fast protein liquid chromatography
GA	Golgi aparatus
GAL	genes regulated by galactose
GFP	green fluorescence protein
HEK	human embryonic kidney cell line
HIS3	selection marker encoding auxtrophy to histidine
HKA	H^+/K^+-ATPase
HPH	hygromycin B phosphotrasferase
HPLC	high performance (pressure) liquid chromatography
IEF	isoelectric focusing
IEX	ion-exchange chromatography
IMP	integral membrane protein
IPTG	isopropyl-β-D-1-thiogalactopyranoside
KAN	kanamycin
LB	Luria-Bertani medium
LDH	lactate dehydrogenase
LEU2	selection marker encoding auxtrophy to leucine
LiAc	lithium acetate
LMNG	laurylmaltose-neopentylglycol
MALDI-TOF	matrix-assisted laser desorption/ionization detected by time of flight detector
MET15	selection marker encoding auxtrophy to methionine
MOPS	3-(N-morpholino)propanesulfonic acid
MS	mass spectrometry

MWCO	molecular weight cut-off
Na-ATP	ATP sodium salt
NKA	Na^+/K^+-ATPase
NMDG	N-methyl-D-glucamine
OD	optical density, absorbance
PC	phosphatidylcholine
PE	phosphatidylethanolamine
PEP	phosphoenolpyruvate
PK	pyruvate kinase
PMCA	Ca^{2+}-ATPase from plasma membrane
PMSF	phenylmethylsulfonylfluoride
PP	polymeric fraction of silymarin
PS	phosphatidylserine
PUFA	polyunsaturated fatty acids
QUE	quercetin
RDP	Rapid-Onset Dystonia Parkinsonism
SA	sinapic acid
SB	silybin
SCH	silychristin
SD	silydianin
SD medium	synthetic drop-out medium
SDS	sodiumdodecylsufate
SDS-PAGE	polyacrylamide gel electrophoresis under denaturing conditions
SEC	size-exclusion chromatography
SERCA	Ca^{2+}-ATPase from sarcoendoplasmic reticulum
SOPS	1-stearoyl-*sn*-glycero-3-phospho-L-serine
TAX	taxifolin
TFA	trifluoracetic acid

TFHPQ	5,6,7,8-tetrafluoro-3-hydroxy-2-phenyl-quinolin-(*1H*)-one
TM	transmembrane
Tris	Tris(hydroxymethyl)aminomethane
TRP1	selection marker encoding auxtrophy to tryptophan
URA3	selection marker encoding auxtrophy to uracil
WT	wild type
YNB	yeast nitrogen base
YP	yeast extract with peptone solution

Introduction

This thesis is focused on the enzyme Na^+/K^+-ATPase (sodium-potassium pump, NKA) which is the first described membrane-bound ATPase from the family of P-type ATPases. Since the discovery of NKA in 1957, the significance of this membrane-bound ATPase has increased. NKA is composed of two main subunits denoted as α and β subunits forming functional heterodimer. The $\alpha\beta$ heterodimer is often associated with the tissue specific regulatory protein from FXYD family. The α subunit is formed by 10 transmembrane helices and three cytoplasmic domains (A, P, N).

In the beginning, the NKA was known mainly as a transporter which translocated sodium and potassium ions across the plasma membrane. Later, other roles of NKA were described, such as involvement in the secondary transport, participating in the water reabsorption in the kidney tissues or the signal transduction in neurons. In general, the dysfunction of NKA can result in the pathological states or diseases such as hyperkalemia [1], cataract [2, 3, 4], hypertension [5, 6, 7] and diabetes [3, 8]. The specific mutations in the genes encoding the NKA isoforms are linked with the development of neurological disorders, e. g. Hemiplegic Migraine [9], Rapid-Onset Dystonia Parkinsonism [10] and Alternating Hemiplegia of Childhood [11]. Furthermore, the recently published study have suggested the correlation between the expression of specific isoforms of α subunit of NKA and the cancer development [12], or a potential role of α expression in the treatment of Alzheimer diseases [13].

Although the biological importance of NKA is clear, the research of human variants of NKA remains challenging for many reasons. For example, the whole enzyme can be prepared by two main techniques – the direct isolation from tissue (e. g. porcine kidney, ox brain, duck nasal gland, shark rectal gland) or the heterologous expression (yeast, insect or mammalian cells). Human proteins can not be isolated directly due to ethical issues making the heterologous expression the only way of the protein preparation.

Unfortunately, the use of yeast expression system, which is widely used for membrane protein expression, needs to be optimized mainly due to the different post-translational modification and membrane lipid composition. On the other hand, the mammalian cells are able to produce heterologous NKA, but the naturally expressed NKA is also present. Another disadvantages of mammalian expression system are a high cost and the low heterologous protein yield. Those obstacles might be overcome by using the directly isolated porcine kidney NKA that shows sequence similarity approximatelly 98% with human kidney variant (based on the comparison of human and porcine α_1 sequences obtained from the Uniprot website [14]).

The interactions between water soluble compounds and cytoplasmic domains can

be examined by using isolated the C23 loop (enzyme N-terminus and A domain) and C45 loop (P and N domains). Both loops may be easily overexpressed in bacteria *E. coli*. As was reported earlier, the isolated C45 loop may be separated from the rest of the NKA and it retained its structural and functional properties [15].

As was mentioned above, the proper function of the NKA is essential for the cells. The NKA inhibitors are mainly represented by the group of natural compounds called cardiotonic steroids (CTS) into which belongs specific NKA inhibitor, ouabain. CTS are currently used in medicine as antiarrhythmic and anticancer agents [16]. The significant disadvantage of CTS is their limited useful concentration due to their toxicity. Finding the potential replacements of CTS is important goal of the current research.

In this thesis, the NKA inhibitory effect of 117 compounds was examined, whereas only 5 compounds were active at biologically relevant concentration (10 μM). Active agents can be separated into three separate groups (flavonolignans, halogenated hydroquinolinones, and platinum-based complexes). The first group of compounds was flavonolignans that are natural compounds used in the traditional medicine for centuries. Flavonolignans are well-known mainly for their hepatoprotective properties. Second examined group was halogenated quinolinones that represent synthetic analogues to flavonolignans. Both flavonolignans and halogenated hydroquinolinones bound to the cytoplasmic part of the enzyme and showed different mode of action in comparison to ouabain. The last group of examined compounds was platinum-based complexes.

Those platinum-based complexes (cisplatin, carboplatin and oxaliplatin) are widely used in the treatment of several types of cancer such as testicular, ovarian, bladder, head, neck and small lung cancer [17, 18, 19]. Namely, cisplatin is a dominant agent in the treatment of testicular cancer, where it reaches cure rate over 90% [17, 18]. On the contrary, patients treated by cisplatin may suffer from many side-effects such as nephrotoxicity, neuropathies, or hearing loss [20, 21]. Moreover, during the early stages of cisplatin-based chemotherapy, the kidney damage may occur [22, 23, 24]. The renal NKA might be potentially influenced by the cisplatin binding, which can result in the kidney damage. The substantial cisplatin inhibition of the porcine kidney NKA published by Kubala *et al.* [25] suggested the association of the kidney damage and with the cisplatin treatment.

Cisplatin is a water soluble compound that enters the cells via passive diffusion or by using the active transporters. In the cells, cisplatin is activated without loss of *Cis*-conformation [26] and forms mono- and diaqua complexes [27, 28]. Several papers reported on the cisplatin binding to proteins in the blood and cytosol [29, 30, 31]. This binding is often processed via reactive species within the protein structure such sulfhydryl (-SH) moiety. Additionally, the recently published crystal structure of NKA with bound cisplatin [32] suggested binding to the methionine and cysteine residues on the cytosol-facing part of the enzyme. Here I examined the interaction of cisplatin with the isolated cytoplasmic domain of NKA represented by C45 loop.

The cisplatin binding to the isolated C45 loop was examined using the set of cysteine mutants where each of the 11 naturally occurring cysteine residues was replaced by serine. All mutants were subjected to the cisplatin treatment and their intact masses were determined by using the mass spectrometry (MS). The intact mass differences between

the cisplatin treated and untreated samples suggested the binding of approximately 5 cisplatin molecules to the C45 loop. Those results corresponded to the number of cysteine residues detected on the surface of the C45 loop. By using this approach, I identified the hotspot for the cisplatin binding on the C45 loop at positions Cys452, Cys456 and Cys457. This sequence of cysteine residues is unique for the renal isoform of NKA associated with the extending cysteine to serine replacements in the α_2 and α_3 isoforms. The binding of cisplatin to this hotspot was confirmed by the detection of tetra cysteine motif by the TC-FlAsH^{TM} reagent.

The main aims of this thesis were:

- to express α_3 β_1 complex of sodium-potassium ATPase in yeast *Saccharomyces cerevisiae* and optimize this process
- to study the interactions of NKA with the selected group of small molecules (platinum-based anti-cancer drugs, quinolinones and flavonolignans)
- to study the interactions of cisplatin with NKA via cysteine residues on the large cytoplasmic loop connecting transmembrane helices M4 and M5 (C45 loop)
- to prepare C45 and C23 loops derived from the human DNA sequence for α_1, α_2 and α_3 isoforms by the heterologous expression in *Escherichia coli*

Chapter 1

Theoretical Basis

1.1 Membrane-Bound ATPases

The ion pumping ATPases, transporting ions at the expense of ATP, are the major players in ion homeostasis maintenance [33]. ATPases are transporters enabling translocation of specific solutes accros the membranes, which form unique ionic compartments between both inside and outside the cells. Transported solutes are mainly inorganic ions that play vital roles in mammalian physiology, in processes such as neural transduction, energy transformation, and nutrient uptake.

The five main classes of the ion pump ATPase family have been described. They are called P-type ATPase, F-type ATPase, V-type ATPase, A-type ATPase and E-type ATPase. The nomenclatures was derived from phosphorylated intermediate (P-type ATPase), factors of oxidative phosphorylation (F-type ATPase) and a pump found initially in vacuoles (V-type ATPase) [34], a pump found in *Archea* (A-type ATPase), and cell surface pump that hydrolyzes nucleotide triphosphate including extracellular ATP (E-type ATPase).

Simple nomenclatures based on pump function or localization make the ATPase field easier to access, and have appeared in recent biochemistry and cell biology texts [35]. However, this nomenclature provides only a partial picture of this family. It does not include the wide array of ABC (ATP binding cassette) transporters, which couple the ATP hydrolysis with transport of several substrates (including amino acids and multiple drugs and other xenobiotics) [33]. This thesis is focused mainly on the member of P-type ATPase class.

Na^+/K^+-ATPase (sodium-potassium pump, NKA) was the first P-type ATPase introduced to the field [36], and was shown to translocate two K^+ ions into cell and export three Na^+ ions, coupling these movements with the hydrolysis of one molecule ATP to ADP and phosphate [37]. Similar ion pumps described subsequently include sarcoplasmic (SERCA) or plasma membrane Ca^{2+}-ATPase (PMCA), gastric H^+/K^+-ATPase (HKA), Cu^{2+}-ATPase linked with the Wilsons and Menkes disease [38], plant or fungal plasma membrane H^+-ATPase, etc. This group of pumps forms acyl phosphoenzyme intermediates from ATP (hence the P-type ATPase) prior to ion translocation,

and shows two distinct kinetic states named as E1 and E2 conformations. During the reaction cycle of P-type ATPases, pumps alternately expose ion binding sites to the intracellular and extracellular compartments [33].

Moreover, the P-type ATPases transport different ions in each direction, so the same binding site evidently reorients to accommodate different ions. Different pump classes show different ion preferences, which are determined by the combination of charge, coordination number or geometry, and distances to the ligand groups. Each pump class is determined by binding affinities to transported ions and ligands.

1.2 Structure of the Sodium-Potassium ATPase

The function of P-type ATPases was illustrated by many crystal structures that have been published so far [39]. Namely, X-ray crystal structures of F_1 element of bovine ATP-synthase [40] and of sarcoplasmic Ca^{2+}-ATPase [41] were important breakthroughs for understanding the mechanism of F-type and P-type ATPases, respectively. For example, the F-ATPase structure is also important for understanding the V-ATPases. Both classes share the considerable sequence homology and high-resolution structure of F-type ATPase may help to determine the unknown structure of V-type ATPase.

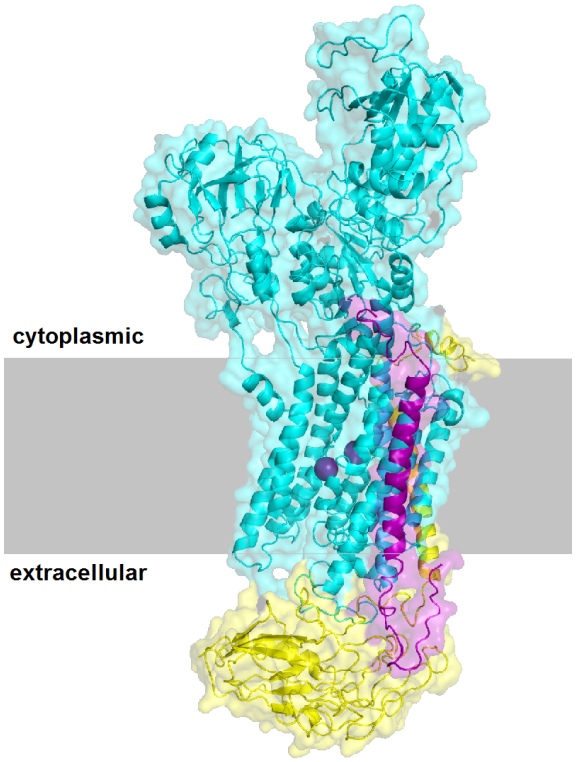

Figure 1: The structure of NKA – the cytoplasmic headpieces of α subunit are widely open towards cytoplasm (upper part of figure). Furthermore, the β (yellow) and α (cyan) subunits form a heterodimer, which is a functional unit of the enzyme. The enzyme is often accompanied by a tissue specific protein from the FXYD family (magenta) which regulates the turnover of the pump. The figure courtesy of Petra Čechová.

Recent research of ATPases is close to discovering a complete picture of how ions are pumped and ATP hydrolyzed at atomic resolution. For example, the structures of the P-type ATPases suggested mechanical movements of their domains during catalytic turnover [33]. For the F-ATPases, the structures revealed the continuous rotation of the γ subunit located at the centre of the $\alpha_3\beta_3$ heterodimer [42, 43]. Crystal structures illustrating ion transport in SERCA have been already published, but detailed structures illustrating reaction cycle of NKA remains unknown. The X-ray structure of NKA was determined in two main conformations – potassium-bound state (often denoted as E2, open conformation) [44, 45] and sodium-bound state (E1 state, closed conformation) [46, 47]. These structures resolved the structure of separate subunits and helped to understand the reaction cycle.

Many P-type ATPases (e. g. SERCA) are formed by one transporting subunit, but some P-type ATPases exhibit more complicated structure. Moreover, of all the members in the P-type ATPases family, only Na^+/K^+-ATPase and H^+/K^+-ATPase require two subunits for active transport of ions. Possibly, this two pumps compose a distinct subfamily within the P-type ATPases. The functional NKA is composed of two essential subunits (named as α and β subunit) and is often associated with regulation protein from the FXYD family (see Figure 1). Human body expresses four different isoforms of α subunit, three β subunits and seven isoforms of FXYD protein in a tissue specific manner [48].

The mass of the α subunit is approximately 112 000 Da, and is also called the catalytic subunit due to its function in the reaction cycle. The β subunit is extensively glycosylated and its molecular weight is approximately 55 kDa depending on the post-translational modification [49]. Moreover, β subunit works as a molecular chaperon that enables folding of alpha subunit into fully functional shape and helps routing an α subunit into the plasma membrane. Finally, the mass of FXYD protein is approximately 10 kDa. The main aim of the FXYD protein is a tissue specific regulation of the pumping carried out by $\alpha\beta$ heterodimer.

In cells, the α and β subunits are expressed at the same ratio. However, for past 40 years, there has been considerable controversy as to whether the protomeric unit of the pump exist in a functional state as an $\alpha\beta$ heterodimer or some higher-order oligomer. Early surveys of the membrane transport proteins suggested that all membrane-bound ATPases had to exist as oligomers [50]. Experiments using a high density expression of α subunit resulted in a close association of α subunits and formation of fixed oligomeric structures. Nevertheless, approximately a half of the α subunits formed monomers, which were found much further apart from oligomeric structures. Surprisingly, the overall activity of functional $\alpha\beta$ heterodimer remained unchanged, suggesting that individual heterodimers were fully functional and correctly localized in the plasma membrane [50]. Although evidence suggested that the $\alpha\beta$ heterodimer is the minimal functional unit, aggregation of the protomeric units is common [50]. This aggregation may be observed for NKA overexpressed in the insect cell or in yeast. Similar behavior shows another P-type ATPase pump, the flipase, overexpressed in *Saccharomyces cerevisiae* [51].

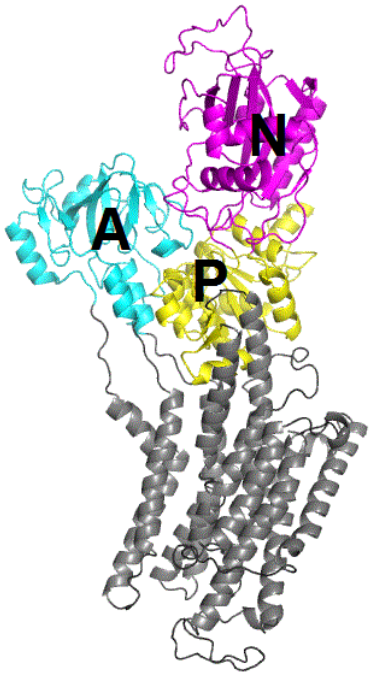

Figure 2: The structure of the α subunit of the NKA. Main domains called A, P and N are highlighted in the structure. The A domain is purple, P domain is yellow and N domain is cyan. The transmembrane part of the enzyme is grey.

1.2.1 α Subunit

The α subunit is composed of three cytoplasmic domains (see Figure 2) named A (actuator), P (phosphorylation), N (nucleotide binding,) and ten transmembrane helices M1 – M10. The α subunit shows very restricted range of divergence in the sequence before a loss of the function (NKA from duck nasal salt gland shows 95.5% similarity and 93.5% identity to that from human kidney). In contrast, similar comparison for the β subunit reveals only 81% similarity and 69% identity between the sequences [50].

The α subunit contains the specific lysine-rich N terminal extension of approximately 40 residues that are able to undergo phosphorylation and serve as platform for protein-protein interaction [52].

The NKA is primarily the pump for sodium ions, however selective filter for potassium ions is less tightly regulated and similar ions can be transported instead. The two binding sites for sodium ions were determined in a good agreement with SERCA (transports two Ca^{2+} ions). But the third binding site has been described recently [47, 46]. Transported ions bound to NKA are illustrated in Figure 3.

The cations are directly coordinated by transmembrane helices M4, M5, M6 and M8 which move during the reaction cycle. By contrast, helices M7, M9 and M10 are anchored in the membrane and their movement is inconsiderable. Consequently, the interaction between FXYD and α subunit is arranged by kinky helix M7 [44].

In the beginning, we would like to note that the sequence numbering is derived from the porcine α_1 isoform. Sites I and II are localized at transmembrane helices M4 – M6 of α subunit (see Figure 4). More specifically, within the site I is Na^+ coordinated by

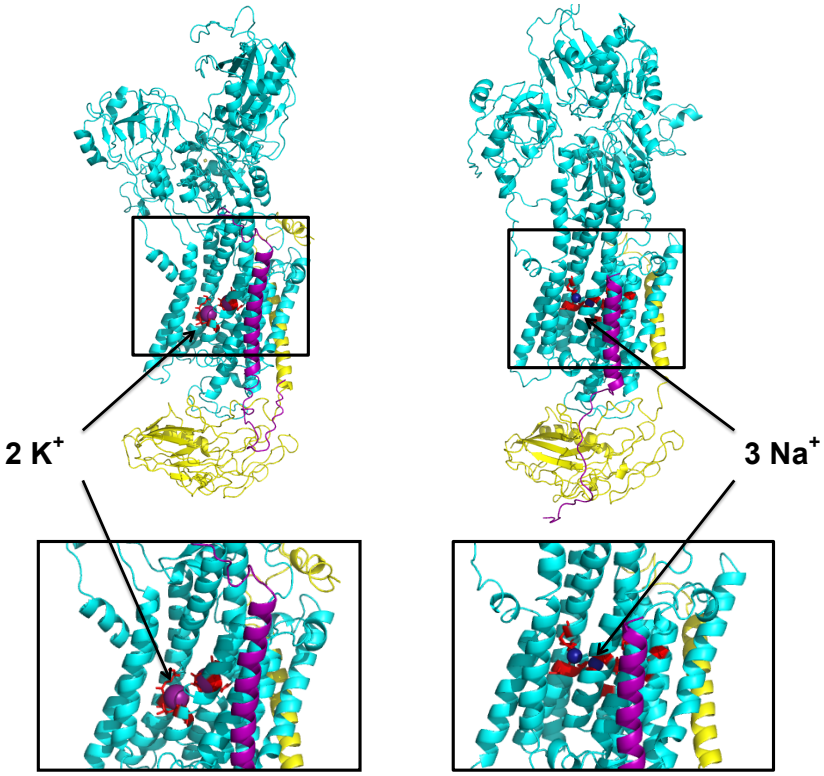

Figure 3: Left: Structure of NKA in open conformation (E2) with bound two K^+ ions. Right: NKA in closed (E1) conformation with bound three Na^+ ions. In the figure are highlighted: α subunit (cyan), β subunit (yellow), FXYD protein (magenta) K^+ ions (purple) and Na^+ ions (dark blue).

residues Asn776, Glu779, Tyr807, Asp808 and Gln923 [53, 54]. Site II involves residues Val322, Ala323, Val325, Glu327 and Asp804 [53, 54]. Two distinct localizations (IIIa and IIIb) were proposed for third Na^+ by [47]. Site IIIa lays between helices M6, M8 and M9 involving residues (Glu954, Tyr771 and Thr807). Site IIIb is localized between helices M5, M7 and M8 interacting with Thr774, Gln854 and Asp926. At site IIIb, the later residue Asp926 is crucial for ion coordination as controlled by C-terminal Gln954 from site IIIa. Involvement of Gln954 for ion coordination suggests cooperative mechanism between both sites (IIIa and IIIb) in Na^+ transport [47].

Consequently, the high-resolution structure published later by [46] proposed only one position of site III corresponding to IIIb site published by [47]. This site is localized at the bottom end of the cytoplasmic half of the M5 helix. Here the M5 helix is slightly unwound and bend towards Pro778. Site III is formed at the cytoplasmic end of the unwound part of M5, between the main chain carbonyl of Tyr771 and Ser775 amide from M5. Side chains of residues on M6 (namely Asp808) and M8 (Gln923) confine the Na^+ to the unwound space in M5. The aromatic ring of Tyr771 forms the ceiling of the binding cavity and provides π-electrons for Na^+ binding. A side wall is formed by Thr774 and Gln923 side chains and seems rigid because of an extensive hydrogen bonding network involving Tyr771 (M5), Gln854 (M7) and Asp926 (M8). The Ser775 hydroxyl coordinates Na^+ in both sites I and III and is likely to make hydrogen bonds with the Asp808 carboxyl. Thus, site III seems very restricted in the axial direction (that is, along the M5 helix) and is indeed too small for K^+ [46].

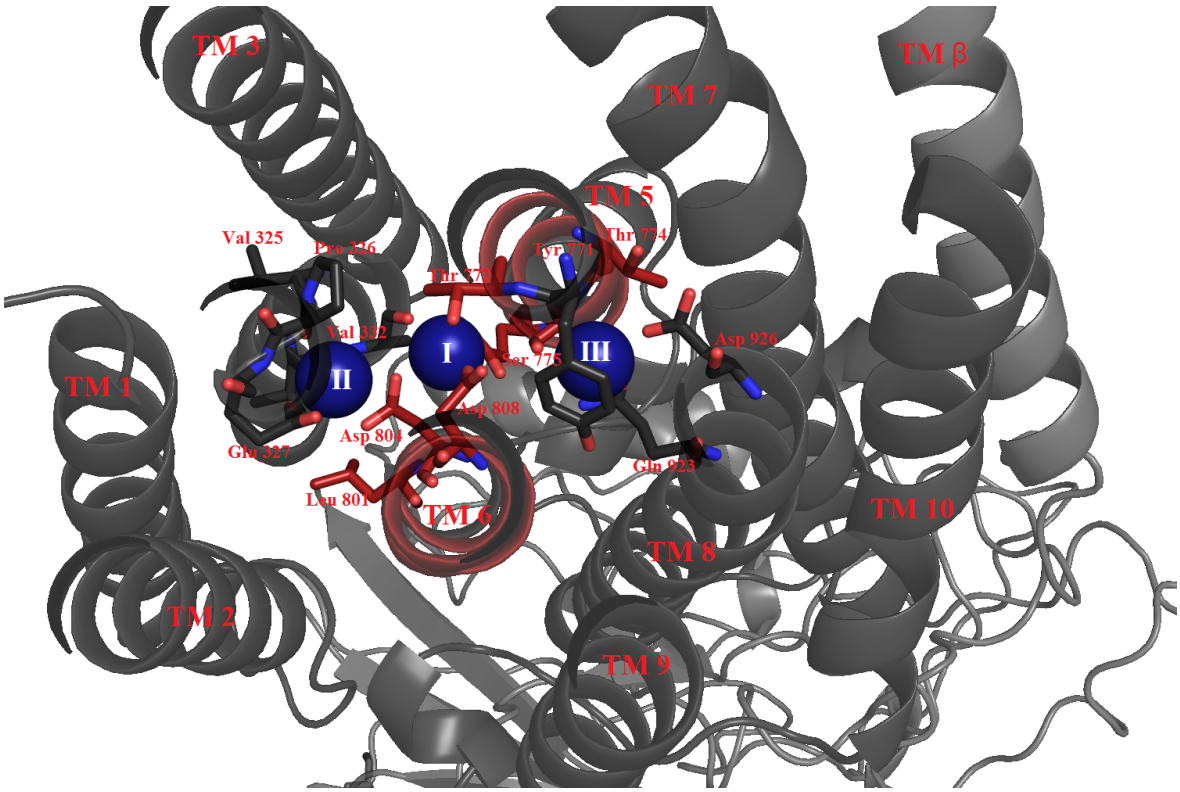

Figure 4: Figure of the human α_1 NKA in closed (E1) conformation with bound three Na^+ ions (dark blue). The homology model was based on crystals with PDB ID 2ZXE [44] and 4HQJ [47]. The figure courtesy of Petra Čechová [55].

K^+ binding site (see Figure 5) poses distorted geometry of bound cations adjusting high affinity for binding. Site I is analogous to SERCA 1a site I for Ca^{2+}. Coordination geometry of this site is very regular, involving six oxygen atoms that can be found approximately 2.7Å from K^+. In this site, the atom of K^+ is coordinated by Ala323, Glu 779, Thr772, Ser775, Asp804 and Asp808. The second site involves the contribution of four side chains and two main chain oxygen atoms of (residues Val325, Pro326, Glu327, Leu801, Asp804 in the Figure 5) [53, 55]. This site contributes to potassium transport, but the selectivity for K^+ is low, suggesting primary transport of Na^+ ions. Site II is localized mainly within M4 helix and is shifted toward the extracellular side. Residue Glu327 influences affinity to K^+, because this residue seals the bound potassium from the cytoplasm [53].

This stabilizations include Gly855 carbonyl which would otherwise be exposed to the hydrophobic core of the membrane bilayer that is energetically unfavorable. In the crystal structure, there is a cholesterol molecule, which is shielding the unwound part of M7 helix from bulk lipid. The cholesterol is stacked there via interaction with Tyr40 from β subunit and Gln856 from α subunit. Surprisingly, Gln856 is the conserved residue suggesting significant function of bound cholesterol [52].

The NKA extracellular ion exit pathway lays between M1, M2, M4 and M6 transmembrane helices and Glu334 was identified as an essential residue for ion binding/gating from both sides of the membrane [54].

Except for the transmembrane domain, the three cytoplasmic domains significantly

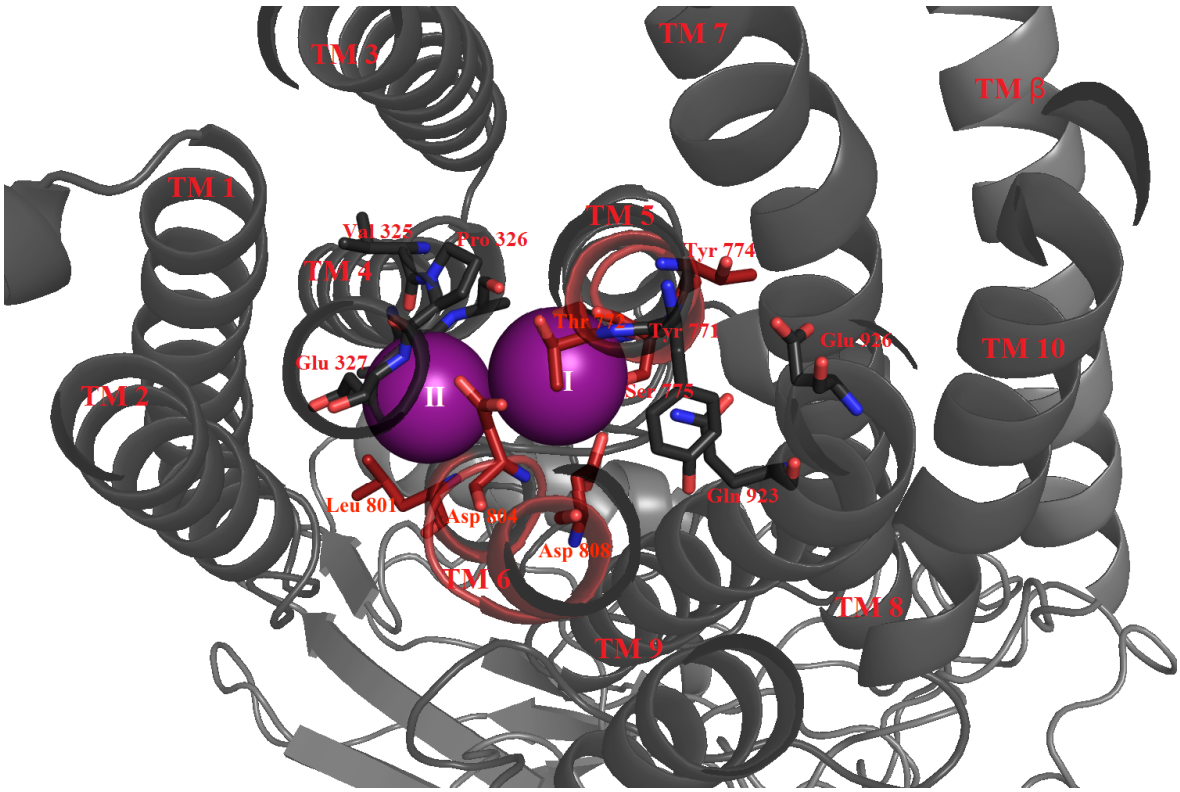

Figure 5: Structure of NKA in open conformation (E2) with bound two K^+ ions (purple). The figure courtesy of Petra Čechová [55].

contribute to the reaction cycle. The N domain recognizes ATP and positions the γ phosphate for nucleophilic attack, whereas a conserved aspartate in the P domain accepts the phosphoryl group and forms a high energy aspartyl-phosphate intermediate [56].

A glutamate in the A domain positions a water molecule for the subsequent hydrolysis which leads to the release of the phosphoryl group. The cytoplasmic domains are connected to the transmembrane segment by five linker regions that form the crucial structural connection between two-steps release of energy on the cytoplasmic side and its conversion into physical translocation of ions through the membrane [54].

A 5 amino acids sequence motif of 369-Asp-Lys-Thr-Asn-Thr-Leu (DKTGTL) is of paramount importance, because aspartic acid at position 369 undergoes phosphorylation during the reaction cycle [50]. A highly conserved motif Thr-Gly-Glu-Ser (TGES) in the A domain and the phosphoryl binding pocket in the P domain contain conserved catalytic residues that stabilize the transition states during phosphorylation. The electrostatic repulsion between ATP γ phosphate and carbonyl of Asp369 is overcome by the charge delocalization caused by the residues Lys702 and Mg^{2+} cofactor. Based on the active site modelling, two residues Asp714 and Asn782 were also proposed as residues coordinating ATP [57].

Release of the γ phosphate from the ATP unlocks interface between the N domain and the P domain, allowing the transition from high energy E1-P state to a lower energy E2-P ground state. N domain disengages from the phosphorylation site, giving space for the A domain, which rotates by 120° and places the TGES motif at the former

position of the ATP. The aspartyl-phosphate is thereby sealed against an unspecific attack and forms a hydrophilic cluster between the A domain and P domain and the upper end of M2 helix. Dephosphorylation is mediated by Thr181 and Glu183 from TGES motif by placing activated water molecule for nucleophilic attack. Also, an arginine at position 544 (Arg544) is localized at the mouth of ATP-binding pocket and is involved in the phosphorylation of NKA [58].

1.2.2 β Subunit

This subunit works as a molecular chaperon ensuring proper membrane integration and packing of newly synthesized α subunit in the endoplasmic reticulum (ER) [59, 60]. Most notably, β routes α to the plasma membrane and prevents it from degradation. The overexpression of the β subunit results in integration of β into plasma membrane, but overexpression of α subunit results in retention of this subunit in the ER [60, 61]. Additionally, β modulates the function of the whole protein by tuning the cation-binding affinity and K^+ occlusion. Furthermore, it was reported that β also modulates the formation of cell-to-cell junctions [49].

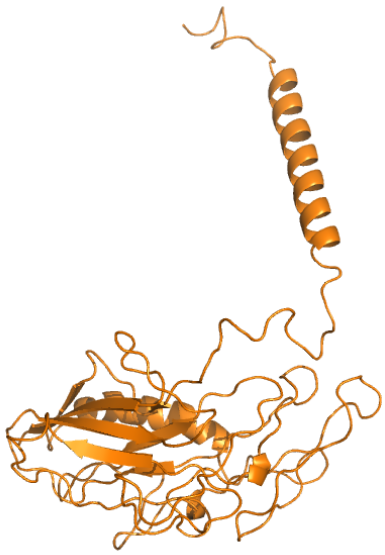

Figure 6: The structure of β subunit of NKA. There is one helical structure associated with the transmembrane part of α subunit, while the protein is anchored in the membrane. The lower part of β subunit works as a lid which opens and closes during the reaction cycle.

The β subunit is extensively glycosylated during the post-translational modification of the protein. From two to four glycosylation sites can be found on the β subunit, but number of these sites depends on the isoform. The glycosylation sites may also regulate the dimer-formation of $\alpha\beta$ complex [52]. β subunit (see Figure 6) is composed of the N terminal domain approximately 30 residues long, one transmembrane helix and a large extracellular domain (denoted as ectodomain). The ectodomain contains 240 residues and covers the external surface of α subunit (complex interaction with loop between helices M7 and M8). The extracellular domain of β subunit is distorted antiparallel β-sheet and a short helix containing 9 residues. The main part of this

subunit is exposed to the extracellular space (80% of overall structure). However, the structure of β subunit is stabilized by three disulfide bonds [52] which are required for heterodimer targeting to the plasma membrane, and are highly resistant to reduction [62]. Several studies revealed that reduction of the disulfide bonds in the extracellular domain resulted in the loss of ATPase activity [63, 64]. In addition, the presence of K^+ ions protected the disulfide bonds against the mentioned reduction and associated loss of function. From those observations was concluded that β subunit was involved in the stabilization of K^+-occluded state [64].

Various $\alpha\beta$ complexes previously exhibited different apparent K^+ affinities [65, 66, 67, 68], since both subunits rearrange significantly during the reaction cycle. Furthermore, a deletion or mutation of the β subunit can result in severe consequences (such as hearing loss, motor disabilities). For instance, in *Drosophilla*, the β subunit regulates sight and hearing that can cause hearing or sight loss. In the mice, deletion of the gene encoding β_2 isoform causes motor disabilities, and the animals die a few weeks after birth. In the human, changes in the expression pattern of β_2 have been linked to glioma development [69] and to occurrence of polycystic kidney disease [70].

1.2.3 FXYD Proteins

The family of FXYD proteins is a group of tissue specific regulators modulating kinetic properties of the whole $\alpha\beta$ heterodimer as well as they are responsible for apparent affinities of transported ions and ATP [71, 49]. FXYD proteins are composed of a single transmembrane helix (adjacent to M7 helix of α subunit), extracellular part containing conserved motif FXYD(Y) and a cytoplasmic part that containing important phosphorylation sites (see Figure 7). The position of conserved motif is just prior to transmembrane helix. Furthermore, the transmembrane domain contains two conserved glycine residues and the most of the functional effect is associated with this part.

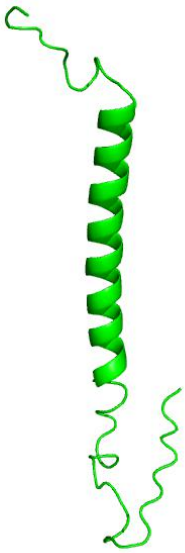

Figure 7: Structure of FXYD protein.

Additionally, the γPhe12 anchors the segment to the β subunit through stacking interaction with βPhe187 and two tyrosine residues (γTyr14 and γTyr16) in the conserved motif form an aromatic cluster with tyrosine residue in the β subunit (βTyr69) and tryptophan residue (αTrp980) from α subunit, thereby sandwiching the β with α [52]. Asp15, the last residue in the FXYD motif caps transmembrane helix.

FXYD motif appears to be important for stabilizing α-β-FXYD interaction. Moreover, FXYD and β change their relative distances during the reaction cycle suggesting the complex modulation of the NKA activity. It seems that isoform specific interaction reflects the special needs of the cell within tissue and mutation in the sequence encoding the γ subunit (FXYD2 protein) is associated with an inherited form of hypomagnesia [70]. Unfortunately, the principle of how FXYD proteins affect binding of Na^+, K^+ and kinetic properties of NKA is unclear.

1.2.4 Isoforms of the Structural Subunits

As mentioned previously, the human α subunit exists in four distinct isoforms, human β can be found in three isoforms and human body expresses seven isoforms of FXYD proteins. Localizations of those isoforms are summarized in Table 1.1.

Studying the human $\alpha_3\beta_1$ complex of NKA which is expressed by neuronal cells, was one aim of this work. Neurons may express α_1, α_2, α_3 or any combination of these isoforms, and evidence suggests that neuronal type is the determining factor. The function or significance of multiple NKA isoforms and their nonuniform expression between neurons, remain unknown [48]. Neurons express $\alpha_3\beta_1$ and rarely $\alpha_3\beta_2$ complexes of the NKA. However, β_1 and β_2 subunits are also expressed in other tissue and cell types. Different types of central and peripheral glia (astrocytes, oligodentrocytes and Schwann cells) express α_1 or α_1 and α_2, but not α_3 isoform. At least two groups of peripheral neurons were functionally identified expressing α_3, the skeletal muscle stretch receptor afferent neurons and γ-motoneurons [48].

One can hypothesize that existence of several isoforms of the NKA subunits is connected with their kinetic differences. The most consistently reported feature of α_3 is a relative insensibility to Na^+ activation (28±8 mM Na^+ for half-activation of α_3 (according to [65, 72, 73, 74, 75, 76]). Additionally, α_3 is relatively independent on voltage as revealed electrophysiological experiments [65, 77, 78, 79]. Finally, this isoform displays the highest ATP affinity for half-activation. For example α_1 requires 400 μM ATP for half-activation, but α_3 requires only 90 to 210 μM ATP [72, 74].

Reviews of these findings suggest that different isoforms of NKA may be complementary to each other in terms of active ion transport in neurons. Thus, α_1 NKA appears to be well suited for control of intracellular Na^+ in resting neurons. The steep voltage dependence of its transport rate enables the α_1 isoform to respond with fast activation during short bursts of action potential associated with depolarization and additional entry of Na^+ through the voltage-dependent channels. α_3 has low Na^+ affinity and shallow voltage dependence making it an ideal transporter for control of the intracellular sodium under extreme conditions such as post-tetanic hyperpolariza-

tion. Furthermore, relatively high ATP affinity of this isoform may be an additional advantage ensuring the activity of α_3 even under low concentration of ATP [48].

Subunit Isoform	Localization	Reference
α_1	mainly kidney, thymus, lung, liver, heart, skeletal muscle, testis, brain and pineal gland	[80, 81]; [82, 83, 84, 85, 86, 87, 88, 89, 90, 91]
α_2	skeletal muscle, heart, brain	[80, 81]; [84, 85, 87, 90, 91]
α_3	brain, pineal gland	[80, 81, 82]
α_4	sperm cells/germ cells	[86, 88, 89]
β_1	kidney, lung, liver, brain, skeletal muscle and heart	[80, 81, 82, 83, 84, 85, 87, 90, 91]
β_2	thymus, skeletal muscle, pineal gland and brain	[80] [83, 85, 86, 87, 88, 89, 90, 91]
β_3	lung, liver, skeletal muscle and testis/germ cells	[80] [83, 85, 86, 87, 88, 89, 90, 91]
FXYD1	heart and skeletal muscle	[92, 93, 71, 94]
FXYD2	kidney	[92, 95, 93, 71]
FXYD3	stomach, colon	[92, 93, 71]
FXYD4	inner and outer medullary collecting duct in kidney	[92, 96, 93, 71]
FXYD5	testis, colon	[92, 93, 71]
FXYD6	brain	[92, 93, 71]
FXYD7	brain	[92, 93, 71]

Table 1.1: Human isoforms of NKA subunits and their localization in the body (according to [48, 49]).

1.2.5 Lipid Enviroment

General lipid-protein interaction depends on the lipid-induced changes with the physiological properties of bilayer [97]. Both chemical and physical properties (hydrophobic thickness, curvature stress, elastic moduli, etc.) of a lipid bilayer affect the final structure and function of the membrane-bound proteins. As reported recently, lipid-protein interactions show strong potential in the distribution of specifically bound lipids at the lipid-protein surface [97]. Moreover, the mutual interaction between lipids and membrane-bound proteins seems to be evolutionarily conserved. Detailed information about membrane architecture can be found in [35].

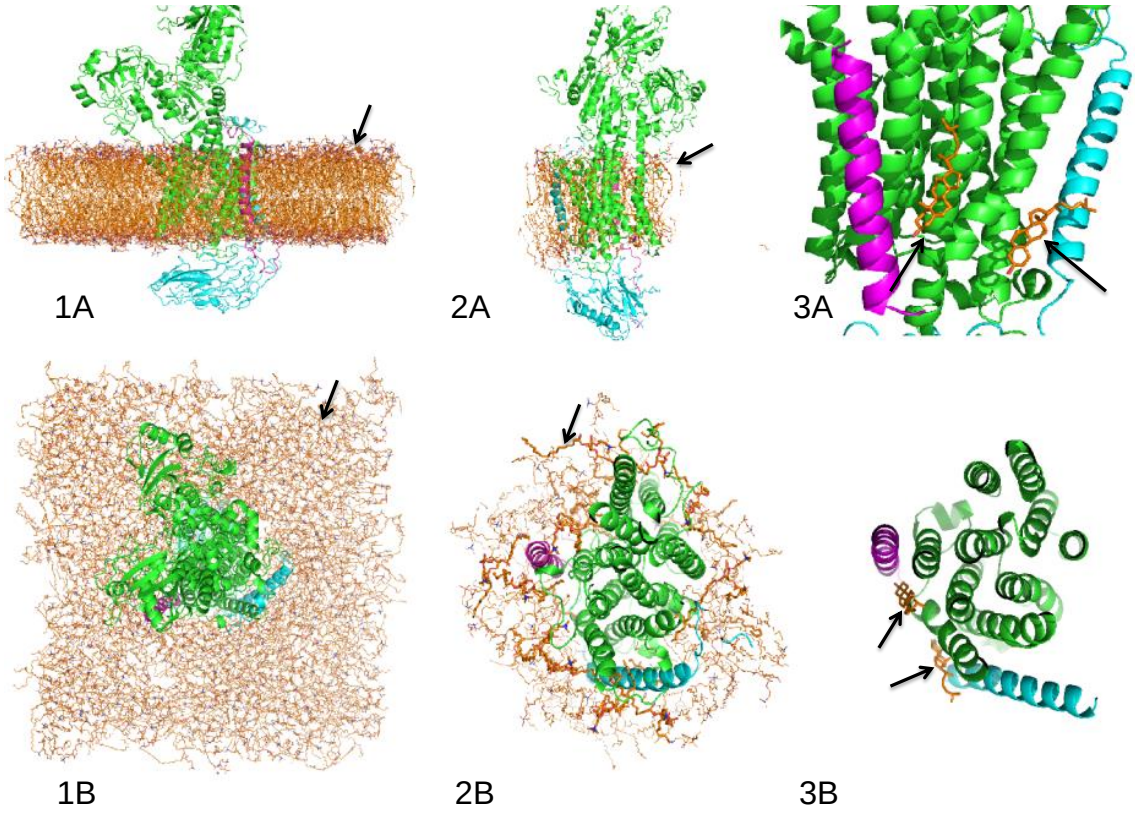

Figure 8: A lipid environment around the NKA – membrane parallel view (A) and membrane perpendicular view (B). Part 1A, B shows free lipids in the membrane, 2A, B illustrate annular lipids which are associated with the protein and 3A, B show specific-bound lipids (non-annular lipids).

The effect of annular lipids and specific-bound lipids (see Figure 8) can examine the functional effects of phospholipids and cholesterol on the structural stability of the NKA. Annular lipids coat the transmembrane surface of the protein and only the protein structure restricts their free motion. Annular lipids associated with NKA are phosphatidylcholine (PC), phosphatidylserine (PS) and cholesterol (CHS). Any phospholipid or molecule of CHS can serve as specific-bound lipid found within NKA structure [98]. The specific-bound lipids (also called nonannular lipids) are tightly associated with the protein in long-term interactions [99]. The specific-bound lipids are found filling the cavities on the protein, fitting into grooves between the transmembrane helices or they are stacked between the subunits. Such positioning significantly distorts their structure and geometry [44, 46, 100].

Structural effects of phospholipids or cholesterol on the structural stability of NKA can be separated into three distinct groups – compounds causing structural stabilization (PS and CHS), compounds with a stimulatory effect (unsaturated phosphatidylethanolamine – PE), and lipids causing inhibition of enzyme activity (PC, sfingomyelin and high concentrations of CHS) [101, 102, 103].

In general, animal plasma membrane contains 30 – 50 % of CHS. Optimal conditions for NKA hydrolytic activity are ranging 20 – 40% of CHS [104]. The increasing activity is in accord with cholesterol-induced increase of the rate determining the E2 → E1 reaction step and the stabilization of the E1 conformation [105]. CHS or 1,2-dioleyl-*sn*-glycero-3-phospho-L-serine (DOPS) dramatically increase the enzyme activity obtained at the optimal bilayer thickness. The results based on the recombinant NKA from *Pichia pastoris* suggested the specific effect of CHS on the NKA/PS complex via the hydrophobic matching system for the transport of sodium and potassium [106, 107, 102, 108].

The lipid interactions may be isoform specific due to the variability of membrane composition of tissue expressing the NKA. For example, renal NKA and its oligomeric states are stabilized by the specific binding of the anionic phospholipids such as PS or cardiolipin. However, the recombinant $\alpha_1\beta_1$FXYD1 complex is structurally selective for synthetic neutral lipids (PE, DOPS, PC and natural brain PS) with polyunsaturated fatty chains [97, 102, 109]. The structural selectivity for the neutral lipid class and the asymmetric saturated plus PUFA (polyunsaturated fatty acids) fatty acyl chain structure is a strong indication for a specific interaction with the NKA [110].

1.3 Function and Regulation of NKA

The electrochemical gradient established by NKA drives many physiological processes, such as secondary transport, osmotic balance and excitability of neurons and muscles. The NKA is ubiquitous in human cells and its proper function is essential. In most cases, altering the number of active pump molecules present in the membrane via endocytosis and exocytosis regulates NKA in cells [5, 111]. Regulation pathways are important for many cellular processes and changes.

For controlling insertion or retrieval of particular membrane protein, it is necessary to establish a specific signal that may modulate this particular pathway. Signals in response to the actions of extracellular effectors, such as dopamine, are produced by phosphorylation of the α subunit of NKA by specific protein kinases at many of sites [111]. The short-term regulation of this type, involving protein-kinase C (PKC) isoforms, has been published recently [6, 112, 113]. The mechanism of interaction is more complex, since the response of the pump may be affected by the intracellular Na^+ concentration [114].

For example, the plasma membrane of cardiac myocytes contains highly active Na^+/Ca^{2+}-exchanger influencing function of cardiac NKA. The cardiac NKA can be partly inhibited by rising of the intracellular Ca^{2+} concentration. Despite the inhibition of essential NKA, this process does not influence the overall cell viability. The mechanism of NKA inhibition is well-known for decades and is often discussed as a positive effect of cardiotonic glycosides that are used in arrhythmia treatment.

1.4 The Reaction Cycle

The knowledge of reaction mechanism of NKA is based to a large extent on early studies of the biochemical properties of the phospho-enzyme intermediates, the partial biochemical reactions catalyzed by the protein, and their relationships to the partial transport reactions (see Figure 9) [115].

In the 1960s, Post and Albers made observations [116, 117] which prompted proposals of a reaction scheme that is commonly known as Post-Albers diagram. The Post-Albers diagram provided a framework for the investigation of the mechanism of the NKA for more than 30 years. It has been shown that principles of Post-Albers digram are applicable to other transport proteins belonging to the general class of P-type ATPases [50].

The kinetic mechanism of the cation transport includes a definition of the properties of the phosphorylated intermediates, occluded states after dephosphorylation, and conformation changes of the protein. In general, the pumping mechanism fits the ping-pong transport mechanism and includes several steps. According to [58], pumping mechanism is described by six steps are:

1. ATP binding with low affinity accelerates inward transport of two K^+ ions coupled to the E2[2K]↔ E1 conformation transition

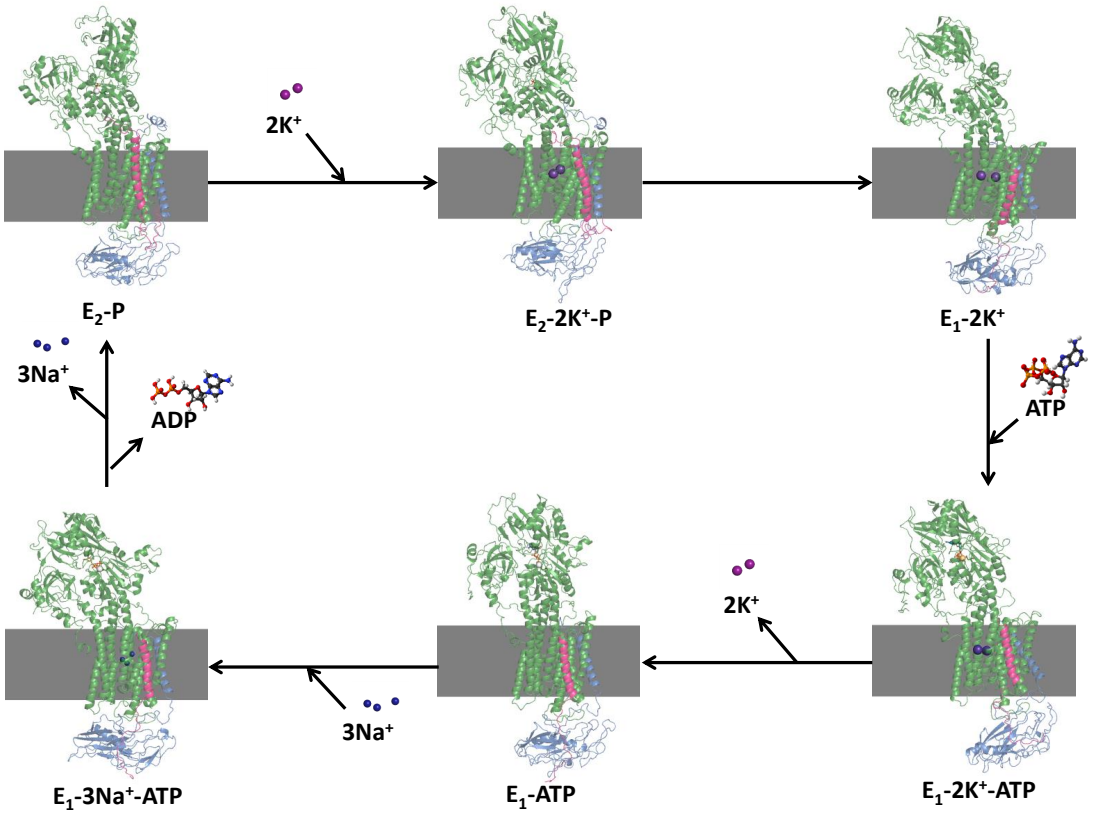

Figure 9: The illustration of the Post-Albers diagram. α subunit is green, β subunit is blue and FXYD protein is magenta. The figures are based on the Na^+-bound structure of the NKA ($E_1 3Na^+$-ATP) with PDB ID 4HQJ [47] and K^+-bound structure ($E_2 2K^+$-P) with PDB ID 2ZXE [45], respectively. The remaining intermediates were obtained by molecular-dynamic simulations performed by Petra Čechová [55].

$$E_2\ [2K] \leftrightarrow E_1\ 2K + ATP \leftrightarrow ATP \cdot E_1 + 2K^+_{cytoplasmic}$$

2. binding of three Na^+ ions at cytoplasmic-oriented sites
   $ATP \cdot E_1 + 3\ Na^+_{cytoplasmic} \leftrightarrow E_1\ ATP + 3Na^+$

3. $Na^+_{cytoplasmic}$-oriented phosphorylation from ATP and occlusion of three Na^+ ions
   $E_1\ ATP\ 3Na^+ \leftrightarrow E_1\text{-}P[3Na] + ADP$

4. outward transport of three Na^+ ions coupled to the E_1-P $\leftrightarrow$ E_2-P conformational transition
   $E_1\text{-}P[3Na] \leftrightarrow E_2P[2Na] + Na^+_{extracellular}$

5. binding of two K^+ ions at extracellularly oriented sites
   $E_2P[2Na] + 2K^+_{extracellular} \leftrightarrow E_2P[2K] + 2Na^+_{extracellular}$

6. $K^+_{extracellular}$-activated dephosphorylation and occlusion of two K^+ ions
   $E_2P[2K] \leftrightarrow E_2[2K] + P_i$

Despite the fact that the most significant steps are known for fifty years, such as the relationship between a biophysically defined pathway (apparently leading to the Na^+ binding site from extracellular medium) and the structurally defined channel in the protein, some sub-steps of the reaction cycle remain controversial [115].

Other authors published alternative schemes of the Post-Albers diagram and can be found in [15, 50, 52, 58, 62, 118, 119, 120, 121, 122, 123].

1.4.1 Diseases Caused by Dysfunction of NKA

NKA generates the sodium gradient which is consequently used by secondary transporters. A malfunction of this pump is linked with pathology of several diseases (e. g. ischemia [70], diabetes[5, 124], hypertension [3], cataract [2], hyperkalemia [3]) and neurological disorders (Familial Hemiplegic Migraine 2 – FHM2 [9, 125], Alternating-Hemiplegia of Childhood – AHC [126, 127, 128], Rapid-Onset Dystonia Parkinsonism – RDP [128, 129, 130], CAPOS syndrome [131, 127, 132]). Recently, the sequencing of patient genome has revealed several mutations in the genes encoding the α subunit of NKA. Consequently, the methods of molecular biotechnology (mutant protein expression in *Xenopus* oocytes, transgenic mice, etc.) are used to determine the biophysical changes caused by the individual mutations that are responsible for the correlations with disorder severity.

In general, mutations in the sequence of different isoforms of α subunits result in the various phenotype. For example, the mutations in *ATP1A1* and *ATP2A3* (encoding human variant of SERCA) are linked with the adrenal aldosterone-producing adenoma. In the gene *ATP1A1* encoding α_1 isoform were identified nine somatic mutations causing outward proton leak under physiological conditions [133]. On the other hand, the investigation of the role of α_2 is more complicated. The gene *ATP1A2* is developmentally regulated and plays no role in early development [134].The research of α_2 role in the muscle contraction demands the experimental animal in which the gene *ATP1A2* is knocked out only in the skeletal muscles. Mentioned strategy overcomes problems with the global α_2 knock-out mouse which dies at birth. Finally, important mutations in the *ATP1A3* gene are described below. Nevertheless, we would like to note that sequence numbering corresponds to human α_1 isoform for better understanding and orientation.

Cerebellar ataxia, areflexia, pes cavus, optic atrophy, and sensorineural hearing loss (CAPOS) syndrome is a rare neurological disorder, which has been reported in a few families [131]. The amino acid replacement at position 828 (Glu828Lys, see Figure 10) in the genome of affected mother was not inherited from either of her unaffected parents and, therefore, must have arose *de novo*. Glu828Lys mutation substitutes a positively charged lysine for a negatively charged glutamate in the C-terminus cation transporting domain of α_3 subunit of NKA [131].

The structure of the C-terminal pathway is also affected by mutations causing another severe neurological disorder – Familial Hemiplegic Migraine 2 (FHM2). In general, the C-terminus of NKA controls the gate to the ion pathway and its structure is crucial for a pump function [9]. Naturally occurring mutations of either arginine,

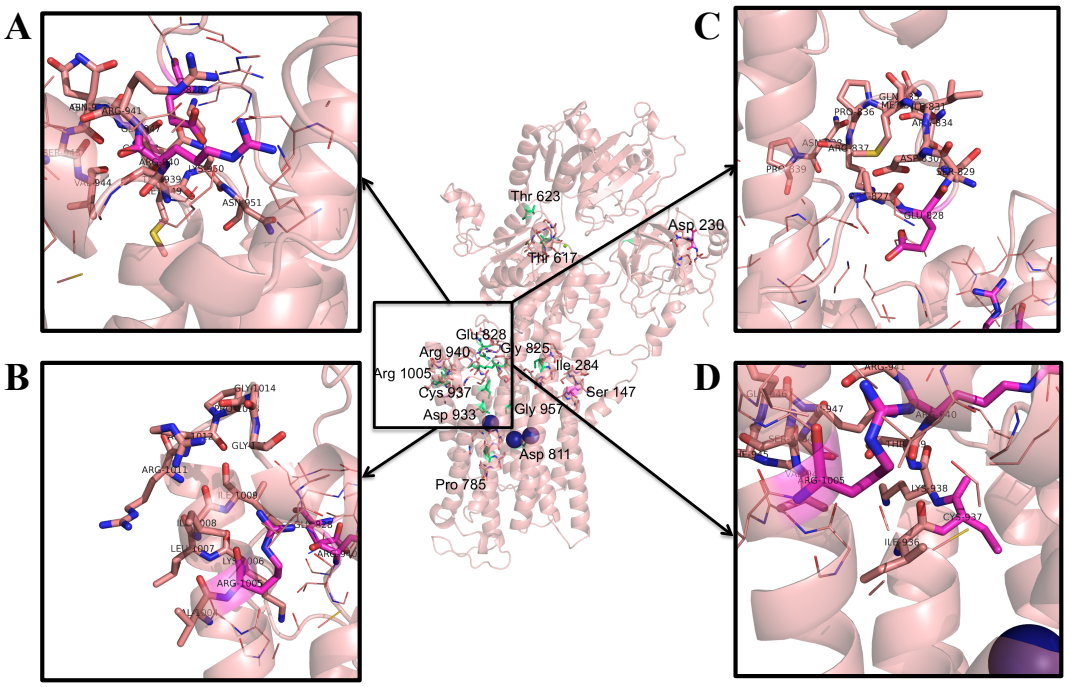

Figure 10: The structure and surrounding environment of residues Arg940 (A), Arg1005 (B), Glu828 (C), and Cys937 (D). All highlighted residues are localized in the transmembrane part of the pump. Their position in the close proximity to the membrane-cytosol interface can play significant role in the translocation of ions. Mutations of these residues can block one of the water translocation pathways [55]. More specifically, residues Arg1005 (localized within transmembrane helix M10) and Arg940 (transmembrane helix M9) comprise the C-terminal pathway [9]. The figures are based on the Na^+-bound structure of the NKA with PDB ID 4HQJ [47].

Arg940Pro (see Figure 10) or Arg1005Gln (see Figure 10) cause FMH2, a severe and dominant form of migraine [9].

In the following part, we will focus on the two main neurological disorders linked with mutations of genes encoding α subunit of NKA – Alternating Hemiplegia of Childhood (AHC) and Rapid-Onset Dystonia Parkinsonism (RDP). AHC is characterized by episodes of alternating hemiplegia or quadriplegia and dystonic or tonic attacks that are associated with permanent neurological deficits including intellectual disability and movement disorders. Paroxysmal events typically start before 18 months of age, and are often precipitated by specific triggers (emotional stress, bathing, cold, fatigue, hypothermia and hyperthermia) [135, 136]. Unfortunately, the exact mechanism of AHC is unknown, although treatment with Flunarizine (a Ca^{2+} influx inhibitor specific for vascular smooth muscle and neurons) has been reported to reduce the symptoms. However, the effectiveness and long-term effects of this treatment are unknown [126].

Neurological investigations did not provide any clue on the pathogenesis of this disease. For individual patients with clinical phenotypes mostly consistent with AHC, the mutations in the *ATP1A2* gene encoding α_2 subunit were identified. Those muta-

tions are also associated with familial hemiplegic migraine. Thus, no biochemical or radiobiological markers exist for AHC, and the diagnosis has been entirely based on clinical criteria (most symptoms listed above) [126].

A heterozygous missense mutation in *ATP1A3* was confirmed in 33 of the 35 patients (Japanese AHC Family Association) by Sanger sequencing. None of the parents showed any *ATP1A3* mutation. All mutations were confirmed as *de novo* mutations. Of the 33 patients with these *ATP1A3* mutations, 12 (36%) had a Glu825Lys mutation (see Figure 11); 10 patients (20%) suffered from a Asp811Asn mutation (see Figure 11); 2 patients had a Cys937Phe mutation (see Figure 10); and the remaining 9 patients had other mutations [126]. More specific mutations are listed in [11, 126].

Common mutations associated with AHC are Asp811Asn in exon 17 and Gly825Lys in exon 18. Notably, these two mutations in adjacent exons were detected in 67% cases from tested cohort, suggesting a possible mutation hotspot in exon 17 and 18. Both mutations are predicted to result in an amino acid change within two conserved functional protein domains and one transmembrane domain: the C-terminal cation transporting ATPase domain and the α subunit of the P-type ATPase domain as well as the transmembrane region 6 of the α_3 NKA [135]. Finally, familial cases of AHC with late onset, mild phenotypes, and autosomal dominant inheritance and concordant occurrence in monozygotic twins was reported, but almost all cases were sporadic. *ATP1A2* gene mutations have been reported as the cause of AHC in atypical familial cases. However, these were identified as rare [126].

Other mutations associated with AHC are Ser147Tyr (see Figure 13), Asp230Asn (see Figure 13), Ile284Asn (see Figure 12), Asp811Asn, Glu825Lys and Gly957Arg (see Figure 11). More specifically, the mutant Asp811Asn showed an increase in the maximum ouabain binding compared to the wild type enzyme. The antagonism between KCl and ouabain was not observed for Asp811Asn and Ser147Tyr mutants. The absence of the antagonism indicates that K^+ is not able to bind to those mutants. In general, AHC mutations are located near or inside one of the transmembrane domains. One exception to this rule appears to be Asp230Asn, located in the cytoplasmic loop between transmembrane helices 2 and 3 (loop C23). Additionally, mutations Glu825Lys and Asp811Asn are located in the GC-rich sequences of *ATP1A3*, and within 6-bp palindrome. These features may be relevant to development of these *de novo* mutations [137].

The evaluation of the crystal structure of NKA predicted that a change from aspartic acid at position 811 to asparagine (Asp811Asn) in AHC will prevent the binding of potassium ions. The aspartate located at amino acid position 811 is highly conserved in NKA in all investigated species, and plays a major role in the cation binding pocket. The structural modelling of the Asp811Asn mutation predicted a direct effect on the binding of potassium ions, reflecting the highly important role of aspartic acid residue at 811 in the coordination of ion binding sites I and II in K^+-occlusion and Na^+-coordination, and also binding of Mg^{2+} ion site II in the high resolution ouabain bound state [11].

However, no significant ATPase activity or phosphorylation level was also detected for Ser137Tyr, Ile284Asn, Glu825Lys and Gly957Arg. Moreover, Ile284Asn,

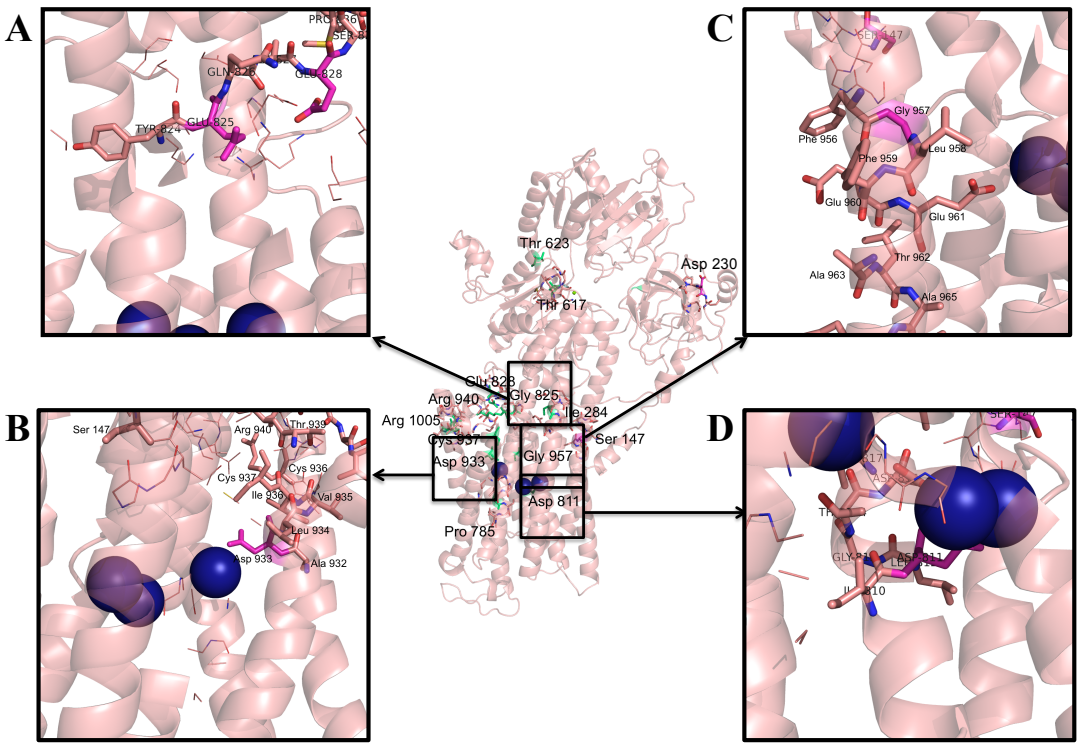

Figure 11: The structure and surrounding environment of residues Glu825 (A), Asp933 (B), Gly957 (C), and Asp811 (D). The residue Glu825 is localized above the binding site for sodium ions. The replacement of Glu by amino acid with bulky side chain can result in a block of ion transport (ions are unable to reach the binding site or to be released). The residues Asp933 and Asp811 are very close to the ion binding site. Moreover, the mutation of the Glu825Lys causes the complete loss of pump function, inability to bind ouabain [11]. Mutation Asp811Asn affects K^+ binding, which is linked with loss of pump function. This mutation does not change the interaction with the NKA specific inhibitor. Mutation Gly957Arg affects Na^+ release, the pump exhibit no activity and no ouabain binding [11]. The figures are based on the Na^+-bound structure of the NKA with PDB ID 4HQJ [47].

Glu825Lys, and Gly957Arg could not bind ouabain, which indicates that these mutations result in a severely affected protein with a complete loss of function.

For mutation at position 825, negatively charged residue at 825 enhances cation shuttling, the presence of a positive residue Lys825 mutant would produce a less favorable environment for cation movement. A cavity large enough to contain water molecules can be found in the protein models extending from Glu825 to Gly957. Although this observation of the cavity seems to be certainly suggestive, no direct evidence supports the involvement of residue 825 in the cation transport. While the loss of proton transport may be relevant to some co-morbidities observed in severe AHC, the *in vivo* significance of a proton transport via NKA has not bee determined yet [132].

Finally, the mutant Gly957Arg is located in the transmembrane helix M9. The structure of an α-helix might be strongly disturbed by the amino acid replacement

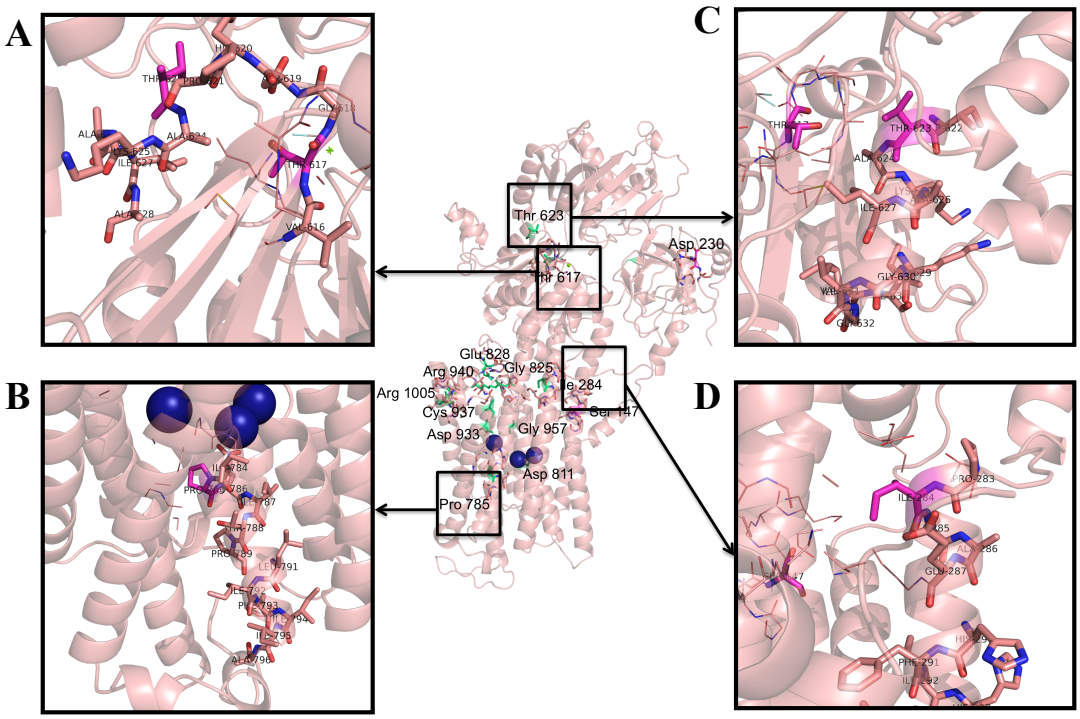

Figure 12: The structure and the surrounding environment of residues Thr617 (A), Pro785 (B), Thr623 (C), and Ile284 (D). Residues Thr617 and Thr623 are localized on A domain and both have polar side chains. On the other hand, the side chain of Pro785 contains heterocyclic ring which can be involved in specific interactions. Ile284 is hydrophobic and is localized in the centre of membrane on the kinky helix M2. The figures are based on the Na^+-bound structure of the NKA with PDB ID 4HQJ [47].

from glycine to arginine. This residue is important for regulation of the C-terminal pathway. In addition, the recently published crystal structure of the Na^+-bound state has suggested that Gly957Arg has affected the IIIa ion binding site of NKA, which has been important for the release of Na^+ ions following transition from E_1P-ADP state to the E_2 state [11].

The most of the AHC causative mutations are localized in the transmembrane domains. One would expect some of the mutations to reduce the level of protein expression, and that the mutations would be distributed through the protein rather than concentrated in the transmembrane domains. Unfortunately, localization of those mutations may affect the ion occlusion and their translocation accros the membrane.

Rapid-Onset Dystonia Parkinsonism is characterized by abrupt onset of dystonia within hours to weeks, and it is associated with Parkinsonism. None of the *ATP1A3* mutations detected in AHC was reported in RDP, suggesting that AHC and RDP are allelic disorders due to the mutations with distinct effects on *ATP1A3* activity. Nevertheless, some overlap exists for the permanent dystonia is found in most AHC patients and it is a core feature of RDP. The paroxysmal dystonia is frequent in AHC cases and may be sometimes observed in RDP [130].

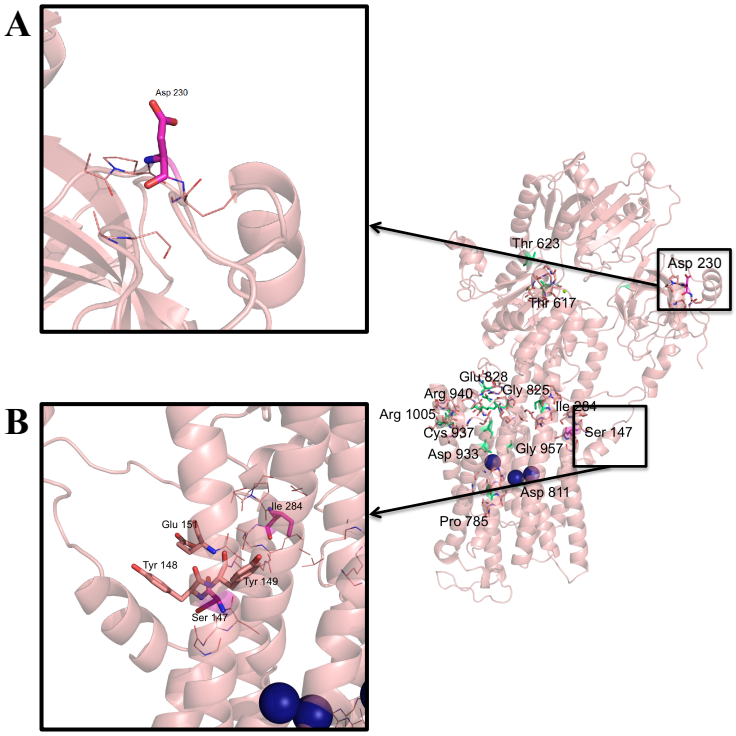

Figure 13: The structure and surrounding environment of residues Asp230 (A) and Ser147 (B). The residue Asp230 is on the C23 loop and represents an exception from the standard localization in the transmembrane part of the enzyme. Ser147 is localized in the transmembrane part of the enzyme and affects the K^+ binding. The figures are based on the Na^+-bound structure of the NKA with PDB ID 4HQJ [47].

The differences in the clinical symptoms between the patients with AHC and RDP are probably caused by variability in the positions of the *ATP1A3* mutations or by amino acid sequence changes. Various amino acid replacements could influence the structure, function, and overall NKA expression in the cells. The mutations in *ATP1A3* can be clearly differentiated for AHC and RDP. Nevetheless, they could be also viewed as an allelic disorder, or as a different aspects on the continuum of a single disease [126].

Despite the inconsistency in the tests on cell cultures, the RDP mutations typically reduce α_3 protein expression, whereas AHC mutations reduce the functional protein levels. These data suggest that *ATP1A3* mutation causes RDP through the hypomorphic effects on the NKA, while the AHC-causing mutations modulate the activity of the pump [10].

Thr617Met (see Figure 12), Pro785Leu (see Figure 12), Asp933Asn (see Figure 11) and Asp933Tyr (see Figure 11) were identified as the most frequent mutations of RDP. The mutation Thr623Met (see Figure 12) was reported in six different families or single patients and accounts for a third of all familial or sporadic cases. Thr623Met mutation suggests the existence of a potential RDP hotspot localized in exon 14 [135]. In contrast, the analysis of the Asp933Asn mutation which was identified in both patients with RDP and familial AHC suggested that protonation at this site was crucial for the movement of Na^+ and K^+ across the cell membrane [128].

Additionally, the familial RDP (FRDP) mutations Pro785Leu and Thr617Met functionally altered NKA by reducing its apparent affinity to cytoplasmic Na^+, but principal mechanism differs between the mutants. The residue Pro785 is localized near the extracellular end of the transmembrane helix M5. An aromatic side chain of Pro785 is important for the Na^+ binding properties, but not for the K^+ binding. The mutation of Pro785 caused no change in the E1 – E2 equilibrium. Thr617 is located in the cytoplasmic part of the molecule near the catalytic site and is universally conserved among P-type ATPases. The effect of Thr617Met mutation is analogous to Pro785Leu mutation, but the mechanism is different. Thr617Met affects the Na^+ affinity via displacement of the conformational equilibrium in favor of E2(K_2) [138].

To determine the exact structural consequences of the mutations in the NKA sequence and functional changes of the whole protein is challenging. The study of this consequence can be the first step in the research with a direct application to a treatment of above mentioned neurological disorders. Furthermore, some authors discuss an abnormal α_3 NKA expression which can be possibly related to cancer development [12, 139]. Unfortunately, this cancer-related abnormal NKA expression includes many processes and regulations. The complicated structure and regulation scheme should be determined before the complete understanding of this relationship.

1.5 Cytoplasmic Loops C23 and C45

The crystal structures of NKA in closed and open conformation were published by many authors [44, 52, 47, 100, 120]. The crystal structures helped to understand the NKA structure and they are useful for the monitoring of transitions between the main conformational states. The crystal structures represent available information about the natural NKA structure and serve as the basis for the computational methods such as molecular dynamics.

Three large domains (named as A, P, N) could be identified on the cytoplasmic side of the membrane. The A domain consists of the N-terminus and loops between the transmembrane helices M2 a M3 (loop C23). The N and P domains are composed of a large cytoplasmic loop connecting helices M4 and M5 (C45 loop) as shown in Figure 14.

Within the conserved sequence of N domain was identified the nucleotide-binding site. Whereas, the central P domain contains the residuum Asp369 that undergoes phosphorylation during the reaction cycle. Many interactions of NKA with the water soluble molecules are limited to the cytoplasmic part of the enzyme. To study interactions of NKA with water soluble molecules, the whole NKA can be represented only by domains which are exposed to the cell exterior such as C23 and C45 loops.

The large cytoplasmic loop C45 connecting transmembrane helices M4 and M5, and smaller loop C23 connecting transmembrane helices M2 and M3 are the most important representatives of the cytoplasmic domains. The structures of both loops are in Figure 15. As published previously, the C45 loop can be isolated from the rest of the enzyme and retains its structural [140, 141, 142] and functional properties [143, 144, 145, 146] including ATP binding [15].

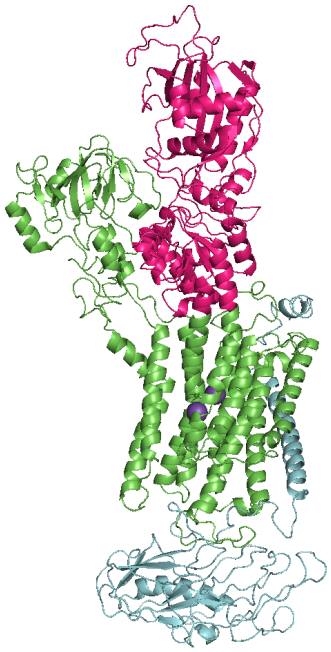

Figure 14: Structure of open NKA with C45 loop. Within green α subunit is C45 loop highlighted in magenta, and β subunit is blue.

Furthermore, there are two binding sites for Mg^{2+} ions within C45. The first magnesium ion is coordinated by Asp710 [147]. Another Mg^{2+} ion is coordinated by Asp369 [46] with potential contribution of Val569 and Phe572 [15]. The second coordination site for magnesium ion is distant from another important sites on the C45 suggesting biological significance. These findings agrees to in SERCA, where the presence of two Mg^{2+} ions was published [147]. Grycova *et al.* [15] also assumed that Mg^{2+} ions play role in the stabilization of the closed conformation of C45. More specifically, the C45 rapidly changes its structure after addition of ATP in the absence of Mg^{2+}. This movement weakens the contact between N and P domains and results in the open conformation of C45 [15].

Finally, we note that the described binding of two magnesium ions according to [15] was based on the SERCA structure and is in good agreement with crystal structures of NKA [44, 46] published later.

Due to the convenient size of those proteins (C45 – 48 kDa, C23 – 13 kDa), they can be prepared by the heterologous expression in bacteria. The structures of both loops are in Figure 15.

1.6 Isolation of the NKA from a Porcine Kidney

Although, NKA is present in most animal cells, it is particularly abundant in secretory and excitatory tissues. The most common sources for purification are kidney, brain, nasal glands, and electric organs [148, 149]. The enzyme can be isolated from various source animals e. g. pig [150, 151], mouse [152], ox [153, 154], shark [155, 44], duck

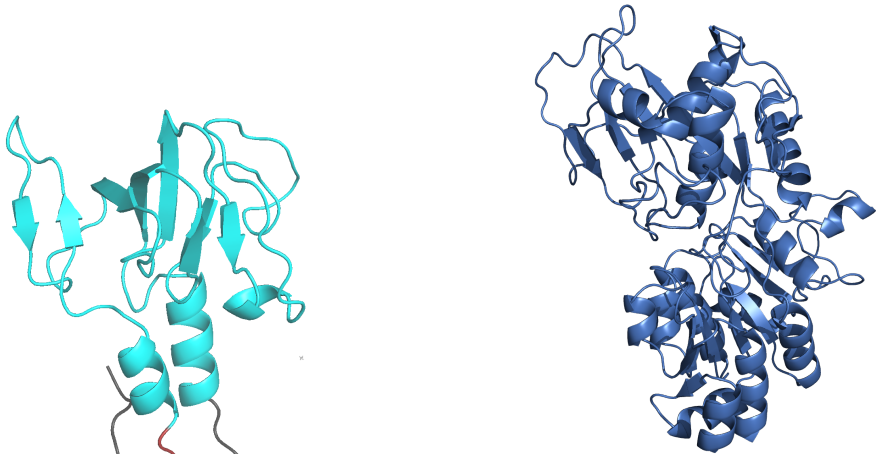

Figure 15: Left: The structure of the C23 loop. Right: The structure of C45 loop. The figure courtesy of Petra Čechová.

[156] and electric eel [157]. The study of the human variant is challenging due to ethical issues and inability of mammalian expression systems to provide sufficient amount of the protein for the research.

Klodos *et al.* [151] described the large-scale preparation of partly purified NKA from porcine kidney with the precise estimation of time consumption, and discussed the final protein yield and purity. Their method was based on a differential centrifugation and SDS-treatment of a microsomal preparation. The yield was 0.4 mg protein per 1 g of tissue with the specific (ouabain-sensitive) activity of 25 – 28 $\mu mol \cdot min^{-1} \cdot mg^{-1}$, and the nucleotide binding capacity of 3 $nmol \cdot mg^{-1}$ [149]. They also determined the protein to lipid ratio as 1:1 (w/w) with the protein purity of approximately 80%.

The basic steps of this method are tissue dissection, rough homogenization, mild-homogenization, and series of centrifugations followed by a microsome fraction preparation. Early studies were using a discontinuous sucrose gradient, where fractions between separate sucrose concentrations were subjected to final centrifugation. The method published by Jorgensen and Skou [158] is technically inconvenient due to small differences between sucrose concentrations, time-consuming gradient preparation, and low purity of the final protein. On the other hand, recent methods use detergent treatment followed by a differential centrifugation, which enables to remove high concentration of detergent used in the treatment. The sodium dodecylsulfate (SDS) is widely used as a detergent for microsomes solubilization in the preparation of NKA from porcine kidney. This ionogenic detergent exhibits high efficiency during short incubation period, and can be easily removed by dialysis.

1.7 Heterologous Protein Expression in *E. coli*

Molecular biotechnology enables production of proteins by metabolic actions of microorganisms (e. g. bacteria *E. coli*) using recombinant DNA method (insertion of the gene from one organism into another organism). The technology of recombinant DNA has far-reaching possibilities in the industrial production of biologically impor-

tant substances (insulin, interferone, growth hormones, viral antigenes). This chapter was based on [159].

1.7.1 Regulation of Transcription in Bacteria

In bacteria, many essential processes (e. g. production of amino acids, nucleotides, replication, transcription, translation, cell growth, and responses to environment) depend on proteins. The transcription of structural genes is regulated by signaling pathways enabling production of the needed proteins. Furthermore, the same regulatory machinery can be used for the down-regulation of transcription.

Frequently, bacteria structural genes that encode proteins required for several steps in a single metabolic pathway are contiguous in the chromosome. This arrangement is often called an operon. One promoter controls a single operon, and operon transcription produces one large mRNA molecule. The placement of a stop codon for one protein close to start codon of the next protein within a multigene mRNA generates a set of discrete proteins during translation. But a ribosome binding site (a Shine-Dalgarno sequence) precedes start codon in each coding sequence.

Each bacteria recognizes a different promoter sequence by the production of several sigma factors (binding site for RNA polymerase on the DNA). Nucleotide sequences in and around the sigma factor (operon region) play an essential role in determining whether an operon is transcribed. For instance, when a regulatory protein (a repressor) bind to an operator region and prevents RNA polymerase from binding to the promoter, the transcription is blocked. However, sometimes the specific low-molecular-weight compounds (effectors) bind to a particular repressor protein and change its conformation. The structurally modified repressor can no longer bind to the operator sequence and transcription is turned on.

Eukaryotes involve more complex regulation machinery, since the initialization of the gene transcription requires binding of several transcription factors. In general, the regulatory pathways vary within the organisms and they often use the specific signal sequences added during the post-translational modification of the synthetized protein.

1.7.2 Technology of Recombinant DNA

The technology of recombinant DNA encompasses a number of experimental approaches leading to production of heterologous products. The combination of techniques is unique for selected protein, but the most widely used steps are following:

1. The DNA (cloned DNA, DNA insert, target DNA or foreign DNA) from a donor organism is extracted, enzymatically cleaved and ligated to another DNA (a cloning vector) to form a new recombinant DNA molecule (cloning construct).
2. This cloning construct is transferred into host cell and maintained within it. This process is called a transformation.

3. Transformed cells are identified and selected.

4. The construct can be used for production of proteins in the host cells.

1.7.3 Cloning Vectors

Plasmids are the most commonly used cloning vectors. Plasmids are self-replicating, double-stranded, circular DNA molecules that are maintained in bacteria cells as independent extrachromosomal DNA. Generally, the plasmids are naturally present in bacteria cells, as they are involved in the utilization of unusual metabolites, encoding the resistance to antibiotics and plasmids can be transferred from one cell to another. Although the plasmids provide the cell with an advantage under specific conditions, they are not essential for their survival. The plasmids in molecular biotechnology contain an origin for DNA replication, multicloning site (a restriction site for several restriction enzymes) and selection markers. Usually, the size of the plasmids is between 1 kbp and 500 kbp. Their number of copies per cell is variable.

The first cloning plasmid was established by F. Bolivar and R. Rodriguez in 1980s. The plasmid was named pBR322. Nowadays, many plasmids are tailored specifically for the purpose of protein expression.

1.7.4 Transformation and Selection

The process of introduction of purified DNA into a host cell is called transformation, and such cell is able to accept this DNA is called competent. Generally, the competence and transformation are not intrinsic properties of bacteria cells. However, the competence can be induced by various treatments (e. g. wash with cold calcium chloride) which enhance the acquisition of DNA by the cell. Several methods for the uptake of exogenous DNA to the cell were developed (a brief heat-shock, electroporation, gene gun, etc.). Unfortunately, the transformation is very inefficient process (efficiency approximately 1‰).

After the transformation, it is necessary to identify the cells that contain plasmids with inserted DNA. This is often accomplished using the genes for antibiotics resistance. Directly after the transformation, the cells are incubated in the medium without antibiotics to allow the expression of resistance genes. Consequently, the transformation mixture is plated onto medium that contains antibiotics. The cells with plasmid grow under these conditions, because they are resistant. In contrast, the nontransformed cells are sensitive to antibiotic and die. This process is called a selection.

1.7.5 Regulable Promoters

Regulable promoters are used for the time and level dependent expression under control of specific promoters. The most widely used are *lac* and *trp* promoter. Each of these promoters interacts with regulatory proteins (repressor, corepressor, inductor), which

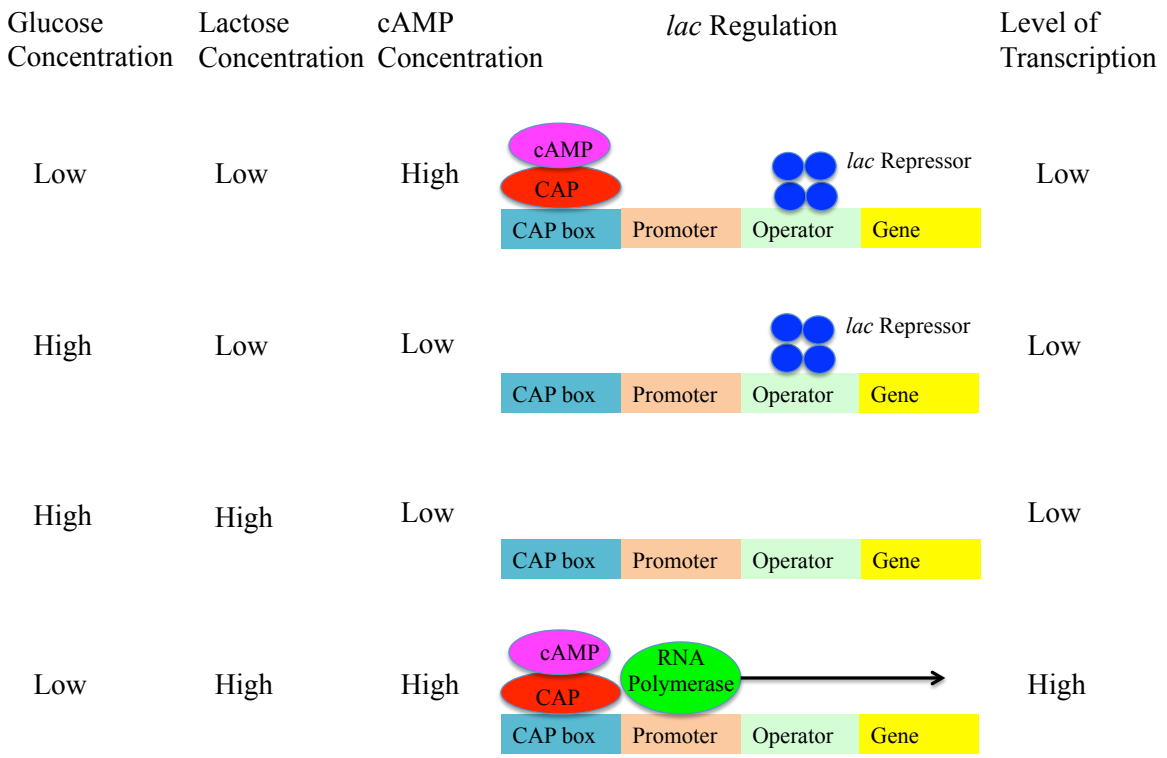

Figure 16: The egulation of the *lac* promoter. The effects of the concentrations of glucose, lactose and cAMP in the medium on the level of transcription from the promoter. *Lac* repressor is a tetramere, which binds to the operator sequence. The cAMP-CAP complex binds to the CAP box on the DNA enhancing the level of gene transcription. The arrow indicates the direction of transcription. The figure is based on [159].

provide a controllable switch for either turning on/off specific transcription of adjacent cloned genes. In addition, these promoters are recognized by the major form of the bacterial RNA polymerase holoenzyme.

More specifically, *lac* operon is constructed from the -10 region of the *lac* promoter (10 nucleotide pairs upstream from the site of the initiation of transcription). The mechanism of *lac* promoter regulation is in Figure 16. If the lactose is absent in the growth medium, the *lac* promoter is repressed by the *lac* repressor protein which prevents the *lac* operon from transcription. The addition of lactose or isopropyl-β-D-thiogalactopyranoside (IPTG) to the medium induces transcription under control of the *lac* promoter. IPTG serves as a synthetic inducer of the protein expression. Both substances (IPTG and lactose) prevent the *lac* repressor from binding to the *lac* operator, thereby enabling the transcription to occur. *Lac* operon contains *lacZ* gene encoding enzyme β-galactosidase which is involved in the cleavage of lactose to galactose and glucose. Moreover, the transcription from the *lac* promoter is also regulated by a catabolite activator protein (CAP or cyclic AMP repressor protein) to the CAP box that is localized upstream of the promoter region. CAP binding to the CAP box increases the level of transcription downstream of the promoter. The affinity of CAP

to its binding site on the DNA is enhanced by its association with cAMP whose level is increasing with decreasing the glucose level.

Thus, when IPTG or lactose is present and no repressor protein binds to the DNA, the high intracellular concentration of cAMP can lead to the high level transcription of genes under control of *lac* promoter. This regulation is illustrated in Figure 16.

1.7.6 Fusion Proteins

Apparent low level of protein expression is often caused by the degradation of the foreign proteins. In many studies, an overexpression of a separate protein ended by proteolysis [159]. When these proteins were synthetized as fusion proteins, they are prevented from degradation. Fusion proteins can contain signal sequence (e. g. sequence for translocation) or tag for purification (e. g. His-tag).

1.8 Heterologous Expression of NKA in Yeast

An alternative method of the protein preparation is a heterologous expression in host cells. Prior to the methods of molecular biotechnology (heterologous protein expression and cloning), the purification of functional NKA was extremely difficult, for the expression of the separate subunits results in the loss of enzyme activity. Consequently, the overexpressed β subunit is transported and inserted into plasma membrane without dramatic functional changes [60, 61]. For the α subunit, the overexpression of the protein results in the retention of the subunit in the ER [60, 61, 160].

Moreover, the most commonly used expression systems show high levels of endogenous NKA which is ubiquitously expressed in eukaryotic expression systems (mammalian cell lines and insect cells) [111]. Signal of the endogenic NKA can be overcome by converting the heterologous enzyme to ouabain-resistant form by the substitution of several amino acids. For low concentration of ouabain, the activity of endogenous NKA is negligible. Under these conditions, the ouabain-resistant form of enzyme is responsible for the observed NKA activity.

Up to now, only two expression systems with low or zero endogenous NKA activity were described – yeast expression system (*Saccharomyces cerevisiae* or *Pichia pastoris*) [103, 161], or insect cells infected with baculovirus (sf9 or High Five lines) [11, 162].

1.8.1 Heterologous Expression of Membrane Proteins in Yeast *Saccharomyces cerevisiae*

Many variables influence and complicate the expression of the human $\alpha_3\beta_1$ complex in yeast (*Saccharomyces cerevisiae*), such as yeast strain for cultivation, specific post-translational modifications, detergent for membrane solubilization, and relipidation of the purified protein. Nevertheless, the studies of NKA presented many remarkable

applications. For instance, Weigand *et al.* [11] studied the changes in the ATPase activity caused by selected mutations which can be found in the *ATP1A3* genes of the AHC and RDP patients [126, 135, 128]. These findings were based on the NKA prepared using a baculovirus-insect cell expression system. The determination of the structural consequences linked with gene mutations, and changes in the overall pump activity or changes in the affinity of ion binding requires further study.

The yeast genome (6000 genes) is approximately four times smaller than the human genome (25000 genes), but the yeast cells possess a similar mechanism of protein synthesis, maturation, and secretory pathway trafficking [163]. Moreover, this simple system enables to perform homologous recombination which is end joining DNA repair [164]. On the other hand, human and yeast cells differ in many way, e. g. lipid composition of the membrane or post-translational modifications. Human cells contain relatively high level of cholesterol. In contrast, yeast contain ergosterol and cholesterol is absent. Yeast and human cells contain similar but not identical amounts of sterols and other lipids. This variable composition of the cell membranes may influence the stability of the expressed protein via lipid-protein interactions. The specific lipid-protein interactions play an important role mainly in the protein folding and trafficking to the membrane [165]. The lipid environment and dynamic cellular responses to the protein expression is also significant for emphasizing the aspects of co-translational machinery, and post-translational modifications [165].

The fundamentals of protein expression are: promoters, host strain and plasmids. These fundamentals we will discuss in the following subsections.

1.8.2 Inducible Promoters

Inducible promoters enable to specify the timing and level of protein expression in the host organism. Promoters play a very important role in the membrane protein expression, since the overexpressed proteins can be toxic for the cells. Expression of toxic proteins may result in the employment of the proteolysis machinery in host cell. The most common inducible promoters are P_{CUP1}, P_{GAL1}, P_{MET25} and P_{PHO5}. These promoters including their regulation are listed in Table 1.2.

GAL genes are, due to their effective and precise regulatory mechanism, the most widely used inducible promotors. The *GAL* genes are a set of structural and regulatory genes that encode enzymes required for galactose utilization [169]. The *GAL* genes products are proteins that transport galactose into cells, convert intracellular galactose to glucose-1-phosphate, and demonstrate galactosidase activity [171]. These genes exhibit three carbon source-dependent states:

1. inactive or repressed by glucose
2. nonrepressed, in the presence of glycerol
3. active or induced to high-level expression by galactose

Glycerol is often used as a carbon source for cultivation and the main nutrient for yeast is glucose. At the induction time, the glucose level is very low, because it was

Inducible promoter	gene	regulation	reference
P_{CUP1}	metallothionein	positive regulation – $Cu^{(II)}$	[166, 167]
P_{GAL1}	galactokinase	negative regulation – glucose, positive regulation – galactose	[168]
$P_{GAL1-10}$	galactokinase	negative regulation – glucose, positive regulation – galactose	[169, 170, 171]
P_{MET25}	methionin	negative regulation – methionin and cysteine synthase	[172]
P_{PHO5}	repressible acid phosphatase	negative regulation – inorganic phosphate	[173]

Table 1.2: Selected inducible promoters for heterologous expression in yeast [163].

metabolized during the cultivation. The induction itself is performed using galactose to activate high-level expression. During the cultivation, the galactose (inductor) is being metabolized, therefore its level decreases in time after induction. This obstacle can be bypassed by the cyclic galactose promoters [174]. More information on the inducible promoters can be found in [175].

1.8.3 Host Strains

Yeast host strains have been developed for auxotrophic and antibiotic selection strategies, however, each cell strain has been developed for an unique characteristic (e. g. protease deficient strain [176], or lipid composition of the membrane [177]).

1.8.4 Selection Strategies

Auxotrophic selection strategy is based on plasmids which are paired with available strains that are auxotrophic for selected amino acid or DNA base by carrying full or functional knock-out of these auxotrophic genes. Auxotrophic selection requires continual selection by growth in minimal media lacking relevant nutrient [178]. Examples of auxotrophic selection markers are *TRP1* [179], *HIS3* [180], *LEU2* [181], *URA3* [181], *MET15* [182], and *ADE2* [182].

The selection with antibiotics is independent of auxotrophic strain limitations and can be used for the selection in rich media (complete media). Common antibiotics used for selection are amminoglycoside phosphotransferase (APT) [183, 184], hygromycin B phosphotransferase (HPH) [185, 186], and the zeocin^{TM} resistance (Sh ble) [187, 188] genes. These antibiotics affect the ribosome function, thus expression studies should be performed in rich liquid media lacking antibiotics.

1.8.5 Plasmids

Plasmids can be cathegorized into three groups such as low-copy plasmids, high-copy plasmids, and integrating plasmids. The low-copy plasmids contain yeast centromere, and autonomous replicating sequence that make these plasmids mitotically stable in yeast. The transformed yeast typically contain one or two plasmid copies per cell [189]. The high-copy plasmids contain 2μ sequence [190, 191, 192], which is a natural plasmid from yeast at approximately 100 plasmid copies per haploid genome [193, 194, 195]. Transformed cells contain 20 plasmid copies per cell [188]. Finally, the integrating plasmids can be used if the cells lose the plasmids (low and high-copy), or if the number of plasmids per cell is unstable [188, 194, 196] during the cultivation. Integrating plasmids are based on the yeast chromosomal DNA and they are used for the targeted integration by the homologous recombination [197, 198].

1.8.6 Expression

The protein expression in yeast can be affected by pH, cultivation temperature, cell-induction concentration, induction strategy, and expression duration. Although, examples described in the literature [199, 200] may serve as a guide for successful membrane protein expression, each target protein needs an optimization of these conditions. For example, lowering the growth temperature reduces the cellular growth rate, but may have other advantages, such as promoting protein folding and membrane insertion, reducing rates of proteolysis, and regulatory cold-shock chaperons that do the protein folding [199].

1.8.7 Post-Translational Modifications

The newly synthetized proteins are subsequently modified by several modifications such as glycosylation, formation of disulfide bonds, or methylation. Post-translational modifications vary between organisms and can influence the stability or function of the prepared protein.

The important biological characters such as immunogenicity, solubility, protein and cellular recognition, resistance to proteolysis, protein folding or biological function are determined by the specific carbohydrates presented on the glycoprotein [201, 202]. Glycosylation is a highly specific and complex post-translational modification.

Glycosylation is performed within ER or within Golgi apparatus (GA). More specifically, inner core of the protein is glycosylated in ER and outer part of the protein can be glycosylated in GA and in ER. N-linked glycosylation occurs at sequence Asn-X-Ser and Asn-X-Tyr, where X can be any amino acid excluding Pro [203]. The preliminary stages of glycosylation occur in the ER and include the attachment of two N-acetylglucoseamine molecules, nine mannose sugars, three glucose sugars to Arg at recognition site. This initial complex is partly removed (three glucose molecules and one mannose) during exiting ER. This preliminary complex is similar to higher eukaryotes, but glycosylation differs in later stages [165].

Higher eukaryotes remove mannoses using mannosidases within GA, but other sugars can be added (galactose or sialic acid) [170]. Nevertheless, yeast does not have mannosidases that enable hyperglycosylation or heterologous addition of many mannoses [204, 202]. Modifications in GA significantly affect function of the final protein. This obstacle can be overcome by site-directed mutagenesis of glycosylation sites or by using specific host-strain (*Pichia pastoris, Hansenula* and many other). Unfortunately, introduction of mutations affects cell growth and cultivation [205].

Another important post-translational modification is formation of disulfide bonds. Disulfide bond formation is favored conformation of two cysteine residues linked covalently. These bonds are often necessary for proper protein folding. In general, yeast cells are able to form disulfide bonds, but maintenance of the proper disulfide bonds during the expression needs special attention. Sometimes, it could be useful to change the strain for expression [206, 207, 208].

1.8.8 Lipids

Biological membranes are composed of diverse lipids. Variations in the lipid headgroup and acyl chain form the unique lipid properties. In addition, differences in the lipid composition affect membrane protein translocation efficiency, topology, stability, complex assembly, transport within the secretory pathway, and function [165]. It should be noted that both lipid biosynthesis and membrane protein biogenesis occur within the membrane of the ER, where both lipid and protein components are balanced [209]. The specific lipid composition of the membrane of yeast is continuously changing.

For the proper topology of membrane proteins, anionic glycerophospholipids (e. g. phosphatidylserine (PS), phosphatidylinositol (PI), phosphatidylcholine (PC) and its phosphorylated derivatives, and cardiolipin (CL)) are required. This glycerophospholipids are mainly located on the cytosolic side of the membrane [210, 211, 212]. PS is a minor component of the organelle membrane in *Saccharomyces cerevisiae*. The only exception in *Saccharomyces cerevisiae* is the plasma membrane, where PS is presented in 34% [213]. PS is selectively arranged on the inner leaflet of the ER and plasma membrane because of the phospholipid flipases [214]. In contrast to PS, PC is the most abundant glycerophospholipid in *Saccharomyces cerevisiae* [215] where it is a major structural component of the organelle membranes.

1.8.9 Purification

The purification of the integral membrane proteins (IMP) can be separated into several steps. The first step is usually the removal of IMP from their natural environment. IMPs exhibit hydrophobic manner, therefore the use of the detergents that mimic lipid properties is indispensable, allowing their extraction from the lipid bilayer. The second steps is purification of the solubilized protein and the third step is the protein reconstitution into liposomes (addition of synthetic lipids, relipidation) for functional studies [216]. The typical purification protocol is illustrated in Figure 17.

Mild and gentle procedures are preferred for the maintaining of the native confor-

mation of the protein and its activity. These techniques also should be as effective as possible to maximize the recovery of the protein of interest and to minimize the contaminants [216].

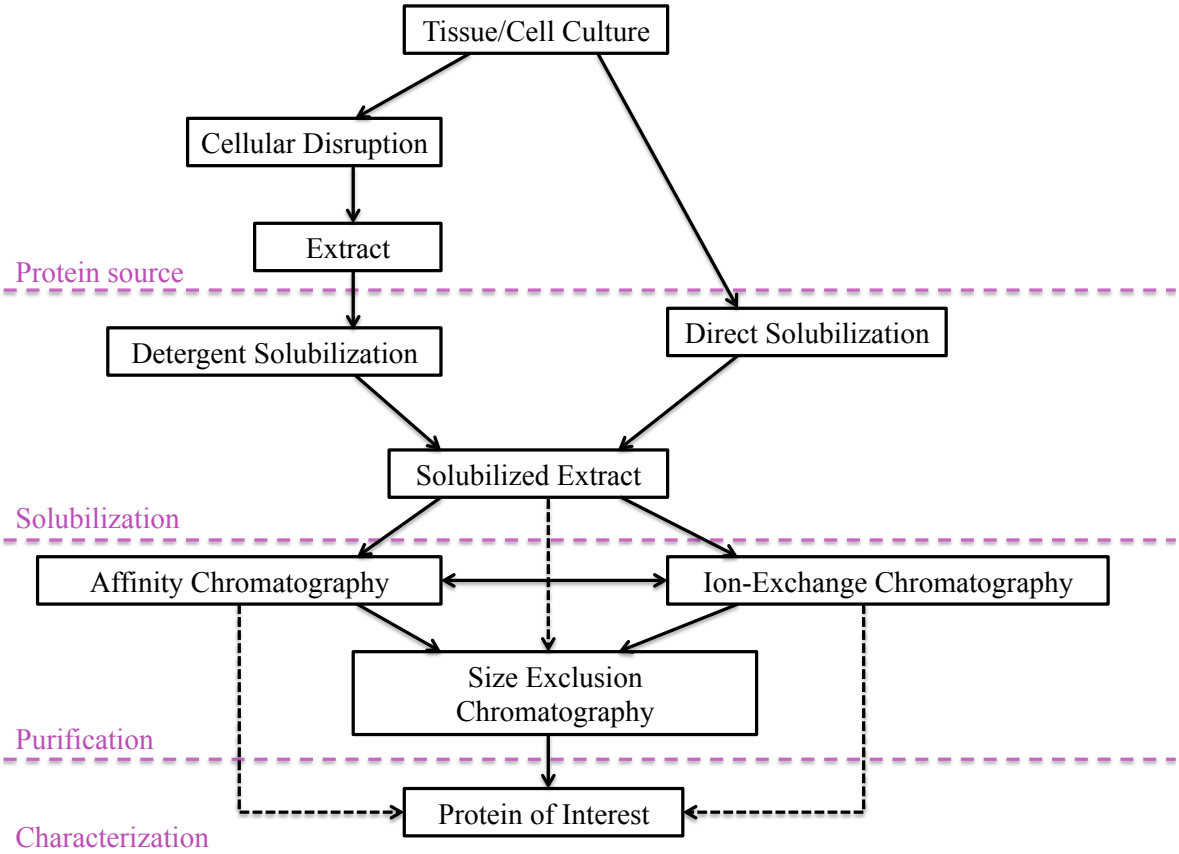

Figure 17: The scheme of the integral membrane protein purification (according to [216]).

An effective solubilization depends on the nature of the protein, lipid composition of the membrane, used detergent, and buffer. During the preparation the protein:lipid:detergent ratio is essential. In general, the purification of IMPs is not significantly different from the purification of soluble proteins, and similar protocols are used. The detergent concentration during the protein preparation should be as low as possible to avoid protein precipitation and aggregation. However, due to the unique physiochemical characteristics of each IMP, the detergent and purification strategy have to be selected individually. In appropriate cases, the analysis of ligand binding can give more direct information about the functional integrity of the solubilized IMP [216].

The most purification steps start with a solubilized IMP extract and involve different chromatographical approaches such as ion-exchange chromatography (IEX), chromatofocusing (CF), isoelectric focusing (IEF), size-exclusion chromatography (SEC), and immobilized metal affinity chromatography (IMAC). In some cases, the IMPs are purified as fusion protein with affinity tag (histidine tag, calmodulin affinity, green fluorescent protein, etc.). The selection of these methods is highly dependent on the protein of interest and further analytical requirements. Thus, each IMP possesses unique physiochemical properties, and requires a specific purification approach.

1.8.10 Solubilization

At the beginning of the IMP purification, the cells undergo mechanical (mechanical homogenizers, French press, ultrasound, etc.) or nonmechanical (repeated freeze and thaw method, osmotic shock, etc.) disruption in the presence of detergents [217].

Protease inhibitors are used extensively to avoid degradation of IMPs. Moreover, the used buffers have to be compatible with the selected detergent [218]. Detergents (or surfactants) are amphiphilic compounds, which means that hydrophilic head-group and hydrophobic tail (hydrocarbon chain) are present within one molecule. Detergents show higher hydrophobicity than lipids making them useful in the solubilization process of IMPs [219, 218, 220, 221]. At low concentrations, the detergents exist as monomers in water, but with increasing concentration, the monomers self-organize into non-covalent aggregates – micelles [221, 222, 223]. The lowest concentration above which the monomers tend to aggregate and form micelles is denoted as the detergent critical micelle concentration (CMC). At CMC, the detergent micelles and monomers are in equilibrium. Increasing concentration results in the micelles formation, but the concentration of the monomers remains without change [221]. The size of the micelle, and the number of detergent molecules forming the micelle vary with the detergent.

According to the their structure, detergents can be separated into three categories – nonionic, ionic, and zwitterionic [224].

Nonionic detergents have uncharged head-groups, either polyoxyethylene or glycosidic groups [216]. They are known as mild and nondenaturing detergents. Their main advantage is that they can solubilize the IMPs in a functional state, due to their ability to break only protein-lipid and lipid-lipid interactions, but not the protein-protein interactions [219]. Examples of nonionic detergents are Triton X-100, digitonin and maltoside such as decyl-β-D-maltopyranoside (DM) and dodecyl-β-D-maltopdyranoside (DDM) [216].

Ionic detergents contain cationic or anionic head-groups. The hydrophilic part of the detergent can be formed by hydrocarbon chain or rigid steroidal structure. Common examples of ionic detergents are sodium dodecyldulfate (SDS) and cetyltrimethylammonium bromide (CTAB) [216].

Finally, zwitterionic detergents contain head-groups bearing anionic and cationic net charges. In general, zwitterionic detergents combine properties of ionic and nonionic detergents. For example 3-[(3-cholamidopropyl)dimethylammonio]-1-propanesulfonate (CHAPS) and fos-choline are representatives of this group [216].

1.9 Membrane Protein Expression in Mammalian Cells

This section briefly summarizes the main steps of membrane protein expression in mammalian cells. Further information can be found in literature [163].

The first approval of a therapeutical protein from mammalian cell line occurred in 1986 [225]. Recently, numerous mammalian cell lines have been used in the membrane protein expression such as Chinese hamster ovary (CHO), human embryonic kidney (HEK), green monkey kidney (COS-1), and baby hamster kidney (BHK). Mammalian systems are widely used in the industry for the production of recombinant high-order eukaryotic membrane proteins [225]. Mammalian cells are often used for correct protein folding and post-translational modifications [226, 227, 228]. Membrane proteins are broad group of molecules including adhesion molecules, transduction factors, and transport proteins (channels and pumps). These molecules require specific post-translational modifications such as glycosylation, phosphorylation, methylation, disulfide bond formation, proteolytic processing, and lipid addition for their functionality [229, 230].

Yeast cells and bacteria cells were used for expression of membrane proteins, however, these proteins were poorly glycosylated or misfolded in yeast [227, 231]; and in bacteria were often accumulated as insoluble aggregates (inclusion bodies) [227, 232]. The main difference between mammalian cells, insect cells, yeast, and bacteria cells is their lipid composition of the membranes [227]. For example, the overexpression of membrane proteins requires proper protein folding that necessitates the presence of cholesterol, which is abundant in mammalian expression systems [233]. Moreover, mammalian cells exhibit just few disadvantages such as low yield of recombinant protein and high cost.

Basically, membrane proteins are difficult to study due to their low expression level in the cell. However, many membrane proteins have an effect on the progression of diseases [234, 235, 236], which makes them an aim of great pharmaceutical importance.

Many expression systems have been developed in recent years in an attempt for the study of these delicate proteins. Studies that utilize a mammalian expression systems may be highly useful for membrane proteins production due to the processing environment of these cells and advantageous nature of protein folding [233].

1.9.1 Culture Types and Media

Depending on the cell type, the cell can be grown in adherent or suspension culture using batch, fed-batch, or perfusion cultures [233].

The cell membrane of adherent cell types contains cell adhesion molecules such as integrins, cadherins, and selectins that bind cells to the surface. Some agents (e. g. trypsin) are necessary of release the culture from the surface of cultivation plate or flask. Furthermore, the composition of the growing media affects the adhesion of the culture, which can be important for functionality of the studied protein. This type of culture grows as continuous layer until becoming confluent. The confluent culture needs to be subcultured to adjust vitality of the culture [233].

For the cell suspension, the confluence depends on the volume of media rather than on the surface area of the container for suspension culture. The cell yield of suspension cultures is higher than for adhesion cell types, which makes them advantageous in high-level production. Subcultivation into fresh media is performed when nutrients are spent and toxic substrates or metabolites start to accumulate [233].

Both, batch and fed-batch cultivation involve growing the cells up in a single suspension or adherent culture process. Maximum density of the cells is reached just before exhausting the nutrients (amino acids in the media, serum, etc.). The culture is often harvested at this time [233].

Perfusion process is a continuous cultivation that requires the continuous addition and removal of several volumes of media per day. Cells can be removed with spent media or hold in the bioreactor in order to reach the highest possible cell densities [233].

It should be noted that different cell growth strategies require unique media composition.

1.9.2 Transfection

To express the protein, the DNA should be cloned into a suitable vector that has a promoter and polyadenylation signal (polyA signal sequence). The mammalian expression vectors also include stable markers such as neomycin, puromycin, and hygromycin. The transfected cells can be stably identified by the selection of cells that are resistant to these antibiotics, nonetheless, an improved techniques have been published recently [237].

1.10 Determination of the Na^+/K^+-ATPase Activity

Two basic methods are available for the determination of NKA activity: Enzyme-coupled assay and Baginsky assay. In principle, both methods detect inorganic phosphate, but they use different approach. Following sections introduce these methods.

1.10.1 Baginsky assay

The ATPase activity can be determined by a direct colourimetric detection of inorganic phosphate, called Baginsky assay [238, 239]. The principle of the Baginsky assay is a monitoring the interaction of ammonium molybdate with a product of ATP hydrolysis (inorganic phosphate), which leads to a colour change measured at 710 nm. The main advantages of this method are its effectivity, low time consumption and the ability to automate the process using an automatic pipetting workstation.

This assay enables the determination of inorganic phosphate in the presence of organic compounds containing labile phosphate. The liberation of phosphate from these compounds during the analysis can lead to errors. This interference is commonly encountered in enzymatic procedures where phosphate released from a substrate is used for the detection of enzyme activity. Any non-enzymatic hydrolysis of the substrate would contribute to the overall phosphate concentration and erroneously increase the

enzyme activity. However, the substrate hydrolysis is continuous, and makes the precise activity determination very difficult [238].

The Baginsky assay is a simple and sensitive procedure for phosphate determination that eliminates error caused by a nonenzymatic phosphate hydrolysis. A unique feature of the method concerns the fact that the reagents form the stable coloured complex with the inorganic phosphate present, but any additional phosphate cannot react with reagents involved in complex formation.

1.10.2 Enzyme-Coupled Method

This method is an alternative to Baginsky assay [238] enabling the determination of the NKA activity. The coupled ATPase assay is used for the determination of mitochondrial Ca^{2+} and Na^+/K^+-ATPase. This method was described by Norby [240], and is based on the following linked reactions:

$$\mathrm{ATP} \xrightarrow{\mathrm{Na^+/K^+ - ATPase}} \mathrm{P_i + ADP} \quad (1)$$

$$\mathrm{P_i + phosphoenolpyruvate} \xrightarrow{\text{pyruvate kinase}} \mathrm{ATP + pyruvate} \quad (2)$$

$$\mathrm{pyruvate + NADH} \xrightarrow{\text{lactate dehydrogenase}} \mathrm{lactate + NAD^+} \quad (3)$$

The addition of NKA starts the reaction. All reactions have reaction equilibrium shifted toward products (proceed to the right side of the reaction). The first step of detection (1) requires NKA cofactor Mg^{2+}, and transported ions (Na^+, and K^+). The rate of the last reaction (3) is determined as a change in absorbance, which is monitored at 340 nm (NADH). The detection proceeds in the steady-state which is established approximately 30 s after initiation of the assay. The steady-state absorbance measures the uninhibited rate of reaction (1) since the steady-state concentration of ADP is always significantly lower than the inhibitory concentrations, and the auxiliary enzymes and their reactants exhibit no influence on the reaction catalyzed by NKA [240]. The steady-state absorbance is proportional to the NKA concentration and rate constant during the assay to the exhaustion of NADH ($+H^+$).

1.11 Small Molecules Influencing NKA Activity

1.11.1 Cardiotonic Steroids and Their Analogues

Cardiotonic glycosides (also known as cardiotonic steroids, CTS, see Figure 18) and ouabain (specific inhibitor of NKA) undergo extensive research for decades due to their

remarkable biological effects (congestive heart failure treatment, arrhythmia treatment, anticancer drugs, diuretics, emetics, and abortificants) [16]. These compounds are often isolated from natural sources (plants and animals), but many of CTS display high toxicity (IC_{50} in range of nanomoles) which also limits their use in the drug development. Plants containing CTS were used for medicinal purposes more than 1500 years ago. For example, the name "ouabain" is derived from Somali word "waabaayo" which means "arrow poison". Englishman William Withering used extract from foxglove (*Digitalis purpurea L.*) and oleander (*Nerium oleander L.*) for treatment of congestive heart failure 250 years ago. This extract contained CTS such as digitalis, digoxin and oleandrin [16].

Nowadays, CTS are used in the prevention and/or treatment of proliferative diseases such as cancer. CTS inhibit cell proliferation and exhibit favorable cytotoxic activity against several cell lines. Their action is mostly based on the induction of apoptosis [241, 242, 243, 244, 245, 246, 247, 248]. More specifically, the inhibition of NKA by CTS leads to the accumulation of sodium and calcium ions in the cells and this reduce the membrane potential and intracellular potassium concentration [249]. Although, CTS are known as antiarrythmic agents, they also increase the level of reactive oxygen species [4] which contributes to mentioned effect through the redox modification of cardiac ryanodine receptors [250, 251].

In hearth, the mechanism of CTS action arises from the inhibition of NKA. Interaction between CTS and NKA results in the NKA inhibition, which leads to increasing sodium concentration in the intracellular space [252]. This elevated sodium level affects the plasma membrane Na^+/Ca^{2+}-exchanger, leading to a significant increase in the intracellular calcium concentration, and heart contraction [253, 254, 255]. This positive ionotropic effect of CTS enables their use as a major therapeutic agent in the management of congestive heart failure [253, 254, 255, 256]. But for this to occur, sufficient number of NKA must be inhibited to significantly increase intracellular sodium concentration, even if this occurs in a limited space in the cytoplasm [6]. Additionally, current research have revealed anticancer properties of CTS. However, their role in the anticancer treatment is still not well established.

It is no surprise that binding site for ouabain is a highly conserved sequence across evolutionary spectrum excluding parasites of *Acokanthera schimperi* and *Strophantus gratus* – plants from which the inhibitor is extracted. The highly conserved binding site for ouabain suggests existence of natural ouabain-like compound which has role of NKA regulator [6].

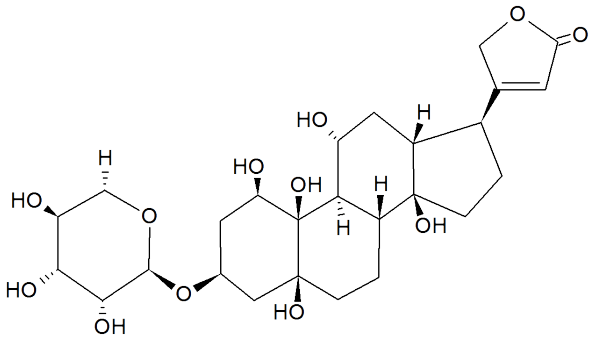

Figure 18: Structure of typical member of cardiotonic steroids family – ouabain.

Binding site for CTS is highly conserved region within animals [257, 258, 259, 260, 261, 262], insects [263] and human [65, 264], but some exceptions exist. For example monarch butterflies [263] and leaf beetles [263] developed a resistance to ouabain since they consume the plant materials containing CTS. The detailed study of their NKA revealed two binding sites for CTS within α subunit [6]. Additionally, the genome sequencing of the mouse and rat α isoforms revealed the replacement of Asn122 by histidine. This replacement is responsible for the relative insensitivity of murine and rat NKA to ouabain. Another site responsible for ouabain resistance can be found at position 111 [257, 259]. Those residues encoding resistance to ouabain enabled expression of NKA in mammalian cells where the natural NKA is also present and can be suppressed by ouabain selection.

The potential involvement of CTS compounds in the cancer treatment was discussed 40 years ago [265, 266]. This research was abandoned due to high toxicity of the compounds. In the 1970s, only murine cell lines were available for testing the potential drugs, and those cell lines were less sensitive to CTS action. Some CTS inhibit cell proliferation of human and monkey cell lines [243, 267, 268, 269, 270] at non-toxic nanomolar concentrations, where they are [271, 272, 273, 274]. Nowadays, CTS should be considered for skin cancer treatment, or they should be investigated for possible adjuvant therapy for malignant diseases [16].

1.11.2 Flavonolignans

Recent drug design has greatly benefited from the functional compounds isolated from plants often used by the traditional medicine. Moreover, these compounds serve as precursors or inspiration for the synthesis of the new active derivatives that can be even more effective in the biochemical interactions.

The scope of our research was included the series of phenolic compounds, called flavonoids, which had been known since ancient times (approximately 4^{th}. century B. C.). In general, flavonoids are a broad class of a secondary metabolites contained in plants, and they are responsible for yellow, red or blue pigmentation of the flowers [275]. Major dietary sources of flavonolignans are tea, red wine, apple, tomato, onion, thyme, parsley, soy beans, legumes, grapefruit, lemon and several vegetables, fruits, and trees such as Ginkgo or neem [276].

Flavonoids can be isolated from *Silybum marianum* as a mixture called silymarin. This extract is currently included in many commercial products. Silymarin is a standardized active extract from plant seeds containing approximately 70 – 80% of the silymarin flavonolignans, and 20 – 30% of a chemically undefined fraction comprising mostly polymeric and oxidized polyphenolic compounds (called phenolic fraction – PP) [277]. By now, 23 flavonolignans have been identified in *Silybum marianum* [278].

The main component of silymarin is silybin (also called silibinin or silybinin, see Figure 19). Silybin is a mixture of two distinct diastereomers, denoted as silybin A and silybin B. Despite the 1:1 proportion of those diastereomers, the isomers were finally separated in 2003 [280]. Other flavonolignans present in silymarin are isosilybin, dehydrosilybin, silychristin, silydianin, and few flavonoids such as taxifolin (see Figure

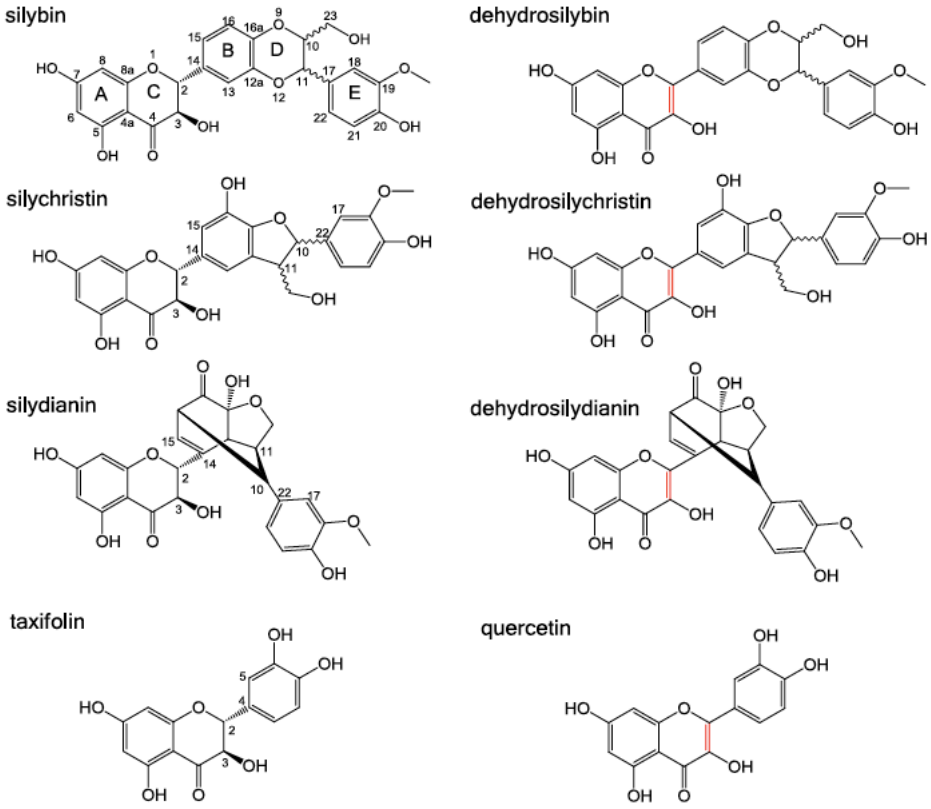

Figure 19: Structures of silybin (SB), silychristin (SCH), silydianin (SD), and their dehydroderivatives (DHSB, DHSCH, DHSD), taxifolin (TAX), and quercetin (QUE). The 2,3-double bond in dehydroderivatives is highlighted in red [279]. The figure courtesy of Michal Biler.

19) [281]. Only silybin (A and B), isosilybin (A and B), silychristin and silydianin are the most important constituents of seed extracts.

White-flowering variant of *Silybum marianum* contain also 3-dehydro-flavonolignans such as silandrin, silymonin, silyhermin, neosilyhermin A and B [282]. The often neglected PP of the silymarin exhibits several effects different from monomeric flavonolignans such as cholesterol sequestrant [283].

Unfortunately, the positive effects of flavonolignans suffers from some controversy. The main controversy of effects is the variability of the silymarin composition caused by the different methods of extract preparation used in published studies. It has been documented previously that the properties of respective compounds in various silymarines depend on the source of seeds (cultivar and planting conditions), processing conditions, and extraction method [277].

Natural flavonoids are antioxidative [284, 285], free-radical scavenging [286], hepato-protective [287], and cytotoxic agents [288]. The main disadvantage of flavonolignans is their limited bioavailibility [289] due to low water-solubility of these compounds. Several approaches were applied to improve the biovailibility of the flavonoids such as the preparation of silybin bis-hemisuccinate [290], the preparation of phosphatidylcholine complex of silybin [290], or the addition of a sugar moiety to silybin scaffold [290].

More information on effects and applications of the flavonolignans can be found in the literature [291, 292].

1.11.3 Halogenated Quinolinones

The synthetic analogues of natural flavonoids based on the 3-hydroxyquinolinone scaffold called quinolinones represent other biologically relevant compounds. They are isosteric to flavoniods – they contain three-member-ring skeleton. The group of pyrrolo-[3, 4-h]quinolin-2-ones was synthetized from furocumarines, and was applied in the skin disease treatment. They compounds can act as photo-induced cell killers after irradiation by long-wave UV light [293]. Quinolinones exhibit the cytostatic and antileukemic activity [294]. Moreover, 2-heptyl-3-hydroxyquinolin-4-one is a bacterial signal molecule that can act as strong antiprotozoal agent due to its role in the cell-to-cell communication system [295, 296]. Copper(II) quinolinonato-7-carboxamido complexes were prepared as analogues to platinum complexes [297]. Finally, the novel structural analogues of quinolinones are being currently prepared to obtain higher activity, low toxicity, and more specific selectivity.

The low solubility of quinolinones limits their bioavailability. Respecting their limited water solubility, current research is focused on the improvement of the bioavailability of selected compounds [298, 299]. Moreover, the delivery system based on the silica nanoparticals was established recently [300].

Except the biological importance, the spectroscopic properties of 3-hydroxyquinolin-4(*1H*)-one were also studied [301].They exhibit dual emission spectra and promising fluorescence quantum yield. Due to this, they can be used as fluorescence labels [296].

The therapeutic properties of quinolones can might be further altered by the chemical modification of the quinolone scaffold, e. g. chloro- and dichloro- derivatives of 3-hydroxy-2-phenylquinolin-4(1*H*)-ones, but biological activity of halogenated quinolinones is unknown.

Acronym	R_1	R_2	R_3	R_4
TFHPQ	F	F	F	F
DFHPQ	H	F	F	H
8CHPQ	H	H	H	Cl
6CHPQ	H	Cl	H	H
DCHPQ	Cl	Cl	H	H

Monochloro- and dichloro-3-phenyl-3-hydroxyqiunolin-4(*1H*)-ones were evaluated as potential anticancer drugs in the National Cancer Institute Bethesda [294]. All tested compounds were subjected to three distinct cell lines, but only three compounds passed NCI's criteria, and were evaluated against the 60 tumor cell lines. Furthermore, 5,6-dichloro-, 5,7-dichloro-, and 7,8-dichloro-3-phenyl-3-hydroxyqiunolin-4(*1H*)-ones inhibited the growth of the cell lines derived from colon and breast cancer [294, 301]. Structures and positions of halogen atoms within the 3-hydroxy-2-phenylquinolin-4(*1H*)-one derivatives are summed in Figure 20.

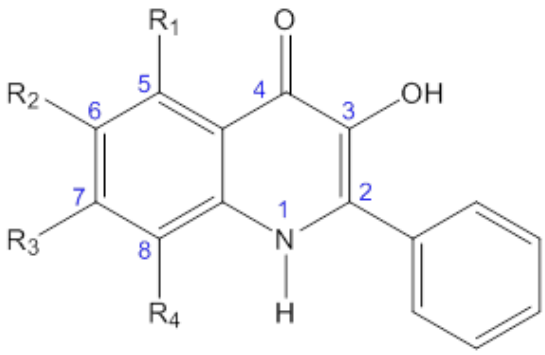

Figure 20: Structure and acronyms of 3-hydroxy-2-phenylquinolin-4(*1H*)-one derivatives [302].

1.11.4 Platinum-Based Drugs

Cisplatin (*Cis*-diamminedichloroplatinum(II), see Figure 21) was approved for the treatment of the both ovarian [17] and testicular cancer [18] in 1978 [303], and it was also administrated for many other types of cancer, e. g. bladder, head and neck, oeasopheral, small cell lung cancer [17] and lymphomas [24]. The first characterization and synthesis of cisplatin was performed by Peyrone in 1845 [304].

Nowadays, the cisplatin treats testicular cancer with cure rate more than 90% efficiency [305]. But some tumors such as colorectal, and non small cell lung cancers [306] exhibit an intrinsic resistance for cisplatin treatment. Furthermore, ovarian and small cell lung cancers were found to acquire the resistance during the early stages of the cisplatin treatment [307].

Oxaliplatin (1,2-diamminocyclohexaneplatinum(II) oxalate, see Figure 21), the only one registered platinum-based agent demonstrating activity against cisplatin-resistant tumors [308]. Another platinum-based drug – carboplatin (*Cis*-diammine(1,1-cyclobutanedicarboxylato)platinum(II), see Figure 21) shows similar action in the cancer treatment as cisplatin with lower toxicity [28, 303].

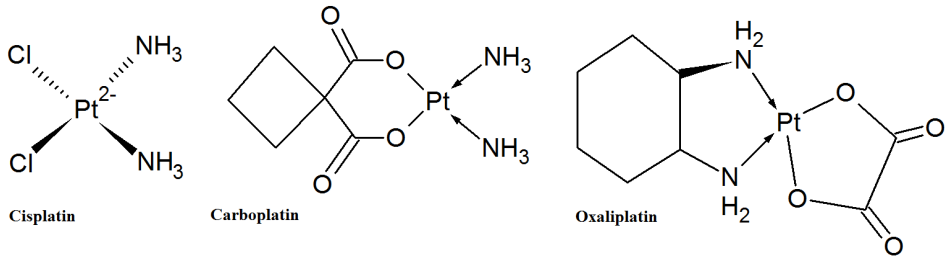

Figure 21: The most widely used platinum-based anticancer drugs – cisplatin, carboplatin, and oxaliplatin.

Selective toxicity to tumor cells is a complex machinery involving the drug uptake, transport to the cell nucleus, formation of adducts with target DNA, and recognition by damage-response proteins [27]. The formation of these adducts and cross-links with target DNA in the cell nucleus inhibits the DNA replication, thus, interfering with

the cell division by mitosis. Subsequently, the signal transduction pathway is transactivated and other nuclear proteins contribute to cell-cycle arrest, attempt to repair damaged DNA, apoptosis and necrosis [28].

Cisplatin enters the cell largely by passive diffusion, but it also utilizes active transport to penetrate through cellular membranes [309, 310]. In general, charged compounds are unable to diffuse through the membranes. For this purpose cisplatin is activated in the cells by aquation involving the exchange of the two chloride moieties with water or hydroxyl ligands, and without change of *Cis* conformation of platinum [26, 25]. Aqua derivatives are readily preserved in the cell cytoplasm, where they bind to intracellular targets (DNA) [28]. The stability of cisplatin in the neutral state is adjusted by high chloride concentration which enables cisplatin to enter the cell and traps cisplatin inside the cell [311]. Moreover, the cisplatin is trapped in the intracellular fluid due to difference in the chloride concentration between extracellular (~ 100 mM) and intracellular fluid (~ 4 – 12 mM) [312].

The loss of chloride ions leads to formation of cationic mono- and diaqua complexes [313, 27, 28] that can loose a proton forming hydroxo- species [314]. These hydroxo-species are able to form hydroxo-bridged platinum(II) multimers [311, 315]. Under physiological conditions, cisplatin forms carbonate [315] and bicarbonate complexes [316]. Finally, aqua diaminoplatinum(II) complex was proved as the most reactive species and hydroxo-bridged species as the least reactive [28]. However, the use of cisplatin is also limited by its low water solubility. Despite those findings, cisplatin is mainly administrated intravenously [317].

As mentioned previously, cisplatin is transported into cells by active transporters [318]. More specifically, copper transporters (P-type ATPases, ATP7B) and organic cation transporters (SLC transporters and ABC transporters) are involved in this transport. Active transport depends on the nature of nonleaving group coordinated to platinum, which play a major role in the uptake effectivity [28]. For example, the organic cation transporters help oxaliplatin in cells and increase its cytotoxicity. In contrast, cisplatin and carboplatin is not accumulated under those conditions and their effect is negliable. Active transporters could possibly explain the activity of oxaliplatin against the colorectal cancer [319]. However, a certain degree of actively transported cisplatin seems to be modulated by other pharmacological agents such as ouabain and the membrane-interactive agents amphotericin and digitonin [318].

After the cisplatin activation, the cisplatin can covalently bind to DNA. As a result, the DNA double helix is slightly unwound and bent [320, 321, 322]. More specifically, the monoaqua cisplatine complex readily forms monofunctional adducts with the N^7 atom of purine bases [27, 323]. Eventually, bifunctional adducts can be formed [324], but adducts were found between two guanines on the opposite strands at d(GpC).d(GpC) sites [325, 326]. Intrastrand adducts are rather rare due to steric inaccessibility [21]. Moreover, cisplatin-carbonato complexes have been reported to form monofunctional [327, 328] and difunctional [328] adducts with target DNA. The study of DNA of cisplatin-treated patients confirmed the presence of approximately 65% 1,2d(GpG), 25% 1,2d(ApG), and 5 – 10% 1,3d(GpNpG) adducts [329, 330, 331, 332, 333]. Oxaliplatin and carboplatin exhibit different DNA-binding kinetics and form disparate adduct profiles [334, 335].

Cisplatin causes many dose-limiting side effects (e. g. severe nausea, myelosupression, neurotoxicity, nephrotoxicity, emetogenesis or ototoxicity [17, 18, 22, 25, 336, 337]). Cisplatin also bind to many blood and cytoplasmic proteins [29, 30, 31, 338]. Moreover, the crystal structure of NKA with bound cisplatin was published in 2012 [339].

Chapter 2

Material and Methods

2.1 Isolation of NKA from Porcine Kidney

2.1.1 Materials

The purification was performed according to [149, 150, 151] with some modifications. All solutions were prepared using ultrapure water and analytical grade reagents. The pH adjustments were carried out using HCl. All solutions, instruments and equipment were cooled down in advance. The isolation was performed in the cold room temperated to 4°C. All used material is listed below:

1. 25 fresh porcine kidneys obtained at a slaughterhouse. Kidneys were immediately cooled and kept on ice.
2. Potter-type homogenizer with teflon pestle and glass pestle.
3. Mixer or kitchen blender with glass container.
4. Scalpels and Rongeur tongs for outer medulla dissection.
5. Buffer I (1 l): 30 mM L-histidine, 250 mM succrose; pH 7.3
6. Buffer II (5 l): 25 mM imidazole, 250 mM succrose, 1 mM EDTA; pH 7.4
7. Buffer III (2 l): 20 mM L-histidine, 250 mM succrose, 0.9 mM EDTA; pH 7.0
8. Ice cubes prepared using buffer II.

2.1.2 Methods

Each kidney was cut longitudinally into slices 0.5 – 1.0 cm thick. The outer medulla (see Figure 22) was dissected by a scalpel and Rongeur tong. The dissected tissue was immedately placed into beaker with ice-cold buffer I in ratio 1:1 (tissue:buffer I).

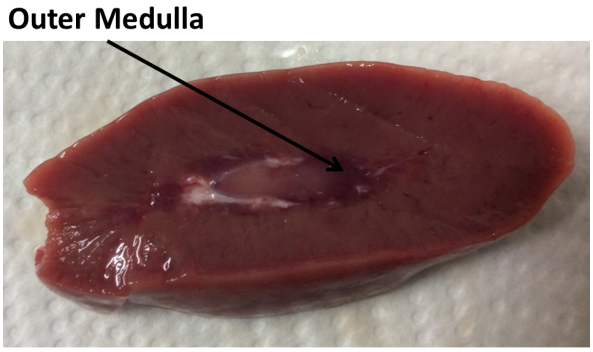

Figure 22: Kidney outer medulla in the longitudinal cut.

The outer medulla tissue (300 g) was mixed with buffer II (300 ml liquid buffer and two ice-packs filled with the same buffer) reaching the final ratio 1:3 (tissue:buffer II). The mixture was roughly homogenized by the kitchen blender. The buffer ice cubes prevent the solution from foaming and protein degradation. The rough homogenate was further gently homogenized by a Potter-type homogenizer (three times up and down). Approximately 1 l of the homogenate was diluted with buffer II up to 3 l. The diluted homogenate was subjected to series of centrifugations. The first centrifugation was at 3700 g for 20 minutes at 4°C. The centrifugation yields supernatant (S1) and pellet (P1). Supernatant S1 is kept on ice while the pellets are resuspended in 1 l of buffer II and homogenization is repeated as described above. The second homogenate was diluted by 1 l of buffer II as before and subjected to a repeated centrifugation (3700 g, 20 minutes, 4°C) yielding supernatant (S2) and pellet (P2). The supernatant S2 was kept on ice and pellets were discarded. Both supernatants (S1 and S2) were combined and subjected to the second centrifugation (7400 g, 20 minutes, 4°C). The supernatant (S3) was kept on ice, and pellet (P3) was discarded. For microsomal fraction collection was used ultracentrifugation (38000 g, 40 minutes, 4°C) where the pellet was saved and supernatant was discarded. Finally, the pellet was resuspended in 200 ml of buffer II and homogenized by glass homogenizer. The microsomal fraction was diluted to the concentration of 5 mg·ml^{-1} and stored at −80°C. The deeply frozen microsomal fraction can be stored for several months.

On the next day the set SDS solution using 1% SDS stock solution in buffer II was prepared. Table 2.1 shows the dilutions used for SDS titration.

One aliquot of the microsomal fraction was thawed on ice and the protein concentration was determined using the Bradford method with BSA as a standard. The concentration was adjusted to 4.6 mg/ml by buffer II. Subsequently, we prepared 14 samples by mixing 80 µl of microsomes with 20 µl of SDS solution in buffer II (according to Table 2.1). All samples were incubated 1 hour at 20°C or 4°C. After the incubation, the Baginsky assay determined the ATPase activity. The dependance of ATPase activity on the SDS concentration should be in good agreement with the typical bell-shape curve [149]. The maximum of the bell-shape curve equals to the optimal concentration for the activation of the microsomal fraction at the next step. The SDS concentration should be ranging from 0.08 to 0.1 %.

The large scale preparation was performed using optimal SDS concentration revealed in the previous step. The thawed aliquot of the microsomal fraction was treated

Sample No.	SDS%	Volume of 1%SDS Stock (μl)	Buffer II (μl)
1	0.00	0	1000
2	0.10	100	900
3	0.20	200	800
4	0.30	300	700
5	0.35	350	650
6	0.40	400	600
7	0.45	450	550
8	0.50	500	500
9	0.55	550	450
10	0.60	600	400
11	0.65	650	350
12	0.70	700	300
13	0.75	750	250
14	0.80	800	200

Table 2.1: Table of SDS solution for microsomes titration (according to [149]).

by SDS and incubated at 20°C overnight under continuous stirring. The next day, the suspension was ultra centrifuged (127000 g, 50 minutes, 4°C), supernatant was discarded and pellet was resuspended in 400 ml of buffer III using glass homogenizer. The pellet was resuspended and centrifuged four times. After the last cycle of centrifugation, the resuspended pellet was aliquoted into small portions which were used for the protein concentration determination, and for the determination of ATPase activity. The protein was diluted using buffer III to the final concentration 1 mg·ml^{-1} and stored at −20°C.

2.2 Expression of NKA in BJ 5457 Strain

2.2.1 Strains and Media

P. A. Pedersen, University of Copenhagen, Denmark kindly provided *Saccharomyces cerevisiae* strain BJ 5457 [161, 340]. This yeast strain was employed as a host organism for the expression of the α_3 β_1 human NKA. The transformed cells were selected on the synthetic minimal medium containing 0.5% glucose and supplemented with leucine (30 mg·l^{-1}) and lysine (20 mg·l^{-1}).

The *Escherichia coli* cells XL1 ([341]) were used as a host organism for the construction of recombinant DNA vector. *E. coli* cells were grown in the Luria-Bertani medium [342] with the appropriate antibiotics.

2.2.2 Transformation of *Saccharomyces cerevisiae* and *Escherichia coli*

This project was solved under the supervision of professor Poul Nissen, Aarhus University, Denmark (yeast expression, HPLC purification) and Per Amstrup Pedersen, University of Copenhagen, Denmark (expression vector construction, detergent screening and optimization of protein expression).

Yeast cells were transformed by homologous recombination according to [343, 344]. 50 ml of yeast culture was cultivated in the rich media to OD_{600} equaling approximately 0.9. Then the culture was harvested by centrifugation (3000 g, 3 minutes), washed with ice cold sterile water, and repeatedly washed in buffer A (10 mM Tris-HCl, 100 mM lithium acetate, 1 mM EDTA; pH 7.5). The cells were resuspended in 250 µl of buffer A and added 30 µl of denatured single stranded salmon sperm DNA (10 µg/µl, Invitrogene). Cell solution was pipetted into sterile eppendorf tubes and mixed with vector DNA. Into mixture was added buffer B (40% PEG4000, 10 mM Tris-HCl, 100 mM lithium acetate, 1 mM EDTA; pH 7.5). The cells were subjected to the heat-shock (42°C, 15 minutes), and consequently incubated at 30°C for 30 minutes. Finally, the cells were harvested by the centrifugation (3000 g, 3 minutes), resuspended in sterile water and plated onto plates with minimal medium. The plates were incubated at 30°C for 72 hours at least.

E. coli strains were transformed by the heat-shock according to [345]. The *E. coli* stock solution was gently thawed and mixed with at least 100 ng of vector DNA. The cells were kept on ice for 30 minutes and consequently subjected to the heat-shock (42°C, 45 seconds). After the heat-shock, the cells were kept for 3 minutes on ice. Cold cells were mixed with standard LB medium and incubated at 37°C for 1 hour. Finally, the cells were placed onto plates with selection antibiotics. The plates were incubated at 37°C for approximately 17 hours.

2.2.3 Plasmid Construction for Expression in Yeast

P. A. Pedersen, University of Copenhagen, Denmark kindly provided the *S. cerevisiae-E. coli* shuffle vector pEMBLyex4 (2259) [161, 340]. The pUC57 vector containing gene for α_3 (PUC57-α_3) or β_1 (pUC57-β_1) were synthetized by GenScript. The *S. cerevisiae-E. coli* shuffle vector was digested by BamHI, HindIII and PstI endonucleases (all from Thermo Fisher) for gene insertion. All selected genes were amplified by PCR using synthetized pUC57-α_3 or pUC57-$beta_1$ vector as a template and with primers 1. – 4. listed in Table 2.2.

The α_3 gene was mutated by the site-directed mutagenesis to produce mutant proteins Asp811Asn, Glu825Lys, Asp933Asn, Asp933Tyr, and Gly957Arg. The PCR products were inserted into vector by homologous recombination. DNA from yeast was purified by the lyticase method, and *E.coli* XL1 cells were transformed to select the constructs. The pEMBLyex4 vector containing the α_3 wild-type (WT) or mutant gene was purified from *E.coli* by GeneJET Plasmid Miniprep Kit (Thermo), and digested by endonuclease NruI (Thermo). The shuffle vector with the inserted β_1 was used as a template for PCR with primers 5. and 6. Table 2.2. The PCR product with

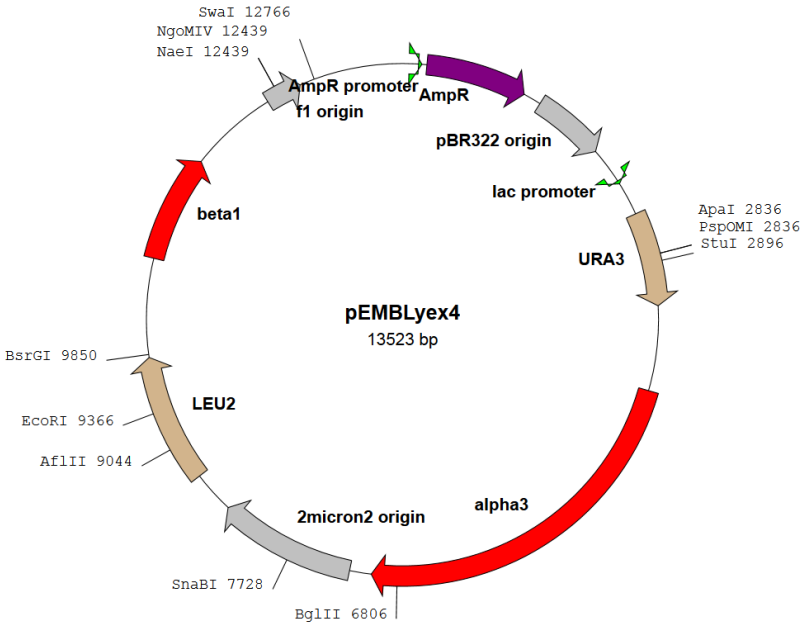

Figure 23: Cloning vector based on pEMBLyex4 vector. This vector contains genes for ampicilin resistance, multicloning site, and two selection markers (*LEU2* and *URA3*). The genes for α and β subunits are placed under the control of the same promoter region (*GAL10*). The complete cloning vector is approximately 13.5 kbp long.

No.	Name	Sequence 5'→3'
1.	H α_3 FwD	ACACAAATACACACACTAAATTACCGGATCAA TTCTAAGATAATTATGGGTGACAAGAAAGACG AT
2.	H α_3 ReD	ACACAAATACACACACTAAATTACCGGATCAA TTCTAAGATAATTATGGGGGACAAGAAAGATG A
3.	H β_1 FwD	ACACAAATACACACACTAAATTACCGGATCAA TTCTAAGATAATTATGCACCATCACCATCACC ATCACCATCACCATGCAAGAGGTAAGGCAAAG GAA
4.	H β_1 ReD	CTTCAATGCTATCATTTCCTTTGATATTGGAA TCATTCATGATTTGACTTCGATCTTAA
5.	H $\alpha_3\beta_1$ FwD	CTAGTCTCTTTCTCGGTCTAGCTAGTTTTACT ACACGCTTCGCTGATTAATTACC
6.	H $\alpha_3\beta_1$ ReD	GCTCAGCAAAGGCAGTGTGATCTAAGATTCTA TCTGATGAAAGGTAGTCTAGTACC

Table 2.2: Primers used for the insertion of α_3 and β_1 subunits into the cloning vector, and for the insertion of α_3 subunit into vector containing β_1.

the β_1 gene was incorporated into the digested pEMBLyex4 vector containing α_3 gene by the homologous recombination. The sequences of final constructs were verified by DNA sequencing. The vector map of the final construct is illustrated in Figure 23.

2.2.4 Site-Directed Mutagenesis

Specific mutations (Asp811Asn, Glu825Lys, Asp933Tyr and Gly957Arg) in the α_3 gene were performed using QuikChange Lightning Site-Directed Mutagenesis Kit (Agilent Technologies). All mutated residues were verified by DNA sequencing (GATC Biotech AG, Germany).

2.2.5 Heterologous Expression in Yeast

The proteins were expressed using galactose-regulated promoters. The yeast cells were grown in shake flasks in synthetic minimal medium containing 0.5% glucose, 3% glycerol as a carbon source, and supplemented with all amino acids except lysine, isoleucine, leucine, glutamine, asparagine, glycine. A single colony of transformed yeast was selectively propagated into 5 ml of synthetic minimal media supplemented with leucine until saturation (according to [161]). An aliquot of 100 µl of the culture was transferred into 5 ml of synthetic minimal media supplemented with lysine but without leucine. The culture was grown until saturation. Then, 500 µl of the culture was transferred into 50 ml of the same media. For the large scale protein preparation 2.0 liters of minimal media with lysine was inoculated. All selected cultures were grown at 30°C until they reached optical density OD_{450} 1.0 and then induced with 2% galactose. The cultures were separated into aliquot containing 1.5 liter, and the other aliquot with 0.5 liter of culture and they were incubated at 15°C and 30°C, respectively. The cultures were harvested by centrifugation after 48 h cultivation. During the cultivation period, 50 ml of the culture were harvested for monitoring of the protein expression.

2.2.6 Isolation of the Yeast Membranes

The isolation of yeast membranes was performed according to Pedersen *et al.* [161]. Galactose-induced yeast cells were harvested at 5800 g for 5 minutes, and washed with ice-cold water. The yeast cells were resuspended in an ice-cold lysis buffer composed of 25 mM imidazole, 1 mM EDTA, 1 mM EGTA, 10% sucrose (w/v), 1 mM PMSF, 1 µg/mg chymostatin, 1 µg/mg leupeptin a 1 µg/ml pepstatin and pH was adjusted to 7.5. The cells were homogenized in an ice-cold Bead Beater (Biospec) three times for 1 minute. The homogenate was centrifuged at 1100 g for 20 minutes. The supernatant was further centrifuged at 3000 g for 20 minutes. The final supernatant was centrifuged at 164600 g for 1.5 h. The resulting crude membrane fraction was homogenized in a Teflon-glass Braun homogenizer in an ice-cold lysis buffer. All centrifugation steps were hold at 4°C. The membranes were stored at −80°C.

2.2.7 Purification of NKA from Crude Membranes

The prepared membranes were thawed and diluted to the final concentration of 2 $mg^{-1}{\cdot}ml^{-1}$ in lysis buffer containing 2 mg/ml of detergent (n-dodecyl-β-D-maltoside, DDM or octaethylene glycol monodecyl ether, $C_{12}E_8$) and supplemented with 1.2

mg/ml cholesteryl hemisuccinate. The solubilisation of membranes was performed at 4°C for 1 h. The solubilized membranes were further centrifuged at 164300 g, at 4°C for 30 minutes. The supernatant was diluted with the ice-cold buffer (25 mM Tris, 10 mM imidazole, 500 mM NaCl and 10% glycerol, pH 7.6) to 1.5 CMC (critical micelle concentration) of detergent. Ni-NTA beads (Qiagen) were added into membranes solution in the ratio of 0.5 ml of beads to 1 ml of supernatant. The solution was incubated at 4°C overnight. The protein was eluted by the series of elution buffers (25 mM Tris, 500 mM NaCl, 10% glycerol, 0.75 mg·ml^{-1} detergent, 0.15 mg·ml^{-1} cholesteryl hemisuccinate and 10 – 500 mM imidazole) with increasing imidazole concentration.

2.3 Expression of NKA in Gal4ΔPep4 and ΔPep4 Strains

2.3.1 Cultivation of Gal4ΔPep4 Strain of *Saccharomyces cerevisae*

Yeast transformation was performed according to a standard LiAc transformation protocol as was described in protocol for BJ5457 strain. One colony from plate was picked up to inoculate 10 ml of SD medium without uracil (synthetic drop-out media from Difco doped with yeast nitrogen base without amino acids (YNB)) containing 2% glucose. The culture was cultivated overnight at 30°C on the shaker. 500 µl of culture was transferred into 10 ml of SD medium without leucine but with 2% glucose. This culture was cultivated overnight on shaker at 30°C. 1 ml of preculture was used to start two aliquots containing 30 ml of SD medium with 2% glucose. These precultures were cultivated at 30°for 24 hours. Subsequently, 2 l of SD medium without leucine with 1% glucose was inoculated by 10 ml of preculture. These large cultures were cultivated at 30°C on shaker (120 rpm) for 36 h.

The temperature was lowered to 17°C at least 2 h before induction. Actual level of glucose was tested using MediTest Glucose (Marchery-Nagel). The induction was performed when glucose concentration decreased to zero. The induction was carried out by addition of 200 ml of 10xYP solution (100 g·l^{-1} yeast extract, 100 g·l^{-1} peptone) and galactose (100 ml of 40% stock solution give 2% final concentration). The cultures were cultivated for 24 h at 17°C on the shaker and a proper aeration was adjusted by slightly opening the flask's lid. After 24 h, the cultures were collected by centrifugation (3500 g, 10 minutes). The cells must be kept on ice while processing due to prevention of produced protein degradation. Then the cells were washed with ice-cold water and resuspend in the lysis buffer (1.4 M sorbitol, 10 mM MOPS/Tris-HCl, 1 mM EDTA, and protease inhibitors cocktail; pH 7.2) establishing ratio 1:10 (cell to buffer). Cells were separated into smaller aliquots (100 ml each). These aliquots were frozen by liquid nitrogen and stored at −80°C.

Furthermore, we would like to note that the cell to buffer ratio influences the preparation of crude membranes. More concentrated cells can be difficult to separate by centrifugation. In general, 1:1 ratio for freezing the cells can be also used, but then the cells lysis by glass beads must be optimized and cells must be diluted.

2.3.2 Crude Membranes Preparation

The cells aliquot in the lysis buffer was gently thawed and mixed with ice-cold glass beads with ratio 1:1 (glass beads to cells). The cells were disrupted by Pulverisette 6 instrument. The cell lysate was filtered to separate beads and solution. The filtered cell lysate was centrifuged at 10000 g at 4°C for 10 minutes. The pellet was removed, and the supernatant was subjected to the ultracentrifugation at 164700 g at 4°C for 1.5 h. The supernatant was removed, and the pellet was resuspended in the membrane buffer (10 mM MOPS/Tris-HCl, 1 mM EDTA, 25% glycerol, and protease inhibitors cocktail; pH 7.2). The crude membranes were quickly frozen in liquid nitrogen and stored at −80°C.

2.3.3 Membrane Solubilisation

Before starting the membrane solubilization, the stock solution containing detergent and lipids (concentrated 100x) must be prepared. The first step was the preparation of 20 mg·ml^{-1} detergent solution, and chloroform solutions containing lipids (the lipids are often delivered as chloroform solution). The chloroform was dried out using nitrogen flow. For the complete removal of chloroform, the nitrogen-dried solution was left in vacuum overnight. The next day, lipids were dissolved in the detergent stock solution up to the final lipids concentration of 10 mg·ml^{-1}.

The membrane solubilization protocol was based on Cohen *et al.* [102]. Crude membranes were gently thawed on ice and then mixed with DDM using detergent to membranes (w/w) ratio equal to 2:1 (final concentration of membranes was 2 mg·ml^{-1} and DDM 4 mg·ml^{-1}). The solubilization buffer (250 mM NaCl, 20 mM Tris-HCl, 5 mM imidazole, 0.5 mM PMSF, 10% glycerol, and protease inhibitors cocktail; pH 7.4) was used for dilution of membranes. The buffer was filtered using 0.22 μm syringe filter. The membrane with detergent solution was incubated at 4°C on the magnetic stirrer for 1 h. The insoluble material was removed by ultracentrifugation at 164000 g for 30 minutes. Pellet was removed and supernatant was kept for protein purification. IMAC resin (TALON, Clontech, USA) was washed by wash buffer (100 mM NaCl, 20 mM Tris-HCl, 10% glycerol, 10 mM imidazole, 0.2 mg·ml^{-1} DDM or 0.1 mg·ml^{-1} $C_{12}E_8$, 0.05 mg·ml^{-1} DOPS or SOPS, 0.01 mg·ml^{-1} CHS, and protease inhibitors cocktail; pH 7.4). The buffer was filtered using 0.22 μm syringe filter just before use. The IMAC resin was mixed with solubilized membranes (100 μl of beads per 10 mg of membranes) and incubated for 1 h at 4°C. After incubation, the solution was loaded into empty gravity flow column. Then, the resin was washed by 5 column volumes of wash buffer. The washing step was repeated. Finally, the His-tag fusion protein was eluted by 1 column volume of elution buffer (100 mM NaCl, 20 mM Tris-HCl, 10% glycerol, 150 mM imidazole, 0.2 mg·ml^{-1} DDM or 0.1 mg·ml^{-1} $C_{12}E_8$, 0.05 mg·ml^{-1} DOPS or SOPS, 0.01 mg·ml^{-1} CHS, and protease inhibitors cocktail; pH 7.4. The buffer was filtered using 0.22 μm syringe filter. Imidazole was dialyzed out in dialysis buffer (100 mM NaCl, 20 mM Tris-HCl, 10% glycerol; pH 7.4). Protein was concentrated by Amicon tubes (molecular weight cut-off (MWCO) 50 kDa) and stored at −20°C.

While optimizing the protocol, we also performed the membrane solubilization according to Morth *et al.* [120]. The membranes were gently thawed on ice and diluted

by 1x solubilization buffer (20 mM KCl, 5 mM KF, 5 mM $MgCl_2$, 100 mM NMDG, 40 mM MOPS-Tris, and protease inhibitors cocktail; pH 7.0) establishing the final concentration of membranes to 4 mg·ml^{-1}. The TALON resin was washed by solubilization buffer before use. After 1 hour solubilization by NMDG, the membrane solution was mixed with TALON resin as described previously. All wash and elution solutions were doped by 100 µl synthetic lipids (0.05 mg·ml^{-1} DOPS or SOPS, 0.01 mg·ml^{-1} CHS). Resin was subsequently washed using low-salt and high-salt washes (see Table 2.3) for contaminants removal. The protein was eluted by the increasing imidazole concentration as suggested Table 2.3. The eluted protein was concentrated using centrifugal filters with MWCO 30 kDa (Amicon) and stored at −20°C.

Step	2xSolubilization Buffer (ml)	Water (ml)	1 M Imidazole (ml)	1 M NaCl (µl)
Low-salt wash 1 (LS1)	5	4.68	0.2	20
High-salt wash (HS)	5	1.37	0.2	3300
Low-salt wash 2 (LS2)	5	4.58	0.3	20
Elution 1 (E1)	5	4.70	0.2	0
Elution 2 (E2)	5	4.00	0.9	0
Elution 3 (E3)	5	2.40	2.5	0
Elution 4 (E4)	5	0.00	4.9	0

Table 2.3: Table of wash and elution buffers used for protein purification based on [120].

2.3.4 Size-Exclusion Chromatography (SEC)

All samples prepared using Gal4ΔPep4 strain were analyzed by SEC. Running buffer based on [102] was composed of 100 mM NaCl, 20 mM Tris-HCl, 10% glycerol, 0.2 mg·ml^{-1} DDM or 0.1 mg·ml^{-1} C_12E_8, 0.05 mg·ml^{-1} DOPS or SOPS, and 0.01 mg·ml^{-1} CHS; pH 7.4. The buffer was filtered using 0.22 µm syringe filter. The running buffer for [120] based protocol was composed of 20 mM KCl, 5 mM KF, 5 mM $MgCl_2$, 100 mM NMNG, 40 mM MOPS-Tris; pH 7.0. The running buffer was filtered as described above.

The SEC was performed using instrument Akta Micro (GE Healthcare, Sweden) and Superdex 200 Increase 3.2/300 column (GE Healthcare, Sweden). The separation was performed at room temperature with cooled column (4°C). Flow rate was set to 0.05 ml·min^{-1} and 100 µl fractions were collected into microwell plate.

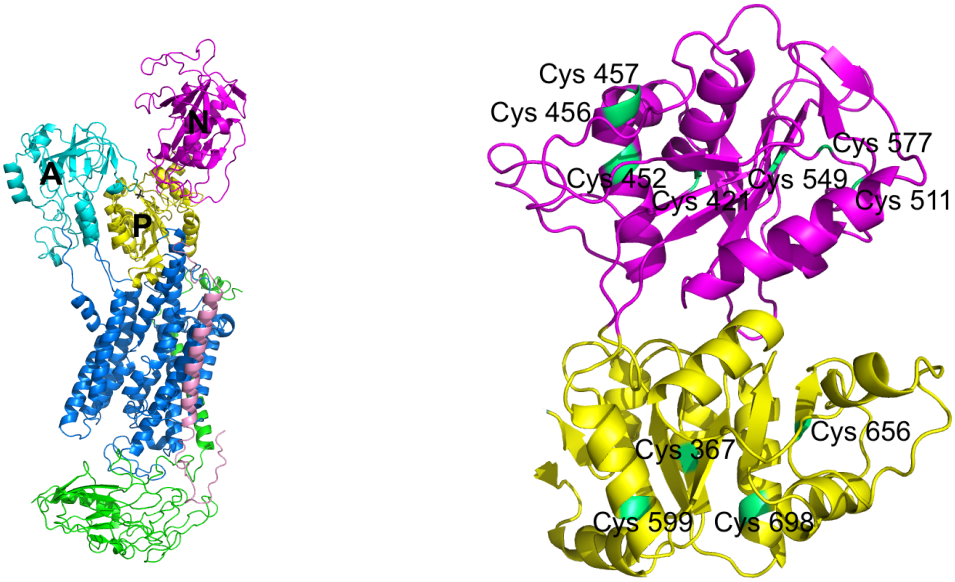

Figure 24: Left: the structure of NKA with highlighted C45 loop formed by the P (yellow) and N (magenta) domains. The transmembrane part of NKA is dark blue, A domain is cyan, P domain is yellow, N domain is maganta, β subunit is green, and FYXD protein is pink. Right: the structure of the mouse brain C45 loop of the NKA. All mutated cysteine residues are highlighted in green and sequence numbering is based on porcine α_1.

2.4 Preparation of the Large Cytoplasmic Loop of NKA (C45 Loop)

The large cytoplasmic segment connecting the transmembrane helices 4 and 5 (C45 loop, residues Leu354 – Ile777 of the mouse brain sequence, see Figure 24) with a $(His)_{10}$-tag at N terminus was expressed in *E. coli* Rosetta DE3 cells (Promega, USA) and purified using Co^{2+}-based affinity resin (TALON resin, Clontech, USA) as described by Grycova *et al.* [15]. The bacteria cultures were cultivated to OD_{600} 0.5 – 0.7 and consequently induced by 10 µM IPTG and 100 µM L-arabinose. The induced cultures were incubated overnight on the shaker at 17°C. The cultures were harvested by centrifugation (5000 g, 5 minutes) and resuspended in lysis buffer (10 mM Tris-HCl, 10 mM NaCl; pH 7.5) containing protease inhibitors (2 $\mu g \cdot ml^{-1}$ leupeptin, 2 $\mu g \cdot ml^{-1}$ pepstatin and 1 mM PMSF) and directly subjected to cell disruption by ultrasound homogenizator model 3000 (BioLogics, USA). The cell lysate was centrifuged (15000 g, 1 hour at 4°C), pellet was removed and supernatant was left to interact with TALON resin. TALON affinity resin was washed with set of wash buffers (wash buffer 1: 20 mM Tris-HCl, 20 mM imidazole, 100 mM NaCl; wash buffer 2: 20 mM Tris-HCl, 20 mM imidazole, 500 mM NaCl; and wash buffer 3: 20 mM Tris-HCl, 30 mM imidazole, 100 mM NaCl. pH of all wash buffers was adjusted to 7.4.). The elution was carried out using elution buffer (500 mM imidazole, 20 mM Tris-HCl, 140 mM NaCl; pH 7.4). Immediately after elution, the protein was dialyzed into dialysis buffer (20 mM Tris-HCl, 140 mM NaCl; pH 7.4) and stored at −20°C. The protein concentration was determined using the Bradford assay [346] with BSA as a standard.

2.4.1 The Set of Cysteine Mutants of the C45 Loop

The cDNA sequence of mouse brain C45 loop was digested at restriction sites of NheI and HindIII for cloning into final vector. The template, 1275 bp DNA of mouse brain C45 loop, was commercially synthetized and cloned using the restriction enzymes NheI, HindIII and sealed by T4 ligase (NEB) into pET28b plasmid. The construct was multiplied by Top 10 *Escherichia coli* bacteria (Thermo Fisher, USA) and isolated using Wizzard Plus SV Minipreps DNA Purification System (Promega). A set of eleven recombinant proteins (Figure 24) containing one point mutation in codon TGC→ AGC or TGT→ AGT (amino acid replacement Cys→ Ser) and one protein containing double replacement of cysteine residues. The primers used for cloning are listed in Table 2.4. The sequences were verified by DNA-sequencing using primers T7-terminator (GCTAGTTATTGCTCAGCGG) and T7-promoter (TAATACGACTCACTATAGGG). Heterologous expression in *E. coli* using vector depicted in the Figure 25 and purification of isolated C45 was described in detail by others (e. g. [15]).

The sequence numbering was based on the mouse brain sequence.

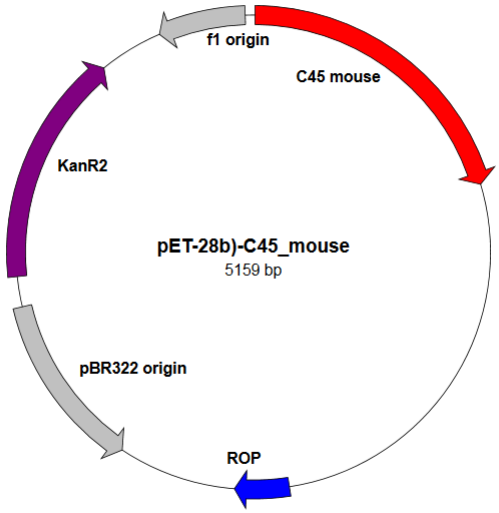

Figure 25: The map of cloning vector for overexpression of the mouse brain C45 loop. The N-terminal His-tag is fused with C45 mouse gene, KanR2 is gene for kanamycin resistance, f1 is an origin of replication, pBR322 is a replication origin and ROP encodes regulatory protein.

2.4.2 C45 Loops Intact Mass Determination

MALDI-TOF analysis for the intact mass determination of the C45 loop was performed on the Microflex LRF20 instrument. Samples of the untreated C45 loop and its derivatives were incubated with cisplatin (molar ratio of 1:20) for 24 h at 4°C, whereas the control samples were mixed with water. The cisplatin-treated and control samples were dialyzed against 2 l of dialysis buffer (20 mM Tris-HCl; pH 7.5) for 72 h at 4°C. All samples were concentrated up to final concentration of 20 $mg{\cdot}ml^{-1}$ using centrifugal filters (Amicon, Merck Millipore) with MWCO 30 kDa. The 1 µl of each sample was

Primer	Sequence (5'→3')
C367S	Construct was synthetized by Generi Biotech, Czech Republic
C421S FwD	CCAGAATTGCTGGTCTCTCTAACAGGGCAGTG TTTCAGG
C452S FwD	CCGAGTCGGCGCTCTTAGAGTCCATCGAGATC TGCTGTGGC
C456S FwD	GCATCGAGATCAGCTGTGGCTCCGTGATGGAG ATGAGG
C457S FwD	GCATCGAGATCTGCAGTGGCTCCGTGATG
C456S+C457S FwD	GCATCGAGATCAGCAGTGGCTCCGTGATGGA GATGAGG
C511S FwD	GGATCCTGGACCGAAGCAGTTCTATCCTCCTCC
C549S FwD	GCGTGTGCTAGGTTTCAGCCACCTCCTTCTGCC TGACG
C577S FwD	GATAACCTCAGCTTCGTGG
C599S FwD	GCTGTGGGCAAAAGCCGCAGCGCTGGGATTAA GG
C656S FwD	CAAGGCCAGTGTAGTACATG
C698S FwD	GCTCATCATTGTGGAGGGCAGCCAGCGGCAGGG

Table 2.4: Primer sequences used for preparation of the set of cysteine mutants. The sequences were derived from the mouse brain C45 loop, and all mutations were confirmed using gene sequencing by Seqme s.r.o., Czech Republic. FwD sequence stands for a forward direction of gene transcription and downstream primers were reverse complement.

placed onto the target plate (MSP BigAnchor Chip TM 96, microScript Target), immediately mixed with 1 µl of matrix (20 mg·ml^{-1} Sinapic acid in 0.1% TFA/acetonitrile, 1:1, v/v) and allowed to dry on air. At least 500 single-pulse spectra were acquired in the linear mode for positive ions. The instrument parameters were as follows: acceleration voltage 20 kV, extraction voltage 18 kV, lens voltage 9.5 kV and delayed extraction time 1000 ns. Then the mass spectrum of each sample was obtained by summing over all these subspectra. The final molecular weight of the protein was averaged from 10 replicates and plotted by Matlab2017a software. The external calibration was performed using a mixture of Protein Calibration Standard II (Bruker Daltonics, Germany, 1:1, v/v).

2.4.3 TC-FlAsH^{TM} Detection

The TC-FlAsH^{TM} reagent (Invitrogene) was used for detection of cysteine residues in the positions C452, C456 and C457. This sequence is similar to the sequence which can be detected by TC-FlAsH^{TM} reagent. The protein samples of C45 WT, C452S, C456S, C457S, and C456S+C457S were diluted to the final concentration approximately 1 mg·ml^{-1} and denatured at 60°C for 30 minutes. Denatured proteins were incubated with working solution of TC-FlAsH^{TM} reagent at room temperature for 10 minutes. Subsequently, the standard SDS-PAGE was performed. The in gel fluorescence from

SDS PAGE gel was visualized using Green: 520 nm/6 filter on the luminescent image analyzer Amersham Imager 600 instrument (GE Healthcare, Sweeden).

2.4.4 Chemical Modification of Cysteine and Methionine Residues

The chemical modification was performed according to [347, 348, 349]. The C45 WT proteins were diluted to the final concentration of 1 mg·ml^{-1} and alkylated by 330 mM iodoacetate in 100 mM ammonium bicarbonate (final concentration of iodoacetate was 55 mM) at room temperature for 30 minutes. The reaction was stopped by adding 10 mM β-mercaptoethanol. The modified C45 WT was dialyzed against 2 l of dialysis buffer (20 mM Tris-HCl, pH 7.5) at 4°C overnight. The modification of methionine residues was performed according to [347, 350, 351]. The C45 WT at concentration 1 mg·ml^{-1} were oxidized by chloramine T in 100 mM ammonium bicarbonate. The molar ratio of chloramine T to methionine was equal to 10. After the modification, the C45 WT was dialyzed as described above. The intact masses of modified C45 WT proteins before and after cisplatin treatment were detected using the same set up as described in the section 2.4.2.

2.5 Preparation of Human C23 and C45 Loops

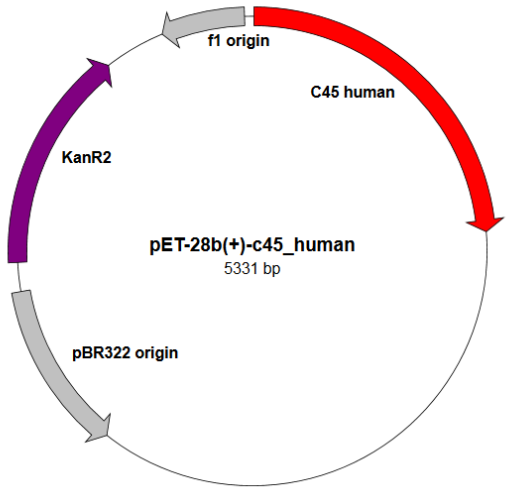

Figure 26: The map of cloning vector for the overexpression of human variants of the C45 loop. The N-terminal His-tag is fused with the C45 gene, KanR2 is a gene for kanamycin resistance, f1 is an origin of replication, pBR322 is a replication origin and ROP encodes regulatory protein.

Thomas Friedrich from Institute of Chemistry, Technical University of Berlin, Germany kindly provided the DNA sequences encoding human α_1, α_2 and α_3 subunits in 3.1x DNA vector. Each sequence of C45 and C23 was multiplied using standard PCR (all used primers are listed in the Table 2.5) and digested by NdeI a XhoI (New England Biolabs) endonucleases. DNA fragment was selected by standard 1% agarose

electrophoresis, and isolated from gel using Wizard SV Gel and PCR Clean-Up System (Promega) mixed with linearized pET28b (New England Biolabs) vector. The vector with C45 gene was sealed using T4-DNA Ligase (New England Biolabs) and inserted into TOP 10 *E. coli* cells (Invitrogene). The construct DNA was isolated with GeneJET Plasmid Miniprep Kit (Thermo). The sequences of all constructs were verified by the DNA sequencing (Seqme s. r. o., Czech Republic). The vector maps for human C45 and C23 loops are illustrated in the Figure 26 and Figure 27, respectively.

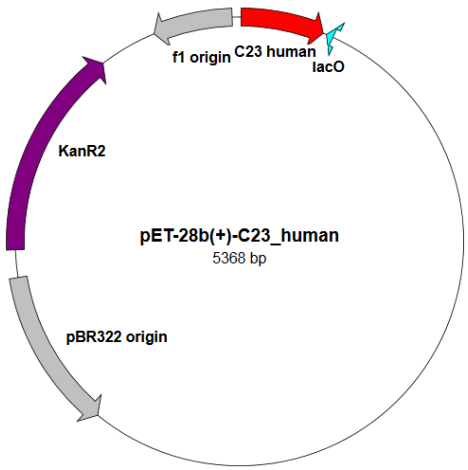

Figure 27: Map of cloning vector for overexpression of human variants of the C45 loop. The N-terminal His-tag is fused with C23 mouse gene, KanR2 is a gene for kanamycin resistance, f1 is an origin of replication, pBR322 is a replication origin and ROP encodes regulatory protein.

2.5.1 Purification of Human C23 Loops

The C23 loop connecting the transmembrane helices 2 and 3 with a $(His)_{10}$-tag at N terminus was expressed in *E. coli* Rosetta DE3 cells (Promega, USA) and purified using Co^{2+}-based affinity resin (Clontech, USA). The cell cultures were grown until OD_{600} 0.6 and consequently, the induction was performed using 500 µM IPTG. Induced cultures were incubated on shaker at 17°C for 20 h. The cultures were harvested by centrifugation (5000 g, 5 minutes) and resuspended in lysis buffer (10 mM Tris-HCl, 10 mM NaCl; pH 7.5) containing protease inhibitors (2 $\mu g \cdot ml^{-1}$ leupeptin, 2 $\mu g \cdot ml^{-1}$ pepstatin and 1 mM PMSF) and directly subjected to cell disruption by ultrasound homogenizator model 3000 (BioLogics, USA). The cell lysate was centrifuged (15000 g, 25 minutes at 4°C), pellet was removed and supernatant was left to interact with TALON resin. TALON affinity resin was washed with set of wash buffers (wash buffer 1: 20 mM Tris-HCl, 20 mM imidazole, 100 mM NaCl; wash buffer 2: 20 mM Tris-HCl, 20 mM imidazole, 500 mM NaCl; and wash buffer 3: 20 mM Tris-HCl, 30 mM imidazole, 100 mM NaCl. pH of all wash buffers was adjusted to 7.4.). The elution was carried out using elution buffer (500 mM imidazole, 20 mM Tris-HCl, 140 mM NaCl; pH 7.4). Immediately after the elution, the protein was dialyzed into dialysis buffer

Primer	Sequence (5'→3')
ALPHA1 C23 FwD	CTGCATATGGCCCTTGTGATTCGAAATGGT
ALPHA1 C23 ReD	TGCCTCGAGCTATCTTCCCATCACAGTGCG
ALPHA1 C45 FwD	CAGCATATGACTGCCAAACGCATGGCAA
ALPHA1 C45 ReD	TACCTCGAGCTAACGACCTTCCTCTACTCC
ALPHA2 C23 FwD	CAGCATATGGCCCTTGTGATCCGGGAGGGAG
ALPHA2 C23 ReD	TATCTCGAGCTAGCGGCCCATCACCGTC
ALPHA2 C45 FwD	CAGCATATGACAGCCAAGCGCATGGCACG
ALPHA2 C45 ReD	TATCTCGAGCTAGCGGCCCTCCTCCACCC
ALPHA3 C23 FwD	CAGCATATGGCCCTGGTGATCCGGGAAG
ALPHA3 C23 ReD	TATCTCGAGCTAACGGCCCATGACAGTGCG
ALPHA3 C45 FwD	TTACATATGACCGCCAAGCGCATGGCCC
ALPHA3 C45 ReD	TATCTCGAGCTAGCGGCCCTCCTCCACCCCTG

Table 2.5: Primer sequences used for the preparation of the human variants of the C45 and C23 loops. The sequences were derived from the human sequences listed in Chapter 4.4 and all mutations were confirmed using gene sequencing by Seqme s.r.o., Czech Republic. FwD sequence stands for a forward direction of gene transcription and ReD stands for a reverse direction.

(20 mM Tris-HCl; pH 7.4) and stored at −20°C. Protein concentration was determined using the Bradford assay [346] with BSA as a standard.

2.5.2 Purification of Human C45 Loops

All C45 loops were expressed and purified using the same protocol as described in Section 2.5.

2.6 Determination of NKA Activity

2.6.1 Enzyme-Coupled Assay

The measurements of NKA activity were performed at Department of Biophysics (Aarhus University, Denmark) in collaboration with Natalya Fedosova.

The reaction was started by adding of the NKA (2 µl at concetration 6.78 mg·ml^{-1}) into reaction buffer (30 mM L-histidine, 130 mM NaCl, 20 mM KCl, 4 mM $MgCl_2$, 1 mM PEP, 3 mM Na-ATP, 0.22 mM NADH, 12.5 U·ml^{-1} PK, and 30 U·ml^{-1} LDH; pH 7.4). After the initialization of the reaction, the absorbance was monitored for 300 s. The reaction stopped by the addition of 500 µM ouabain, and residual absorbance was determined by absorbance at 340 nm measurement for 300 s. Final concentration of inorganic phosphate produced by NKA was calculated using formula:

$$c = \frac{MW \cdot V}{\epsilon \cdot d \cdot v \cdot 1000} \cdot \Delta A,$$

where c is a concentration of the reaction product in mg·ml^{-1}, MW is a molecular weight of NADH (663,43 g·mol^{-1}), ϵ is an extinction coefficient of NADH at 340 nm (6300 M^{-1}·cm^{-1}), d is an optical pathway, V is a final volume of the reaction solution, and v is a volume of the enzyme.

The NKA activity was determined by following formula:

$$Activity_{ATPase} = \frac{n_{Pi}}{m_{enzyme} \cdot t},$$

where n_{Pi} is an amount of produced inorganic phosphate, m_{enzyme} is weight of the used enzyme in milligrams, and t is a time in hours.

2.6.2 Baginsky Assay

The NKA activity was measured using modified Baginsky assay protocol by Baginsky *et al.* [238] with some modifications [239]. Baginsky assay demands relatively low amount of samples and provides a wide range of reproducible results in comparison with other methods. This colourimetric method relies on the detection of inorganic phosphate which interacts with ammonium molybdate. The reaction results in a colour change which can be monitored as a change of absorbance at 710 nm measurable using microplate reader Synergy Mx (BioTek, USA). Baginsky assay was easily automatized using the automated pipetting station Freedom EVO (Tecan, Switzerland).

The reaction buffer was composed of 325 mM NaCl, 50 mM KCl, 7.5 mM $MgCl_2$, and 75 mM imidazole, pH 7.2. The NKA (0.1 mg·ml^{-1}) isolated from porcine kidney was mixed with reaction buffer without ATP. All inhibitors were solubilized in methanol immediately before measurement. Subsequently, 10 µl of inhibitor solution was added into 20 µl of reaction buffer with enzyme and incubated for 2 minutes. For the control sample, only 10 µl of reaction buffer without enzyme was added.

The reaction started by the adding 7.5 mM ATP into 30 µl of reaction buffer with the pump. Then, the sample was incubated for 6 minutes at room temperature. The produced inorganic phosphate was detected using 75 µl of the staining solution composed of 160 mM ascorbic acid, 3.7 % (v/v) acetic acid, 3 % (w/v) SDS and 0.5 % ammonium molybdate. The staining reaction was incubated for 8 minutes at room temperature, and then the reaction was stopped by adding 125 µl of solution composed of 0.9 % (w/v) bismuth citrate, 0.9 % (w/v) sodium citrate and 3.7 % HCl. Bubbles from the surface were removed and absorbance at 710 nm was read. The calibration line was determined using of KH_2PO_4 solutions, in 0 – 37.5 nM concentration range.

The ATPase activity of untreated NKA decreases to approximately 10 % in the presence of ouabain, which serves as a specific inhibitor of Na^+/K^+-ATPase. 10 mM ouabain was used to reveal residual activity of ATPases. The residual activity in presence of ouabain has been subtracted from the total estimated ATPase activity.

I have tested using the Baginsky assay several compounds belonging into group of flavonolignans. Namely silybin (SB), silydianin (SD), silychristin (SCH) a taxifolin (TAX), and their dehydro- derivatives dehydrosilybin (DHSB), dehydrosilydianin (DHSD), dehydrosilychristin (DHSCH), and quercetin (QUE) were examinated in the paper III [279]. We have also tested the group of halogenated quinolinones and platinum-based complexes (cisplatin, oxaliplatin, and carboplatin).

Chapter 3

Results and Discussion

3.1 Isolation of NKA from Porcine Kidney

The 234 g of the outer medulla tissue was dissected from 3.6 kg of whole porcine kidneys. The centrifugation 3 yielded 23.52 g of pellet, which was subjected to ultracentrifugation. Series of ultracentrifugation and pellet resuspendation enabling to reach high purity of the final protein. The steps of purification are illustrated in Figure 28, and Figure 29 shows SDS-PAGE of the selected steps of the isolation.

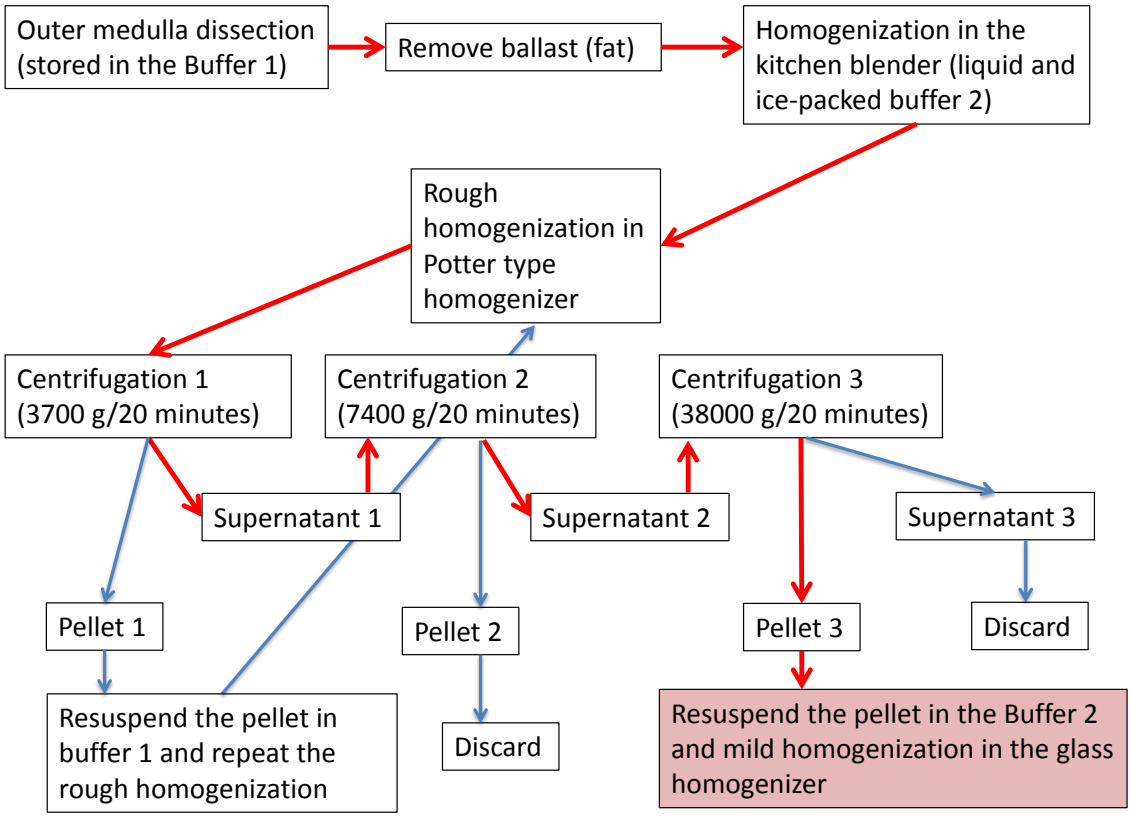

Figure 28: The scheme of NKA isolation from porcine kidney.

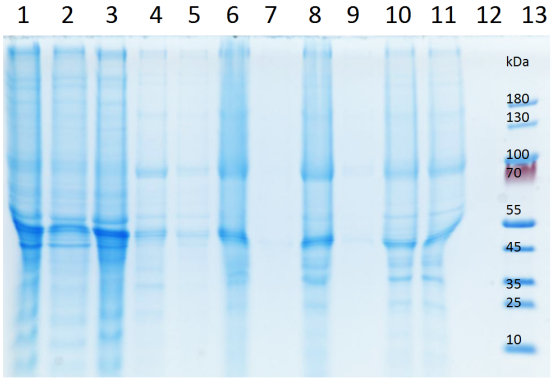

Figure 29: SDS-PAGE illustrating purification of NKA from porcine kidney. Samples were loaded in the following order: 1 and 2 – microsomes 4.6 mg·ml^{-1}, 3 – ultracentrifugation 1 (pellet), 4 – ultracentrifugation 1 (supernatant), 5 – ultracentrifugation 2 (pellet), 6 – ultracentrifugation 2 (supernatant), 7 – ultracentrifugation 3 (pellet), 8 – ultracentrifugation 3 (supernatant), 9 – ultracentrifugation 4 (pellet), 10 – ultracentrifugation 4 (supernatant), 11 – pure protein 1 mg·ml^{-1}, 12 – empty, and 13 – marker.

Using this method, I prepared 370 mg of microsomes that exhibited unspecific ATPase activity of 41.0 µmol·mg^{-1}·h^{-1}, and specific (ouabain-sensitive) activity of 9.9 µmol·mg^{-1} · µh^{-1}. I used method of titration by SDS to find out the most effective SDS concentration for membrane solubilization (see Figure 30). We tested two different temperatures for membrane solubilization. Our results suggested that optimal conditions were 0.8 mg·ml^{-1} (0.08%) SDS and incubation temperature 20°C. A large-scale preparation of the NKA (used in the functional studies) was performed under these conditions.

Two aliquots of 10 ml microsomes (4.0 mg·ml^{-1}) were treated by two distinct concentrations of SDS (0.8 mg·ml^{-1} and 2.0 mg·ml^{-1}). Using 0.8 mg·ml^{-1} SDS, we obtained 17.1 mg of the pure protein that exhibited the specific activity of 109.8 µmol·mg^{-1}·h^{-1} and the unspecific activity of 164.9 µmol·mg^{-1}·h^{-1}.

Sample	Concentration (mg·ml^{-1})	Specific ATPase activity (µmol·mg^{-1}·h^{-1})	Unspecific ATPase activity (µmol·mg^{-1}·h^{-1})
Microsomes	4.0	9.9	41.0
NKA+0.8 mg·ml^{-1} SDS	4.0	30.1	64.3
NKA+2.0 mg·ml^{-1} SDS	4.0	36.3	76.5
Pure NKA	1.0	109.8	164.9

Table 3.1: Summary of the NKA preparation from the porcine kidney. The specific ATPase activity is ouabain-sensitive activity, and the unspecific activity is overall activity of all ATPases present in the sample.

The microsomes, which were treated by higher SDS concentration (2.0 mg·ml^{-1}) yielded lower specific and unspecific activity. Activities of the samples from the most important steps of the purification process are presented in Table 3.1.

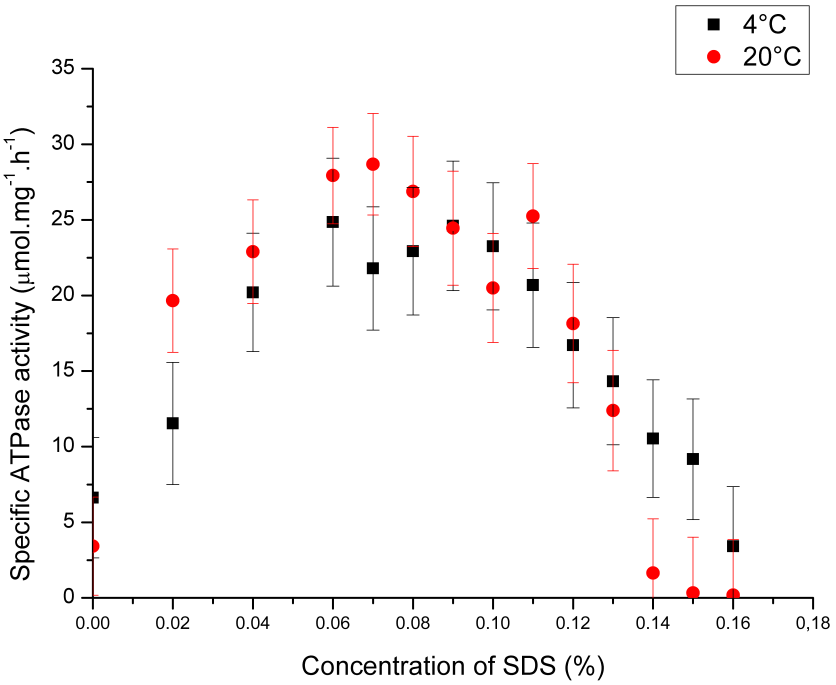

Figure 30: Specific ATPase activity of samples that were treated by different concentrations of SDS. Solubilization was performed at two distinct temperatures – 4°C and 20°C.

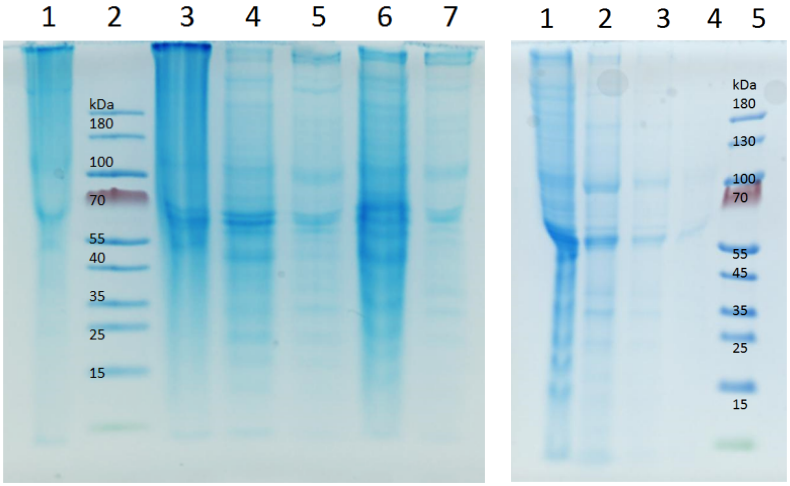

Figure 31: Left: SDS-PAGE of the purified NKA without homogenization with the ice-packed Buffer 2. The samples were loaded as follows: 1 – porcine kidney NKA isolated using the differential ultracentrifugation on the sucrose gradient, 2 – marker, 3 – crude membranes 4 mg·ml^{-1}, 4 – membranes solubilized by 0.8 mg·ml^{-1} SDS, 5 – pure protein solubilized by 0.8 mg·ml^{-1} SDS (final concentration of 1.0 mg·ml^{-1}), 6 – membranes solubilized by 2.0 mg·ml^{-1} SDS, 7 – pure protein solubilized by 2.0 mg·ml^{-1} SDS (final concentration of 0.7 mg·ml^{-1}). Right: SDS-PAGE of the purified NKA without homogenization with the ice-packed Buffer 2. The samples were following 1 – microsomes 4.6 mg·ml^{-1}, 2 – pure protein 1 mg·ml^{-1}, 3 – pure protein 0.2 mg·ml^{-1}, 4 – pure protein 0.1 mg·ml^{-1}, and 5 – marker.

One purification from 25 kidneys yielded approximately 87.0 mg of pure NKA with specific activity approximately 164.9 $\mu mol \cdot mg^{-1} \cdot h^{-1}$. The concentration and purity of the final pure protein was estimated using Bradford assay and SDS-PAGE (see Figure 31) We used centrifugal filters to increase the protein concentration and for removal of contaminants with small molecular weight. The concentrated protein exhibited improved purity, but the loss of ATPase activity appeared within days.

3.2 Expression of NKA in Yeast Strain BJ5457

In general, some useful expression strategies for the integral membrane protein expression were published previously [340, 343, 352]. Unfortunately, the expression of NKA excludes the use of the GFP fusion protein expression due to protein misfolding caused by GFP fusion. NKA cannot be GFP-tagged neither within α subunit (both N- and C-termini), nor within β subunit without significant change of the complex association (personal communication with Per Amstrup Pedersen). However, the whole NKA complex can be expressed in yeast with high yield (according to [46, 126, 232, 161, 344, 343]).

The effective purification can be performed using N-terminal $(His)_{10}$-tag placed on the β subunit (see vector map in Figure 23). Similar approach using BJ5457 yeast strain was previously used for purification of the porcine $\alpha_1\beta_1$ complex [161, 353]. Furthermore, [354] developed simple protocol for the increase of yield produced membrane proteins using yeast expression system.

I prepared the expression vector for co-expression of human complex of $\alpha_3\beta_1$ in yeast *Saccharomyces cerevisiae* (strain BJ5457). I also expressed a set of mutant proteins (D811N, E825K and G957 in human α_1 numbering). These mutations are often mentioned as a possible causative mutations for AHC and RDP [135, 128, 10]. I would like to note that for easier understanding I will keep using the human α_1 numbering.

The both genes (encoding α_3 and β_1 subunit) were placed into expression vector pEMBLye4 under control of the same promoter sequence which was positively regulated by galactose and negatively regulated by glucose. The yeast strain BJ5457 also contained cyclic galactose promoter enabling a high yield protein expression under selected conditions. Moreover, we monitored the time-dependent protein expression and we tested two distinct cultivation temperatures (15°C, 30°C) after the induction of protein expression. For the optimization of membrane solubilization, αDDM and $C_{12}E_8$ detergents were used. Obtained results are presented in the following section.

Yeast strain BJ5457 expressed NKA complex as illustrated in Figure 32. The molecular weight of the prepared complex is in good agreement with the control sample (porcine kidney NKA).

The size of the β subunit expressed in yeast exhibited lower molecular weight (approx. 40 kDa) than β subunit from porcine kidney NKA complex (approx. 50 kDa), as can be seen in Figure 33. For example, the methylotrophic yeast *Pichia pastoris* expresses the β subunit as two strains with molecular weight 44 and 47 kDa [107]. I assume, that the molecular weight difference was linked with the post-translational

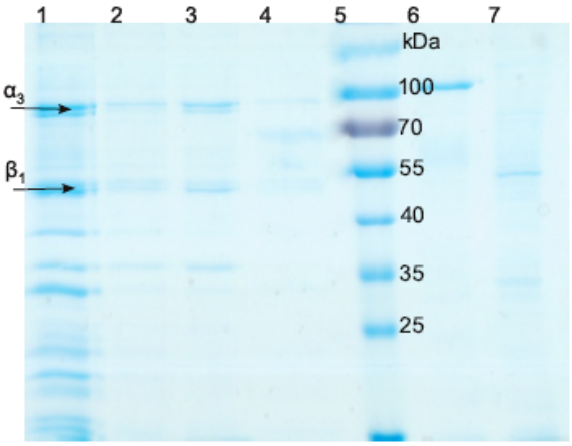

Figure 32: The pure NKA protein analyzed by SDS-PAGE. Positive control is represented by NKA isolated from porcine kidney and plasma membrane Ca^{2+}-ATPase (PMCA) expressed in yeast as negative control. Samples were loaded in the following order: 1 – α_3Gly957Arg+β_1WT, 2 – α_3Glu825Lys+β_1WT, 3 – α_3Asp811Asn+β_1WT, 4 – α_3WT+β_1WT, 5 – marker, 6 – porcine kidney NKA, and 7 – PMCA as a negative control.

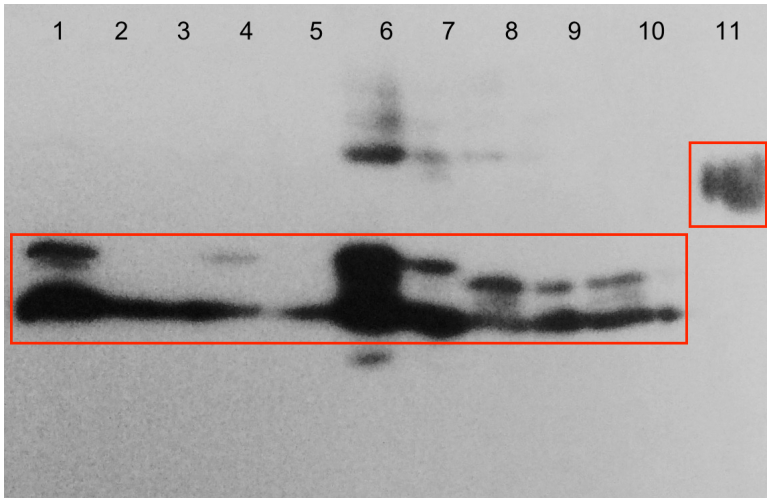

Figure 33: Western blot of crude membranes isolated from Gal4ΔPep4 and ΔPep4 strains. The protein was detected using the specific anti-human α_3 antibody. In the figure is highlighted position of β subunit. The crude membrane samples were loaded in the following order: 1 – α_3Asp811Asn+β_1WT (48 h cultivation at 30°C), 2 – α_3Asp811Asn+β_1WT (48 h cultivation at 15°C), 3 – α_3Glu825Lys+β_1WT (48 h cultivation at 30°C), 4 – α_3Glu825Lys+β_1WT (48 h cultivation at 15°C), 5 – α_3Gly957Arg+β_1WT (48 h cultivation at 30°C), 6 – α_3WT+β_1WT (48 h cultivation at 15°C), 7 – α_3Gly957Arg+β_1WT (12 h cultivation at 30°C), 8 – α_3Gly957Arg+β_1WT (12 h cultivation at 15°C), 9 – α_3Gly957Arg+β_1WT (16 h cultivation at 30°C), 10 – α_3Gly957Arg+β_1WT (16 h cultivation at 15°C), and 11 – porcine kidney NKA.

modifications, more specifically with glycosylation. The β is highly glycosylated in the animal cells and those glycosylations may be chemically removed. β subunit without glycosylations then exhibited the same molecular weight for both, heterologous and porcine protein [102].

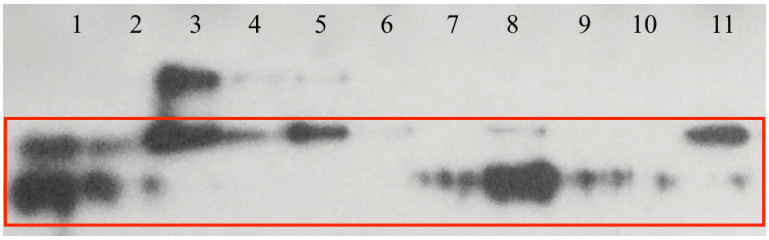

Figure 34: Western blots for crude membranes containing NKA prepared from yeast. For specific protein detection were used antibodies for human α_3 subunit. In the figure is highlighted position of α subunit. Samples were loaded in the following order: 1 – porcine kidney NKA (7.9 µg), 2 – porcine kidney NKA (3.9 µg), 3 – α_3WT+β_1WT (48 h cultivation at 15°C, 2.4 µg), 4 – α_3WT+β_1WT (48 h cultivation at 15°C, 1.2 µg), 5 – α_3WT+β_1WT (48 h cultivation at 30°C, 1.8 µg), 6 – α_3WT+β_1WT (48 h cultivation at 30°C, 0.9 µg), 7 – α_3WT+β_1WT (4 h cultivation at 15°C, 7.7 µg), 8 – α_3WT+β_1WT (4 h cultivation at 30°C, 8.7 µg), 9 – α_3WT+β_1WT (8 h cultivation at 15°C, 8.5 µg), 10 – α_3WT+β_1WT (8 h cultivation at 30°C, 8.4 µg), 11 – α_3WT+β_1WT (24 h cultivation at 15°C, 12.5 µg), and 12 – α_3WT+β_1WT (24 h cultivation at 30°C, 10.0 µg).

Furthermore, several bands for β subunit were observed. Those results agreed with the results obtained for heterologously expressed NKA [103, 106, 97, 110, 355]. The presence of multiple bands for β subunits were considered as different levels of glycosylations.

The α subunit was expressed as a full size protein with molecular weight approximately 110 kDa which correlated with expected weight (the porcine kidney NKA α subunit). In contrast to β subunit, the α subunit is not glycosylated and was expressed as a single peptide without differences in the molecular weight.

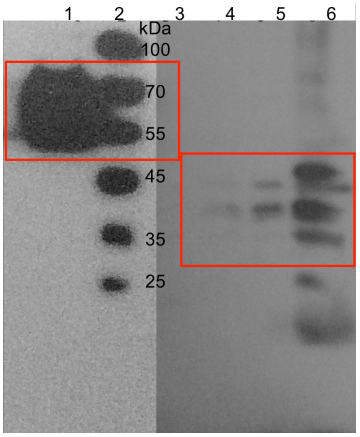

Figure 35: Pure proteins analyzed by Western blotting. The specific antibodies for β_1 subunit were used for the protein detection. In the figure is highlighted the position of β subunit. The samples were loaded in the following order: 1 – porcine kidney NKA, 2 – marker, 3 – α_3WT+β_1WT, 4 – α_3Asp811Asn+β_1WT, 5 – α_3Glu825Lys+β_1WT, and 6 – α_3Gly957Arg+β_1WT.

The temperature and glucose concentration at the time of induction plays a major role in the α subunit expression. For example, if the induction was performed at higher temperature than 15°C, a truncated product was observed (see Figure 34). In

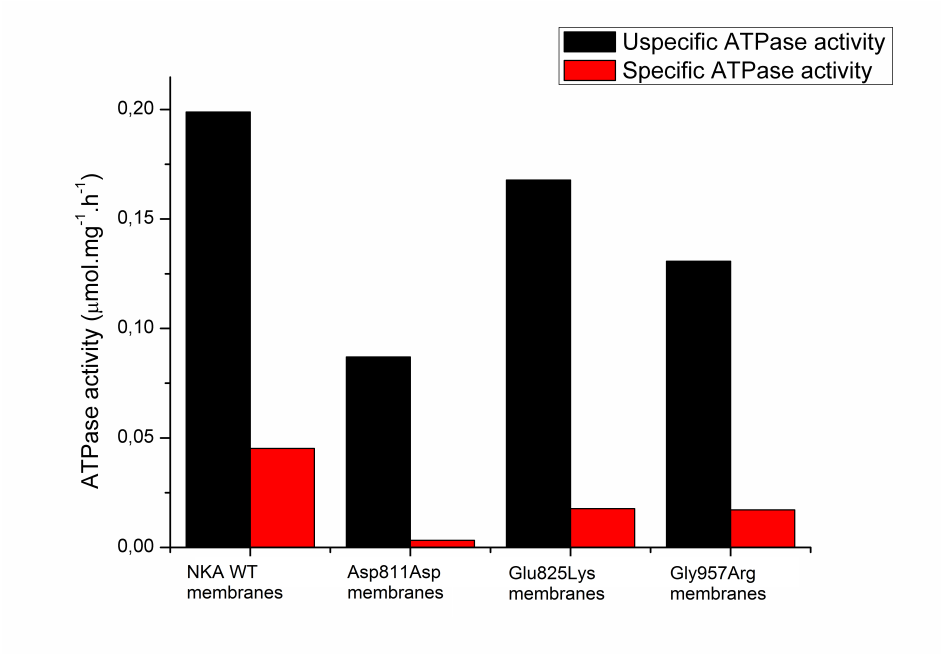

Figure 36: Activity of NKA expressed in yeast strain BJ5457 detected by Baginsky assay. The NKA expressed in yeast exhibited activity only if incorporated in the membranes. After the membrane solubilization NKA lost its function.

the presence of residual glucose, the level of expression was suppressed decreasing the total complex yield. The induction temperature and residual glucose concentration had dramatic influence on the quality and quantity of the prepared protein.

Furthermore, the highest expression level is detected using 48 hours long cultivation time at 15°C (see Figures 33 and 34). Thus, a large scale preparation of NKA was conducted at 15°C for 48 hours.

Moreover, two detergents at 1.5 CMC were also used for the solubilization of yeast membranes prepared under mentioned conditions. The better solubilization was observed for αDDM detergent than for $C_{12}E_8$. The use of detergent depends on the composition of the membrane that should be solubilized. For the NKA purification from porcine kidney, I used SDS detergent due to its low prize and high efficiency. This detergent may be too drastic for the mild solubilization of yeast membranes.

The Baginsky assay was used for the determination of specific ATPase activity with NKA isolated from porcine kidney as a standard (see Figure 37). The expressed proteins seemed deactivated after their isolation from membranes. These results were in good agreement with the ATPase activity measured by the enzyme coupled method (see Figure 36).

Finally, the local environment is a crucial parameter ensuring the protein function [97]. Although, the protein preparations described above were carried out only in the presence of CHS, the ATPase activity of membrane samples was detected. Nevertheless, the lipid composition of a reconstituted membrane around the expressed protein should be optimized in the future.

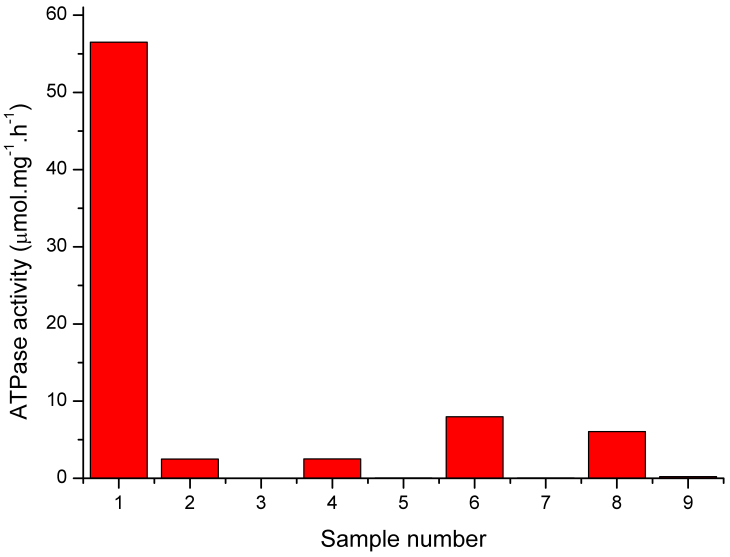

Figure 37: Activity of NKA expressed in yeast strain BJ5457. The detected activities were determined using enzyme-coupled of ATPase activity determination. The samples numbering corresponds to 1 – porcine kidney NKA, 2 – α_3WT+β_1WT membranes, 3 – α_3WT+β_1WT pure protein, 4 – α_3Asp811Asn+β_1WT membranes, 5 – α_3Asp811Asn+β_1WT pure protein, 6 – α_3Glu825Lys+β_1WT membranes, 7 – α_3Glu825Lys+β_1WT pure protein, 8 – α_3Gly957Arg+β_1WT membranes, 9 – α_3Gly957Arg+β_1WT pure protein. The tested membrane samples exhibit ATPase activity, yet the activity of purified proteins was below the detection limits of this method.

3.3 Expression of NKA in Yeast Strains Gal4ΔPep4 and ΔPep4

3.3.1 Gal4ΔPep4 and ΔPep4 Strains

The yeast strains Gal4ΔPep4 and ΔPep4 [356] were also used for NKA production. These strains were kindly provided by Poul Nissen and the optimization of the protein isolation was performed in the collaboration of student under my supervision Veronika Kolomazníková. Selected strains varied mainly in the post-translational modifications – specifically in glycosylations. In comparison to BJ5457 strain, the cultivation was shortened due to the absence of the cyclic galactose promoter. This cyclic promoter enables to cultivate yeast to high optical densities without decreasing the galactose concentration after induction (galactose is not consumed by yeast).

The Figure 38 illustrates the crude membranes prepared from both selected strains. Furthermore, better results were obtained using Gal4ΔPep4 strain (see Figure 38 or Figure 39). Therefore this strain was used for the consequent preparations.

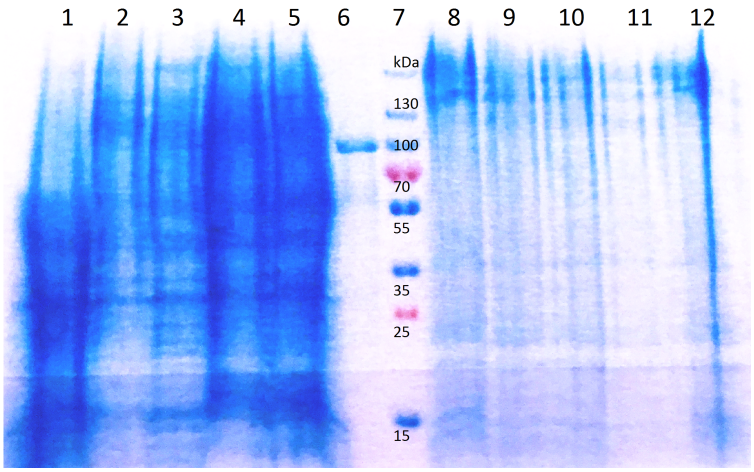

Figure 38: SDS-PAGE of crude membranes isolated from Gal4ΔPep4 and ΔPep4 strains. The crude membrane samples were following: 1,8 – empty vector pEMBLyex4, 2,9 – α_3WT+β_1WT, 3,10 – α_3Asp811Asn+β_1WT, 4,11 – α_3Glu825Lys+β_1WT, 5,12 – α_3Gly957Arg+β_1WT, 6 – porcine kidney NKA, and 7 – marker. Samples 1 – 5 were prepared from Gal4ΔPep4 strain and samples 8 – 12 were prepared from ΔPep4 strain.

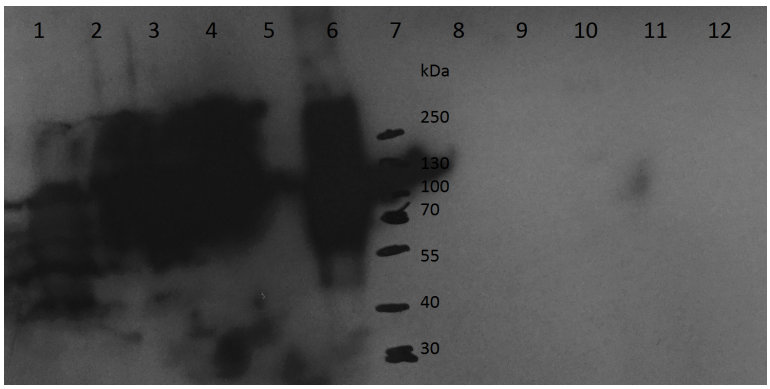

Figure 39: Western blot of crude membranes isolated from Gal4ΔPep4 and ΔPep4 strains. The protein was detected using specific anti-human α_3 antibody. Crude membrane samples were loaded in the following order: 1,8 – empty vector pEMBLyex4, 2,9 – α_3WT+β_1WT, 3,10 – α_3Asp811Asn+β_1WT, 4,11 – α_3Glu825Lys+β_1WT, 5,12 – α_3Gly957Arg+β_1WT, 6 – porcine kidney NKA, and 7 – marker. Samples 1 – 5 were prepared from Gal4ΔPep4 strain and samples 8 – 12 were prepared from ΔPep4 strain.

3.3.2 Optimization of Preparation Protocol

The protocol of the pure protein preparation used for BJ5457 strain exhibited low yield when applied to Gal4ΔPep4 and ΔPep4 strains. The optimization of the protein expression was based on the protocol published by [102] for the NKA preparation from methylotrophic yeast *Pichia pastoris*. The second protocol used for optimization was based on the potassium-bound state of NKA published by Morth *et al.* [120]. Unfortunately, the second mentioned protocol yielded protein, which was not able to retain its activity. This loss of the enzyme activity was caused by the presence of potassium in the buffers [102, 41]. The proteins prepared using both protocols were subjected to HPLC analysis, Western blotting and activity determination.

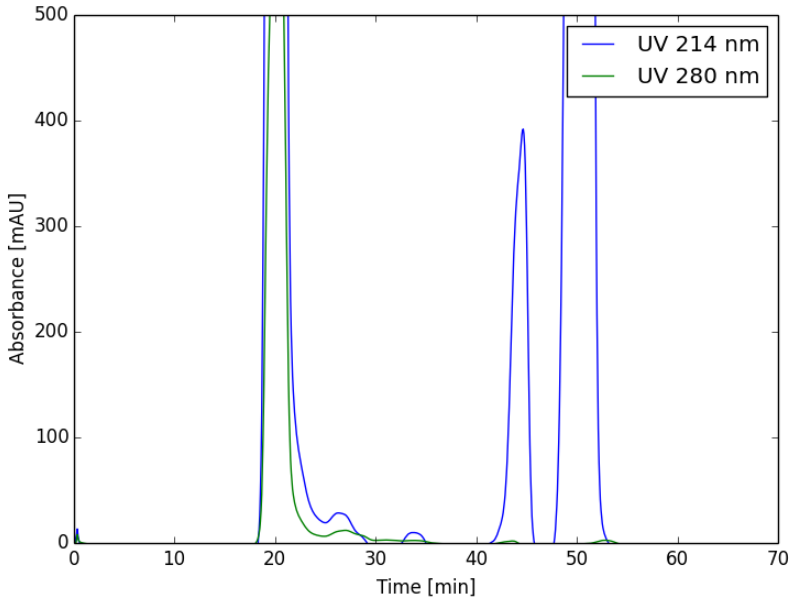

Figure 40: Elution profile of the ribosome solution. Absorbances at 214 nm and 280 nm are highlighted in blue and green, respectively. The void peak (green elution profile) containing aggregates was eluted at retention time of 20 minutes. Other peak in the elution profile shows low absorbance at 280 nm and was eluted at retention time of 28 minutes.

Before the separation of the prepared protein using compact fast protein liquid chromatography (FPLC) we tested the separation method using large aggregates to detect the void peak elution time. Solution containing ribosomes was used for this purpose. The position of the void containing aggregates was eluted at retention time of 20 minutes after separation initialization (see Figure 40).

Then the same conditions were applied to samples prepared according to Cohen *et al.* [102] and Morth *et al.* [120], respectively (Figure 41).

From the elution profile (see Figure 42), I assume that conditions of preparation resulted in the protein denaturation. Haviv *et al.* [103] published the protocol derived from Cohen *et al.* [102], where the protein after elution is stored at −20°C in the presence of a high concentration of imidazole. However, my results suggest that protein was denatured under these conditions (see elution profile in the Figure 41). Due to the protein denaturation, I added a dialysis step just after the protein elution. Dialyzed proteins exhibited different elution profile when separated by HPLC (see Figure 42).

The elution profile showed a typical double peak which suggested the presence of a dimer and monomer form of NKA. Furthermore, similar elution profiles were obtained for other P-type ATPases (personal communication with Joseph Lyons). I also observed multiple bands for β subunit due to presence of several forms with different glycosylation levels. I significantly reduced the presence of those forms using urea treatment during crude membranes preparation. The cell lysate was centrifuged (1000 g, 10 minutes) and immediately mixed with 2 M urea and 100 mM KCl. The cell lysate was incubated for 25 minutes at 4°C. Then, the urea-treated lysate was subjected to centrifugation (20 000 g, 20 minutes) and preparation continued standardly. Urea

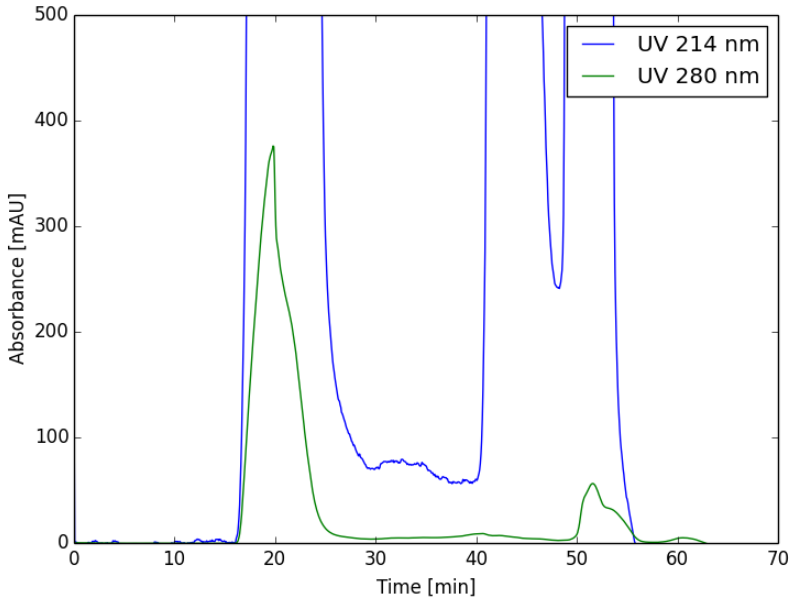

Figure 41: Elution profile of pure protein prepared using Cohen *et al.* [102] protocol. Absorbances at 214 nm and 280 nm are highlighted in blue and green, respectively. The peak-shape suggested an immediate elution of the aggregated NKA just after the void peak at retention time of 20 minutes.

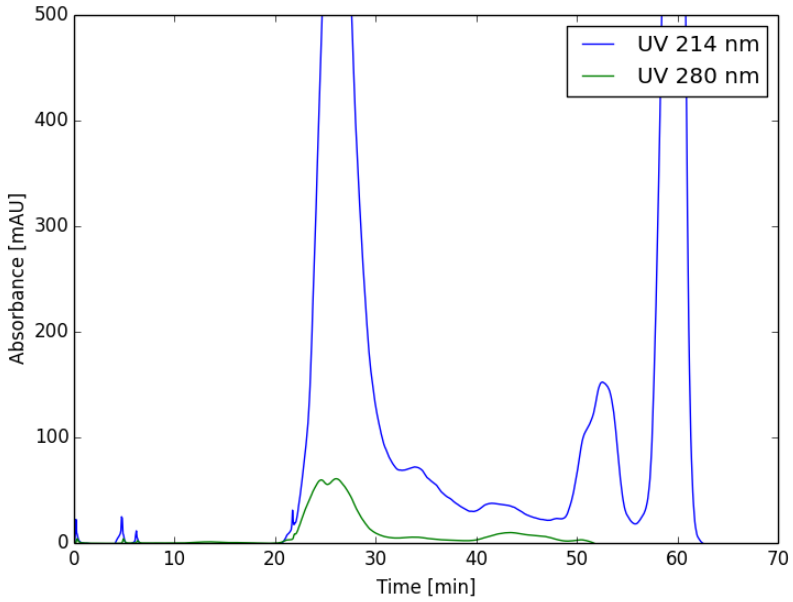

Figure 42: Elution profile of the dialyzed pure protein prepared according to Cohen *et al.* [102] protocol with added dialysis step (dialysis overnight against 2 l of the dialysis buffer). absorbances at 214 nm and 280 nm are highlighted in blue and green, respectively. The double peak was detected at time retention time of approximately 25 minutes after separation initialization. The peak can be interpreted as elution of NKA in the dimeric and monomeric form.

treated samples showed approximately 2 main bands for β subunit instead of 4 or more bands (see Figure 43).

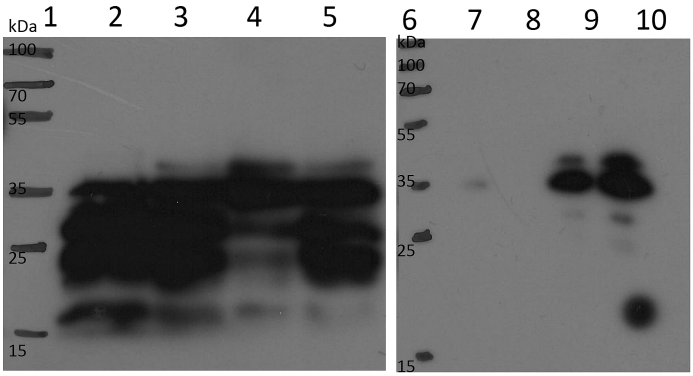

Figure 43: SDS-PAGE of urea treated and untreated membranes isolated from Gal4ΔPep4 strain. The samples were loaded in the following order: 1 – marker, 2 – pure protein Gly957Arg α_3+β_1 WT, 3 – pure protein Glu825Lys α_3+β_1 WT, 4 – pure protein Asp811Asn α_3+β_1 WT, 5 – pure protein α_3WT+β_1 WT, 6 – marker, 7 – α_3WT+β_1 WT low salt wash, 8 – α_3WT+β_1 WT high salt wash, 9 – α_3WT+β_1 WT eluted protein, 10 – α_3WT+β_1 WT concentrated pure protein (0.27 mg·ml^{-1}).

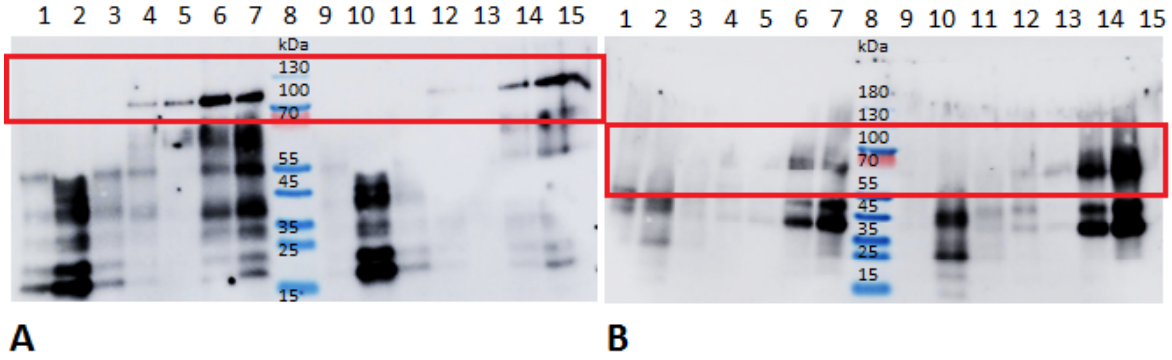

Figure 44: The prepared proteins were detected by specific antibody against α_3 subunit (A) and against β_1 subunit (B). Samples 1 – 7 were solubilized using αDDM and samples 9 – 15 were solubilized using βDDM. The samples were loaded in the following order: 1 – solubilized sample, 2 – removed insoluble material, 3 – IMAC fall through, 4 – wash, 5 – elution before dialysis, 6 – elution after dialysis, 7 – concentrated pure protein, 8 – marker, 9 – solubilized sample, 10 – removed insoluble material, 11 – IMAC fall through, 12 – wash, 13 – elution before dialysis, 14 – elution after dialysis, 15 – concentrated pure protein.

Despite the promising elution profile and western-blots, the pure protein completely lost its function. Due to the loss of a function we optimized detergent solubilization (time of solubilization and detergent type) and artificial membrane reconstitution.

I tested 6 distinct detergents (namely SDS, LMNG, $C_{12}E_8$, αDDM, βDDM, and DM) and two solubilization times (2 or 17 hours). The results are illustrated in Figure 44, Figure 45 and Figure 46. I also tested 6 different lipid solutions based on [97, 102, 103, 106, 109], which are listed in Table 3.2.

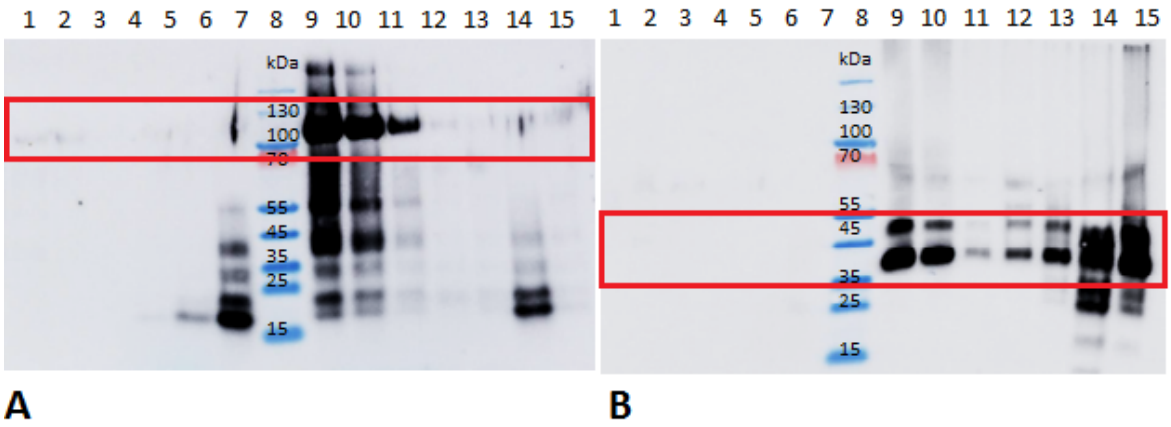

Figure 45: Western blot of the samples prepared using DM and SDS detergents. The prepared proteins were detected by specific antibody against α_3 subunit (A) and against β_1 subunit (B). The samples 1 – 7 were solubilized using DM and samples 9 – 15 were solubilized using SDS. The samples were loaded in the following order: 1 – solubilized sample, 2 – removed insoluble material, 3 – IMAC fall through, 4 – wash, 5 – elution before dialysis, 6 – elution after dialysis, 7 – concentrated pure protein, 8 – marker, 9 – solubilized sample, 10 – removed insoluble material, 11 – IMAC fall through, 12 – wash, 13 – elution before dialysis, 14 – elution after dialysis, 15 – concentrated pure protein.

Mixture No.	Composition	Concentration ($mg \cdot ml^{-1}$)
1.	60% DOPS 20% PC 20% CHS	0.25 0.25 0.10
2.	80% DOPS 20% CHS	0.25 0.10
3.	60% DOPS 40% CHS	0.25 0.10
4.	100% DOPS	0.25
5.	100% Brain PS	0.25
6.	100% Brain polar extract	0.25

Table 3.2: Used lipid solutions for artificial membrane reconstitution. All lipids were dissolved in the chloroform, dried out in stream of nitrogen and dissolved in the detergent solution.

Unfortunately, any lipid composition used for an artificial membrane reconstitution did not improve the function of the purified enzyme. Due to the loss of NKA function and due to losing a considerable amount of the α subunit caused by IMAC, we decided to prepare the protein using analogous approach to isolation from porcine kidney. The crude membranes were subjected to a series of centrifugations to obtain the pure protein. I screened the same set of detergents as in the previous protocol (see Figure 47, Figure 48, and 49).

I determined the NKA activity of the prepared crude membranes and of the pure

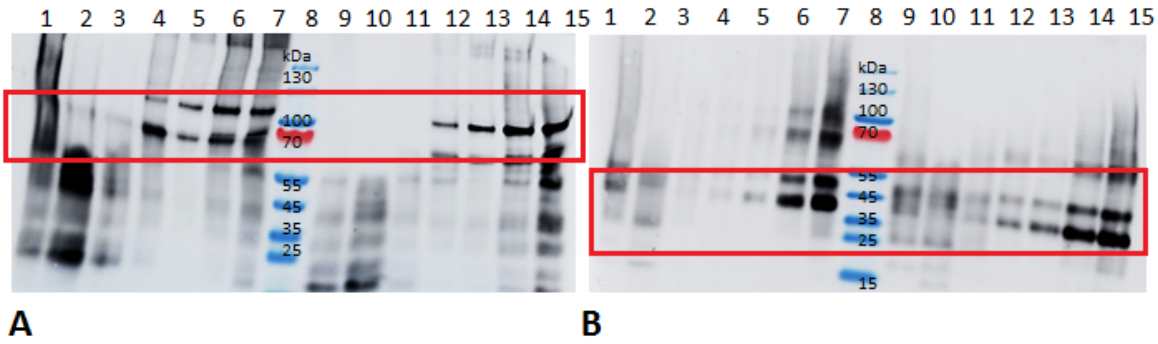

Figure 46: Western blots of the samples prepared using $C_{12}E_8$ and LMNG detergents. The prepared proteins were detected by specific antibody against α_3 subunit (A) and against β_1 subunit (B). The samples 1 – 7 were solubilized using $C_{12}E_8$ and samples 9 – 15 were solubilized using LMNG. The samples were loaded in the following order: 1 – solubilized sample, 2 – removed insoluble material, 3 – IMAC fall through, 4 – wash, 5 – elution before dialysis, 6 – elution after dialysis, 7 – concentrated pure protein, 8 – marker, 9 – solubilized sample, 10 – removed insoluble material, 11 – IMAC fall through, 12 – wash, 13 – elution before dialysis, 14 – elution after dialysis, 15 – concentrated pure protein.

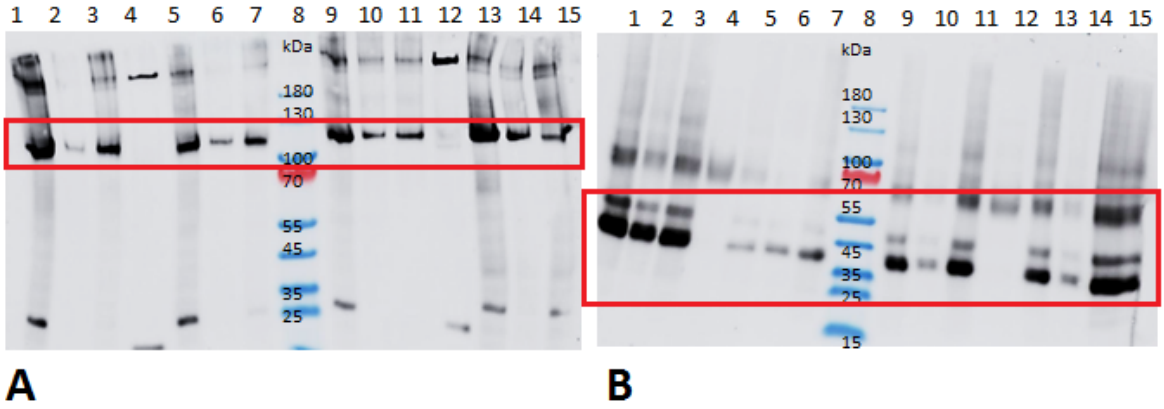

Figure 47: Western blot of the samples prepared using αDDM, βDDM, DM and SDS detergents. The prepared proteins were detected by the specific antibody against α_3 subunit (A) and against β_1 subunit (B). The samples 1 – 3 were prepared using αDDM, 5 – 7 βDDM, 9 – 11 DM, 13 – 15 SDS, and as positive control porcine kidney NKA was used. The samples were loaded in the following order: 1 – solubilized sample (αDDM), 2 – pure protein (αDDM), 3 – concentrated pure protein(αDDM), 4 – porcine kidney NKA, 5 – solubilized sample (βDDM), 6 – pure protein (βDDM), 7 – concentrated pure protein(βDDM), 8 – marker, 9 – solubilized sample (DM), 10 – pure protein (DM), 11 – concentrated pure protein (DM), 12 – porcine kidney NKA, 13 – solubilized sample (SDS), 14 – pure protein (SDS), 15 – concentrated pure protein (SDS).

proteins using standard Baginsky assay. The crude membrane samples showed high background possibly caused by other ATPases and the activity of the pure proteins was below the detection limit of used method. Therefore, on that account, I optimized the protocol for Baginsky assay by adding other nonspecific ATPases inhibitors such as KNO_3, NaN_3 and Na_2MO_4 at final concentrations of 50 mM, 5 mM, and 0.25 mM, respectively. Despite this optimization we did not improve obtained results. I

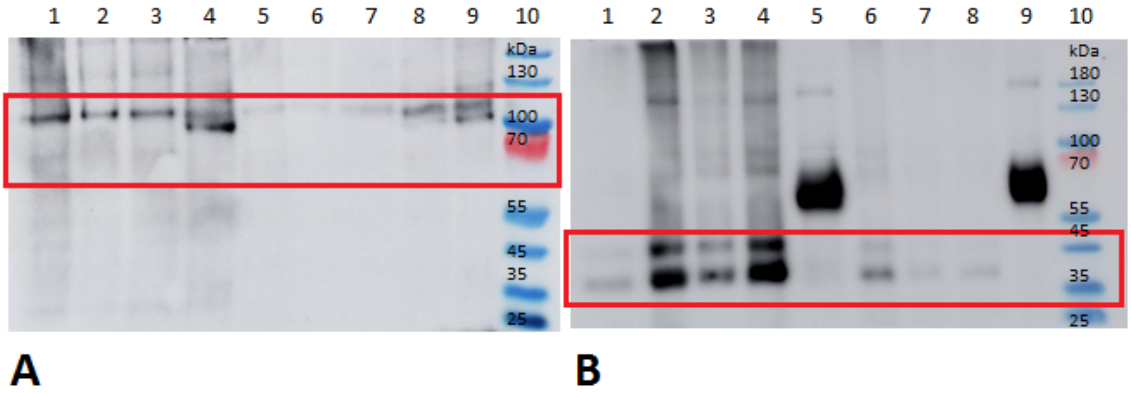

Figure 48: Western blot of the samples prepared using $C_{12}E_8$ and LMNG detergents. The prepared proteins were detected by the specific antibody against α_3 subunit (A) and against β_1 subunit (B). The samples were loaded in the following order: 1 – solubilized sample (LMNG), 2 – pure protein (LMNG), 3 – concentrated pure protein (LMNG), 4 – porcine kidney NKA, 5 – solubilized sample ($C_{12}E_8$), 6 – pure protein ($C_{12}E_8$), 7 – concentrated pure protein ($C_{12}E_8$), 8 and 9 – porcine kidney NKA.

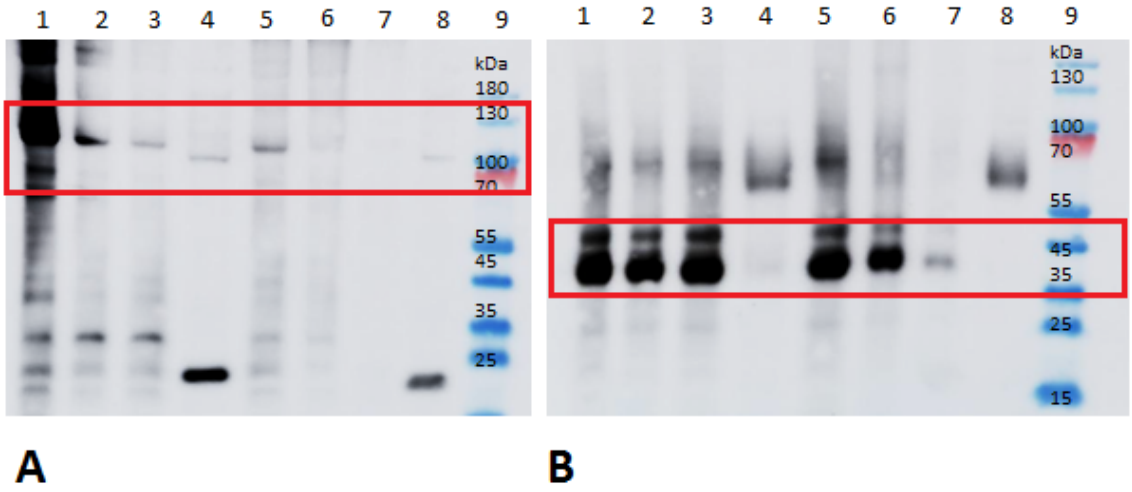

Figure 49: Western blot of the samples prepared using $C_{12}E_8$ and LMNG detergents. The prepared proteins were detected by the specific antibody against α_3 subunit (A) and against β_1 subunit (B). The samples were loaded in the following order: 1 – concentrated pure protein (αDDM), 2 – concentrated pure protein (βDDM), 3 – concentrated pure protein (DM), 4 – porcine kidney NKA, 5 – concentrated pure protein (SDS), 6 – concentrated pure protein ($C_{12}E_8$), 7 – concentrated pure protein (LMNG), 8 – porcine kidney NKA, 9 – marker.

assume that the NKA activity was not detected due to the low concentration of expressed protein, insufficient glycosylation or inappropriate composition of the artificial membrane.

3.4 Interaction of NKA With Small Molecules

3.4.1 Flavonolignans

My findings of the interaction between porcine kidney NKA and flavonolignans were published in paper III [279]. In this study I examined the inhibitory effect of SB, SD, SCH, TAX, DHSB, DHSD, DHSCH and QUE on the NKA activity. In the beginning, all compounds were tested in the initial screening at the final concentration of 10 μM, and the most active compounds were selected for the molecular modelling performed by Petra Čechová.

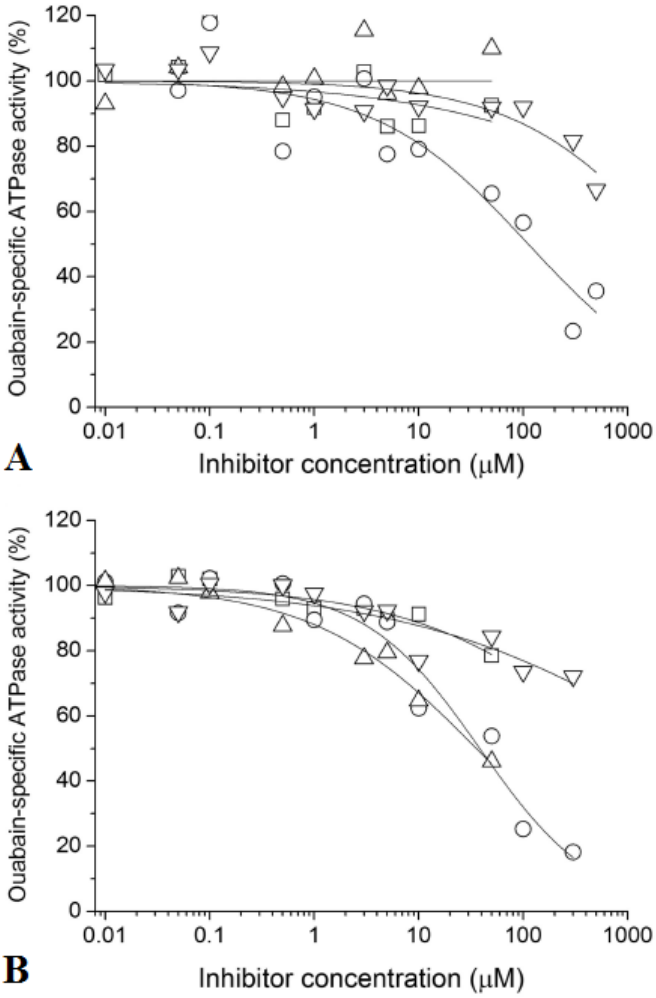

Figure 50: A: Inhibition of NKA by SB (squares □), SCH (circles ○), SD (up triangles △), TAX (down triangles ▽). B: Inhibition of NKA by corresponding dehydroderivatives DHSB, DHSD, DHSCH and QUE, respectively. The reference value (100%) represents ouabain-specific activity of untreated NKA, and each point is represented as mean of four replicates. The error values were typically smaller than symbol size.

The ouabain-sensitive ATPase activity was measured for the increasing concentration of all selected compounds (see Figure 50). Substantial inhibition caused by the compound at final concentration of 10 μM was observed only for SCH, DHSCH and

DHSD. IC_{50} values calculated for those compounds were 110 ± 40 μM, 138 ± 8 μM and 36 ± 14 μM, respectively.

The determined Hill coefficients exceeded 1 indicating the presence of multiple binding sites and negative cooperativity. The active compounds (SCH, DHSCH, DHSD) were subjected to deeper analysis of their inhibitory mechanism. There was no change in IC_{50} for ouabain or in K^+/ouabain antagonism in the presence of active compounds (Figure 51 A). In contrast to ouabain, which elevates $K_{0.5}(K^+)$, none of the tested flavonolignans altered the K^+-dependence of the NKA activity (Figure 51 B).

We used molecular docking tools for the prediction of the potential binding sites for

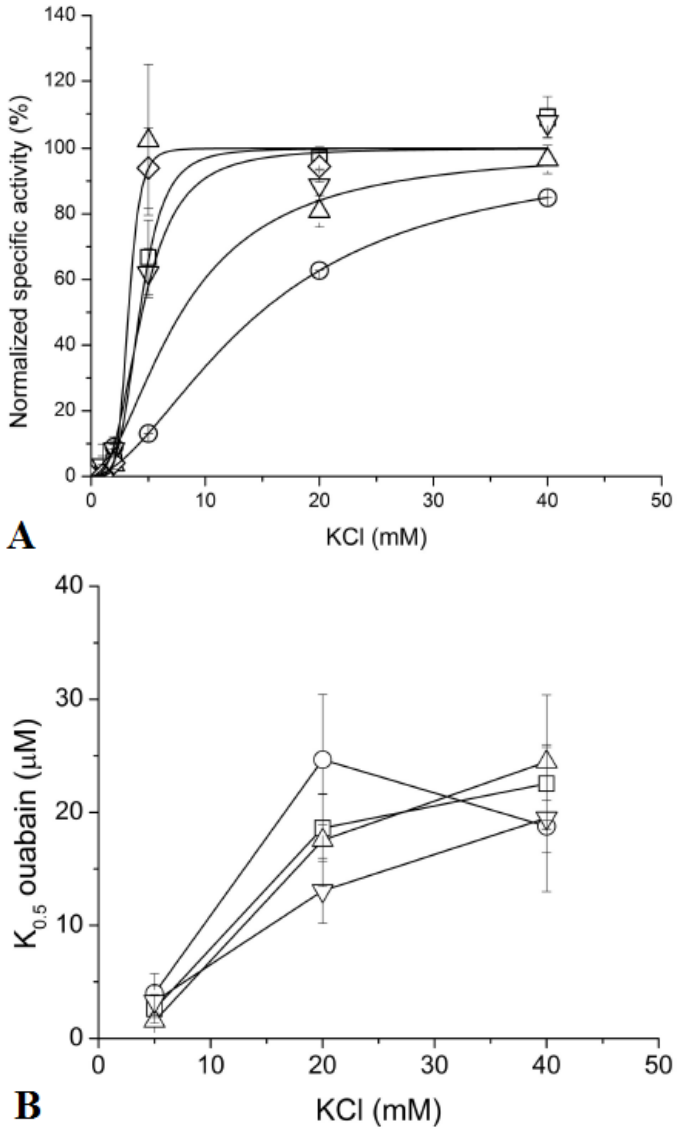

Figure 51: A: the K^+-dependence of the NKA activity in the absence of any ligand (squares □) or in the presence of ouabain (circles ○), SCH (up triangles △), DHSCH (down triangles ▽) or DHSD (diamonds ◇). B: the K^+/ouabain antagonism in the absence or in the presence of 40 μM SCH (circles ○), DHSCH (up triangles △) or DHSD (down triangles ▽) [279]. Each data point is represented as the mean ± S. E. M. of four replicates.

selected compounds (see Figure 52). All five major binding sites were localized mostly on the large cytoplasmic loop connecting transmembrane helices M4 and M5 (C45 loop). Furthermore, all compounds exhibited similar affinities (−11 to −9 kcal.mol^{-1}) to all predicted binding sites in both major enzyme conformations. We identified five major binding sites, but only three of them were conserved in open and closed conformations. The binding site in the close proximity of residue Asn733 was observed only in the open conformation, and binding to Arg248 was limited to close conformation.

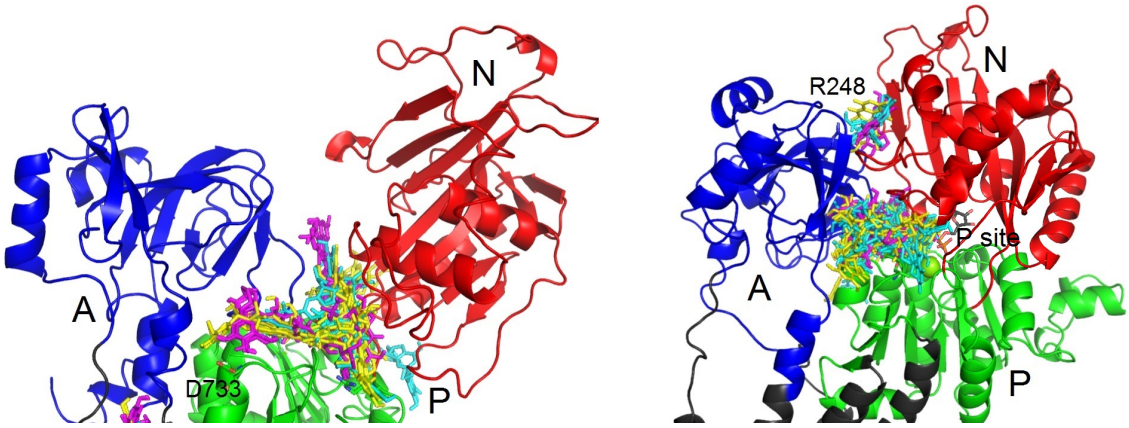

Figure 52: Zoom to the binding sites of SCH (yellow), DHSCH (cyan) and DHSD (magenta) on cytoplasmic loop in the open (left) and close (right) structure. The α is composed of A domain (blue), P domain (green) and N domain (red) [279]. The figure courtesy of Petra Čechová.

The C45 represents more than 40% of the mass of the whole α subunit of NKA, and serves as a target for interaction with soluble molecules due to its position. Consequently, an isolated C45 loop was prepared in bacteria *E. coli* to verify the binding of flavonolignans to cytoplasm-facing part of NKA. The changes in the fluorescence spectra for SCH, DHSCH and SD confirmed the interaction with C45 (performed by Martin Kubala, see Figure 53) as suggested by the molecular modelling (performed by Petra Čechová).

3.4.2 Halogenated Hydroquinolinones

In paper I [302], we described the NKA inhibitory effect of selected halogenated hydroquinones.

I tested halogenated hydroquinolinones as potential NKA inhibitors. The initial screening of quinolinones (31 compounds) at final concentration of 10 μM revealed only one significantly active molecule – 5,6,7,8-tetrafluoro-3-hydroxy-2-phenylquinolin-4(1H)-one (TFHPQ). In contrast to dichlor- or difluor- derivatives, this compound decreased the NKA activity to ca. 45% of its initial activity (see Figure 54). The observed inhibitory effect of TFHPQ depended on concentration – increasing concentration of inhibitor decreased the NKA activity. However, the limited water solubility of TFHPQ significantly limited the IC_{50} determination. The determination of IC_{50} or Hill coefficient requires estimated value of the minimal activity in the presence of inhibitor, which was out of available concentration range. Indeed, at concentration higher

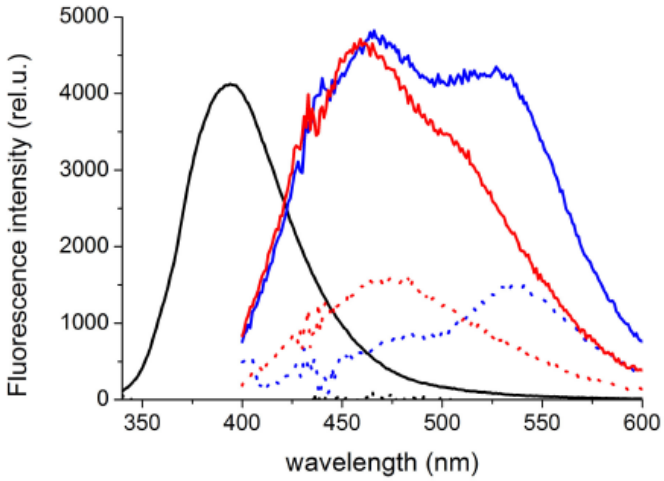

Figure 53: Fluorescence emission spectra of 5 μM SCH (black), DHSCH (blue), and DHSD (red) in the presence of (solid line) and absence (dotted line) of 5 μM C45 loop. The fluorescence intensity in the spectrum of SCH in the presence of C45 was adjusted to fit the graph [279]. The figure courtesy of Martin Kubala.

than 15 μM, the aggregates appeared. Due to the poor control of the real aggregated and non-aggregated TFHPQ concentration in solution, these data were excluded from quantitative analysis. Therefore, the NKA activity in the presence of 10 μM yielded 45% of the initial NKA activity, from which I assumed that the IC_{50} value was near 10 μM.

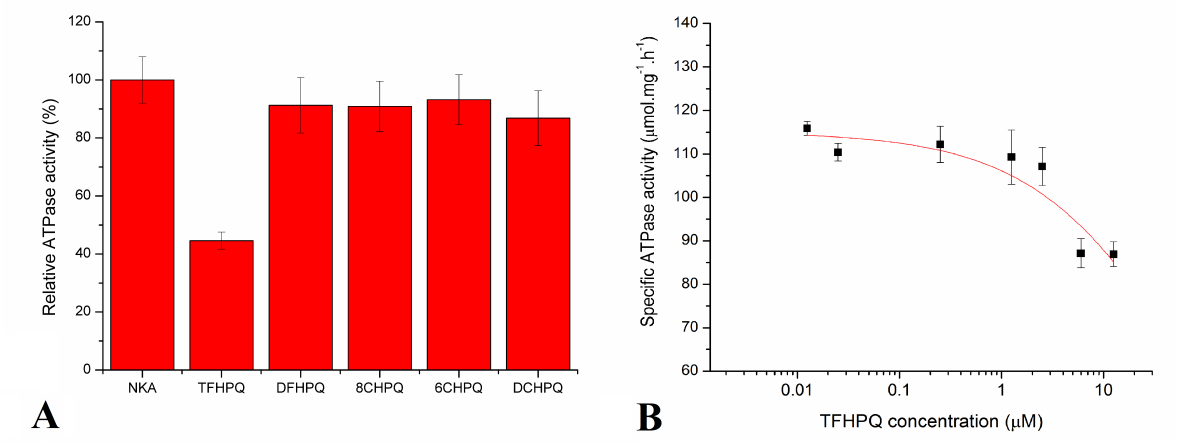

Figure 54: A: The changes of the relative ATPase activity caused by the halogenated quinolinones at final concentration of 10 μM. B: The relative ATPase activities were obtained by normalizing the ATPase activity of the quinolinone-treated enzyme by the activity of the enzyme incubated without inhibitor. The inhibitory effect caused by TFHPQ at increasing concentration. Each data point represents average of four replicates [302].

TFHPQ was subjected to molecular docking to predict the potential binding sites. The closed structure determined TFHPQ binding to αTyr970, αTrp988 and γPhe33 which was localized in the transmembrane domain. However, the crystal structure contain the cholesterol molecule bind in this position suggesting that this site might be inaccessible in the native environment.

The docking into the open conformation suggested the position of the potential binding site for TFHPQ in the open conformation in the close proximity of the C-terminal end of the protein (residuum αTyr1022 and βTrp12) as showed in Figure 55. This site corresponds to one of the binding sites proposed for flavonolignans.

The other compounds could bind to the C-terminal binding site in the open structure, but with lower affinities than TFHPQ. Moreover, they occupied several other binding poses on the protein that were not available for TFHPQ. In the closed conformation, they bound to the similar sites as TFHPQ, but again, with lower affinities.

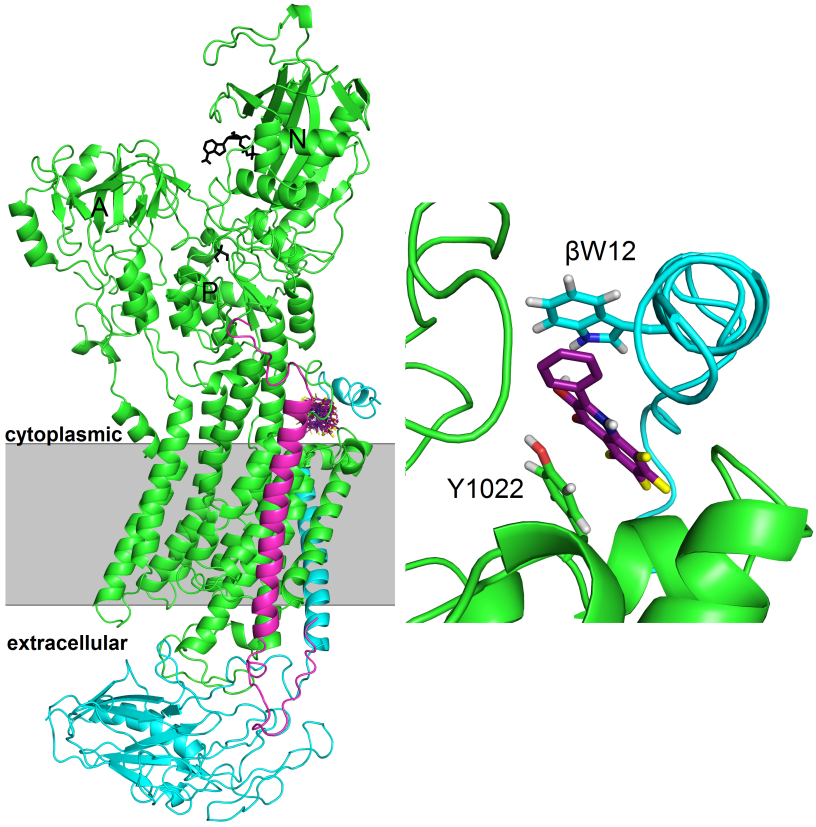

Figure 55: Localization of TFHPQ binding site in the open conformation of the protein (left), and zoom (right). The docked TFHPQ is highlighted in purple, α subunit is in green, β subunit is in cyan, and the FXYD protein is in magenta [302]. The figure courtesy of Petra Čechová.

In order to better understand the TFHPQ inhibition, I evaluated its effect on NKA activation by Na^+, K^+ or ATP (Figure 56). TFHPQ exhibited an effect on the Na^+ dependent NKA activation, altering the enzyme affinity for Na^+. The activity at high NaCl concentration was decreased only to 45% of maximal activity in the presence of THFPQ (Figure 56 A). Similarly, the NKA activity was insignificantly decreased by TFHPQ at high K^+ concentrations, reaching only 45% of the control (Figure 56 B). The shape of the curve was not substantially affected by the presence of TFHPQ (Figure 56 C). Again, the affinity for K^+ slightly decreased suggesting that the TFHPQ inhibition leads to the decrease of the enzyme affinity for transported cations. The ATP-dependence of NKA activity follows the well-known bell-shaped curve [357], which suggests unchanged mechanism of ATP binding.

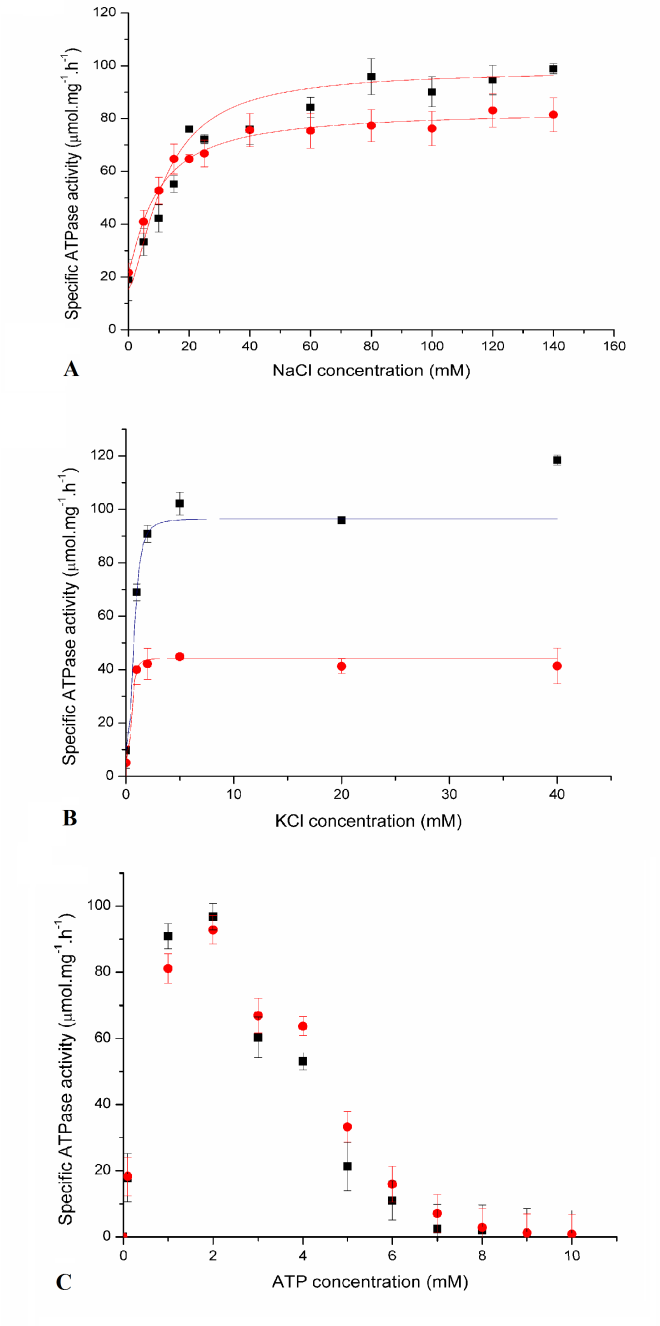

Figure 56: The Na^+-dependence (A), K^+-dependence (B) and ATP-dependence of the NKA activity in the absence of any inhibitor (■) and in the presence of 12.5 μM TFHPQ (●). Each data point represents average of four replicates [302].

3.4.3 Platinum-Based Drugs

In the paper V [25], I examined inhibition of porcine kidney NKA by selected platinum-based anticancer drugs (cisplatin, oxaliplatin and carboplatin). In the recent study [358], paper II, I have analyzed the cisplatin binding to the cysteine residues on the cytoplasmic domain (represented by the C45 loop) of NKA.

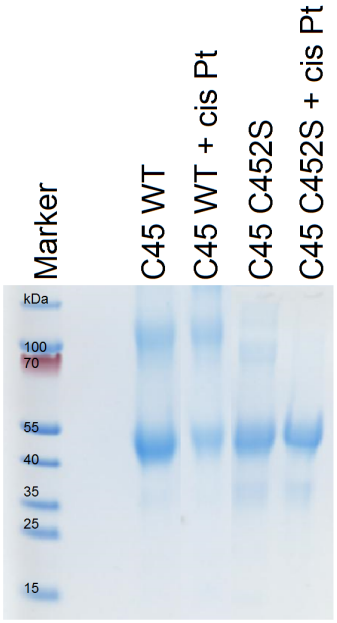

Figure 57: The purity of isolated C45 loops determined by SDS-PAGE. The overall protein yield and purity was not affected by the introduced mutation or by the cisplatin treatment as suggested similar band intensity of analyzed proteins.

Protein	Intact mass (m/z) Without Cisplatin	Standard Deviation (m/z)	Intact mass (m/z) With Cisplatin	Standard Deviation (m/z)	Mass Difference (m/z)
C45 WT	48316	31	49491	20	1175
Cys367Ser	48243	15	48580	62	1337
Cys421Ser	48330	16	49607	31	1277
Cys452Ser	48319	15	49274	36	955
Cys456Ser	48321	20	49337	19	1016
Cys457Ser	48321	72	49252	23	931
Cys456Ser+ Cys457Ser	48181	41	48803	33	623
Cys511Ser	48522	25	49831	31	1575
Cys549Ser	48310	10	49449	36	1139
Cys577Ser	48427	22	49421	21	994
Cys599Ser	48632	17	49835	26	1203
Cys656Ser	48317	18	49265	34	948

Table 3.3: The intact masses detected for C45 WT and mutant proteins in the presence and absence of cisplatin.

Interactions of cisplatin and other platinum-based anticancer drugs (carboplatin and oxaliplatin) with NKA were reported recently [25]. Kubala *et al.* revealed that only cisplatin exhibited the substantial inhibition of porcine kidney NKA. The understanding of this interaction on the molecular level is far from clear and could be the

first step in the elimination of inevitable side-effects. More specifically, nephrotoxicity of cisplatin is limiting its use as a drug [18, 309, 311].

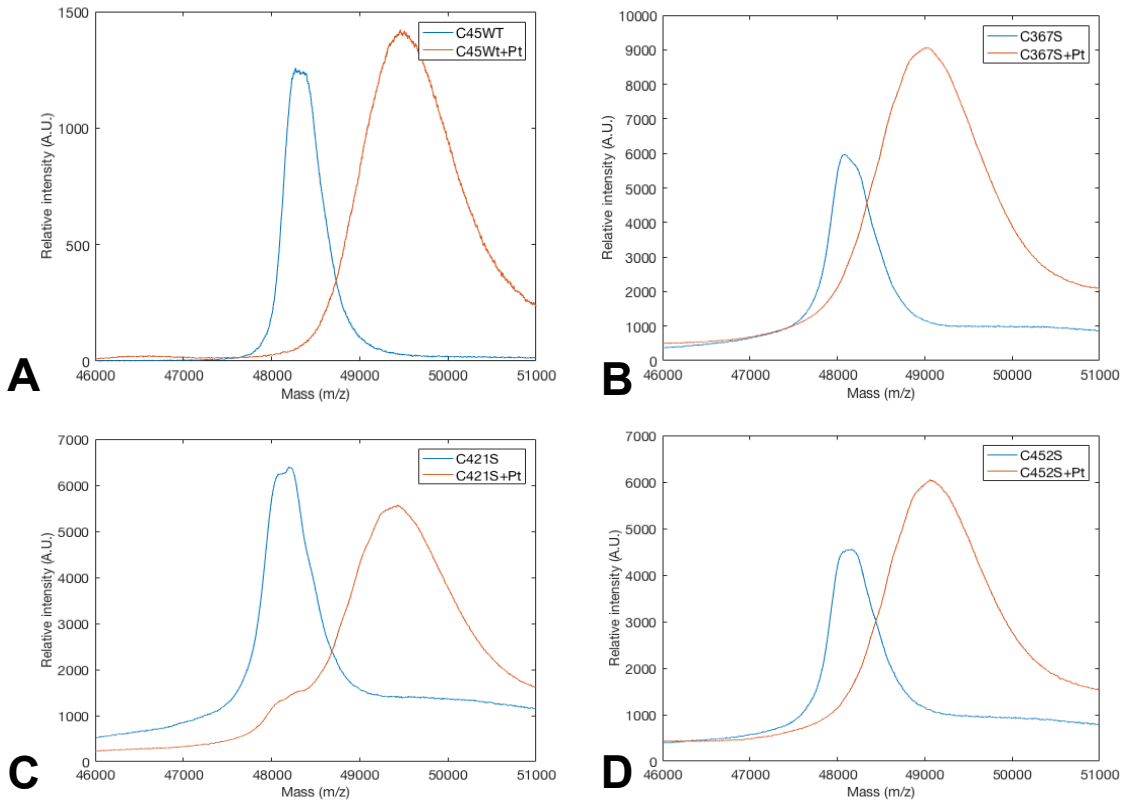

Figure 58: The intact masses for C45 WT (A), Cys367Ser mutant (B), Cys421Ser mutant (C), and Cys452Ser mutant (D) treated by cisplatin (red line), and cisplatin untreated proteins (blue line) detected by mass spectroscopy. The data are presented as intact mass (m/z) and each data point is represented as the mean ± S.E.M. of ten replicates.

The most reactive functional groups within the protein structures toward cisplatin are cysteine residues [359, 360, 361]. I assumed that the interaction between NKA and cisplatin is taking place within the cytosol-facing domain of NKA (C23 and C45 loop). Thus, the isolated large cytoplasmic loop C45 (soluble in buffered aqueous solutions) presents a useful system for examining the cisplatin interactions with NKA [15].

Although, whole C45 loop contains 11 cysteine residues, I assume that binding of cisplatin is restricted to only few residues. The C45 loop contains segment with cysteines Cys452, Cys456 and Cys457 that lay in the close proximity of the protein surface. This segment is accessible from solvent and can be hypothetically involved in many processes.

Therefore, the sequential single amino acid replacement (cysteine to serine) of all cysteine residues could be helpful in the identification of the cisplatin binding site. The Cys456Ser+Cys457Ser mutant (with two adjacent cysteine residues) was also prepared and its interaction with cisplatin tested. Moreover, nor the single amino-acid

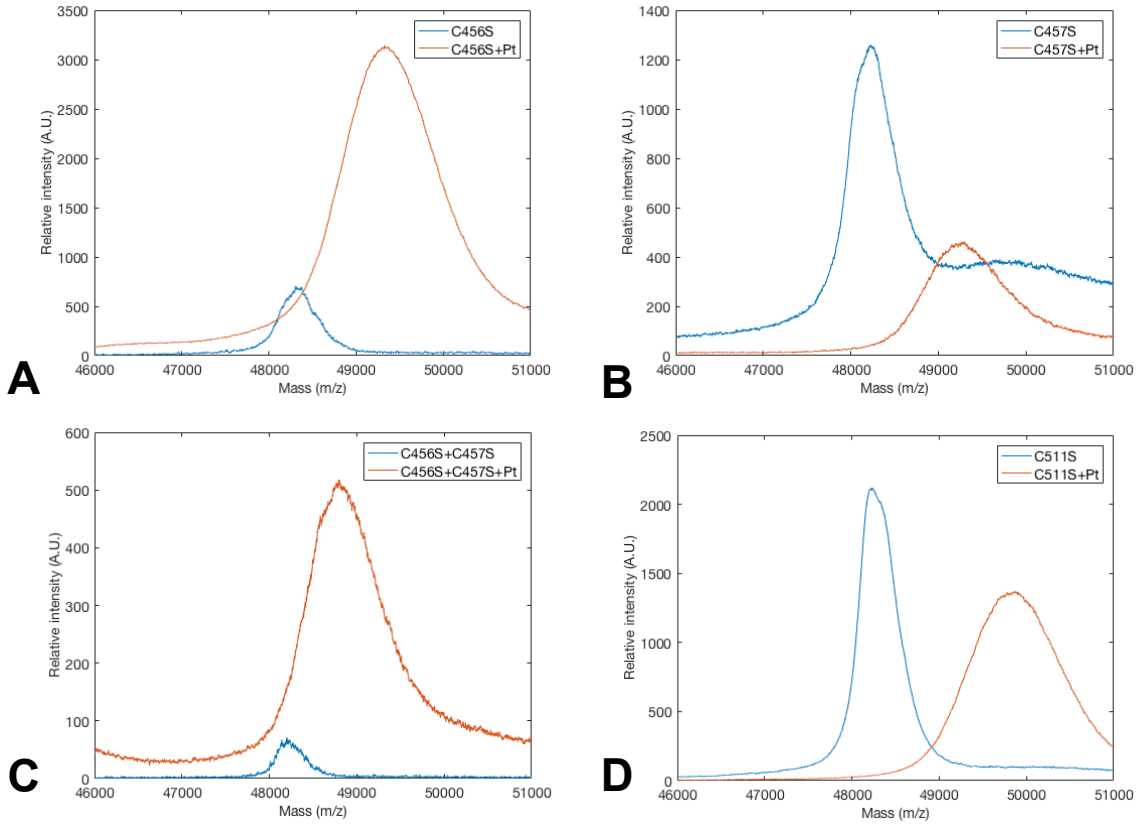

Figure 59: The intact masses for Cys456Ser (A), Cys457Ser mutant (B), Cys456Ser+Cys457Ser mutant (C), and Cys511Ser mutant (D) treated by cisplatin (red line), and cisplatin untreated proteins (blue line) detected by mass spectroscopy. The data are presented as intact mass (m/z) and each data point is represented as the mean ± S.E.M. of ten replicates.

replacements neither cisplatin treatment did alter overall protein yield and purity as documented by SDS-PAGE (Figure 57).

Unfortunately, the solvation of cisplatin is solute-dependent [19, 28, 311], moreover, the changes in ligands of the platinum complex can be observed depending on the media [32]. This fact could largely influence the measured total mass of the protein-cisplatin systems.

I detected intact masses for a complete set of C45 proteins (WT and mutants with replaced cysteine residues) in the presence and absence of cisplatin. For C45 WT, I determined intact mass in the presence of two other platinum complexes (carboplatin and oxaliplatin) (see Figure 61). Carboplatin and oxaliplatin were excluded from detailed study of binding to the C45 loop due to their negligible effects on the overall NKA activity. The detected intact masses for cisplatin untreated and treated proteins are summarized in Table 3.3 and in Figure 58, Figure 59, and Figure 60.

The intact masses of the C45 loops were detected using MALDI-TOF mass spectrometry that provided a molecular mass value of 48316 ± 31 Da, which is in good agreement with mass detected by SDS-PAGE and with previously published data [339]. The intact mass of cisplatin-treated C45 WT protein was determined as 49490 ± 20 Da

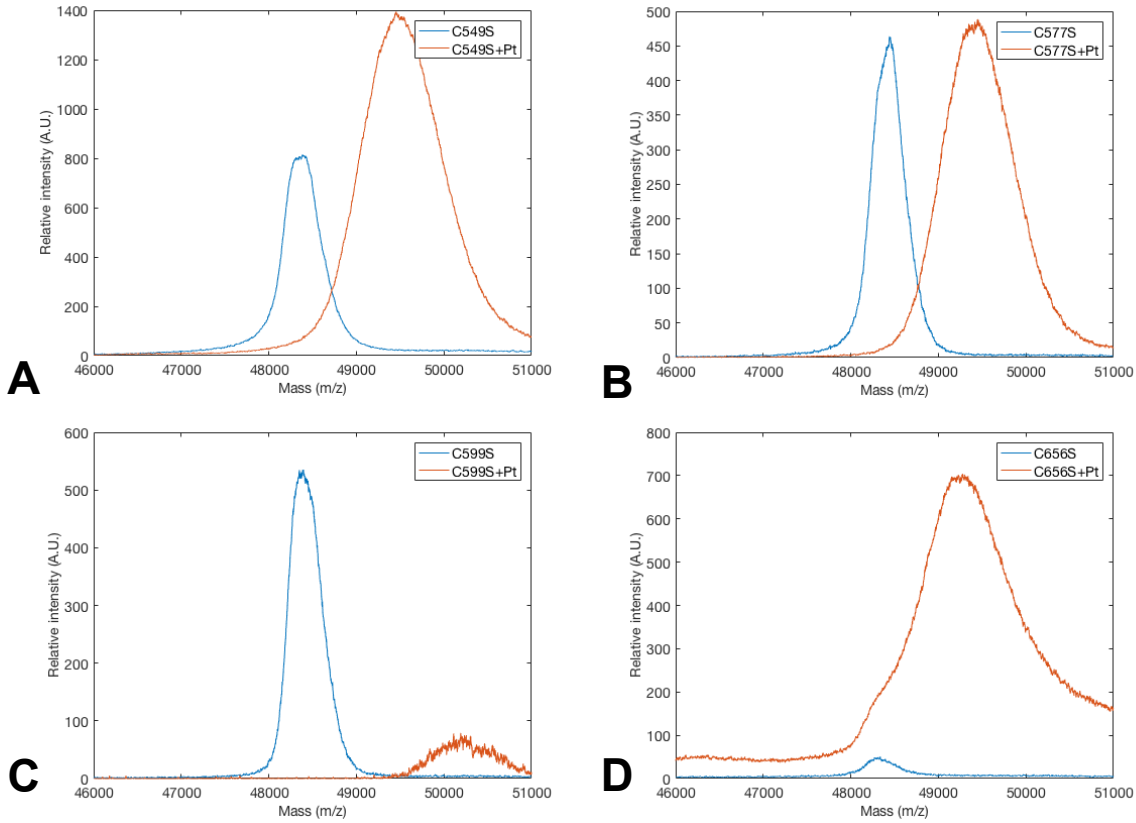

Figure 60: The intact masses for Cys549Ser (A), Cys577Ser mutant (B), Cys599Ser mutant (C), and Cys656Ser mutant (D) treated by cisplatin (red line), and cisplatin untreated proteins (blue line) detected by mass spectroscopy. The data are presented as intact mass (m/z) and each data point is represented as the mean ± S.E.M. of ten replicates.

(see Figure 62). The molecular mass difference between the treated and untreated C45 WT was approximately 1170 Da which suggested the formation of four or five adducts with cisplatin (see Figure 62).

The similar differences between treated and untreated proteins were observed for residues Cys367Ser, Cys421Ser, Cys549Ser and Cys599Ser. The lower value of molecular mass difference was detected for the residues Cys452Ser, Cys456Ser, Cys457Ser, Cys577Ser and Cys656Ser (Figure 62, Table 3.3) and was accounted for approximately 250 Da, indicating that these residues interact with cisplatin. For double mutant Cys456Ser+Cys457Ser the molecular weight of cisplatin untreated protein was 48181 ± 41 Da and cisplatin treated sample was 48803 ± 33 Da. The molecular weight difference detected for double mutant was only 620 Da which suggested the loss of binding of two cisplatin molecules (see Figure 62).

The abnormal mass difference was detected only for Cys511Ser mutant which exhibited mass difference 1573 ± 40 Da. This abnormal difference may be related with the potential protein misfolding.

Furthermore, the localization of cysteine residues were detected by the chemical modification using iodoacetate. The chemical modification increases the intact mass

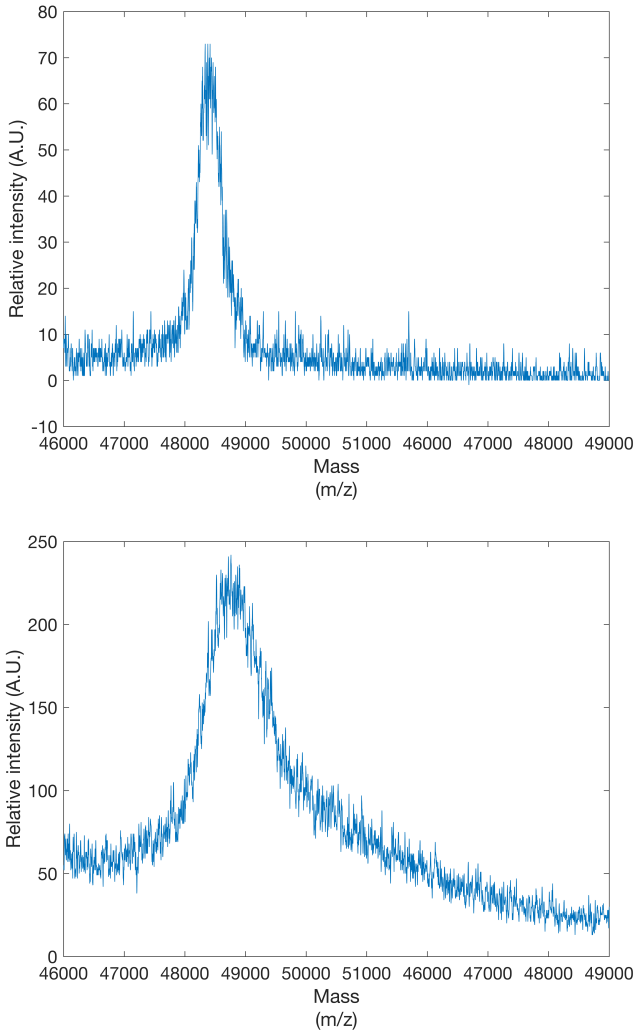

Figure 61: Intact masses of C45 WT loop detected by MALDI TOF mass spectrometry. The carboplatin treated C45 WT exhibited intact mass approximately 48910 Da (upper figure). Intact mass of oxaliplatin was approximately 49581 Da (lower figure).

of the protein in ratio 57 Da per one modified residue. For C45 WT was detected intact mass of 48428 ± 31 Da that suggested the modification of five cysteine residues. This difference remained constant after the cisplatin treatment which supported the hypothesis that cisplatin was not able to bind to the modified cysteine residues (see Figure 63).

Involvement of cysteine Cys367 which is only two residues apart from phosphorylation site at position Asp369 [57] was suggested by [339]. We detected negligible difference between molecular mass shifts of Cys367Ser mutant and C45 WT suggesting that impairment of NKA function is not caused by impairment of the phosphorylation.

The sequence of residues Cys452, Cys456 and Cys457 enables detection of the C45 loop by TC-FlAsH^{TM} reagent. This arsenic-based reaction may be used for detection of specific peptide consisting of amino acid sequence Cys-Cys-Gly-Pro-Cys-Cys. Within C45 loop can be found similar sequence, namely Cys-Ile-Glu-Ile-Cys-Cys. The binding of the TC-FlAsH^{TM} reagent to this sequence on C45 loop resulted in detected fluorescence signal (see Figure 64). For C45 WT we detected fluorescence signal similar to the

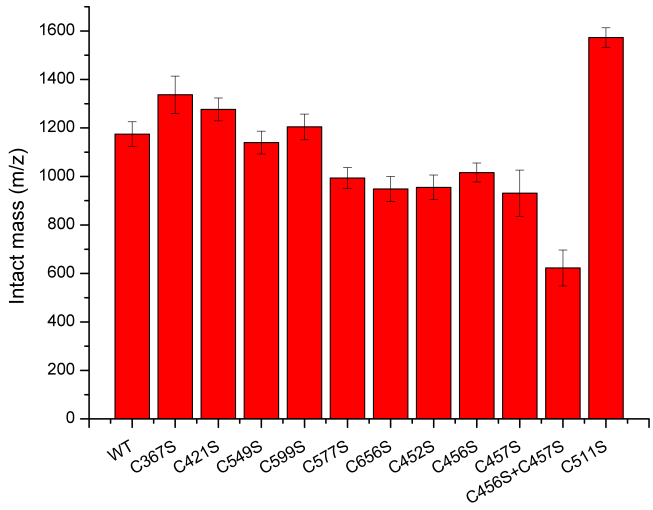

Figure 62: Relative changes in the intact mass of cisplatin untreated C45 WT and cisplatin treated C45 loops.

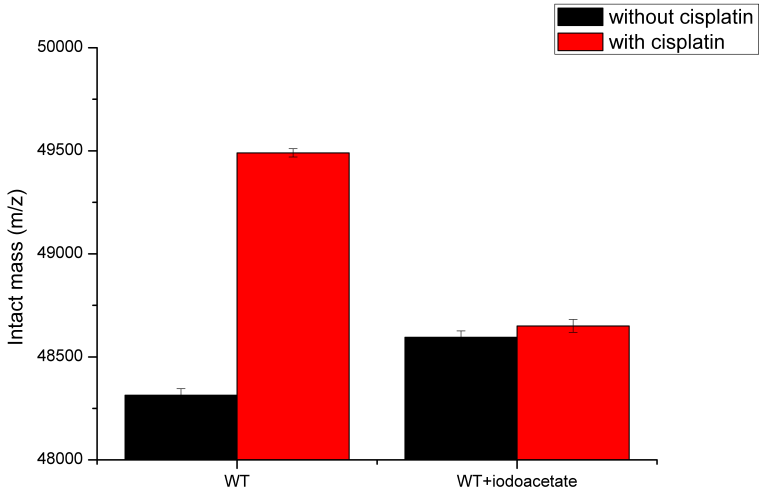

Figure 63: The changes in the intact mass of C45 WT proteins after chemical modification of cysteine residues. One aliquot of C45 WT protein without any modification was used as a control (WT) and two aliquots of C45 WT were subjected to chemical modification of cysteine residues (WT+iodoacetate). The intact mass was detected after the chemical modification (black) and after cisplatin treatment (red).

intensity of Coomassie stained band on SDS-PAGE. For C45 WT with bound cisplatin we detected the decrease in the fluorescence intensity due to cisplatin binding. For Cys452Ser mutant we detected strong fluorescence signal in the absence of cisplatin that decreases in the presence of cisplatin. We assume that the TC-FlAsH^{TM} reagent binds weakly to Cys456Ser and Cys457Ser already occupied by bound cisplatin. Similar situation was obtained for Cys457Ser, and C456S+C457S mutants. Additionally, the residue Cys456 possibly plays a key role in the binding of the TC-FlAsH^{TM} reagent.

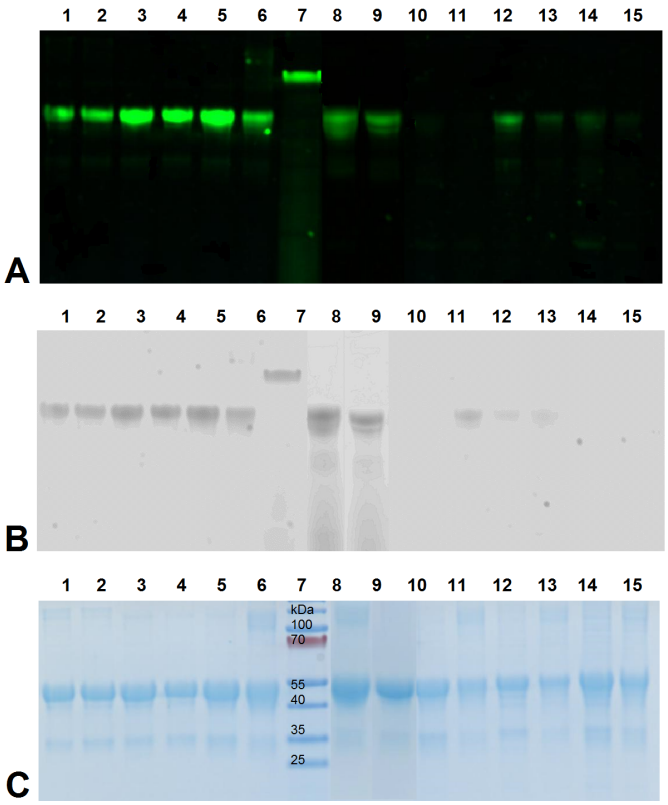

Figure 64: The SDS-PAGE and in gel fluorescence of TC-FlAsH^{TM}-tagged C45 WT, Cys452Ser, Cys456Ser, Cys457Ser, and Cys456Ser+Cys457Ser proteins, where the detected in gel fluorescence (A), negative image (B), and Coomassie stained SDS-PAGE gel. The samples were loaded in the following order: 1 – C45 WT the first elution before dialysis, 2 – C45 WT the second elution before dialysis, 3 – C45 WT the first elution after dialysis, 4 – C45 WT the second elution after dialysis, 5 – C45 WT without cisplatin, 6 – C45 WT with cisplatin, 7 – marker, 8 – Cys452Ser without cisplatin, 9 – Cys452Ser with cisplatin, 10 – Cys456Ser without cisplatin, 11 – Cys456Ser with cisplatin, 12 – Cys457Ser without cisplatin, 13 – Cys457Ser with cisplatin, 14 – Cys456Ser+Cys457Ser without cisplatin, 15 – C456S+C457S with cisplatin.

The mutation of this residue results in the loss of the fluorescence signal caused by reagent's inability to bind to the C45 loop.

The only controversy was observed for Cys511Ser mutant for which was not detected using the fluorescence signal. For Cys511Ser we also observed abnormal intact mass difference between cisplatin treated and untreated proteins. This protein is possibly misfolded and the observed abnormalities may be result of a conformational change.

3.5 Expression and Purification of Human C23 and C45 Loops

Some isoform-specific interactions can be evaluated using isolated C23 a C45 loops derived from main human variants of NKA (α_1, α_2 and α_3). For this purpose, we prepared the set of His-tagged C23 and C45 loops based on the human α sequences (sequences are listed in the supplementary material) and optimized the purification protocol.

The mouse brain C45 is standardly used in our laboratory. Its structure begins with amino acid sequence Leu354-Glu355-Ala356-Val357-Glu358 and ends with the sequence Leu773-Thr774-Ser775-Asn776-Ile777, which is localized on the transmembrane helix M5 (see Figure 65).

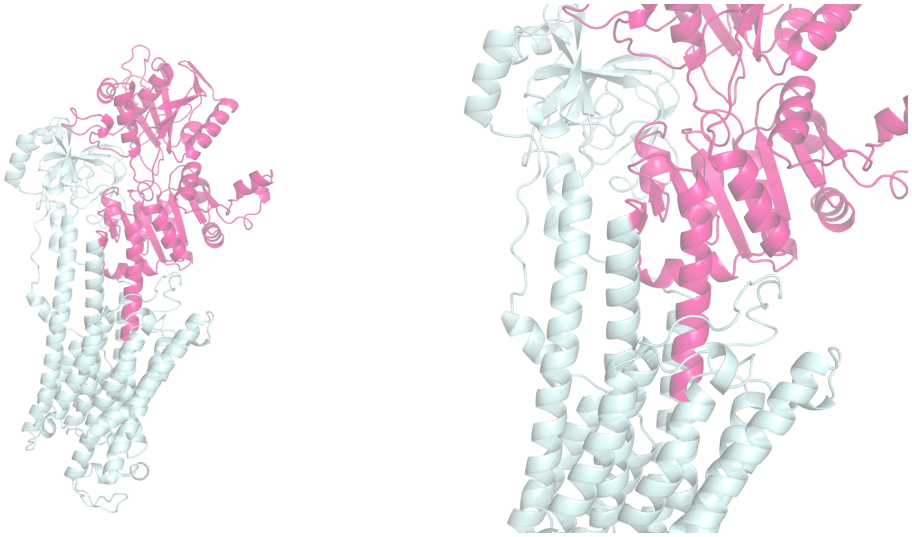

Figure 65: Left: The overall structure of mouse brain C45 loop. Right: The zoomed structure of the cytosol facing interface.

On the other hand, all human-based C45 loops begins with amino acid sequence Thr347-Ala348-Lys349-Arg350-Met351 and ends with the sequence Val762-Glu763-Glu764-Gly765-Arg766 (see Figure 66). These human variants of C45 loop are 14 amino acids longer on the C-terminus and 18 amino acids shorter on the C-terminus. But no significant changes in the protein yield or stability were detected.

The expression and purification of α_1 C45 and α_3 C45 is illustrated in Figure 67. Expression and purification of both proteins was optimized in collaboration with student under my supervision Martina Jamečná. We identified both proteins α_1 C45 and α_3 C45 in the elution. For efficient protein expression was used the low concentration of IPTG as well as the low cell density. Under those conditions we were able to prepare sufficient amount of the protein which was used for study of platinum-based complexes. Nonetheless, the α_2 C45 struggles to express as full size protein (see Figure 68). The human α_2 C45 possibly acquires the construct reclonning for the stable protein expression. None of the tested conditions (IPTG concentration, cell density, time and temperature of cultivation after induction) improved significantly the full size pro-

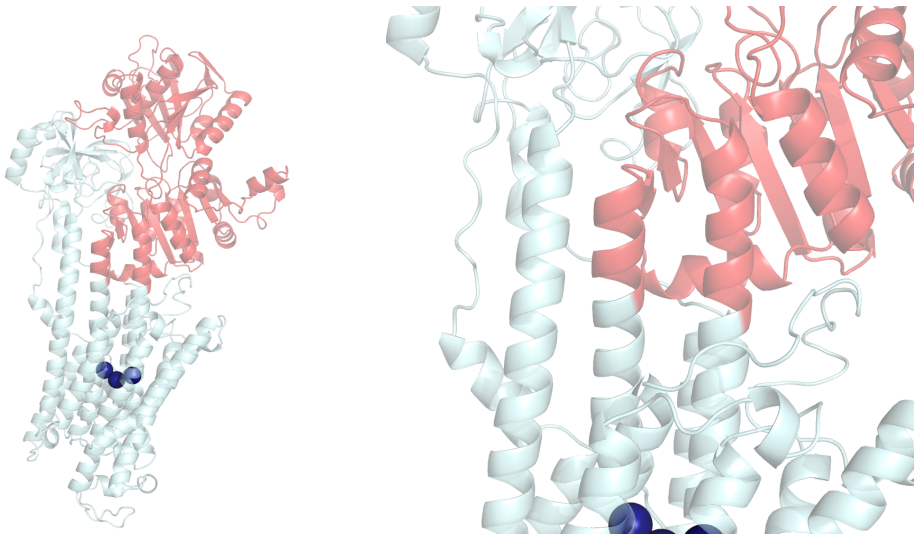

Figure 66: Left: The overall structure of human α_1 C45 loop. Right: The zoomed structure of the cytosol facing interface.

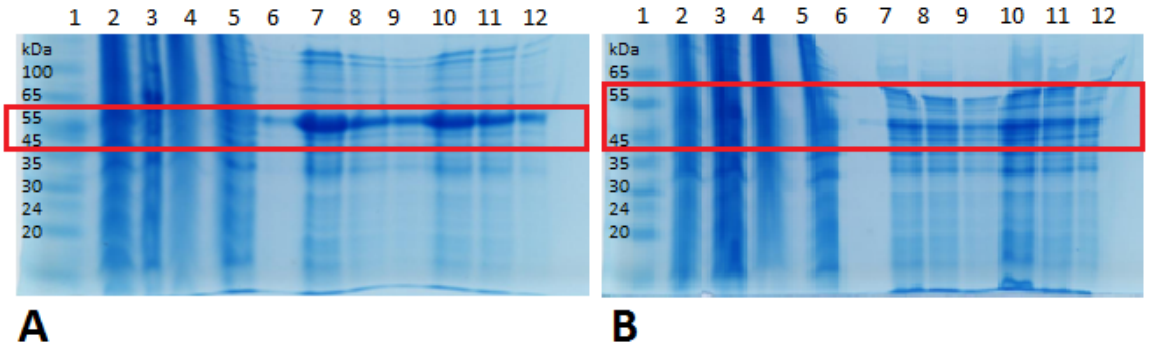

Figure 67: SDS-PAGE for α_1 (A) and α_3 (B) C45 loop. In the figure is highlighted in red the position of the C45 loop. The samples were loaded in the following order: 1 – marker, 2 – cells before disruption, 3 – supernatant from centrifugation, 4 – pellet from centrifugation, 5 – IMAC fall through, 6 – washes, 7 – 1st elution before dialysis, 8 – 2nd elution before dialysis, 9 – 3rd elution before dialysis, 10 – 1st elution after dialysis, 11 – 2nd elution after dialysis and 12 – 3rd elution after dialysis.

tein expression. Based on the analysis of the protocol used for the protein expression optimization, I assume that the difficulties occurs on the expression level.

Consequently, the C23 loops seems to be more complicated to prepare due to its small size and its interaction with the membrane. My construct missed the helices which are normally near the membrane (see Figure 15). I decided to prepare the truncated form of the loop due to aggregation of full-size construct. Unfortunately, it seemed that the protein preparation was not significantly improved, because no C23 was detected in elution when IMAC was used for protein purification (see samples 9 – 13 in Figure 68). The loss of the protein during IMAC might have been caused by the incorrect protein folding that resulted in the inaccessibility of the His-tag. I was able to obtain the protein using the centrifugal filters with two distinct MWCO (30

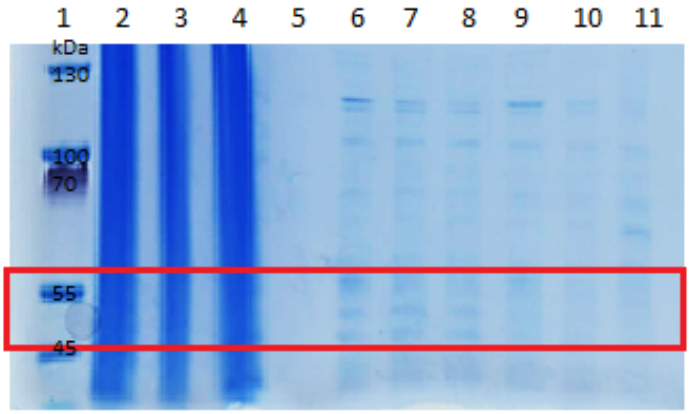

Figure 68: SDS-PAGE for α_2 C45 loop. In the figure is highlighted in red the position of the C45 loop. The samples were loaded in the following order: 1 – marker, 2 – supernatant from centrifugation, 3 – pellet from centrifugation, 4 – IMAC fall through, 5 – low salt washes (1 + 2), 6 – high salt wash, 7 – 1st elution before dialysis, 8 – 2nd elution before dialysis, 9 – 3rd elution before dialysis, 10 – 1st elution after dialysis, 11 – 2nd elution after dialysis and 12 – 3rd elution after dialysis.

kDa and 3 kDa, respectively). Nonetheless, the yield and purity of the final protein remained low (see samples 1 – 4 in Figure 69).

The prepared α_1 C45 and α_3 C45 loops were treated by the platinum-based complexes (cisplatin, carboplatin and oxaliplatin) that exhibited the toxicity to different cells and their intact mass was determined by mass spectroscopy.

For mouse brain C45, I detected approximately two molecules of carboplatin and three molecules of oxaliplatin interacting with C45. Unfortunately, I was not able to detect a complete set of intact masses for human α_1 and α_3 C45 loops treated by all three platinum complexes due to low signal detection (see Figure 70). Obtained results can be the starting point for the future research.

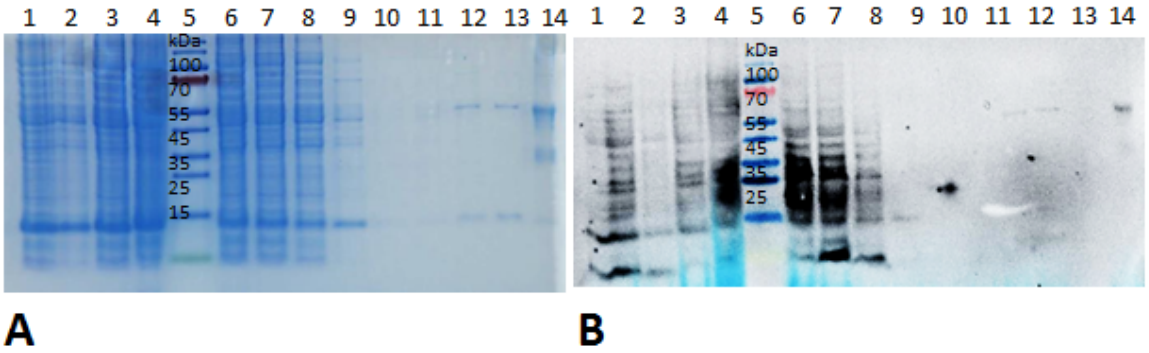

Figure 69: SDS-PAGE (A) and Western blot (B) of the C23 loop prepared using centrifugal filters (samples 1 – 4) and IMAC (samples 6 – 13). The Western blot detected the proteins using specific antibody against His-tag. The samples were loaded in the following order: 1 – supernatant from centrifugation, 2 – fall through filter with MWCO 30 kDa, 3 – concentrated protein using filter with MWCO 3 kDa, 4 – retained solution from 30 kDa MWCO filter, 5 – marker, 6 – supernatant centrifugation, 7 – fall through IMAC, 8 – low salt wash 1, 9 – high salt wash, 10 – low salt wash 2, 11 – 1st elution before dialysis, 12 – 2nd elution before dialysis, 13 – 3rd elution before dialysis, 14 – C45 WT (positive control).

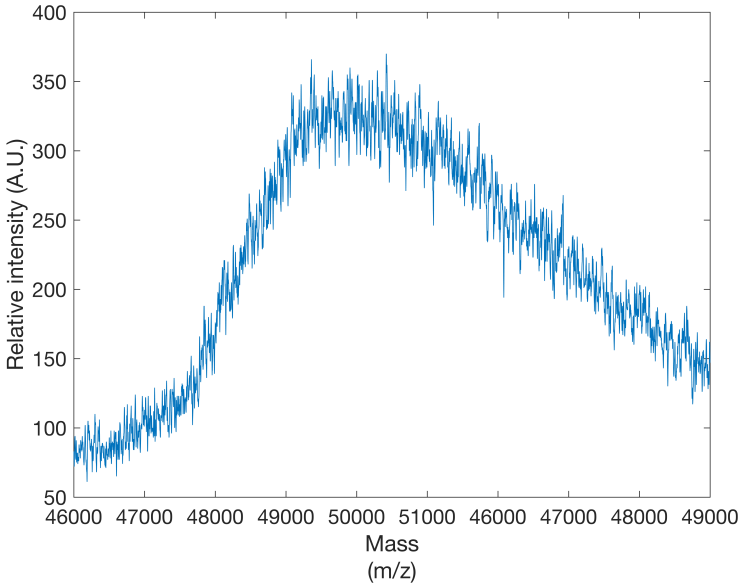

Figure 70: The intact mass for human α_1 C45 WT treated by cisplatin.

Chapter 4

Conclusions

4.1 Expression of NKA in Yeast

NKA is an essential membrane protein establishing the membrane potential by actively pumping sodium and potassium ions across the plasma membrane. I used and optimized two basic methods of NKA preparation – direct isolation from tissue and heterologous expression.

I prepared the cloning vector for the expression of human $\alpha_3\beta_1$ complex of NKA in the yeast, and I tested three distinct yeast strains (BJ5457, Gal4ΔPep4 and ΔPep4) for protein expression. I verified the presence of both (α and β) subunits in the membrane fraction, and in the final pure protein sample for all tested strains. The protocol for cultivation and purification was subjected to detailed optimization (in collaboration with my Bc. student Veronika Kolomazníková).

Furthermore, I prepared a set of single amino acid mutants linked with the neurological disorders (Asp811Asn, Glu825Lys and Gly957Arg mutants). All proteins (WT and mutants) exhibited similar expression level suggesting no influence of the protein expression caused by mutation.

4.2 Isolation of NKA From Porcine Kidney

Our laboratory standardly prepares the NKA from porcine kidney using the protocol based on procedure reported by Fedosova *et al.* [149] with some modifications. Namely, I introduced the step of the rough homogenization of dissected tissue (in the kitchen blender) before the homogenization in the teflon homogenizer. This step significantly improved the protein yield, purity and stability.

The enzyme prepared using this method may be used for the ATPase activity determination using both Baginsky assay and Enzyme coupled method. In this thesis, I preferably used the Baginsky assay for its experimental convenience, low time and

financial consumptions. Moreover, the Baginsky assay was automated using the pipetting station and used for the testing of a large number of the potential NKA inhibitors.

4.3 Interaction of NKA With Small Molecules

All compounds were tested on the porcine kidney NKA isolated by the above mentioned method, and the final concentration of tested compounds was 10 μM.

In this thesis, I examined the interactions of NKA with selected small molecules (flavonolignans, halogenated quinolinones, and platinum-based complexes). I evaluated the inhibitory effect of these small molecules and determined the mechanism of their inhibition.

4.3.1 Flavonolignans

I tested eight flavonolignans (SB, SD, SCH, QUE, DHSB, DHSD, DHSCH, and TAX) from which only three (DHSD, SCH, and DHSCH) exhibited the substantial NKA inhibition. Flavonolignans showed the limited water solubility which is their main disadvantage. Despite the limited range of useful concentrations, the IC_{50} values for DHSD, SCH, and DHSCH were determined and were accounted for 36 ± 14 μM, 110 ± 40 μM, and 38 ± 8 μM, respectively.

I determined the Na^+, K^+, and ATP-dependent NKA activation in the presence or absence of flavonolignans or ouabain. My results suggested that the inhibitory mechanism of flavonolignans differ from ouabain, the specific inhibitor of NKA and typical representative of the cardiotonic steroid family.

I prepared the isolated cytoplasmic loop C45, and verified that flavonolignans bind there as predicted by molecular docking.

4.3.2 Halogenated Hydroquinolinones

Halogenated hydroquinolinones are chemical analogues of flavonolignans. From the large group of tested halogenated hydroquinolinones only one compound, called TFHPQ, significantly inhibited the NKA activity. By contrast, the monochloro- and dichloro-derivatives did not exhibit substantial NKA inhibition.

Similarly to flavolignans, halogenated hydroquinolinones showed limited solubility, therefore the determination of the IC_{50} value was proceeded with low precision. At 10 μM concentration, TFHPQ decreased the NKA activity to approximately 45% suggesting the IC_{50} value to be slightly below 10 μM. For future use, the solubility should be improved by the chemical modification, or by the encapsulation which might increase the bioavaibility of TFHPQ.

The predicted binding site for TFHPQ was found in the close proximity of C-

terminal pathway. The binding of TFHPQ into this site may cause the steric impairment of the ion transport. This mechanism of the inhibition varied from the mechanism described for ouabain.

4.3.3 Platinum-Based Drugs

I tested the influence of anti-cancer agents – cisplatin, carboplatin and oxaliplatin – on the porcine kidney NKA. Carboplatin and oxaliplatin did not seem to inhibit the NKA. By contrast, cisplatin completely supressed the NKA activity. The inhibition by cisplatin was studied in detail.

I identified 5 cysteine residues (Cys452Ser, Cys456Ser, Cys457Ser, Cys577Ser, and Cys656Ser) on the C45 loop interacting with cisplatin. They represents the binding sites of cisplatin on the C45 loop as unambiguously determined and confirmed by mass spectrometry.

4.4 Human C23 and C45 Loops

I prepared a set of C23 and C45 loops derived from the human α_1, α_2, and $\alpha 3$ sequences. All those loops were overexpressed in bacteria cells. The isolated human α_1 and α_3 C45 loops were successfully prepared using the heterologous protein expression method. The protocol for this preparation was optimized (in the collaboration with my Bc. student Martina Jamečná). Unfortunately, human α_2 C45 was prepared in the truncated form. The used vector for the protein expression should be improved in order to obtain the natural structure of the human α_2 C45 protein. Current results may be the starting point for investigation of the isoform-related NKA inhibition.

Bibliography

[1] Hana R Pohl, John S Wheeler, and H Edward Murray. Interrelations between Essential Metal Ions and Human Diseases. In *Metal Ions in Life Sciences*, volume 13, pages 29–47. Springer, 2013.

[2] N. A. Delamere, S. Tymiya, and S. Tamiya. Lens ion transport: from basic concepts to regulation of Na^+/K^+-ATPase activity. *Experimental Eye Research*, 6(9):2166–2171, 2008.

[3] Mohd Suhail. Na^+/K^+-ATPase : Ubiquitous Multifunctional Transmembrane Protein and its Relevance to Various Pathophysiological Conditions. *Journal of Clinical Medicine Research*, 2(1):1–17, 2010.

[4] P. Babula, M. Masarik, V. Adam, I. Provaznik, and R. Kizek. From $Na^+[K^+$-ATPase and Cardiac Glycosides to Cytotoxicity and Cancer Treatment. *Anti-Cancer Agents in Medicinal Chemistry*, 13(March):1069–87, 2013.

[5] A. G. Therien and R. Blostein. Mechanisms of Sodium Pump Regulation. *American journal of physiology. Cell physiology*, 279(3):C541–66, 2000.

[6] J. B. Lingrel. The Physiological Significance of the Cardiotonic Steroid/Ouabain-Binding Site of the Na^+/K^+-ATPase. *Annual Review of Physiology*, 72:395–412, 2010.

[7] Vladimir V. Matchkov and Igor I. Krivoi. Specialized Functional Diversity and Interactions of the Na^+/K^+-ATPase. *Frontiers in Physiology*, 7(MAY), 2016.

[8] A. G. Therien and R. Blostein. Mechanisms of Sodium Pump Regulation. *American journal of physiology. Cell physiology*, 279(3):C541–66, 2000.

[9] H. Poulsen, H. Khandelia, J. P. Morth, M. Bublitz, O. G. Mouritsen, J. Egebjerg, and P. Nissen. Neurological Disease Mutations Compromise a C-Terminal Ion Pathway in the $Na^+[K^+$-ATPase. *Nature*, 467(7311):99–102, 2010.

[10] E. L. Heinzen, K. J. Swoboda, Y. Hitomi, F. Gurrieri, B. de Vries, F. D. Tiziano, B. Fontaine, N. M. Walley, M. T. Sweney, T. M. Newcomb, L. Viollet, C. Huff, B. Lynn, S. P. Reyna, K. J. Murphy, K. V. Shianna, and C. E. Gumbs. *De novo* Mutations in *ATP1A3* Cause Alternating Hemiplegia of Childhood. *Nature Genetics*, 44(9):1030–1034, 2013.

[11] K. M. Weigand, M. Messchaert, H. G. P. Swarts, F. G. M. Russel, and J. B. Koenderink. Alternating Hemiplegia of Childhood Mutations Have a Differential Effect on $Na^+[K^+$-ATPase Activity and Ouabain Binding. *Biochimica et Biophysica Acta - Molecular Basis of Disease*, 1842(7):1010–1016, 2014.

[12] Alexey Bogdanov, Fedor Moiseenko, and Michael Dubina. Abnormal expression of *ATP1A1* and *ATP1A2* in breast cancer. *F1000 Research*, 6:10, 2017.

[13] Li Nan Zhang, Yong Jun Sun, Shuo Pan, Jun Xia Li, Yin E. Qu, Yao Li, Yong Li Wang, and Zi Bin Gao. Na^+/K^+-ATPase, a Potent Neuroprotective Modulator Against Alzheimer Disease. *Fundamental and Clinical Pharmacology*, 27(1):96–103, 2013.

[14] Alex Bateman, Maria Jesus Martin, Claire O'Donovan, Michele Magrane, Rolf Apweiler, Emanuele Alpi, Ricardo Antunes, Joanna Arganiska, Benoit Bely, Mark Bingley, Carlos Bonilla, Ramona Britto, Borisas Bursteinas, Gayatri Chavali, Elena Cibrian-Uhalte, Alan Da Silva, Maurizio De Giorgi, Tunca Dogan, Francesco Fazzini, Paul Gane, Leyla Garcia Castro, Penelope Garmiri, Emma Hatton-Ellis, Reija Hieta, Rachael Huntley, Duncan Legge, Wudong Liu, Jie Luo, Alistair Macdougall, Prudence Mutowo, Andrew Nightingale, Sandra Orchard, Klemens Pichler, Diego Poggioli, Sangya Pundir, Luis Pureza, Guoying Qi, Steven Rosanoff, Rabie Saidi, Tony Sawford, Aleksandra Shypitsyna, Edward Turner, Vladimir Volynkin, Tony Wardell, Xavier Watkins, Hermann Zellner, Andrew Cowley, Luis Figueira, Weizhong Li, Hamish McWilliam, Rodrigo Lopez, Ioannis Xenarios, Lydie Bougueleret, Alan Bridge, Sylvain Poux, Nicole Redaschi, Lucila Aimo, Ghislaine Argoud-Puy, Andrea Auchincloss, Kristian Axelsen, Parit Bansal, Delphine Baratin, Marie Claude Blatter, Brigitte Boeckmann, Jerven Bolleman, Emmanuel Boutet, Lionel Breuza, Cristina Casal-Casas, Edouard De Castro, Elisabeth Coudert, Beatrice Cuche, Mikael Doche, Dolnide Dornevil, Severine Duvaud, Anne Estreicher, Livia Famiglietti, Marc Feuermann, Elisabeth Gasteiger, Sebastien Gehant, Vivienne Gerritsen, Arnaud Gos, Nadine Gruaz-Gumowski, Ursula Hinz, Chantal Hulo, Florence Jungo, Guillaume Keller, Vicente Lara, Philippe Lemercier, Damien Lieberherr, Thierry Lombardot, Xavier Martin, Patrick Masson, Anne Morgat, Teresa Neto, Nevila Nouspikel, Salvo Paesano, Ivo Pedruzzi, Sandrine Pilbout, Monica Pozzato, Manuela Pruess, Catherine Rivoire, Bernd Roechert, Michel Schneider, Christian Sigrist, Karin Sonesson, Sylvie Staehli, Andre Stutz, Shyamala Sundaram, Michael Tognolli, Laure Verbregue, Anne Lise Veuthey, Cathy H. Wu, Cecilia N. Arighi, Leslie Arminski, Chuming Chen, Yongxing Chen, John S. Garavelli, Hongzhan Huang, Kati Laiho, Peter McGarvey, Darren A. Natale, Baris E. Suzek, C. R. Vinayaka, Qinghua Wang, Yuqi Wang, Lai Su Yeh, Meher Shruti Yerramalla, and Jian Zhang. UniProt: A hub for protein information. *Nucleic Acids Research*, 43(D1):D204–D212, 2015.

[15] L. Grycova, P. Sklenovsky, Z. Lansky, M. Janovska, M. Otyepka, E. Amler, J. Teisinger, and M. Kubala. ATP and Magnesium Drive Conformational Changes of the Na^+/K^+-ATPase Cytoplasmic Headpiece. *Biochimica et Biophysica Acta - Biomembranes*, 1788(5):1081–1091, 2009.

[16] R. A. Newman, P. Yang, A. D. Pawlus, and K. I. Block. Cardiac Glycosides as Novel Cancer Therapeutic Agents. *Molecular Interventions*, 8:36–49, 2008.

[17] G. Giaccone. Clinical Perspectives on Platinum Resistance. *Drugs*, Suppl 4:9–17, 2000.

[18] Victoria Cepeda, Miguel Fuertes, Josefina Castilla, Carlos Alonso, Celia Quevedo, and Jose Perez. Biochemical Mechanisms of Cisplatin Cytotoxicity. *Anti-Cancer Agents in Medicinal Chemistry*, 7(1):3–18, 2007.

[19] Viktor Brabec, Ondrej Hrabina, and Jana Kasparkova. Cytotoxic platinum coordination compounds . DNA binding agents. *Coordination Chemistry Reviews*, (May):1–30, 2017.

[20] A. Dzagnidze, Z. Katsarava, J. Makhalova, J. Liendert, M. S. Yoon, H. Kaube, and Et Al. Repair Capacity for Platinum-DNA Adducts Determines the Severity of Cisplatin-Induced Peripheral Neuropathy. *Journal of Neuroscience*, 27:9451–9457, 2007.

[21] K. Barabas, R. Milner, D. Lurie, and C. Adin. Cisplatin: a Review of Toxicities and Therapeutic Applications. *Veterinary and Comparative Oncology*, 6:1–18, 2008.

[22] F. Ries and J. Klastersky. Nephrotoxicity induced by cancer-chemotherapy with special emphasis on cisplatin toxicity. *American Journal of Kidney Diseases*, 8:368–379, 1989.

[23] N. Pabla and Z. Dong. Cisplatin Nephrotoxicity: Mechanisms and Renoprotective Strategies. *Kidney International*, 73:994–1007, 2008.

[24] R. P. Miller, R. K. Tadagavadi, G. Ramesh, and W. B. Reeves. Mechanisms of cisplatin nephrotoxicity. *Toxins*, 2:2490–2518, 2010.

[25] Martin Kubala, Jaroslava Geleticova, Miroslav Huliciak, Martina Zatloukalova, Jan Vacek, and Marek Sebela. Na^+/K^+-ATPase inhibition by cisplatin and consequences for cisplatin nephrotoxicity. *Biomedical Papers*, 158(2):194–200, 2014.

[26] M. F. Howe-Grant and S. J. Lippard. *Metals Ions in Biochemical Systems*. Marcel Dekker, New York, USA, 1980.

[27] E. R. Jamieson and S. J. Lippard. Structure, Recognition, and Processing of Cisplatin-DNA Adducts. *Chemical Reviews*, 99:2467–2498, 1999.

[28] Yongwon Jung and Stephen J Lippard. Direct Cellular Responses to Platinum-Induced DNA Damage Direct Cellular Responses to Platinum-Induced DNA Damage. *Chemical reviews*, 107(5):1387–1407, 2007.

[29] T. Ishikawa and F. Aliosman. Glutathione-Associated Cis-Diamminodichloroplatinum(II) Metabolism and ATP-Dependent Efflux from Leukemia Cells - Molecular Characterization of Glutathione-Platinum Complex and Its Biological Significance. *Journal of Biological Chemistry*, 268:20116–20125, 1993.

[30] C. G. Hartinger, W. H. Ang, A. Casisni, L. Messori, B. K. Keppler, and B. K. Dyson. Mass Spectroscopic Analysis of Ubiquitin-Platinum Interactions of Leading Anticancer Drugs: MALDI Versus ESI. *Journal of Analytical Atomic Spectrometry*, 22:960–967, 2007.

[31] C. G. Hartinger, Y. O. Tsybin, J. Fuchser, and P. J. Dyson. Characterization of Platinum Anti-Cancer Drug Protein-Binding Sites Using a Top-Down Mass Spectrometric Approach. *Inorganic Chemistry*, 47:17–19, 2008.

[32] Miroslav Huliciak, Linda Reinhard, Mette Laursen, Natalya Fedosova, Poul Nissen, and Martin Kubala. Crystals of Na^+/K^+-ATPase with Bound Cisplatin. *Biochemical Pharmacology*, 92:494–498, 2014.

[33] M. Futai, Y. Wada, and J. H. Kaplan, editors. *Handbook of ATPases*. WILEY-VCH, Weinheim, Germany, 1. st edition, 2004.

[34] P. L. Pedersen and E. Carafoli. Ion Motive ATPases. I. Ubiquity, Properties, and Significance to Cell Function. *Trends in Biochemical Sciences*, 12:146–150, 1987.

[35] B. Alberts, A. Johnson, J. Lewis, and M. Raff. *Molecular Biology of the Cell*. Garland Science, New York, USA, fifth eddi edition, 2008.

[36] J. C. Skou. The Influence of Some Cations on an Adenosin Triphosphatase From Peripheral Nerves. *Biochimica et Biophysica Acta (BBA)*, 23:394–401, 1957.

[37] A. K. Sen and R. L. Post. Stoichiometry and Localization of Adenosine Triphosphoate-Dependent Sodium and Potassium Transport in the Erythrocyte. *The Journal of biological chemistry*, 239(1):345–52, 1964.

[38] S. Lutsenko and J. Kaplan. Organization of P-type ATPases Significance of Structural Diversity. *Biochemistry*, 34(48):6003–6013, 1995.

[39] C. Toyoshima and F. Cornelius. New crystal structures of PII-type ATPases: excitement continues. *Current Opinion in Structural Biology*, 23:507–514, 2013.

[40] J. P. Abrahams, A. G. W. Leslie, R. Lutter, and J. Walker. Structure at 2.8 Â Resolution of F1-ATPase from Bovine Heart Mitochondria. *Nature*, 370:621–628, 1994.

[41] C. Toyoshima, M. Nakasako, H. Nomura, and H. Ogawa. Crystal Structure of the Calcium Pump of Sarcoplasmic Reticulum at 2.6 ÅResolution. *Nature*, 405:647–655, 2000.

[42] M. Noji, R. Yasuda, M. Yoshida, and K. Kinoshita. Direct Observation of the Rotation of F1-ATPase. *Nature*, 386:299–302, 1997.

[43] Y. Sambongi, Y. Iko, M. Tanabe, H. Omote, A. Iwamoto-Kihara, I. Ueda, T. Yanagida, Y. Wada, and M. Futai. Mechanical Rotation of the C Subunit Oligomer in ATP Synthase (F0F1): Direct Observation. *Science*, 286:1722–1724, 1999.

[44] T. Shinoda, H Ogawa, F. Cornelius, and C. Toyoshima. Crystal Structure of the Sodium-Potassium Pump at 2.4 ÅResolution. *Nature*, 459(7245):446–50, may 2009.

[45] H. Ogawa, T. Shinoda, F. Cornelius, and C. Toyoshima. Crystal Structure of the Sodium-Potassium Pump ($Na^+[K^+$-ATPase) with Bound Potassium and Ouabain. *Proceedings of the National Academy of Sciences of the United States of America*, 106(33):13742–7, aug 2009.

[46] R. Kanai, H. Ogawa, B. Vilsen, F. Cornelius, and C. Toyoshima. Crystal Structure of a Na^+-bound Na^+[K^+-ATPase Preceding the E1P State. *Nature*, 502(7470):201–6, 2013.

[47] M. Nyblom, L. Reinhard, M. Andersson, E. Lindahl, N. Fedosova, and P. Nissen. Crystal Structure of Na^+[K^+-ATPase in the Na^+-Bound State. *Science*, 342(2013):123–127, 2013.

[48] M. Dobretsov and J. R. Stimers. Neuronal Function and α_3 Isoform of the Na^+[K^+-ATPase. *Front iers in Bioscience*, 10:2373–2396, 2005.

[49] K. Geering. Functional Roles of Na^+[K^+-ATPase Subunits. *Current Opinion in Nephrology and Hypertension*, 17(5):526–532, 2008.

[50] D. W. Martin. Structure-Function Relationships in Na^+[K^+-pump. *Seminars in Nephrology*, 25(5):282–91, sep 2005.

[51] H. Azouaoui, C. Montigny, T. Dieudonn, P. Champeil, A. Jacquot, J. L. Vázquez-Ibar, P. Le Maréchal, J. Ulstrup, M. R. Ash, J. A. Lyons, G. Lenoir, and Poul Nissen. High Phosphatidylinositol 4-Phosphate (PI4P)-Dependent ATPase Activity for the Drs2p-Cdc50p Flippase After Removal of its N- and C-Terminal Extensions. *The Journal of Biological Chemistry*, 292:7954–7970, 2017.

[52] C. Toyoshima, R. Kanai, and F. Cornelius. First Crystal Structures of Na^+[K^+-ATPase: New Light on the Oldest Ion Pump. *Structure*, 19(12):1732–1738, 2011.

[53] Haruo Ogawa and Chikashi Toyoshima. Homology modeling of the cation binding sites of Na^+/K^+-ATPase. *Proceedings of the National Academy of Sciences of the United States of America*, 99(25):15977–15982, 2002.

[54] Maike Bublitz, Hanne Poulsen, J. Preben Morth, and Poul Nissen. In and Out of the Cation Pumps: P-type ATPase Structure Revisited. *Current Opinion in Structural Biology*, 20(4):431–9, aug 2010.

[55] P. Čechová, K. Berka, and M. Kubala. Ion Pathways in the Na^+[K^+-ATPase. *Journal of Chemical Information and Modeling*, 2:acs.jcim.6b00353, 2016.

[56] M. Hilge, G. Siegal, G. W. Vuister, P. Güntert, S. M. Gloor, and J. P. Abrahams. ATP-induced conformational changes of the nucleotide-binding domain of Na^+,K^+-ATPase. *Nature Structural and Molecular Biology*, 10:469–474, 2003.

[57] P. A. Pedersen. Importance of Conserved α Subunit Segment 709GDGVND for Mg^{2+} Binding, Phosphorylation, and Energy Transduction in Na^+[K^+-ATPase. *Journal of Biological Chemistry*, 275(48):37588–37595, sep 2000.

[58] P. L. Jorgensen, K. O. Hakansson, and S. J. D. Karlish. Structure and Mechanism of Na^+[K^+-ase: Functional Sites and Their Interactions. *Annual Review of Physiology*, 65(1):817–849, 2003.

[59] Käthi Geering. The Functional Role of β Subunits in Oligomeric P-type ATPases. *Journal of Bioenergetics and Biomembranes*, 33(5):425–438, 2001.

[60] C. Gatto, S. M. McLoud, and J. H. Kaplan. Heterologous Expression of Na^+/K^+-ATPase in Insect Cells: Intracellular Distribution of Pump Subunits. *American journal of physiology. Cell physiology*, 281(3):C982–C992, 2001.

[61] M. D. Laughery, M. L. Todd, and J. H. Kaplan. Mutational Analysis of α-β Subunit Interactions in the Delivery of Na^+/K^+-ATPase Heterodimers to the Plasma Membrane. *Journal of Biological Chemistry*, 278(37):34794–34803, 2003.

[62] R. E. Dempski. The β Subunit of the $Na^+[K^+$-ATPase Follows the Conformational State of the Holoenzyme. *The Journal of General Physiology*, 125(5):505–520, apr 2005.

[63] L. Kirley. Inactivation of Na^+/K^+-ATPase by β-Mercaptoethanol. *The Journal of Biological Chemistry*, 265:4227–4232, 1990.

[64] S. Lutsenko and J. H. Kaplan. An Essential Role for the Extracellular Domain of the Na^+/K^+-ATPase β Subunit in Cation Occlusion. *Biochemistry*, 32(26):6737–6743, 1993.

[65] G. Crambert, U. Hasler, A. Beggah, N. Yu, N. N. Modyanov, J. D. Horisberger, L. G. Lelievre, and K. Geering. Transport and Pharmacological Properties of Nine Different Human Na^+/K^+-ATPases Isozymes. *Journal of Biological Chemistry*, 275:1976–1986, 2000.

[66] L. Zhang, K. J. Morris, and Y. C. Ng. Fiber Type-Specific Immunostaining of the Na^+/K^+-ATPase Subunit Isoforms in Skeletal Muscle: Age-Associated Differential Changes. *Biochimica et Biophysica Acta (BBA)*, 1762:783–793, 2006.

[67] B. R. Larsen, M. Assentoft, M. L. Cotrina, S. Z. Hua, M. Nedergaard, K. Kaila, J. Voipio, and N. MacAulay. Contributions of the Na^+/K^+-ATPase, NKCC1, and Kir4.1 to Hippocampal K^+ Clearance and Volume Responses. *Glia*, 62:608–622, 2014.

[68] M. DiFranco, H. Hakimjavadi, J. B. Lingrel, and J. A. Heiny. Na^+/K^+-ATPase Activity in Mammalian Skeletal Muscle T-Tubules is Acutely Stimulated by Extracellular K^+. *Journal of General Physiology*, 146:281–294, 2015.

[69] F. Hilbers, W. Kopec, T. J. Isaksen, T. H. Holm, K. Lykke-Hartmann, P. Nissen, H. Khandelia, and H. Poulsen. Tuning of the $Na^+[K^+$-ATPase by the β Subunit. *Nature Scientific Reports*, 6(October 2015):20442, 2016.

[70] P D Wilson, O Devuyst, X Li, L Gatti, D Falkenstein, S. Robinson, D. Fambrough, and C. R. Burrow. Apical Plasma Membrane Mispolarization of Na^+/K^+-ATPase in Polycystic Kidney Disease Epithelia Is Associated with Aberrant Expression of the β_2 Isoform. *The American Journal of Pathology*, 156(1):253–268, 2000.

[71] K. Geering. FXYD Proteins: New Regulators of Na^+/K^+-ATPase. *American Journal of Renal Physiology*, 290:F241–F250, 2006.

[72] E. A. Jewell and J. B. Lingrel. Comparison of the Substrate Dependence Properties of the Rat Na^+/K^+-ATPase α_1, α_2, and α_3 Isoforms Expressed in HeLa Cells. *Journal of Biological Chemistry*, 266:16925–16930, 1991.

[73] J. S. Munzer, S. E. Daly, E. A. Jewell-Motz, J. B. Lingrel, and R. Blostein. Tissue- and Isoform-Specific Kinetic Behavior of the Na^+/K^+-ATPase. *Journal of Biological Chemistry*, 269:16668–16676, 1994.

[74] G. Bianco, G. Sanchez, and R. W. Mercer. Comparison of the Enzymatic Properties of the Na^+/K^+-ATPase $\alpha_3\beta_1$ and $\alpha_3\beta_2$ Isozymes. *Biochemistry*, 34:9897–9903, 1995.

[75] A. G. Therien, N. B. Nestor, W. J. Ball, and R. Blostein. Tissue-Specific Versus Isoform-Specific Differences in Cation Activation Kinetics of the Na^+/K^+-ATPases. *Journal of Biological Chemistry*, 271:7104–7112, 1996.

[76] R. Zahler, Z.-T. Zhang, M. Manor, and W. F. Boron. Sodium Kinetics of Na^+/K^+-ATPase a Isoforms in Intact Transfected HeLa Cells. *Journal of General Physiology*, 213:201–213, 1997.

[77] V. V. Senatorov, D. Mooney, and B. Hu. The Electrogenic Effects of Na^+/K^+-ATPase in Rat Auditory Thalamus. *Journal of Physiology*, 502:375–385, 1997.

[78] V. V. Senatorov and B. Hu. Differential Na^+/K^+-ATPase Activity in Rat Lemniscal and Non-Lemniscal Auditory Thalami. *Journal of Physiology*, 502:387–395, 1997.

[79] D. M. Balshaw, L. A. Millette, K. Tepperman, and E. T. Wallick. Combined Allosteric and Competitive Interaction Between Extracellular Na^+ and K^+ During Ion Transport by α_1, α_2, α_3 Isoform of the Na^+/K^+-ATPase. *Biophysical Journal*, 79:853–862, 2000.

[80] A. W. Shyjan and R. Levenson. Antisera Specific for the α_1, α_2, α_3, and β Subunits of the Na^+/K^+-ATPase: Differential Expression of α and β Subunits in Rat Tissue Membranes. *Biochemistry*, 28:4531–4535, 1989.

[81] O. Urayama, H. Shutt, and K. J. Sweadner. Identification of There Isozyme Proteins of the Catalytic Subunit of the Na^+/K^+-ATPase in Rat Brain. *Journal of Biological Chemistry*, 264:8271–8280, 1989.

[82] A. W. Shyjan, V. Cena, D. C. Klein, and R. Levenson. Differential Expression and Enzymatic Properties of the Na^+/K^+-ATPase α_3 Isoenzyme in Rat Pineal Glands. *Proceedings of the National Academy of Sciences of the United States of America*, 87:1178–1182, 1990.

[83] Y. Sun and W. J. Ball. Determination of Na^+/K^+-ATPase α and β Isoforms and Kinetic Properties in Mammalian Liver. *American Journal of Physiology*, 262:C1491–C1499, 1992.

[84] K. J. Sweadner, K. M. McGrail, and B. A. Khaw. Discoordinate Regulation of Isoforms of Na^+/K^+-ATPase and Myosin Heavy Chain in the Hypothyroid Postnatal Rat Heart and Skeletal Muscle. *Journal of Biological Chemistry*, 267:769–773, 1992.

[85] H. S. Hundal, A. Marette, T. Ramlal, Z. Liu, and A. Klip. Expression of β Subunit Isoforms of the Na^+/K^+ is Muscle Type-Specific. *FEBS Letters*, 328:253–258, 1993.

[86] O. I. Shamraj and J. B. Lingrel. A Putative Fourth Na^+/K^+-ATPase α - Subunit Gene is Expressed in Testis. *Proceedings of the National Academy of Sciences of the United States of America*, 91:12952–12956, 1994.

[87] C. B. Thompson and A. A. McDonough. Skeletal Muscle Na^+/K^+-ATPase α and β Subunit Protein Levels Respond to Hypokalemia Challenge with Isoform and Muscle Type Specificity. *Journal of Biological Chemistry*, 271:32653–32658, 1996.

[88] G. Blanco, G. Sanchez, R. J. Melton, W. G. Tourtellotte, and R. W. Mercer. The α_4 Isoform of the Na^+/K^+-ATPase is Expressed in the Germ Cells of the Testes. *Journal of Histochemistry and Cytochemistry*, 48:1023–1032, 2000.

[89] A. L. Woo, P. F. James, and J. B. Lingrel. Sperm Motility is Dependent on a Unique Isoform of the Na^+/K^+-ATPase. *Journal of Biological Chemistry*, 275:20693–20699, 2000.

[90] S. He, D. A. Shelly, A. E. Moseley, P. F. James, J. H. James, R. J. Paul, and J. B. Lingrel. The α_1 and α_2 Isoforms of Na^+/K^+-ATPase Play Different Roles in Skeletal Muscle Contractility. *American Journal of Physiology. Regulatory, Integrative and Comparative Physiology*, 281:R917–R925, 2001.

[91] J. R. Fowles, H. J. Green, and J. Ouyang. Na^+/K^+-ATPase in Rat Skeletal Muscle: Content, Isoform, and Activity Characteristics. *Journal of Applied Physiology*, 96:316–326, 2004.

[92] K. J. Sweadner and E. Rael. The FXYD Gene Family of Small Ion Transport Regulators or Channels: cDNA Sequence, Protein Signature Sequence, and Expression. *Genomics*, 68:41–56, 2000.

[93] I. Lubarski, K. Pihakaski-Maunsbach, S. J. D. Karlish, A. B. Maunsbach, and H. Garty. Interaction with the Na^+/K^+-ATPase and Tissue Distribution of FXYD5 (Related to Ion Channel). *Journal of Biological Chemistry*, 280:37717–37724, 2005.

[94] J.R. Bell, E. Kennington, W. Fuller, K. Dighe, P. Donoghue, J. E. Clark, L. G. Jia, A. L. Tucker, J. R. Moorman, M. S. Marber, P. Eaton, M. J. Dunn, and M. J. Shattock. Characterization of the Phospholemman Knockout Mouse Heart: Depressed Left Ventricular Function with Increased Na^+/K^+-ATPase Activity. *American journal of physiology. Heart and Circulatory Physiology*, 294:H613–H621, 2008.

[95] D. H. Jones, T. Y. Li, E. Arystarkhova, K. J. Barr, R. K. Wetzel, J. Peng, K. Markham, K. J. Sweadner, G. H. Fong, and G. M. Kidder. Na^+/K^+-ATPase from Mice Lacking the γ Subunit (FXYD2) Exhibits Altered Na^+ Affinity and Decreased Thermal Stability. *Journal of Biological Chemistry*, 280:19003–19011, 2005.

[96] I. Goldschimdt, F. Grahammer, R. Warth, A. Schulz-Baldes, H. Garty, R. Greger, and M. Bleich. Kidney and Colon Electrolyte Transport in CHIF Knockout Mice. *Cell Physiology and Biochemistry*, 14:113–120, 2004.

[97] F. Cornelius, M. Habeck, R. Kanai, C. Toyoshima, and S. J. D. Karlish. General and Specific Lipid-Protein Interactions in $Na^+[K^+$-ATPase. *Biochimica et Biophysica Acta - Biomembranes*, 1848(9):1729–1743, 2015.

[98] M. Esmann, D. Watt, and D. Marsh. Spin-label studies of lipid-protein interactions in Na, K-ATPase membranes from Squalus acanthias. *Biochemistry*, 24:1386–1393, 1985.

[99] N. P. Barrera, M. Zhou, and C. V. Robinson. The Role of Lipids in Defining Membrane Protein Interactions: Insights from Mass Spectrometry. *Trends in Cell Biology*, 23(1):1–8, 2013.

[100] M. Laursen, L. Yatime, P. Nissen, and N. Fedosova. Crystal Structure of the High-Affinity $Na^+[K^+$-ATPase-Ouabain Complex with Mg^{2+} Bound in the Cation Binding Site. *Proceedings of the National Academy of Sciences of the United States of America*, 110(27):10958–63, 2013.

[101] Y. Hayashi, K. Mimura, H. Matsui, and T. Takagi. High-Performance Gel Chromatography of Active Solubilized Na^+/K^+-ATPase Maintained by Exogenous Phosphatidylserine. *Progress in Clinical and Biological Research*, 268A:205–210, 1988.

[102] E. Cohen, R. Goldshleger, A. Shainskaya, D. M. Tal, C. Ebel, M. le Maire, and S. J. D. Karlish. Purification of Na^+/K^+-ATPase Expressed in *Pichia pastroris* Revealed an Essential Role of Phospholipid-Protein Interaction. *Journal of Biological Chemistry*, 280:16610–16618, 2005.

[103] H. Haviv, E. Cohen, Y. Lifshitz, D. M. Tal, R. Goldshleger, and S. J. D. Karlish. Stabilization of Na^+/K^+-ATPase Purified from *Pichia pastoris* Membranes by Specific Interactions with Lipids. *Biochemistry*, 46:12855–12867, 2007.

[104] M. Esmann and D. Marsh. Lipid-Protein Interactions with the Na^+/K^+-ATPase. *Chemistry and Physics of Lipids*, 141:94–104, 2006.

[105] F. Cornelius, N. Turner, and H. R. Christensen. Modulation of Na^+/K^+-ATPase by Phospholipids and Cholesterol. II. Presteady-State Kinetics. *Biochemistry*, 42:8441–8549, 2003.

[106] Y. Lifshitz, E. Petrovich, H. Haviv, R. Goldshleger, D. M. Tal, H. Garty, and S. J. D. Karlish. Purification of Human α_2 Isoform of Na^+/K^+-ATPase Expressed in *Pichia pastoris*. Stabilization by Lipids and FXYD1. *Biochemistry*, 46:14937–14950, 2007.

[107] D. Strugatsky, R. Goldshleger, E. Bibi, and S. J. D. Karlish. Expression of Na^+/K^+-ATPase in *P. pastoris*: Fe^{2+}-Catalyzed Cleavage of the Recombinant Enzyme. *Annals of the New York Academy of Sciences*, 986:247–248, 2003.

[108] A. Katz, Y. Lifshitz, E. Bab-Dinitz, E. Kapri-Pardes, R. Goldshleger, D. M. Tal, and S. J. D. Karlish. Selectivity of Digitalis Glycosides for Isoforms of Human Na^+/K^+-ATPase. *Journal of Biological Chemistry*, 285:19582–19592, 2010.

[109] H. Haviv, M. Habeck, R. Kanai, C. Toyoshima, and S. J. D. Karlish. Neutral Phospholipids Stimulate Na^+/K^+-ATPase Activity: A Specific Lipid-Protein Interaction. *Journal of Biological Chemistry*, 288:10073–10081, 2013.

[110] M. Habeck, H. Haviv, A. Katz, E. Kapri-Pardes, S. Ayciriex, A. Shevchenko, H. Ogawa, C. Toyoshima, and S. J. D. Karlish. Stimulation, Inhibition or Stabilization of Na^+/K^+-ATPase Caused by Specific Lipid Interactions at Distinct Sites. *Journal of Biological Chemistry*, 290:4829–4842, 2015.

[111] J. H. Kaplan. The Na^+/K^+-ATPase: A Current Overview. In M. Futai, Y. Wada, and J. H. Kaplan, editors, *Handbook of ATPases*, chapter Chapter4, pages 89–97. Wiley-VCH, Weinheim, Germany, 1. edition edition, 2004.

[112] C. H. Pedemont and A. M. Bertorello. Short-Term Regulation of the Proximal Tubule Na^+/K^+-ATPase: Increased/Decreased Na^+/K^+-ATPase Activity Mediated by Protein Kinase C Isoforms. *Journal of Bioenergetics and Biomembranes*, 33:439–447, 2001.

[113] Z. Xie and A. Askari. $Na^+[K^+$-ATPase as a Signal Transducer. *European Journal of Biochemistry*, 269(10):2434–2439, 2002.

[114] R. Efendiev, C. E. Budu, A. R. Cinelli, A. M. Betorello, and C. H. Pedemonte. Intracellular Na^+ Regulates Dopamine and Angiotensin II Receptors Availability at the Plasma Membrane and Their Cellular Responses in Renal Epithelia. *Journal of Biological Chemistry*, 278(31):28719–28726, 2003.

[115] J. H. Kaplan. Biochemistry of $Na^+[K^+$-ATPase. *Annual Review of Biochemistry*, 71(1):511–535, 2002.

[116] R. L. Post. A Phosphorylated Dependent Intermediate in Adenosine Sodium and Potassium Transport across Kidney Membranes. *The Journal of Biological Chemistry*, 240(3):1437–1445, 1965.

[117] R. W. Albers. Biochemical Aspects of Active Transport. *Annual Review of Biochemistry*, October 19:727–756, 1967.

[118] L. A. Vasilets and W. Schwarz. Structure-Function Relationships of Cation Binding in the $Na^+[K^+$-ATPase. *Biochimica et Biophysica Acta (BBA)*, 1154:201–222, 1993.

[119] I. M. Glynn. A Hundred Years of Sodium Pumping. *Annual Review of Physiology*, 64:1–18, 2002.

[120] J. P. Morth, B. P. Pedersen, M. S. Toustrup-Jensen, T. L. M. Sørensen, J. Petersen, J. P. Andersen, B. Vilsen, and P. Nissen. Crystal Structure of the Sodium-Potassium Pump. *Nature*, 450(7172):1043–9, dec 2007.

[121] A. Takeuchi, N. Reyes, P. Artigas, and D. C. Gadsby. The Ions Pathway Through the Opened $Na^+[K^+$-ATPase Pump. *Nature*, 456(7220):413–416, 2009.

[122] L. Yatime, M. Laursen, J. P. Morth, M. Esmann, P. Nissen, and N. Fedosova. Structural Insights into the High Affinity Binding of Cardiotonic Steroids to the $Na^+[K^+$-ATPase. *Journal of Structural Biology*, 174(2):296–306, may 2011.

[123] H.-J. Apell. Mechanistic Principles of Ion Transport in the Na^+/K^+-ATPase. *Russian Journal of Electrochemistry*, 53(3):237–247, 2017.

[124] G. Sweeney and A. Klip. Regulation of the Na^+/K^+-ATPase by insulin: why and how? *Molecular and Cell Biochemistry*, 182:121–133, 1998.

[125] M. S. Toustrup-Jensen, A. P. Einholm, V. R. Schack, H. N. Nielsen, R. Holm, M. J. Sobrido, J. P. Andersen, T. Clausen, and B. Vilsen. Relationship Between Intracellular Na^+ Concentration and Reduced Na^+ Affinity in Na^+/K^+-ATPase Mutants Causing Neurological Disease. *Journal of Biological Chemistry*, 289(6):3186–3197, 2014.

[126] M. Sasaki, A. Ishii, and Y. Saito. Genotype – Phenotype Correlations in Alternating Hemiplegia of Childhood. *Neurology*, 82:482–490, 2014.

[127] M. Li, D. Jazayeri, B. Corry, K. M. McSweeney, E. L. Heinzen, D. B. Goldstein, and S. Petrou. A Functional Correlate of Severity in Alternating Hemiplegia of Childhood. *Neurobiology of Disease*, 77:88–93, 2015.

[128] E. L. Heinzen, A. Arzimanoglou, A. Brashear, S. J. Clapcote, F. Gurrieri, D. B. Goldstein, S. H. Jóhannesson, M. A. Mikati, B. Neville, S. Nicole, L. J. Ozelius, H. Poulsen, T. Schyns, K. J. Sweadner, A. van den Maagdenberg, B. Vilsen, and H. Sigurður. Distinct neurological disorders with *ATP1A3* mutations. *Lancet Neurology*, 13(5):503–514, 2015.

[129] P. De Carvalho Aguiar, K. J. Sweadner, J. T. Penniston, J. Zaremba, L. Liu, M. Caton, G. Linazasoro, M. Borg, Marina A J Tijssen, Susan B. Bressman, William B. Dobyns, Allison Brashear, and Laurie J. Ozelius. Mutations in the $Na^+[K^+$-ATPase α_3 gene *ATP1A3* are Associated with Rapid-Onset Dystonia Parkinsonism. *Neuron*, 43(2):169–175, 2004.

[130] A. Roubergue, E. Roze, S. Vuillaumier-Barrot, M. J. Fontenille, A. Méneret, M. Vidailhet, B. Fontaine, D. Doummar, B. Philibert, F. Riant, and S. Nicole. The Multiple Faces of the *ATP1A3*-Related Dystonic Movement Disorder. *Movement Disorders*, 28(10):1457–1459, 2013.

[131] M. K. Demos, Cl. D. van Karnebeek, C. J. Ross, S. Adam, Y. Shen, S. H. Zhan, C. Shyr, G. Horvath, M. Suri, A. Fryer, S. J. Jones, and J. M. Friedman. A Novel Recurrent Mutation in *ATP1A3* Causes CAPOS Syndrome. *Orphanet journal of rare diseases*, 9(1):15, 2014.

[132] M. Li, D. Jazayeri, B. Corry, K. M. McSweeney, E. L. Heinzen, D. B. Goldstein, and S. Petrou. A functional correlate of severity in alternating hemiplegia of childhood. *Neurobiology of Disease*, 77:88–93, 2015.

[133] E. A. Azizan, H. Poulsen, P. Tuluc, J. Zhou, M. V. Clausen, A. Lieb, C Maniero, S Garg, E. G. Bochukova, W. Zhao, L. H. Shaikh, C. A. Brighton, A. E. Teo, A. P. Davenport, T. Dekkers, B. Tops, B. Küsters, J. Ceral, G. S. Yeo, S. G. Neogi, I. McFarlane, N. Rosenfeld, F. Marass, J. Hadfield, W. Margas, K. Chaggar, M. Solar, J. Deinum, A. C. Dolphin, I. S. Farooqi, J. Striessnig, P. Nissen, and M. J. Brown. Somatic Mutations in *ATP1A1* and *CACNA1D* Underlie a Common Subtype of Adrenal Hypertension. *Nat Genet*, 45(9):1055–1060, 2013.

[134] T. L. Radzyukevich, J. C. Neumann, T. N. Rindler, N. Oshiro, D. J. Goldhamer, J. B. Lingrel, and J. A. Heiny. Tissue-Specific Role of the $Na^+[K^+$-ATPase $alpha_2$

Isozyme in Skeletal Muscle. *Journal of Biological Chemistry*, 288(2):1226–1237, 2013.

[135] H. Rosewich, H. Thiele, A. Ohlenbusch, U. Maschke, J. Altmüller, P. Frommolt, B. Zirn, F. Ebinger, H. Siemes, P. Nürnberg, K. Brockmann, and J. Gärtner. Heterozygous *de-novo* Mutations in *ATP1A3* in Patients with Alternating Hemiplegia of Childhood: A Whole-Exome Sequencing Gene-Identification Study. *The Lancet Neurology*, 11(9):764–773, 2012.

[136] B. G. Neville and M. Ninan. The treatment and management of alternating hemiplegia of childhood. *Developmental Medicine and Child Neurology*, 49:777–780, 2007.

[137] A. Ishii, Y. Saito, J. Mitsui, H. Ishiura, J. Yoshimura, H. Arai, S. Yamashita, S. Kimura, H. Oguni, S. Morishita, S. Tsuji, M. Sasaki, and S. Hirose. Identification of *ATP1A3* Mutations by Exome Sequencing as the Cause of Alternating Hemiplegia of Childhood in Japanese Patients. *PLoS ONE*, 8(2), 2013.

[138] V. Rodacker, M. Toustrup-Jensen, and B. Vilsen. Mutations Phe785Leu and Thr618Met in $Na^+[K^+$-ATPase, Associated with Familial Rapid-Onset Dystonia Parkinsonism, Interfere with Na^+ Interaction by Distinct Mechanisms. *Journal of Biological Chemistry*, 281(27):18539–18548, 2006.

[139] T. Mijatovic, F. Dufrasne, and R. Kiss. Na^+/K^+-ATPase and Cancer. *Pharmaceutical Patent Analyst*, 1:91–106, 2012.

[140] E Capieaux, C Rapin, D Thinès, Y Dupont, and a Goffeau. Overexpression in *Escherichia coli* and Purification of an ATP-Binding Peptide from the Yeast Plasma Membrane H^+-ATPase. *The Journal of biological chemistry*, 268(29):21895–900, 1993.

[141] Craig Gatto, April X. Wang, and Jack H. Kaplan. The M4M5 Cytoplasmic Loop of the Na^+/K^+-ATPase, Overexpressed in *Escherichia coli*, Binds Nucleoside Triphosphates with the Same Selectivity as the Intact Native Protein. *Journal of Biological Chemistry*, 273(17):10578–10585, 1998.

[142] M. Kubala, R. Krumscheid, and W. Schoner. Phe 475 and Glu 446 but not Ser 445 participate in ATP-binding to the α subunit of $Na^+[K^+$-ATPase. *Biochemical and Biophysical Research Communications*, 297(2002):154–159, 2002.

[143] M. Kubala, J. Teisinger, R. Krumscheid, and W. Schoner. Eight Amino Acids Form the ATP Recognition Site of $Na^+[K^+$-ATPase. *Biochemistry*, 42:6446–6452, 2003.

[144] M. Kubala, J. Plášek, and E. Amler. Limitations in Linearized Analyses of Binding Equilibria: Binding of TNP-ATP to the H4-H5 Loop of Na^+/K^+-ATPase. *European Biophysics Journal*, 32(4):363–369, 2003.

[145] Z. Lansky, M. Kubala, R. Ettrich, M. Kuty, J. Plasek, J. Teisinger, W. Schoner, and E. Amler. The Hydrogen Bonds between Arg 423 and Glu 472 and Other Key Residues, Asp 443 , Ser 477, and Pro 489, Are Responsible for the Formation and a Different Positioning of TNP-ATP and ATP within the Nucleotide-Binding Site of $Na^+[K^+$-ATPase †. *Biochemistry*, 43:8303–8311, 2004.

[146] M. Kubala, Jaromír Plášek, and E. Amler. Fluorescence Competition Assay for the Assessment of ATP Binding to an Isolated Domain of Na+,K+-ATPase. *Physiological Research*, 53(1):109–113, 2004.

[147] T. L. M. Sorensen, J. V. Moller, and P. Nissen. Phosphoryl Transfer and Calcium Ion Occlusion in the Calcium Pump. *Science*, 304:1672–1675, 2004.

[148] L. Plesner, B. Karlsmose, and M. E. Luscher. [32P]ATP synthesis in steady state from [32p]p i and ADP by Na+/K+-ATPase from ox brain and pig kidney. Activation by K +. *Biochimica et Biophysica Acta (BBA)*, 1040:167–174, 1990.

[149] N. Fedosova. P-Type ATPases: Methods and Protocols. In Maike Bublitz, editor, *Springer Protocols - Methods in Molecular Biology: Purification of Na, K-ATPase from Pig Kidney*, pages 5–10. Springer, 2016.

[150] P. L. Jorgensen. Purification of Na^+[K^+-ATPase: Enzyme Sources, Preparative Problems, and Preparation from Mammalian Kidney. *Methods in Enzymology*, 156(1982):29–43, 1988.

[151] I. Klodos, M. Esmann, and R. L. Post. Large-Scale Preparation of Sodium-Potassium ATPase from Kidney Outer Medulla. *Kidney International*, 62:2097–2100, 2002.

[152] S. Kaur, M. Panchal, M. Faisal, V. Madan, P. Nangia, and B. N. Mallick. Long Term Blocking of GABA-A Receptor in *Locus Coeruleus* by Bilateral Microinfusion of Picrotoxin Reduced Rapid Eye Movement Sleep and Increased Brain Na^+[K^+-ATPase Activity in Freely Moving Normally Behaving Rats. *Behavioural Brain Research*, 151(1-2):185–190, 2004.

[153] I. Klodos. Large-Scale Preparation of Na^+[K^+-ATPase from Ox Brain. *Analytical Biochemistry*, 403:397–403, 1975.

[154] J. L. Gregersen, D. Mattle, N. Fedosova, P. Nissen, and L. Reinhard. Isolation, Crystallization and Crystal Structure Determination of Bovine Kidney Na^+[K^+-ATPase. *Acta Crystallographica Section F: Structural Biology Communications*, 72:282–287, 2016.

[155] P Silva, J Stoff, M Field, L Fine, J N Forrest, and F H Epstein. Mechanism of active chloride secretion by shark rectal gland: role of Na^+/K^+-ATPase in chloride transport. *The American journal of physiology*, 233(4):F298–306, 1977.

[156] D. W. Martin and J. R. Sachs. Preparation of Na^+[K^+-ATPase with Near Maximal Specific Activity and Phosphorylation Capacity: Evidence That the Reaction Mechanism Involves All of the Sites. *Biochemistry*, 38(23):7485–7497, 1999.

[157] A. Yoda and S. Yoda. A New Simple Preparation Method for Na^+[K^+-ATPase-Rich Membrane Fragments. *Analytical Biochemistry*, 110(1):82–88, 1981.

[158] P. L. Jorgensen and J. C. Skou. Purification and Characterisation of Na^+,K^+-ATPase. I- The Influence of Detergents on thr Activity Na^+,K^+-ATPase in Preparations from the Outer Medulla of Rabbit KIdney. *Biochimica et Biophysica Acta*, 233:366–371, 1971.

[159] B. R. Glick and J. J. Pasternak. *Molecular Biotechnology: Principles and Applications of Recombinant DNA*. ASN Press, Washington, USA, 4. edition, 2010.

[160] K. Geering. Topogenic Motifs in P-Type ATPases. *Journal of Membrane Biology*, 174:181–190, 2000.

[161] P. A. Pedersen, J. H. Rasmussen, and P. L. Jorgensen. Expression in High Yield of Pig $\alpha_1\beta_1$ $Na^+[K^+$-ATPase and Inactive Mutants D369N and D807N in *Saccharomyces cerevisiae*. *The Journal of Biological Chemistry*, 271(5):2514–2522, 1996.

[162] A. W. De Tomaso, G. Blanco, and R. W. Mercer. Expression, Targeting, and Assembly of Functional Na^+/K^+-ATPase Polypetides in *baclovirus*-Infected Insect Cells. *Journal of Biological Chemistry*, 268:1470–1778, 1993.

[163] A. S. Robinson, editor. *Production of Membrane Proteins - Strategies for Expression and Isolation*. Wiley-VCH, Weinheim, Germany, first edition, 2011.

[164] A. Wach. PCR-Synthesis of Marker Cassettes with Long Flanking Homology Regions for Gene Disruption in *S. cerevisiae*. *Yeast*, 12:259–265, 1996.

[165] Z. Britton, C. Young, Ö. Can, P. McNeely, A. Naranjo, and A. S. Robinson. Membrane Protein Expression in *Saccharomyces cerevisiae*. In A. S. Robinson, editor, *Production of Membrane Proteins: Strategies for Expression and Isolation*, pages 37–73. Wiley-VCH, Weinheim, Germany, first edition, 2011.

[166] Z. Wang. Controlled Expression of Recombinant Genes and Preparation of Cell-Free Extracts in Yeast. *Methods in Molecular Biology*, 313:317–331, 2006.

[167] T. Etcheverry. Induces Expression Using Yeast Copper Methallothionein Promoter. *Methods in Enzymology*, 185:319–329, 1990.

[168] S. A. Johnston, J. M. Salmeron, and S. S. Dincher. Interaction of Positive and Negative Regulatory Proteins in the Galactose Regulon of Yeast. *Cell*, 50:143–146, 1987.

[169] M. Johnston. A Model Fungal Gene Regulatory Mechanism: The *GAL* Genes of *Saccharomyces cerevisiae*. *Microbiology Reviews*, 51:458–476, 1987.

[170] M. A. Romanos, C. A. Scorer, and J. J. Clare. Foreign Gene Expression in Yeast: A Review. *Yeast*, 8:317–331, 1992.

[171] D. Lohr, P. Venkov, and J. Zlatanovova. Transcriptional Regulation in the Yeast *GAL* Gene Family: A Complex Genetic Network. *FASEB Journal*, 9:777–787, 1995.

[172] D. Mumberg, R. Muller, and M. Funk. Regulable Promoters of *Saccharomyces cerevisiae*: Comparison of Transcriptional Activity and Their Use for Heterologous Expression. *Nucleic Acids Research*, 22:5767–5768, 1994.

[173] A. Hinnen, B. Meyhack, and J. Hein. Heterologous Gene Expression in Yeast. *Biotechnology*, 13:193–213, 1989.

[174] S. Chen, R. W. West, J. Ma, S. L. Johnson, H. Gam, and G. Woldehawariat. TSFl to TSFG, Required for Silencing the *Saccharomyces cerevisiae GAL* Genes, Are Global Regulatory Genes. *Genetics Socienty of America*, 134:701–716, 1993.

[175] D. Maya, M. J. Quintero, M. de la Cruz Muñoz-Centeno, and S. Chávez. Systems for Applied Gene Control in *Saccharomyces cerevisiae*. *Biotechnology Letters*, 30:979–987, 2008.

[176] E. W. Jones. Tackling the Protease Problem in *Saccharomyces cerevisiae*. *Methods in Enzymology*, 194:428–453, 1991.

[177] C. Duport, J. Loeper, and A. D. Strosberg. Comparative Expression of the Human β_2 and β_3 Adrenergic Receptors in *Saccharomyces cerevisiae*. *Biochimica et Biophysica Acta (BBA)*, 1629:34–43, 2003.

[178] C. Guthrie (ed.). Guide to Yeast Genetics and Molecular Biotechnology. *Methods in Enzymology*, 194:1–863, 1991.

[179] G. Tschumper and J. Carbon. Sequence of a yeast DNA fragment containing a chromosomal replicator and TRP1 gene. *Gene*, 10:157–166, 1980.

[180] K. Struhl and R. W. Davis. A Physical, Genetic and Transcriptional Map of the Cloned *his3* Gene Region of *Saccharomyces cerevisiae*. *Journal of Molecular Biology*, 136:309–332, 1980.

[181] M. Rose, P. Grisafi, and D. Botstein. Structure and Function of the Yeast *URA3* Gene: Expression in *Escherichia coli*. *Gene*, 29:113–124, 1984.

[182] C. B. Brachmann, A. Davies, G. J. Cost, E. Caputo, J. Li, P. Hieter, and J. D. Boeke. Designer Deletion Strains Derived from *Saccharomyces cerevisiae* S288C: A Useful Set of Strains and Plasmids for PCR-Mediated Gene Disruption and Other Applications. *Yeast*, 14:115–132, 1998.

[183] C. Hadfield, B. E. Jordan, R. C. Mount, G. H. Pretorius, and E. Burak. G418-Resistance as a Dominant Marker and Reporter for Gene Expression in *Saccharomyces cerevisiae*. *Current Genetics*, 18:303–313, 1990.

[184] J. Davies and B. D. Davis. Misreading of Ribonucleic Acid Code Words Induced by Aminoglycoside Antibiotics. The Effect of drug concentration. *Journal of Biological Chemistry*, 243:3312–2216, 1968.

[185] M. J. Cabanas, D. Vazquez, and J. Modolell. Dual Interference of Hygromycin B with Ribosomal Translation and with Aminoacyl-tRNA Recognition. *European Journal of Biochemistry*, 87:21–27, 1978.

[186] L. Gritz and J. Davies. Plasmid-Encoded Hygromycin B Resistance: the Sequence of Hygromycin B Phosphotransferase Gene and Its Expression in *Escherichia coli* and *Saccharomyces cerevisiae*. *Gene*, 25:179–188, 1983.

[187] A. Gatignol, H. Durand, and G. Tiraby. Bleomycin Resistance Conferred by Drug-Binding Protein. *FEBS Letters*, 230:171–175, 1988.

[188] T. W. Christianson. Multifunctional Yeast High-Copy-Number Shuttle Vectors. *Gene*, 110:119–122, 1992.

[189] L. Clarke and J. Carbon. Isolation of a Yeast Centromere and Construction of Functional Small Circular Chromosomes. *Nature*, 287:504–509, 1980.

[190] S. A. Parent, C. M. Fenimore, and K. A. Bostian. Vector System for the Expression, Analysis and Cloning of DNA Sequences in *S. cerevisiae*. *Yeast*, 1:83–138, 1985.

[191] J. R. Broach. Construction of High Copy Yeast Vectors Using 2μ Circle Sequences. *Methods in Enzymology*, 101:307–325, 1983.

[192] K. A. Armstrong, T. Som, F.C. Volkert, A. Rose, and J. R. Broach. Propagation and Expression of Genes in Yeast Using 2μ Circle Vectors. *Biotechnology*, 13:165–192, 1989.

[193] J. A. Murray. Bending the Rules: the 2μ Plasmid of Yeast. *Molecular Microbiology*, 1:1–4, 1987.

[194] A. B. Futcher. The 2μ Circle Plasmid of *Saccharomyces cerevisiae*. *Yeast*, 4:27–40, 1988.

[195] F. C. Volkert, D. W. Wilson, and J. R. Broach. Deoxyribonucleic Acid Plasmids in Yeast. *Microbiology Reviews*, 53:299–317, 1989.

[196] D. J. Mead, D. C. Gradner, and S. G. Oliver. The Yeast 2μ Plasmid: Strategies for the Survival of a Selfish DNA. *Molecular Genetics and Genomics*, 205:417–421, 1986.

[197] T. L. Orr-Weaver, J. W. Szostak, and R. J. Rothstein. Genetic Applications on Yeast Transformation with Linear and Gapped Plasmids. *Methods in Enzymology*, 101:228–245, 1983.

[198] R. S. Sikorski and P. Hieter. A System of Shuttle Vector and Yeast Host Strains Designed for Efficient Manipulation of DNA in *Saccharomyces cerevisiae*. *Genetics*, 122:19–27, 1989.

[199] N. Bonander, K. Hedfalk, C. Larsson, P. Mostad, C. Chang, L. Gustafsson, and R. M. Bill. Design of Improved Membrane Protein Production Experiments: Quantification of the Host Response. *Protein Science*, 14:1729–1740, 2005.

[200] A. Wedekind, M. A. O'Malley, R.T. Niebauer, and A. S. Robinson. Optimization of the Human Adenosine A2a Receptor Yields in *Saccharomyces cerevisiae*. *Biotechnology Progress*, 22:1249–1255, 2006.

[201] K. Olden, B. A. Bernard, S. L. White, and J. B. Parent. Function of the Carbohydrate Moieties of Glycoproteins. *Journal of Cellular Biochemistry*, 18:313–335, 1982.

[202] C. Wang, M. Eufemi, C. Turano, and A. Giartosio. Influence of the Carbohydrate Moiety on the Stability of Glycoproteins. *Biochemistry*, 35:7299–7307, 1996.

[203] J. P. Aubert, G. Biserte, and M. H. Loucheux-Lefebvre. Carbohydrate-Peptide Linkage in Glycoproteins. *Archives of Biochemistry and Biophysics*, 175:410–418, 1976.

[204] M. A. Romanos. Advances in the Use of *Pichia pastoris* for High-Level Gene-Expression. *Current Opinion in Biotechnology*, 5:527–533, 1995.

[205] M. R. Eckart and C. M. Bussineau. Quality and Authenticity of Heterologous Proteins Synthetized in Yeast. *Current Opinion in Biotechnology*, 7:525–530, 1984.

[206] M. Karlsson, D. Fotiadis, S. Sjovall, S. Johanson, K. Hedfalk, A. Engel, and P. Kjellbom. Reconstitution of water channel function of an aquaporin overexpressed in *Pichia pastoris*. *FEBS Letters*, 537:68–72, 2003.

[207] S. Tornroth-Horsefield, Y. Wang, K. Hedfalk, U. Johanson, M. Karlsson, E. Tajkhorshid, R. Neutze, and P. Kjellbom. Structural mechanism of plant aquaporin gatting. *Nature*, 439:688–694, 2006.

[208] S. G. Aller, J. Yu, A. Ward, Y. Weng, S. Chittaboina, R. Zhuo, P. m. Harrell, Y. T. Trinh, Q. Zhang, I. L. Urbatsch, and G. Chang. Structure of P-Glycoprotein Reveals a Molecular Basis for Poly-Specific Drug Binding. *Science*, 323:1718–1722, 2009.

[209] R. Schneiter and A. Toulmay. The Role of Lipids in the Biogenesis of Integral Membrane Proteins. *Applied Microbiology and Biotechnology*, 73:1224–1232, 2007.

[210] W. van Klompenburg, I. Nilsson, G. von Heijne, and B. de Kruijff. Anionic Phospholipids are Determinants of Membrane Protein Topology. *EMBO Journal*, 16:4261–4266, 1997.

[211] A. van Dalen and B. de Kruijff. The role of Lipids in Membrane Insertion and Translocation of Bacterial Protein. *Biochimica et Biophysica Acta (BBA)*, 1964:97–109, 2004.

[212] A. R. Osborne, T. A. Rapoport, and B. van den Berg. Protein Translocation by the Sec61/SecY Channel. *Annual Reviev of Cell and Developmental Biology*, 21:529–550, 2005.

[213] E. Zinser, C. D. Sperka-Gottlieb, E. V. Fasch, S. D. Kohlwein, F. Paltauf, and G. Daum. Phospholipid Synthesis and Lipid Composition of Subcellular Membranes in the Unicellular Eukaryote *Saccharomyces cerevisiae*. *Journal of Bacteriology*, 173:2026–2034, 1991.

[214] M. S. Bretscher. Asymmetrical Lipid Bilayer Structure for Biological Membranes. *Nature New Biology*, 236:11–12, 1972.

[215] J. A. Butz, R. T. Niebauer, and A. S. Robinson. Co-Expression of Molecular Chaperones Does Not Improve the Heterologous Expression of Mammalian G-Protein Coupled Receptor Expression in Yeast. *Biotechnology and Bioengeneering*, 84:292–304, 2003.

[216] V. Lórenz-Fonfría, A. Perálvarez-Marín, E. Padrós, and T. Lazarova. Solubilization, Purification, and Characterization of Integral Membrane Proteins. In A. S. Robinson, editor, *Production of Membrane Proteins: Strategies for Expression and Isolation*, pages 317–360. Wiley-VCH, Weinheim, Germany, first edition, 2011.

[217] K. Ohlendieck. Extraction of Membrane Proteins. *Methods in Molecular Biology*, 244:283–293, 2004.

[218] I. M. Rosenberg. *Protein Analysis and Purification: Benchtop Technique*. Birkhäuser, Boston , Massachussets, second edition, 2005.

[219] M. le Maire, P. Champeil, and J. V. Moller. Interaction of Membrane Proteins and Lipids with Solubilizing Detergents. *Biochimica et Biophysica Acta (BBA)*, 1508:86–111, 2000.

[220] S. H. Lin and G. Guidotti. Purification of Membrane Proteins. *Methods in Enzymology*, 463:616–629, 2009.

[221] D. Linke. Detergents: An Overview. *Methods in Enzymology*, 463:603–617, 2009.

[222] T. Arnold and D. Linke. The Use of Detergents to Purify Membrane Proteins. *Current Protocols in Protein Science*, 4:8.1–8.30, 2008.

[223] T. Arnold and D. Linke. Phase Separation in the Isolation and Purification of Membrane Proteins. *Biotechniques*, 43:427–430, 2007.

[224] J. M. Neugebauer. Detergents: An Overview. *Methods in Enzymology*, 183:239–253, 2009.

[225] C. Mohan, Y. G. Kim, J. Koo, and G. M. Lee. Assessment of Cell Engineering Strategies for Improved Therapeutic Protein Production in CHO Cells. *Biotechnology*, 3:624–630, 2008.

[226] F. M. Wurm. Production of Recombinant Protein Therapeutics in Cultivated Mammalian Cells. *Nature Biotechnology*, 22:1393–1398, 2003.

[227] N. Eifler, M. Duckely, L. T. Sumanovski, T. M. Egan, A. Oksche, J. B. Konopka, A. Lüthi, A. Engel, and P. J. Werten. Functional Expression of Mammalian Receptors and Membrane Channels in Different Cells. *Journal of Structural Biology*, 159:179–193, 2007.

[228] T. Omasa, M. Onitsuka, and W. D. Kim. Cell engeneering and cultivation of Chinese hamster ovary (CHO) cells. *Current Pharmacology and Biotechnology*, 11:233–240, 2010.

[229] K. Lundstrom. Semliki Forest Virus Vectors for Rapid and High-Level Expression of Integral Membrane Proteins. *Biochimica et Biophysica Acta (BBA)*, 1610:90–96, 2003.

[230] K. Lundstrom. Semliki Forest Virus Vectors for Rapid and High-Level Expression of Integral Membrane Proteins. *Biochimica et Biophysica Acta (BBA)*, 1610:90–96, 2003.

[231] M. Lu, F. Echeverri, and B. D. Moyer. Endoplasmic Reticulum Retention, Degradation, and Aggregation of Olfactory G-Protein Coupled Receptors. *Traffic*, 4:416–433, 2003.

[232] D. Drew, D. J. Slotboom, G. Friso, T. Reda, P. Genevaux, M. Rapp, N. M. Meindl-Beinker, W. Lambert, M. Lerch, D. O. Daley, K. J. Van Wijk, J. Hirst, E. Kunji, and J. W. De Gier. A Scalable, GFP-Based Pipeline for Membrane Protein Overexpression Screening and Purification. *Protein Science*, 14:2011–2017, 2005.

[233] D. Hizal, E. Ohsfeldt, S. Mai, and M. J. Betenbaugh. Membrane Protein Expression in Mammalian Cells. In A. Robinson, editor, *Production of Membrane Proteins: Strategies for Expression and Isolation*, pages 139–166. Wiley-VCH, Weinheim, Germany, first edition, 2011.

[234] T. Holbro, G. Civenni, and N. E. Hynes. The ErbB Receptors and Their Role in Cancer Progression. *Experimental Cell Research*, 284:99–110, 2003.

[235] S. E. Bane, J. E. Velasques, and A. S. Robinson. Expression and Purification of Milligram Levels of Inactive G-Protein Coupled Receptors in *E. coli*. *Protein Expression and Purification*, 52:348–355, 2007.

[236] S. O'Connor, E. Li, B. S. Majors, L. He, J. Placone, D. Baycin, M. J. Betenbaugh, and K. Hristova. Increased Expression of the Integral Membrane Protein ErbB2 in Chinese Hamster Ovary Cells Expressing the Anti-Apoptotic Gene *Bcl-XL*. *Protein Expression and Purification*, 67:41–47, 2009.

[237] G. B. Karlsson and P. Liljestrom. Delivery and Expression of Heterologous Genes in Mammalian Cells Using Self-Replicating α Virus Vectors. *Methods in Molecular Biology*, 246:543–557, 2004.

[238] E. Baginski, L. M. Weiner, and B. Zak. The Simple Determination of Nucleotide Phosphorus. *Clinica Chimica Acta*, 10:378–379, 1964.

[239] L. Cariani, L. Thomas, J. Brito, and J. R. Del Castillo. Bismuth citrate in the quantification of inorganic phosphate and its utility in the determination of membrane-bound phosphatases. *Analytical Biochemistry*, 324(1):79–83, 2004.

[240] Jens G. Nørby. Coupled Assay of Na^+/K^+-ATPase Activity. *Biochemistry*, 324(1984):116–119, 1988.

[241] J. M. Rovinsky, G. L. Tewalt, and A. T. Sneden. Maquiroside A, a New Cytotoxic Cardiac Glycoside from *Maquira calophylla*. *Journal of Natural Products*, 50:211_216, 1987.

[242] D. A. Gentile, J. Henry, A. J. Katz, and D. P. Skoner. Inhibition of Peripheral Blood Mononuclear Cell Proliferation by Cardiac Glycosides. *Annuls of Allergy, Asthma and Immunology*, 78:466–472, 1997.

[243] J. Haux. Digitoxin is a Potent Anticancer Agent for Several Types of Cancer. *Medical Hypotheses*, 53:543–548, 1999.

[244] S. Johansson, P. Lindholm, J. Gullbo, P. Larsson, and L. Bohlin. Cytotoxicity of Digitoxin and Related Cardiac Glycosides in Human Tumor Cells. *Anti-Cancer Drugs*, 12:475–483, 2001.

[245] V. Rosenkranz and M. Wink. Induction of Apoptosis by Alkaloids, Non-Protein Amino Acids, and Cardiac Glycosides in Human Promyelotic HL-60 Cells. *Zeitschrift für Naturforschung C*, 62:458–466, 2007.

[246] A. M. Y. Moustafa, A. I. Khodair, and M. A. Saleh. Structural Elucidation and Evaluation of Toxicity and Anti-tumor Activity of Cardiac Glycosides Isolated from *Leptadenia pyrotechnica*. *Pharmaceutical Biology*, 47:826–834, 2008.

[247] S. Serra, S. Cheng, R. B. Zavareh, C. Simpson, A. Schimmer, S. Ezzat, and S. L. Asa. The Response of Pancreatic Endocrine Tumors to Cardiac Glycosides. *Histopathology*, 53:112, 2008.

[248] Q. Zhao, Y. W. Guo, B. Feng, L. Li, C. G. Huang, and B. H. Jiao. Neriifolin from Seeds of *Cerebera manghas L.* Induces Cell Cycle Arrest and Apoptosis in Human Carcinoma HepG2 Cells. *Fitoterapica*, 82:735–741, 2011.

[249] Z. W. Xu, F. M. Wang, M. J. Gao, X. Y. Chen, W. L. Hu, and R. C. Xu. Targeting the Na^+/K^+-ATPase α_1 Subunit of Hepatoma HepG2 Cell Line to Induce Apoptosis and Cell Cycle Arresting. *Biological and Pharmaceutical Bulletin*, 33:743–751, 2010.

[250] T. Sagawa, K. Sagawa, J. E. Kelly, R. G. Tsushima, and J. A. Wasserstrom. Activation of Cardiac Ryanodine Receptors by Cardiac Glycosides. *American journal of physiology. Heart and Circulatory Physiology*, 282:H1118–1126, 2002.

[251] H. T. Ho, S. C. W. Stevens, R. Terentyeva, C. A. Carnes, D. Terentyev, and S. Gyorke. Arrhythmogenic Adverse Effects of Cardiac Glycosides are Mediated by Redox Modification of Rhyanodine Receptors. *Journal of Physiology (London)*, 589:4697–4708, 2011.

[252] J. Liu, J. Tian, M. Haas, J. I. Shapiro, A. Askari, and Z. Xie. Ouabain Interaction with Cardiac $Na^+[K^+$-ATPase Initiates Signal Cascades Independent of Changes in Intracellular Na^+ and Ca^{2+} Concentrations. *Journal of Biological Chemistry*, 275(36):27838–27844, 2000.

[253] T. Akera and T. M. Brody. Ionotropic Action of Digitalis and Ion Transport. *Life Sciences*, 18:135–142, 1976.

[254] T. Akera and Y. C. Ng. Digitalis Sensitivity of Na^+/K^+-ATPase, Myocytes and the Heart. *Life Sciences*, 48:97–106, 1991.

[255] D. A. Eisner and T. W. Smith. *The Heart and Cardiovascular System*. Raven Press, New York, USA, 2. edditio edition, 1992.

[256] The Digitalis Investigational Group. The Effect of Digoxin on Mortality and Morbidity in Patients with Heart Failure. *New England Journal of Medicine*, 336:525–533, 1997.

[257] T. Akera, F. S. Larsen, and T. M. Brody. The Effect of Ouabain on Sodium-and Potassium-Activated Adenosine Triphosphatase form Hearts of Several Mammalian Species. *Journal of Pharmacology and Experimental Therapeutics*, 170:17–26, 1969.

[258] Y. A.-C. Liu and P. J. Bentley. A Comparison of the Cytotoxicity of Ouabain *in vivo* and *in vitro* in the Frog, *Rana pipiens*, and the Toad, *Bufo marinus*. *Comparative and General Pharmacology*, 2:476–478, 1971.

[259] A. Schwartz, G. E. Lindenmayer, and J. C. Allen. The Sodium-Potassium Adenosine Triphosphatase: Pharmacological, Physiological and Biochemical Aspects. *Pharmacological Reviews*, 27:3–134, 1976.

[260] M. Y. Abeywardena, E. J. McMurchie, G. R. Russel, and J. S. Charnock. Species Variation in the Ouabain Sensitivity of Cardiac Na^+/K^+-ATPase. A Possible Role for Membrane Lipids. *Biochemical Pharmacology*, 33:3649–3654, 1984.

[261] W. J. O'Brien, J. B. Lingrel, and E. T. Wallick. Ouabain Binding Kinetics of the Rat α_2 and α_3 Isoforms of the Sodium-Potassium Adenosine Triphospatase. *Archives of Biochemistry and Biophysics*, 310:32–39, 1994.

[262] J. F. Morris, F. Ismail-Beigi, V. P. Butler, I. Gati, and D. Lichtstein. Ouabain-Sensitive Na^+/K^+-ATPase Activity in Toad Brain. *Comparative Biochemistry and Physiology*, 118:599–606, 1997.

[263] R. M. Lebovitz, K. Takeyasu, and D. Fambrough. Molecular Characterization and Expression of the (Na^+/K^+)-ATPase α-Subunit in *Drosophila melanogaster*. *EMBO Journal*, 8:193–202, 1989.

[264] J. Wang, J. B. Velotta, A. A. McDonough, and R. A. Farley. All Human Na^+/K^+-ATPase α Subunit Isoforms Have a Similar Affinity for Cardiotonic Glycosides. *American Journal of Physiology. Cell Physiology*, 281:1336–1343, 2001.

[265] O. Shiratori. Growth Inhibitory Effects of Cardiac Glycosides and Aglycones on Neoplastic Cells: *In vitro* and *in vivo* studies. *Gann*, 58:521–528, 1967.

[266] J. L. Hartwell and B. J. Abbot. Antineoplastic Principles in Plants: Recent Developments in the Field. *Advanced Pharmacology*, 7:117–209, 1969.

[267] B. Stenkvist. Is Digitalis a Therapy for Breast Cancer? *Oncology Reports*, 6:493–496, 1999.

[268] J.-Q. Chen, R. G. Contreras, R. Wang, S. V. Fernandez, L. Shoshani, I. H. Russo, M. Cereijido, and J. Russo. Sodium,Potassium ATPase (Na^+/K^+-ATPase) and Ouabain/Related Cardiac Glycosides: A New Paradigm for Development of Anti-Cancer Drugs? *Breast Cnacer Research and Treatment*, 96:1–15, 2006.

[269] W. Schoner, M. Frese-Scharper, A.-C. Andres, D. Miescher, B. Zumkehr, and R. A. Schmidt. Cadiac Glycosides Initiate Apo2L/TRAIL Induced Apoptosis in Non-Small Cell Lung Cancer Therapy. *Cancer Research*, 66:6867–6874, 2006.

[270] T. Mijatovic, E. Van Quaquebeke, B. Delest, O. Debeir, F. Darro, and R. Kiss. Carditonic Steroids on the Road to Anti-Cancer Therapy. *Biochimica et Biophysica Acta (BBA)*, 1776:32–57, 2007.

[271] E. Erdmann and W. Schoner. Ouabain-Receptor Interactions in (Na^+/K^+)-ATPase Preparations from Different Tissues and Species. *Biochimica et Biophysica Acta (BBA)*, 307:386–398, 1973.

[272] R. S. Gupta, A. Chopra, and D. K. Stetsko. Cellular Basis for the Species Differences in Sensitivity to Cardiac Glycosides (Digitalis). *journal of Cellular Physiology*, 127:197–206, 1986.

[273] S. Pathak, A. S. Multani, S. Marayan, V. Kumar, and R. A. Newman. Anvirzel ™, an Extract from *Nerium oleander*, Induces Cell Death in Human but not Murine Cancer Cells. *Anticancer Drugs*, 11:455–463, 2000.

[274] P. B. Raghavendra, Y. Sreenivasan, and S. K: Manna. Oleandrin Induces Apoptosis in Human, but not Murine Cells: Dephosporylation of Akt, Expression of FasL, and Alteration of Membrane Fluidity. *Molecular Immunology*, 44:2292–2302, 2007.

[275] D. Biedermann, E. Vavříková, L. Cvak, and V. Křen. Chemistry of Silybin. *Natural Product Report*, 31(9):1138–1157, 2014.

[276] D. K. Sharma. Pharmacological Properties of Flavonoids Including Flavonolignans - Integration of Petrocrops with Drug Development from Plants. *Journal of Scientific and Industrial Research*, 65(6):477–484, 2006.

[277] Radek Gažák, Daniela Walterová, and Vladimír Křen. Silybin and Silymarin – New and Emerging Applications in Medicine. *Current medicinal chemistry*, 14(3):315–338, 2007.

[278] Dezső Csupor, Attila Csorba, and Judit Hohmann. Recent Advances in the Analysis of Flavonolignans of *Silybum marianum*. *Journal of Pharmaceutical and Biomedical Analysis*, 130:301–317, 2016.

[279] M. Kubala, P. Čechová, J. Geletičová, M. Biler, T. Štenclová, P. Trouillas, and D. Biedermann. Flavonolignans as a Novel Class of Sodium Pump Inhibitors. *Frontiers in Physiology*, 7(March):1–10, 2016.

[280] N.-C. Kim, T. N. Graf, C. M. Sparacino, M. C. Wani, and M. E. Wall. Complete Isolation and Structure Identification of Silybins and Isosilybins from the Milk Thistle (*Silybum marianum*). *Organic Biomolecules Chemistry*, 1:1684–1689, 2003.

[281] V. Šimánek, V. Křen, J. Ulrichová, J. Vičar, and L. Cvak. Silymarin: What is in the Name...? An Appeal for a Change of Editorial Policy. *Hepatology*, 32:442, 2000.

[282] I. Szilági, P. Tétènzi, S. Antus, O. Selingmann, V. M. Chari, M. Seitz, and H. Wagner. Structure of Silandrin and Silymonin, two New Flavanolignans from a White Blooming *Silybum marianum* Variety. *Planta Medica*, 43:121–127, 1981.

[283] L. Sobolová, N. Škottová, R. Večeřa, and K. Urbánek. Effect of Silymarin and its Polyphenolic Fraction on Cholesterol Absorption in Rats. *Pharmacological Research*, 53:104–112, 2006.

[284] J. Vacek, M. Zatloukalova, T. Desmier, V. Nezhodova, J. Hrbac, M. Kubala, V. Kren, J. Ulrichova, and P. Trouillas. Antioxidant, Metal-Binding and DNA-Damaging Properties of Flavonolignans a Joint Experimental and Computational Highlight Based on 7-Galloylsilybin. *Chemico-Biological Interactons*, 205:173–180, 2013.

[285] M. Pyszkova, M. Biler, D. Biedermann, K. Valentova, M. Kuzma, J. Vrba, J. Vrba, J. Ulrichova, R. Sokolova, M. Mojovic, M. Popovic-Bijelic, A.and Kubala, P. Trouillas, V. Kren, and J. Vacek. Flavonolignan 2,3-dehydroderivatives: Preparation, Anti-radical and Catoprotective Activity. *Free Radical Biology and Medicine*, 90:114–125, 2015.

[286] L. Mira, M. Silva, and C. F. Manso. Scavenging of Reactive Oxygen Species by Silibinin Dihemisuccinate. *Biochemical Pharmacology*, 17:753–759, 1994.

[287] C. Longuercio and D. Pesci. Silybin and the Liver: from Basic Research to Clinical Practice. *World Journal of Gastroenterology*, 17:2288, 2011.

[288] R. Agarwal, C. Agarwal, H. Ichikawa, R. P. Singh, and B. B. Aggarwal. Anticancer Potential of Silymarin: From Bench to Bed Side. *Anticancer Research*, 26:4457–4498, 2006.

[289] R. Weyhenmeyer, H. Mascher, and J. Birkmayer. Study on Dose-Linearity of the Pharmacokinetics of Silibinin Diastereomers Using a New Stereospecific Assay. *International Journal of Clinical Pharmacology and Theoretical Toxicology*, 30:134–138, 1992.

[290] V. Křen, J. Kubisch, Petr Sedmera, Petr Halada, V. Přikrylová, Alexandr Jegorov, Ladislav Cvak, Rolf Gebhardt, J. Ulrichová, and V. Šimánek. Glycosylation of Silybin. *Optimization*, pages 2467–2474, 1997.

[291] Vladimir Kren and Daniela Walterova. Silybin and Silymarin - New Effects and Applications. *Biomedical Papers*, 149(1):29–41, 2005.

[292] Oyvind M Andersen and Kenneth R Markham. *Flavonoids. Chemistry, Biochemistry and Applications*, volume 45. CRC Press, 1. edition edition, 2006.

[293] P. Barraja, P. Diana, A. Montalbano, A. Carbone, G. Viola, G. Basso, A. Salvador, D. Vedaldi, F. Dall'Acqua, and G. Cirrincione. Pyrrolo-[3,4-h]-quinolinones a New Class of Photochemotherapeutics Agents. *Bioorganic and Medicinal Chemistry*, 19:2326–2341, 2011.

[294] P. Hradil, P. Krejci, J. Hlavac, I. Wiedermannova, A. Lycka, and V. Bertolasi. Synthesis, NMR Spectra and X-Ray Data of Chloro and Dichloro Derivatives of 3-Hydroxy-2-Phenylquinolin-4(*1H*)-Ones and Their Cytostatic Activity. *Journal of Heterocyclic Chemistry*, 41(3):375–379, 2004.

[295] E. C. Pesci, J. B. J. Milbank, J. P. Pearson, S. McKnight, A. S. Kende, E. P. Greenberg, and B. H. Iglewski. Quinolone Signaling in the Cell-to-Cell Communication System of *Pseudomonas aeruginosa*. *Proceedings of the National Academy of Sciences*, 96(20):11229–11234, 1999.

[296] J. Kadrić, K. Motyka, P. Džubák, M. Hajdúch, and M. Soural. Synthesis, Cytotoxic Activity, and Fluorescence Properties of a Set of Novel 3-Hydroxyquinolin-4(*1H*)-Ones. *Tetrahedron Letters*, 55(26):3592–3595, 2014.

[297] R. Krikavova, J. Vanco, Z. Travnicek, R. Buchtik, and Z. Dvorak. Copper(II)quinolinonato-7-carboxamido Complexes as Potent Anti-tumor Agents with Broad Spectra and Selective Effects. *Royal Society of Chemistry*, 6:3899–3899, 2015.

[298] M. di Cagno, J. Styskala, J. Hlaváč, M. Brandi, A. Bauer-Brandl, and N. Skalko-Basnet. Liposomal Solubilization of New 3-hydroxy-quinolinone Derivatives with Promising Anti-Cancer Activity: A Screening Method to Identify Maximum Incorporation Capacity. *Journal ofo Liposome Research*, 21:272–278, 2011.

[299] M. di Cagno, P. C. Stein, J. Styskala, J. Hlaváč, N. Skalko-Basnet, and A. Bauer-Brandl. Overcoming Instability and Low Solubility of New Cytostatic Compounds: A Comparison of Two Approaches. *European Journal of Pharmacology and Biopharmacology*, 80:657–662, 2012.

[300] K. Bürglová, J. Hlaváč, and J. R. Bartlett. Synthesis of Silica Nanoparticals for Encapsulation of Oncology Drugs with Low Water Solubility: Effect of Processing Parameters in Structural Evolution. *Journal of Nanoparticle Research*, 17:123, 2015.

[301] M. Grepl, J. Roithova, P. Hradil, and K. Lemr. Ionisation and Fragmentation of Monochloro-Isomers of 3-Hydroxy-2-Phenyl-4(*1H*)-Quinolinone. *Rapid communications in mass spectrometry : RCM*, 22:2905–2914, 2008.

[302] Jaroslava Šeflová, Michal Biler, Pavel Hradil, Martin Kubala, Petra Čechová, Michal Biler, Pavel Hradil, and Martin Kubala. Inhibition of Na^+/K^+-ATPase by 5,6,7,8-tetrafluoro-3-hydroxy-2-phenylquinolin-4(1H)-one. *Biochemie*, 138:56–61, 2017.

[303] C. Monneret. Platinum Anti-Cancer Drugs. From Serendipity to Rational Design. *Annales Pharmaceutiques Francaises*, 69:286–295, 2011.

[304] M. Peyrone. Über die Einwirkung des Ammoniaks auf Platinchlorür [On the Influence of Ammonia on Platinum Chloride]. *Annals of Chemical Pharmacy*, 51:1, 1844.

[305] G. J. Bosl, D. F. Bajorin, J. Sheinfeld, and R. Motzer. *Cancer of the Testis*. Lippincott Wiliams and Wilkins, Phialdeplhia, Pennsylvania, 6. edditio edition, 2001.

[306] T. Boulikas and M. Vougiouka. Recent Clinical Trials Using Cisplatin, Carboplatin and Their Combination Chemotherapy Drugs. *Oncology Reports*, 11:559–595, 2004.

[307] M. A. Fuertes, C. Alonso, and J. M. Perez. Biochemical Modulation of Cisplatin Mechanisms of Action: Enhancement of Antitumor Activity and Circumvention of Drug Resistance. *Chemical Reviews*, 103:645–662, 2003.

[308] E. Cvitkovic. A Historical Perspective on Oxaliplatin: Rethinking the Role of Platinum Compounds and Learning from Near Misses. *Seminars in Oncology*, 25:1_3, 1998.

[309] R. Safaei. Role of Copper Transporters in the Uptake and Efflux of Platinum Containing Drugs. *Cancer Letters*, 234:34–39, 2006.

[310] A. Yonezawa and K. Inui. Organic Cation Transporter OCT/SLC22A and H^+/Organic Cation Antiporter MATE/SLC47A are Key Molecules for Nephrotoxicity of Platinum Agents. *Biochemical Pharmacology*, 81:563–568, 2011.

[311] M. C. Lim and R. B. Martin. The Nature of Cis-Amine Pd(II) and Anti-tumor Cis-Amine Pt(II) Complexes in Aqueous Solutions. *Journal of Inorganic and Nuclear Chemistry*, 38:1911–1914, 1976.

[312] B. Rosenberg. Anti-Cancer Activity of Cis-Dichloroammineplatinum(II) and Some Relevant Chemistry. *Cancer Treatment Reports*, 63:1433–1438, 1979.

[313] S. E. Miller and D. A. House. The Hydrolysis Products of Cis-diamminedichloroplatinum(II) 5. The Anation Kinetics of Cis-Pt(X)(NH3)2(OH2)+(X=Cl, OH) with Glycine, Monohydrogen Malonate and Chloride. *Inorganica Chimica Acta*, 187:125, 1991.

[314] A. L. Pinto and S. J. Lippard. Binding of the Anti-tumor Drug Cis-Diamminedichloroplatinum(II) (Cisplatin) to DNA. *Biochimica et Biophysica Acta (BBA)*, 780:167–180, 1985.

[315] R. Faggiani, B. Lippert, C. J. L. Lock, and B. Rosenberg. Hydroxo-Bridged Platinum(II) complexes. 1. Di-μ-hydroxo-bis[diammineplatinum(II)] Nitrate, $[(NH_3)_2Pt(OH)_2Pt(NH_3)_2](NO_3)_2$. Crystalline structure and vibrational spectra. *Journal of American Chemical Society*, 99:777–781, 1977.

[316] C. R. Centerwall, J. Goodisman, D. J. Kerwood, and J. C. Dabrowiak. Cisplatin Carbonato Complexes. Implications for Uptake, Antitumor Properties, and Toxicity. *Journal of American Chemical Society*, 127:12768–12769, 2005.

[317] E. Wong and C. M. Giandomenico. Current Status of Platinum-Based Antitumor Drugs. *Chemical Reviews*, 99:2451–2466, 1999.

[318] D P Gately and S B Howell. Cellular accumulation of the anticancer agent cisplatin: a review. *British journal of cancer*, 67(6):1171–6, 1993.

[319] J. L. Misset, H. Bleiberg, W. Sutherland, M. Bekradda, and E. Cvitkovic. Oxaliplatin Clinical Activity: A Review. *Critical Reviews in Oncology and Hematology*, 35:75–93, 2000.

[320] G. L. Cohen, W. R. Bauer, J. K. Barton, and S. J. Lippard. Binding of Cis- and Trans-Dichlorodiammineplatinum(II) to DNA: Evidence for Unwinding and Shortening of the Double Helix. *Science*, 203:1014–1060, 1979.

[321] D. S. Pilch, N. Poklar, C. A. Gelfand, S. M. Law, K. J. Breslauer, E. E. Baird, and P. B. Dervan. Binding of a Hairpin Polyamide in the Minor Groove of DNA: Sequence-Specific Enthalpic Discrimination. *Proceedings of the National Academy of Sciences of the United States of America*, 93:8306–8311, 1996.

[322] Franck Coste, Jean Marc Malinge, Laurence Serre, William Shepard, Michel Roth, Marc Leng, and Charles Zelwer. Crystal Structure of a Double-Stranded DNA Containing a Cisplatin Interstrand Cross-Link at 1.63 Å Resolution: Hydration at the Platinated Site. *Nucleic Acids Research*, 27(8):1837–1846, 1999.

[323] M. S. Davies, S. J. Berners-Price, and T. W. Hambley. Slowing of Cisplatin Aquation in the Presence of DNA but Not in the Presence of Phosphate: Improved Understanding of Sequence Selectivity and the Roles of Monoaquated and Diaquated Species in the Binding of Cisplatin to DNA. *Inorganic Chemistry*, 39:5603–5613, 2000.

[324] D. P. Bancroft, C. A. Lepre, and S. J. Lippard. Platinum-^{195}NMR Kinetic and Mechanistic Studies of Cis- and Trans-Diamminedichloroplatinum(II) Binding to DNA. *Journal of American Chemical Society*, 112:6860–6871, 1990.

[325] Paul B. Hopkins, Julie T. Millard, Jinsuk Woo, Margaret F. Weidner, James J. Kirchner, Snorri Th Sigurdsson, and Stanley Raucher. Sequence Preferences of DNA Interstrand Cross-Linking Agents: Importance of Minimal DNA Structural Reorganization in the Cross-Linking Reactions of Mechlorethamine, Cisplatin and Mitomycin C. *Tetrahedron*, 47(14-15):2475–2489, 1991.

[326] M. A. Lemaire, A. Schwertz, A. R. Rahmouni, and M. Leng. Interstrand Cross-Links are Preferentially Formed at the d(GC) Sites in the Reaction Between Cis-Diamminedichloroplatinum (II) and DNA. *Proceedings of the National Academy of Sciences of the United States of America*, 88:1982–1985, 1991.

[327] A. Binter, J. Goodisman, and J. C. Dabrowiak. Formation of Monofunctional Cisplatin-DNA Adducts in Carbonate Buffer. *Journal of Inorganic Biochemistry*, 100:1219, 2006.

[328] A. J. di Pasqua, J. Goodisman, D. J. Kerwood, B. B. Toms, R. L. Dubowy, and J. C. Dabrowiak. Activation of Carboplatin by Carbonate. *Chemical Research in Toxicology*, 19:139–149, 2006.

[329] A. Eastman. The Formation, Isolation and Characterization of DNA Adducts Produced by Anticancer Platinum Complexes. *Pharmacological Therapy*, 34:155–166, 1987.

[330] S. L. Bruhn, J. H. Toney, and S. J. Lippard. *Progress in Inorganic Chemistry, Bioorganic Chemistry*. Wiley-VCH, New York, USA, 1. edditio edition, 1990.

[331] J. Reedijk. The Relevance of Hydrogen Bonding in the Mechanism of Action of Platinum Antitumor Compounds. *Inorganica Chimica Acta*, 198:873–881, 1992.

[332] M. Sip and M. Leng. *DNA, Cis-Platinum and Intercalators: Catalytic Activity of the DNA Double Helix*, volume 7. Springer Verlag, Berlin Heidelberg, 1. edditio edition, 1993.

[333] M. Kartalou and J. M. Essigmann. Mechanisms of Resistance to Cisplatin. *Mutation Research*, 478:23–43, 2001.

[334] R. B. Weiss and M. C. Christian. New Cisplatin Analogues in Development. *Drugs*, 46:360–377, 1993.

[335] C.P. Saris, PJ.M. van de Vaart, R.C. Rietbroek, and FA. Bloramaert. *In vitro* Formation of DNA Adducts by Cisplatin, Lobaplatin and Oxaliplatin in Calf Thymus DNA in Solution and in Cultured Human Cells. *Carcinogenesis*, 17(12):2763–2769, 1996.

[336] P. Pil and Stephen J Lippard. *Encyclopedia of Cancer*. Academic Press, San Diego, California, 1. edditio edition, 1997.

[337] S. R. McWhinney, R. M. Goldberg, and H. L. McLeod. Platinum Neurotoxicity Pharmacogenetics. *Molecular Cancer Therapy*, 8:10–16, 2009.

[338] B. Odenheimer and W. Wolf. Reactions of Cisplatin with Sulfur-Containing Amino Acids and Peptides. 1. Cysteine and Glutathione. *Inorganica Chimica Acta*, 66:L41–L43, 1982.

[339] M. Huliciak, J. Vacek, M. Sebela, E. Orolinova, J. Znaleziona, M. Havlikova, and M. Kubala. Covalent Binding of Cisplatin Impairs the Function of $Na^+[K^+$-ATPase by Binding to its Cytoplasmic Part. *Biochemical Pharmacology*, 83(11):1507–1513, 2012.

[340] L. Steffensen and P. A. Pedersen. Heterologous Expression of Membrane and Soluble Proteins Derepresses *GCN4* mRNA Translation in the Yeast *Saccharomyces cerevisiae*. *Eukaryotic Cell*, 5(2):248–261, 2006.

[341] W. O. Bullock, J. M. Fernandez, and J. M. Short. XL1-Blue: A High Efficiency Plasmid Transforming recA *Escherichia coli* Strain with β-Galactosidase Selection. *Biotechniques*, 5:376–389, 1987.

[342] G. Bertani. Studies on Lysogenesis. I. The Mode of Phage Liberation by Lysogenic *Escherichia coli*. *Journal of bacteriology*, 62(3):293–300, 1951.

[343] D. Drew, S. Newstead, Y. Y. Sonoda, H. Kim, and G. Von Heijne. GFP-Based Optimization Scheme for the Overexpression and Purification of Eukaryotic Membrane Proteins in *Saccharomyces cerevisiae*. *Nature Protocols*, 3(5):784–798, 2009.

[344] F. Sherman. Getting Started with Yeast. *Methods in Enzymology*, 350(2002):3–41, 2002.

[345] A. Nishimura, M. Morita, Y. Nishimura, and Y. Sugino. A Rapid and Highly Efficient Method for Preparation of Competent *Escherichia coli* Cells. *Nucleic Acids Research*, 18(20):6169, 1990.

[346] M. M. Bradford. Rapid and Sensitive Method for the Quantitation of Microgram Quantities of Protein Utilizing the Principle of Protein-Dye Binding. *Analytical Biochemistry*, 72:248–254, 1976.

[347] R. L. Lundblad and C. M. Noyes. *Chemical Reagents for Protein Modification*. CRC Press, Boca Ralton, Florida, 1. edition, 1984.

[348] M. Kalimi and K. Love. Role of Chemical Reagents in the Activation of Rat Hepatic Glucocoticoid-Receptor Complex. *Journal of Biological Chemistry*, 255:4687–4690, 1980.

[349] J. Beinhauer, R. Lenobel, D. Loginov, I. Chamrád, P. Řehulka, M. Sedlářová, M. Marchetti-Deschmann, G. Allmaier, and M. Šebela. Identification of *Brenia lactucae* and *Oidium neolycopersici* proteins extracted for intact spore MALDI mass spectrometric biotyping. *Electrophoresis*, 37:2940–2952, 2016.

[350] P. de la Llosa, A. el Abed, and M. Roy. Oxidation of methionine residues in lutropin. *Canadien Journal of Biochemistry*, 58:745–748, 1980.

[351] Yoram Shechter, Yigal Burstein, and Abraham Patchornik. Selective Oxidation of Methionine Residues in Proteins. *Biochemistry*, 14:4497–4503, 1976.

[352] P. Scharff-Poulsen and Per Amstrup Pedersen. *Saccharomyces cerevisiae*-Based Platform for Rapid Production and Evaluation of Eukaryotic Nutrient Transporters and Transceptors for Biochemical Studies and Crystallography. *PLoS ONE*, 8:e76851, 2013.

[353] J. H. Rasmussen, Per A Pedersen, and P. L. Jorgensen. High Yield Fermentation of Pig $\alpha_1\beta_1$ Na^+/K^+-ATPase in *Saccharomyces cerevisiae*. *Annals of the New York Academy of Sciences*, 834:469–471, 1997.

[354] J. L. Parker and S. Newstead. Method to Increase the Yield of Eukaryotic Membrane Protein Expression in *Saccharomyces cerevisiae* for Structural and Functional Studies. *Protein Science*, 23:1309–1314, 2014.

[355] J. B. Koenderink and H. G. P. Swarts. Expression of Na^+/K^+-ATPase and H^+/K^+-ATPase Isoforms with the *Baculovirus* Expression System. In M. Bublitz, editor, *P-Type ATPases: Methods and Protocols*, pages 71–78. Springer, 1. edditio edition, 2016.

[356] G. Lenoir, T. Menguy, F. Corre, P. Falson, P. A Pedersen, and D. Thine. Overproduction in Yeast and Rapid and Efficient Purification of the Rabbit SERCA1a Ca^{2+}-ATPase. *Culture*, 1560:67–83, 2002.

[357] J. C. Skou. Further Investigations on a Mg^{++} + Na^+-Activated Adenosinetriphosphatase, Possibly Related to the Active, Linked Transport of Na^+ and K^+ Across the Nerve Membrane. *Biochimica et biophysica acta*, 42:6–23, 1960.

[358] J. Šeflová, P. Čechová, K. M. Šišková, J. Kapitán, M. Kubala, M. Šebela, and P. Mojzeš. Cisplatin Interacting with Cytoplasmic Loop (C45) of the Na^+/K^+-ATPase: Role of Cysteine Residues. *X*, X:X, 2017.

[359] A. K. Boal and A. C. Rosenzweig. Crystal Structure of Cisplatin Bound to a Molecular Copper Chaperone. *Journal of American Chemical Society*, 131:14196–14197, 2009.

[360] J. C. Dabrowiak. *Metals in Medicine*. Wiley-VCH, Weinheim, Germany, first edition, 2009.

[361] Elena A. Dergousova, Irina Yu Petrushanko, Elizaveta A. Klimanova, Vladimir A. Mitkevich, Rustam H. Ziganshin, Olga D. Lopina, and Alexander A. Makarov. Effect of Reduction of Redox Modifications of Cys-residues in the Na^+,K^+-ATPase α_1-subunit on its Activity. *Biomolecules*, 7(1):1–11, 2017.

4.5 Mouse Brain C45 Sequence

In the following section we will list the sequences of all used genes that were inserted into cloning vectors. The sequence of mouse brain C45 loop used for site-directed mutagenesis is listed below.

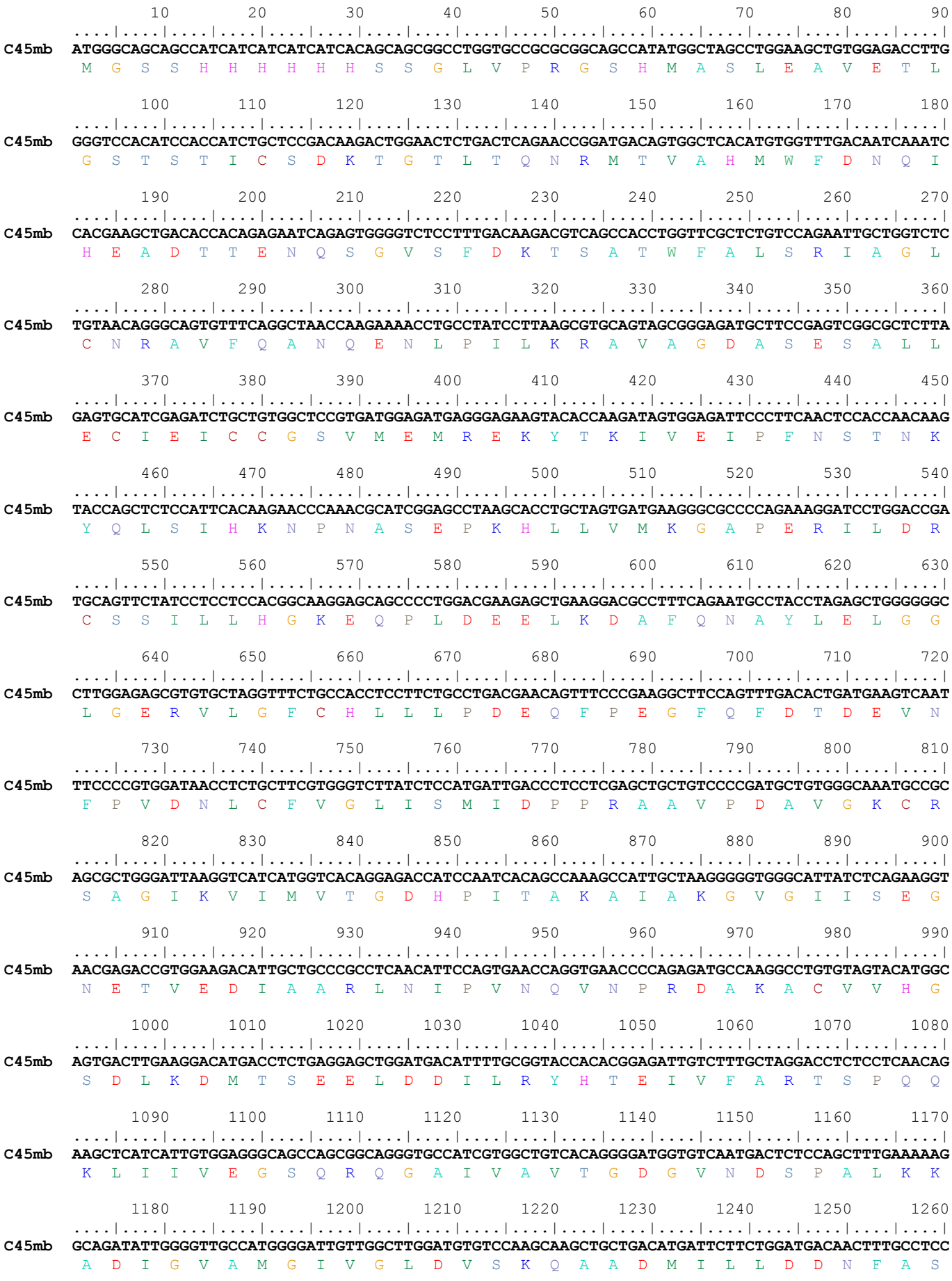
10 20 30 40 50 60 70 80 90
C45mb ATGGGCAGCAGCCATCATCATCATCATCACAGCAGCGGCCTGGTGCCGCGCGGCAGCCATATGGCTAGCCTGGAAGCTGTGGAGACCTTG
M G S S H H H H H H S S G L V P R G S H M A S L E A V E T L
100 110 120 130 140 150 160 170 180
C45mb GGGTCCACATCCACCATCTGCTCCGACAAGACTGGAACTCTGACTCAGAACCGGATGACAGTGGCTCACATGTGGTTTGACAATCAAATC
G S T S T I C S D K T G T L T Q N R M T V A H M W F D N Q I
190 200 210 220 230 240 250 260 270
C45mb CACGAAGCTGACACCACAGAGAATCAGAGTGGGGTCTCCTTTGACAAGACGTCAGCCACCTGGTTCGCTCTGTCCAGAATTGCTGGTCTC
H E A D T T E N Q S G V S F D K T S A T W F A L S R I A G L
280 290 300 310 320 330 340 350 360
C45mb TGTAACAGGGCAGTGTTTCAGGCTAACCAAGAAAACCTGCCTATCCTTAAGCGTGCAGTAGCGGGAGATGCTTCCGAGTCGGCGCTCTTA
C N R A V F Q A N Q E N L P I L K R A V A G D A S E S A L L
370 380 390 400 410 420 430 440 450
C45mb GAGTGCATCGAGATCTGCTGTGGCTCCGTGATGGAGATGAGGGAGAAGTACACCAAGATAGTGGAGATTCCCTTCAACTCCACCAACAAG
E C I E I C C G S V M E M R E K Y T K I V E I P F N S T N K
460 470 480 490 500 510 520 530 540
C45mb TACCAGCTCTCCATTCACAAGAACCCAAACGCATCGGAGCCTAAGCACCTGCTAGTGATGAAGGGCGCCCCAGAAAGGATCCTGGACCGA
Y Q L S I H K N P N A S E P K H L L V M K G A P E R I L D R
550 560 570 580 590 600 610 620 630
C45mb TGCAGTTCTATCCTCCTCCACGGCAAGGAGCAGCCCCTGGACGAAGAGCTGAAGGACGCCTTTCAGAATGCCTACCTAGAGCTGGGGGGC
C S S I L L H G K E Q P L D E E L K D A F Q N A Y L E L G G
640 650 660 670 680 690 700 710 720
C45mb CTTGGAGAGCGTGTGCTAGGTTTCTGCCACCTCCTTCTGCCTGACGAACAGTTTCCCGAAGGCTTCCAGTTTGACACTGATGAAGTCAAT
L G E R V L G F C H L L L P D E Q F P E G F Q F D T D E V N
730 740 750 760 770 780 790 800 810
C45mb TTCCCCGTGGATAACCTCTGCTTCGTGGGTCTTATCTCCATGATTGACCCTCCTCGAGCTGCTGTCCCCGATGCTGTGGGCAAATGCCGC
F P V D N L C F V G L I S M I D P P R A A V P D A V G K C R
820 830 840 850 860 870 880 890 900
C45mb AGCGCTGGGATTAAGGTCATCATGGTCACAGGAGACCATCCAATCACAGCCAAAGCCATTGCTAAGGGGGTGGGCATTATCTCAGAAGGT
S A G I K V I M V T G D H P I T A K A I A K G V G I I S E G
910 920 930 940 950 960 970 980 990
C45mb AACGAGACCGTGGAAGACATTGCTGCCCGCCTCAACATTCCAGTGAACCAGGTGAACCCCAGAGATGCCAAGGCCTGTGTAGTACATGGC
N E T V E D I A A R L N I P V N Q V N P R D A K A C V V H G
1000 1010 1020 1030 1040 1050 1060 1070 1080
C45mb AGTGACTTGAAGGACATGACCTCTGAGGAGCTGGATGACATTTTGCGGTACCACACGGAGATTGTCTTTGCTAGGACCTCTCCTCAACAG
S D L K D M T S E E L D D I L R Y H T E I V F A R T S P Q Q
1090 1100 1110 1120 1130 1140 1150 1160 1170
C45mb AAGCTCATCATTGTGGAGGGCAGCCAGCGGCAGGGTGCCATCGTGGCTGTCACAGGGGATGGTGTCAATGACTCTCCAGCTTTGAAAAAG
K L I I V E G S Q R Q G A I V A V T G D G V N D S P A L K K
1180 1190 1200 1210 1220 1230 1240 1250 1260
C45mb GCAGATATTGGGGTTGCCATGGGGATTGTTGGCTTGGATGTGTCCAAGCAAGCTGCTGACATGATTCTTCTGGATGACAACTTTGCCTCC
A D I G V A M G I V G L D V S K Q A A D M I L L D D N F A S

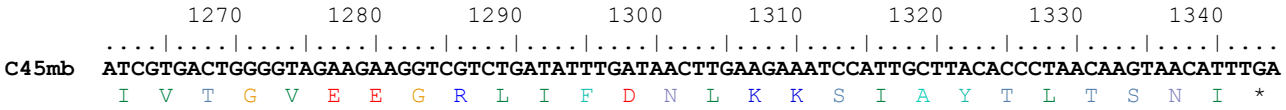
1270 1280 1290 1300 1310 1320 1330 1340
C45mb ATCGTGACTGGGGTAGAAGAAGGTCGTCTGATATTTGATAACTTGAAGAAATCCATTGCTTACACCCTAACAAGTAACATTTGA
I V T G V E E G R L I F D N L K K S I A Y T L T S N I *

4.6 Human α_1, α_2, and α_3 C45 Sequences

All sequences of C45 loops derived from human α_1, α_2, and α_3 genes are listed below.


10 20 30 40 50 60 70 80 90
A1 C45 ATGGCAAGGAAAAACTGCTTAGTGAAGAACTTAGAAGCTGTGGAGACCTTGGGGTCCACGTCCACCATCTGCTCTGAT
M A R K N C L V K N L E A V E T L G S T S T I C S D
100 110 120 130 140 150 160 170 180
A1 C45 AAAACTGGAACTCTGACTCAGAACCGGATGACAGTGGCCCACATGTGGTTTGACAATCAAATCCATGAAGCTGATACGACAGAGAATCAG
K T G T L T Q N R M T V A H M W F D N Q I H E A D T T E N Q
190 200 210 220 230 240 250 260 270
A1 C45 AGTGGTGTCTCTTTTGACAAGACTTCAGCTACCTGGCTTGCTCTGTCCAGAATTGCAGGTCTTTGTAACAGGGCAGTGTTTCAGGCTAAC
S G V S F D K T S A T W L A L S R I A G L C N R A V F Q A N
280 290 300 310 320 330 340 350 360
A1 C45 CAGGAAAACCTACCTATTCTTAAGCGGGCAGTTGCAGGAGATGCCTCTGAGTCAGCACTCTTAAAGTGCATAGAGCTGTGCTGTGGTTCC
Q E N L P I L K R A V A G D A S E S A L L K C I E L C C G S
370 380 390 400 410 420 430 440 450
A1 C45 GTGAAGGAGATGAGAGAAAGATACGCCAAAATCGTCGAGATACCCTTCAACTCCACCAACAAGTACCAGTTGTCTATTCATAAGAACCCC
V K E M R E R Y A K I V E I P F N S T N K Y Q L S I H K N P
460 470 480 490 500 510 520 530 540
A1 C45 AACACATCGGAGCCCCAACACCTGTTGGTGATGAAGGGCGCCCCAGAAAGGATCCTAGACCGTTGCAGCTCTATCCTCCTCCACGGCAAG
N T S E P Q H L L V M K G A P E R I L D R C S S I L L H G K
550 560 570 580 590 600 610 620 630
A1 C45 GAGCAGCCCCTGGATGAGGAGCTGAAAGACGCCTTTCAGAACGCCTATTTGGAGCTGGGGGGCCTCGGAGAACGAGTCCTAGGTTTCTGC
E Q P L D E E L K D A F Q N A Y L E L G G L G E R V L G F C
640 650 660 670 680 690 700 710 720
A1 C45 CACCTCTTTCTGCCAGATGAACAGTTTCCTGAAGGGTTCCAGTTTGACACTGACGATGTGAATTTCCCTATCGATAATCTGTGCTTTGTT
H L F L P D E Q F P E G F Q F D T D D V N F P I D N L C F V
730 740 750 760 770 780 790 800 810
A1 C45 GGGCTCATCTCCATGATTGACCCTCCACGGGCGGCCGTTCCTGATGCCGTGGGCAAATGTCGAAGTGCTGGAATTAAGGTCATCATGGTC
G L I S M I D P P R A A V P D A V G K C R S A G I K V I M V
820 830 840 850 860 870 880 890 900
A1 C45 ACAGGAGACCATCCAATCACAGCTAAAGCTATTGCCAAAGGTGTGGGCATCATCTCAGAAGGCAATGAGACCGTGGAAGACATTGCTGCC
T G D H P I T A K A I A K G V G I I S E G N E T V E D I A A
910 920 930 940 950 960 970 980 990
A1 C45 CGCCTCAACATCCCAGTCAGCCAGGTGAACCCCAGGGATGCCAAGGCCTGCGTAGTACACGGCAGTGATCTAAAGGACATGACCTCCGAG
R L N I P V S Q V N P R D A K A C V V H G S D L K D M T S E
1000 1010 1020 1030 1040 1050 1060 1070 1080
A1 C45 CAGCTGGATGACATTTTGAAGTACCACACTGAGATAGTGTTTGCCAGGACCTCCCCTCAGCAGAAGCTCATCATTGTGGAAGGCTGCCAA
Q L D D I L K Y H T E I V F A R T S P Q Q K L I I V E G C Q

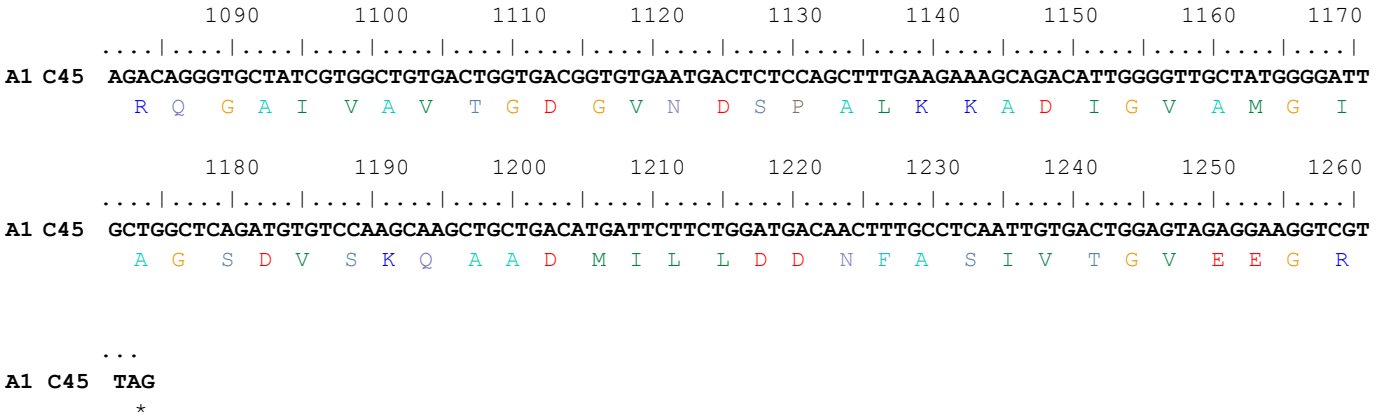
1090 1100 1110 1120 1130 1140 1150 1160 1170
A1 C45 AGACAGGGTGCTATCGTGGCTGTGACTGGTGACGGTGTGAATGACTCTCCAGCTTTGAAGAAAGCAGACATTGGGGTTGCTATGGGGATT
R Q G A I V A V T G D G V N D S P A L K K A D I G V A M G I
1180 1190 1200 1210 1220 1230 1240 1250 1260
A1 C45 GCTGGCTCAGATGTGTCCAAGCAAGCTGCTGACATGATTCTTCTGGATGACAACTTTGCCTCAATTGTGACTGGAGTAGAGGAAGGTCGT
A G S D V S K Q A A D M I L L D D N F A S I V T G V E E G R
...
A1 C45 TAG
*

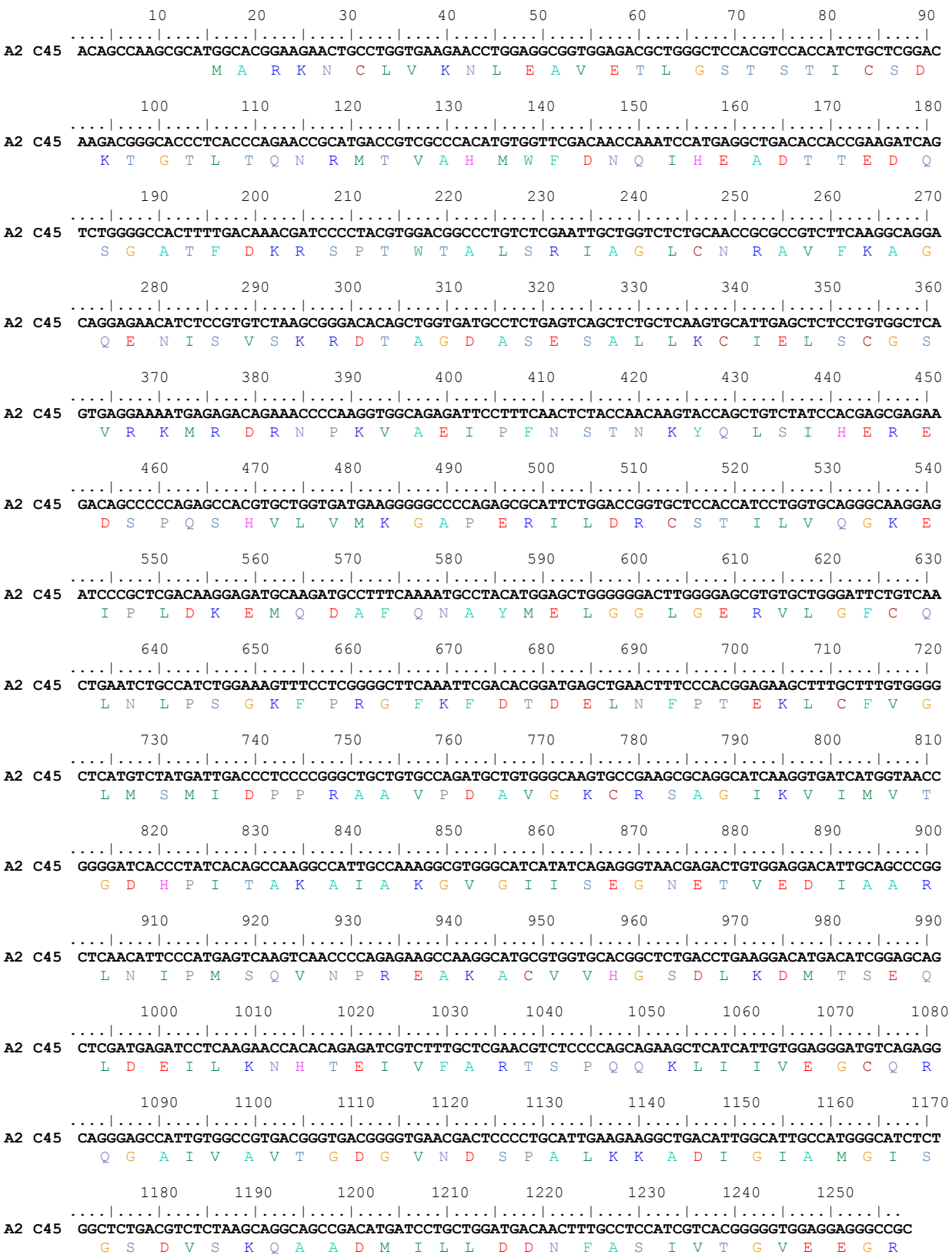
10 20 30 40 50 60 70 80 90
A2 C45 ACAGCCAAGCGCATGGCACGGAAGAACTGCCTGGTGAAGAACCTGGAGGCGGTGGAGACGCTGGGCTCCACGTCCACCATCTGCTCGGAC
M A R K N C L V K N L E A V E T L G S T S T I C S D
100 110 120 130 140 150 160 170 180
A2 C45 AAGACGGGCACCCTCACCCAGAACCGCATGACCGTCGCCCACATGTGGTTCGACAACCAAATCCATGAGGCTGACACCACCGAAGATCAG
K T G T L T Q N R M T V A H M W F D N Q I H E A D T T E D Q
190 200 210 220 230 240 250 260 270
A2 C45 TCTGGGGCCACTTTTGACAAACGATCCCCTACGTGGACGGCCCTGTCTCGAATTGCTGGTCTCTGCAACCGCGCCGTCTTCAAGGCAGGA
S G A T F D K R S P T W T A L S R I A G L C N R A V F K A G
280 290 300 310 320 330 340 350 360
A2 C45 CAGGAGAACATCTCCGTGTCTAAGCGGGACACAGCTGGTGATGCCTCTGAGTCAGCTCTGCTCAAGTGCATTGAGCTCTCCTGTGGCTCA
Q E N I S V S K R D T A G D A S E S A L L K C I E L S C G S
370 380 390 400 410 420 430 440 450
A2 C45 GTGAGGAAAATGAGAGACAGAAACCCCAAGGTGGCAGAGATTCCTTTCAACTCTACCAACAAGTACCAGCTGTCTATCCACGAGCGAGAA
V R K M R D R N P K V A E I P F N S T N K Y Q L S I H E R E
460 470 480 490 500 510 520 530 540
A2 C45 GACAGCCCCCAGAGCCACGTGCTGGTGATGAAGGGGGCCCCAGAGCGCATTCTGGACCGGTGCTCCACCATCCTGGTGCAGGGCAAGGAG
D S P Q S H V L V M K G A P E R I L D R C S T I L V Q G K E
550 560 570 580 590 600 610 620 630
A2 C45 ATCCCGCTCGACAAGGAGATGCAAGATGCCTTTCAAAATGCCTACATGGAGCTGGGGGGACTTGGGGAGCGTGTGCTGGGATTCTGTCAA
I P L D K E M Q D A F Q N A Y M E L G G L G E R V L G F C Q
640 650 660 670 680 690 700 710 720
A2 C45 CTGAATCTGCCATCTGGAAAGTTTCCTCGGGGCTTCAAATTCGACACGGATGAGCTGAACTTTCCCACGGAGAAGCTTTGCTTTGTGGGG
L N L P S G K F P R G F K F D T D E L N F P T E K L C F V G
730 740 750 760 770 780 790 800 810
A2 C45 CTCATGTCTATGATTGACCCTCCCCGGGCTGCTGTGCCAGATGCTGTGGGCAAGTGCCGAAGCGCAGGCATCAAGGTGATCATGGTAACC
L M S M I D P P R A A V P D A V G K C R S A G I K V I M V T
820 830 840 850 860 870 880 890 900
A2 C45 GGGGATCACCCTATCACAGCCAAGGCCATTGCCAAAGGCGTGGGCATCATATCAGAGGGTAACGAGACTGTGGAGGACATTGCAGCCCGG
G D H P I T A K A I A K G V G I I S E G N E T V E D I A A R
910 920 930 940 950 960 970 980 990
A2 C45 CTCAACATTCCCATGAGTCAAGTCAACCCCAGAGAAGCCAAGGCATGCGTGGTGCACGGCTCTGACCTGAAGGACATGACATCGGAGCAG
L N I P M S Q V N P R E A K A C V V H G S D L K D M T S E Q
1000 1010 1020 1030 1040 1050 1060 1070 1080
A2 C45 CTCGATGAGATCCTCAAGAACCACACAGAGATCGTCTTTGCTCGAACGTCTCCCCAGCAGAAGCTCATCATTGTGGAGGGATGTCAGAGG
L D E I L K N H T E I V F A R T S P Q Q K L I I V E G C Q R
1090 1100 1110 1120 1130 1140 1150 1160 1170
A2 C45 CAGGGAGCCATTGTGGCCGTGACGGGTGACGGGGTGAACGACTCCCCTGCATTGAAGAAGGCTGACATTGGCATTGCCATGGGCATCTCT
Q G A I V A V T G D G V N D S P A L K K A D I G I A M G I S
1180 1190 1200 1210 1220 1230 1240 1250
A2 C45 GGCTCTGACGTCTCTAAGCAGGCAGCCGACATGATCCTGCTGGATGACAACTTTGCCTCCATCGTCACGGGGGTGGAGGAGGGCCGC
G S D V S K Q A A D M I L L D D N F A S I V T G V E E G R


10 20 30 40 50 60 70 80 90
A3 C45 ACCGCCAAGCGCATGGCCCGGAAGAACTGCCTGGTGAAGAACCTGGAGGCTGTAGAAACCCTGGGCTCCACGTCCACCATCTGCTCAGAT
M A R K N C L V K N L E A V E T L G S T S T I C S D
100 110 120 130 140 150 160 170 180
A3 C45 AAGACAGGGACCCTCACTCAGAACCGCATGACAGTCGCCCACATGTGGTTTGACAACCAGATCCACGAGGCTGACACCACTGAGGACCAG
K T G T L T Q N R M T V A H M W F D N Q I H E A D T T E D Q
190 200 210 220 230 240 250 260 270
A3 C45 TCAGGGACCTCATTTGACAAGAGTTCGCACACCTGGGTGGCCCTGTCTCACATCGCTGGGCTCTGCAATCGCGCTGTCTTCAAGGGTGGT
S G T S F D K S S H T W V A L S H I A G L C N R A V F K G G
280 290 300 310 320 330 340 350 360
A3 C45 CAGGACAACATCCCTGTGCTCAAGAGGGATGTGGCTGGGGATGCGTCTGAGTCTGCCCTGCTCAAGTGCATCGAGCTGTCCTCTGGCTCC
Q D N I P V L K R D V A G D A S E S A L L K C I E L S S G S
370 380 390 400 410 420 430 440 450
A3 C45 GTGAAGCTGATGCGTGAACGCAACAAGAAAGTGGCTGAGATTCCCTTCAATTCCACCAACAAATACCAGCTCTCCATCCATGAGACCGAG
V K L M R E R N K K V A E I P F N S T N K Y Q L S I H E T E
460 470 480 490 500 510 520 530 540
A3 C45 GACCCCAACGACAACCGATACCTGCTGGTGATGAAGGGTGCCCCCGAGCGCATCCTGGACCGCTGCTCCACCATCCTGCTACAGGGCAAG
D P N D N R Y L L V M K G A P E R I L D R C S T I L L Q G K
550 560 570 580 590 600 610 620 630
A3 C45 GAGCAGCCTCTGGACGAGGAAATGAAGGAGGCCTTCCAGAATGCCTACCTTGAGCTCGGTGGCCTGGGCGAGCGCGTGCTTGGTTTCTGC
E Q P L D E E M K E A F Q N A Y L E L G G L G E R V L G F C
640 650 660 670 680 690 700 710 720
A3 C45 CATTATTACCTGCCCGAGGAGCAGTTCCCCAAGGGCTTTGCCTTCGACTGTGATGACGTGAACTTCACCACGGACAACCTCTGCTTTGTG
H Y Y L P E E Q F P K G F A F D C D D V N F T T D N L C F V
730 740 750 760 770 780 790 800 810
A3 C45 GGCCTCATGTCCATGATCGACCCACCCCGGGCAGCCGTCCCTGACGCGGTGGGCAAGTGTCGCAGCGCAGGCATCAAGGTCATCATGGTC
G L M S M I D P P R A A V P D A V G K C R S A G I K V I M V
820 830 840 850 860 870 880 890 900
A3 C45 ACCGGCGATCACCCCATCACGGCCAAGGCCATTGCCAAGGGTGTGGGCATCATCTCTGAGGGCAACGAGACTGTGGAGGACATCGCCGCC
T G D H P I T A K A I A K G V G I I S E G N E T V E D I A A
910 920 930 940 950 960 970 980 990
A3 C45 CGGCTCAACATTCCCGTCAGCCAGGTTAACCCCCGGGATGCCAAGGCCTGCGTGATCCACGGCACCGACCTCAAGGACTTCACCTCCGAG
R L N I P V S Q V N P R D A K A C V I H G T D L K D F T S E
1000 1010 1020 1030 1040 1050 1060 1070 1080
A3 C45 CAAATCGACGAGATCCTGCAGAATCACACCGAGATCGTCTTCGCCCGCACATCCCCCCAGCAGAAGCTCATCATTGTGGAGGGCTGTCAG
Q I D E I L Q N H T E I V F A R T S P Q Q K L I I V E G C Q

```
                1090      1100      1110      1120      1130      1140      1150      1160      1170
          ....|....|....|....|....|....|....|....|....|....|....|....|....|....|....|....|....|....|
A3 C45    AGACAGGGTGCAATTGTGGCTGTGACCGGGGATGGTGTGAACGACTCCCCCGCTCTGAAGAAGGCCGACATTGGGGTGGCCATGGGCATC
            R  Q   G   A   I   V   A   V   T   G   D   G   V   N   D   S   P   A   L   K   K   A   D   I   G   V   A   M   G   I

                1180      1190      1200      1210      1220      1230      1240      1250      1260
          ....|....|....|....|....|....|....|....|....|....|....|....|....|....|....|....|....|....|
A3 C45    GCTGGCTCTGACGTCTCCAAGCAGGCAGCTGACATGATCCTGCTGGACGACAACTTTGCCTCCATCGTCACAGGGGTGGAGGAGGGCCGC
            A   G   S   D   V   S   K   Q   A   A   D   M   I   L   L   D   D   N   F   A   S   I   V   T   G   V   E   E   G   R


          ...
A3 C45    TAG
          *
```

4.7 Human α_1, α_2, and α_3 C23 Sequences

All sequences of C23 loops derived from human α_1, α_2, and α_3 genes are listed below.

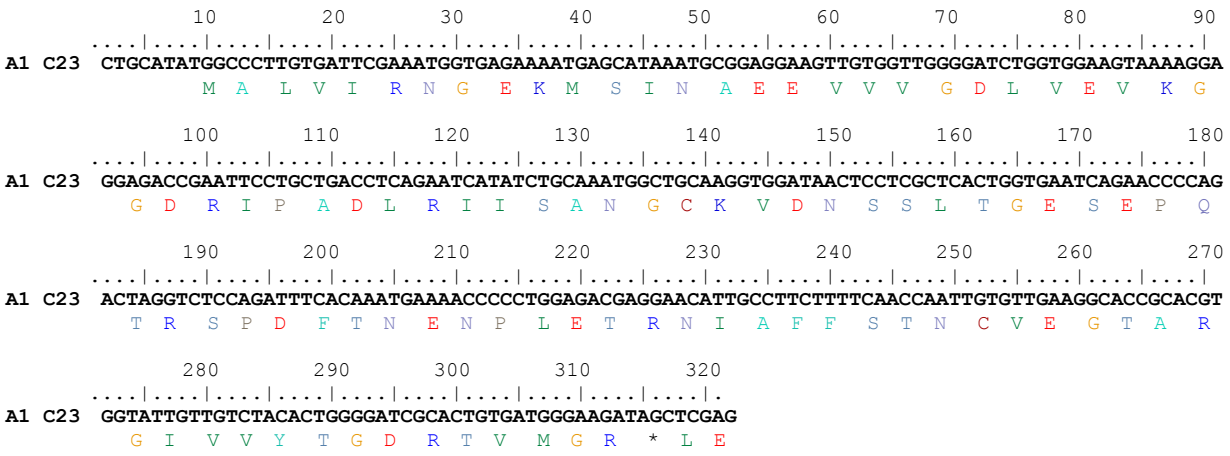
10 20 30 40 50 60 70 80 90
A1 C23 CTGCATATGGCCCTTGTGATTCGAAATGGTGAGAAAATGAGCATAAATGCGGAGGAAGTTGTGGTTGGGGATCTGGTGGAAGTAAAAGGA
M A L V I R N G E K M S I N A E E V V V G D L V E V K G
100 110 120 130 140 150 160 170 180
A1 C23 GGAGACCGAATTCCTGCTGACCTCAGAATCATATCTGCAAATGGCTGCAAGGTGGATAACTCCTCGCTCACTGGTGAATCAGAACCCCAG
G D R I P A D L R I I S A N G C K V D N S S L T G E S E P Q
190 200 210 220 230 240 250 260 270
A1 C23 ACTAGGTCTCCAGATTTCACAAATGAAAACCCCCTGGAGACGAGGAACATTGCCTTCTTTTCAACCAATTGTGTTGAAGGCACCGCACGT
T R S P D F T N E N P L E T R N I A F F S T N C V E G T A R
280 290 300 310 320
A1 C23 GGTATTGTTGTCTACACTGGGGATCGCACTGTGATGGGAAGATAGCTCGAG
G I V V Y T G D R T V M G R * L E

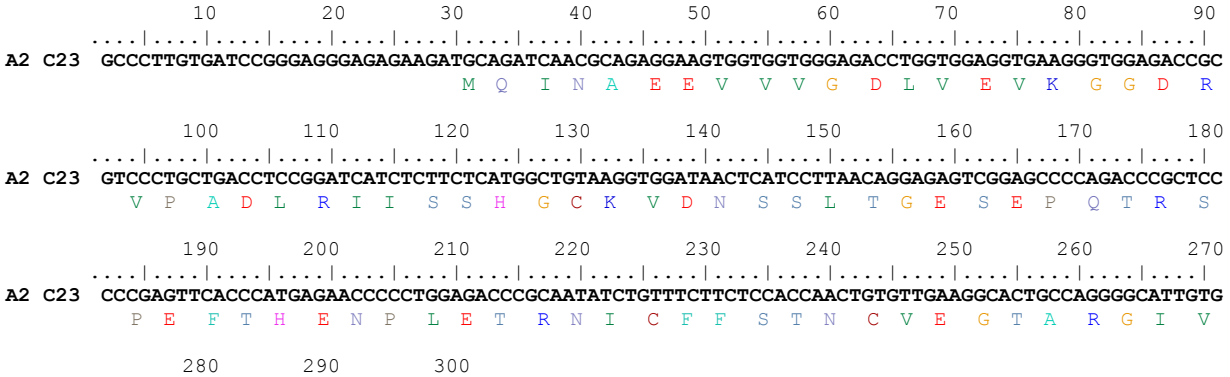
10 20 30 40 50 60 70 80 90
A2 C23 GCCCTTGTGATCCGGGAGGGAGAGAAGATGCAGATCAACGCAGAGGAAGTGGTGGTGGGAGACCTGGTGGAGGTGAAGGGTGGAGACCGC
M Q I N A E E V V V G D L V E V K G G D R
100 110 120 130 140 150 160 170 180
A2 C23 GTCCCTGCTGACCTCCGGATCATCTCTTCTCATGGCTGTAAGGTGGATAACTCATCCTTAACAGGAGAGTCGGAGCCCCAGACCCGCTCC
V P A D L R I I S S H G C K V D N S S L T G E S E P Q T R S
190 200 210 220 230 240 250 260 270
A2 C23 CCCGAGTTCACCCATGAGAACCCCCTGGAGACCCGCAATATCTGTTTCTTCTCCACCAACTGTGTTGAAGGCACTGCCAGGGGCATTGTG
P E F T H E N P L E T R N I C F F S T N C V E G T A R G I V
280 290 300
A2 C23 ATTGCCACAGGAGACCGGACGGTGATGGGCCGCTAG
I A T G D R T V M G R *

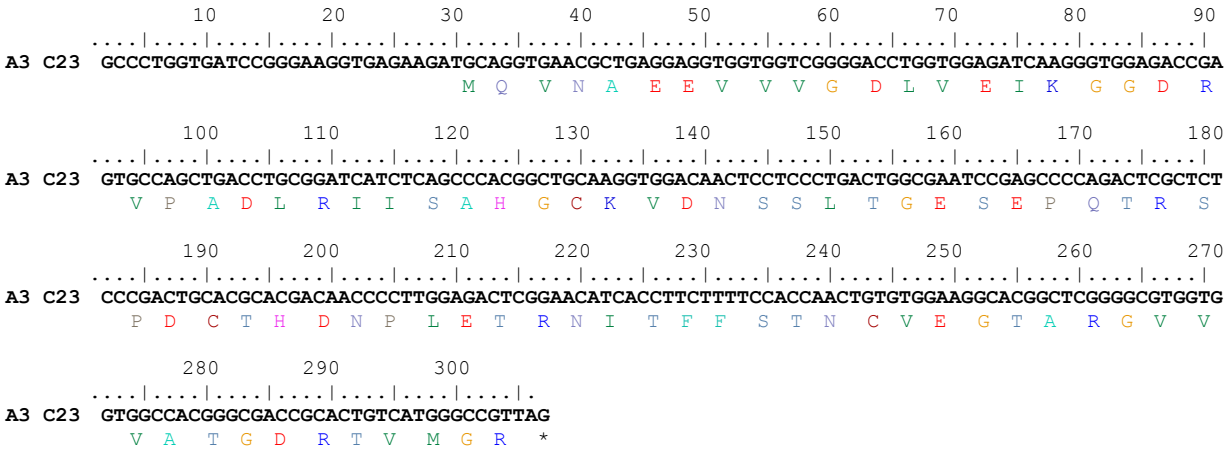
10 20 30 40 50 60 70 80 90
A3 C23 GCCCTGGTGATCCGGGAAGGTGAGAAGATGCAGGTGAACGCTGAGGAGGTGGTGGTCGGGGACCTGGTGGAGATCAAGGGTGGAGACCGA
M Q V N A E E V V V G D L V E I K G G D R
100 110 120 130 140 150 160 170 180
A3 C23 GTGCCAGCTGACCTGCGGATCATCTCAGCCCACGGCTGCAAGGTGGACAACTCCTCCCTGACTGGCGAATCCGAGCCCCAGACTCGCTCT
V P A D L R I I S A H G C K V D N S S L T G E S E P Q T R S
190 200 210 220 230 240 250 260 270
A3 C23 CCCGACTGCACGCACGACAACCCCTTGGAGACTCGGAACATCACCTTCTTTTCCACCAACTGTGTGGAAGGCACGGCTCGGGGCGTGGTG
P D C T H D N P L E T R N I T F F S T N C V E G T A R G V V
280 290 300
A3 C23 GTGGCCACGGGCGACCGCACTGTCATGGGCCGTTAG
V A T G D R T V M G R *

4.8 Alignment of the Human α_3 Sequences for Expression in the Mammalian Cells and in Yeast

Alignment of human α_3 sequences – sequence (1) codon-optimized sequence of human α_3 used for expression in yeast *Sacharomyces cerevisiae*, and (2) sequence of human α_3 for expression in mammalian cells. The similarity of those sequences is only about 70%, but the translated proteins are equal. The codon optimization is based on the yeast codon-preference.

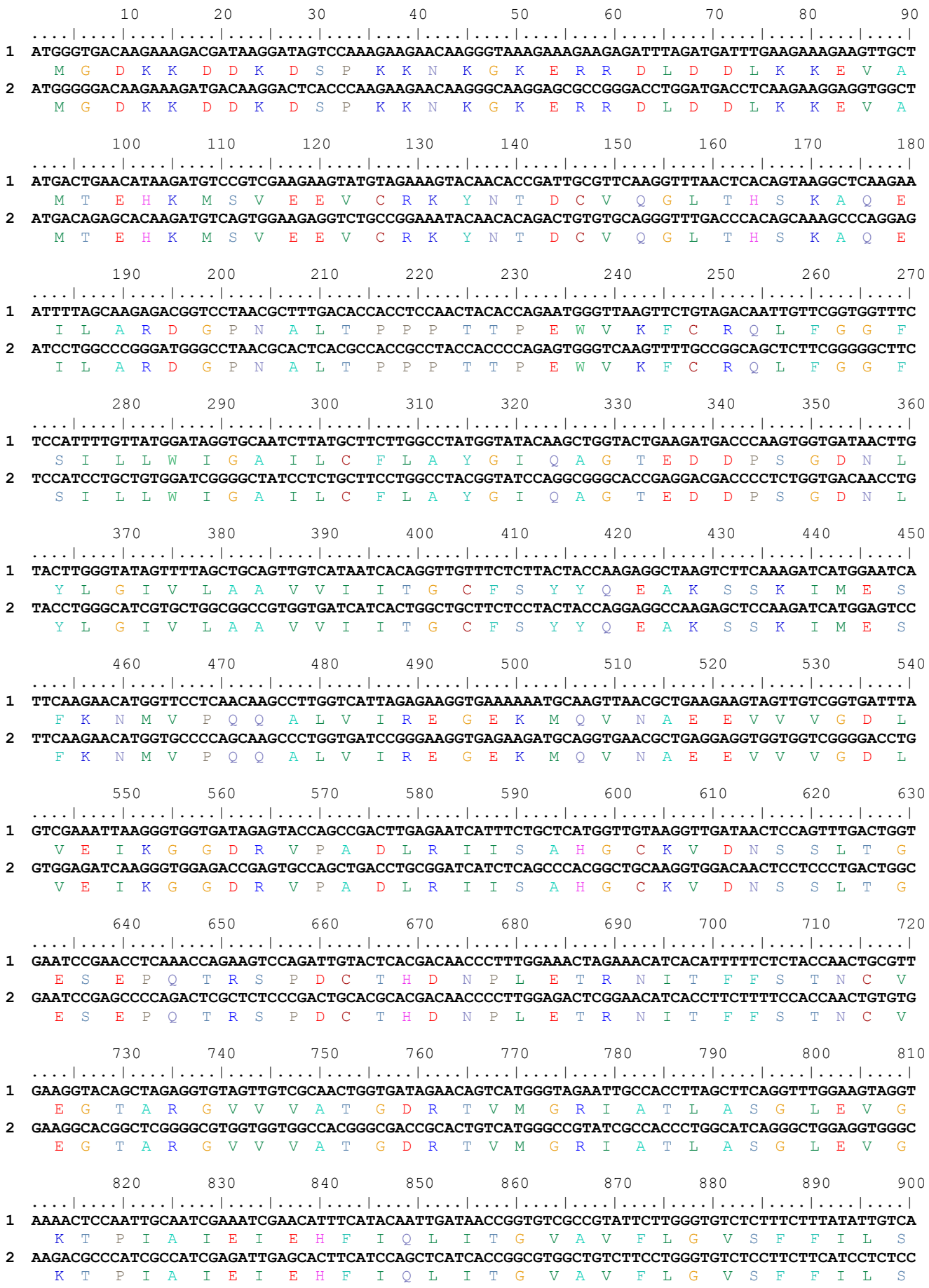
10 20 30 40 50 60 70 80 90
1 ATGGGTGACAAGAAAGACGATAAGGATAGTCCAAAGAAGAACAAGGGTAAAGAAAGAAGAGATTTAGATGATTTGAAGAAAGAAGTTGCT
M G D K K D D K D S P K K N K G K E R R D L D D L K K E V A
2 ATGGGGGACAAGAAAGATGACAAGGACTCACCCAAGAAGAACAAGGGCAAGGAGCGCCGGGACCTGGATGACCTCAAGAAGGAGGTGGCT
M G D K K D D K D S P K K N K G K E R R D L D D L K K E V A
100 110 120 130 140 150 160 170 180
1 ATGACTGAACATAAGATGTCCGTCGAAGAAGTATGTAGAAAGTACAACACCGATTGCGTTCAAGGTTTAACTCACAGTAAGGCTCAAGAA
M T E H K M S V E E V C R K Y N T D C V Q G L T H S K A Q E
2 ATGACAGAGCACAAGATGTCAGTGGAAGAGGTCTGCCGGAAATACAACACAGACTGTGTGCAGGGTTTGACCCACAGCAAAGCCCAGGAG
M T E H K M S V E E V C R K Y N T D C V Q G L T H S K A Q E
190 200 210 220 230 240 250 260 270
1 ATTTTAGCAAGAGACGGTCCTAACGCTTTGACACCACCTCCAACTACACCAGAATGGGTTAAGTTCTGTAGACAATTGTTCGGTGGTTTC
I L A R D G P N A L T P P P T T P E W V K F C R Q L F G G F
2 ATCCTGGCCCGGGATGGGCCTAACGCACTCACGCCACCGCCTACCACCCCAGAGTGGGTCAAGTTTTGCCGGCAGCTCTTCGGGGGCTTC
I L A R D G P N A L T P P P T T P E W V K F C R Q L F G G F
280 290 300 310 320 330 340 350 360
1 TCCATTTTGTTATGGATAGGTGCAATCTTATGCTTCTTGGCCTATGGTATACAAGCTGGTACTGAAGATGACCCAAGTGGTGATAACTTG
S I L L W I G A I L C F L A Y G I Q A G T E D D P S G D N L
2 TCCATCCTGCTGTGGATCGGGGCTATCCTCTGCTTCCTGGCCTACGGTATCCAGGCGGGCACCGAGGACGACCCCTCTGGTGACAACCTG
S I L L W I G A I L C F L A Y G I Q A G T E D D P S G D N L
370 380 390 400 410 420 430 440 450
1 TACTTGGGTATAGTTTTAGCTGCAGTTGTCATAATCACAGGTTGTTTCTCTTACTACCAAGAGGCTAAGTCTTCAAAGATCATGGAATCA
Y L G I V L A A V V I I T G C F S Y Y Q E A K S S K I M E S
2 TACCTGGGCATCGTGCTGGCGGCCGTGGTGATCATCACTGGCTGCTTCTCCTACTACCAGGAGGCCAAGAGCTCCAAGATCATGGAGTCC
Y L G I V L A A V V I I T G C F S Y Y Q E A K S S K I M E S
460 470 480 490 500 510 520 530 540
1 TTCAAGAACATGGTTCCTCAACAAGCCTTGGTCATTAGAGAAGGTGAAAAAATGCAAGTTAACGCTGAAGAAGTAGTTGTCGGTGATTTA
F K N M V P Q Q A L V I R E G E K M Q V N A E E V V V G D L
2 TTCAAGAACATGGTGCCCCAGCAAGCCCTGGTGATCCGGGAAGGTGAGAAGATGCAGGTGAACGCTGAGGAGGTGGTGGTCGGGGACCTG
F K N M V P Q Q A L V I R E G E K M Q V N A E E V V V G D L
550 560 570 580 590 600 610 620 630
1 GTCGAAATTAAGGGTGGTGATAGAGTACCAGCCGACTTGAGAATCATTTCTGCTCATGGTTGTAAGGTTGATAACTCCAGTTTGACTGGT
V E I K G G D R V P A D L R I I S A H G C K V D N S S L T G
2 GTGGAGATCAAGGGTGGAGACCGAGTGCCAGCTGACCTGCGGATCATCTCAGCCCACGGCTGCAAGGTGGACAACTCCTCCCTGACTGGC
V E I K G G D R V P A D L R I I S A H G C K V D N S S L T G
640 650 660 670 680 690 700 710 720
1 GAATCCGAACCTCAAACCAGAAGTCCAGATTGTACTCACGACAACCCTTTGGAAACTAGAAACATCACATTTTTCTCTACCAACTGCGTT
E S E P Q T R S P D C T H D N P L E T R N I T F F S T N C V
2 GAATCCGAGCCCCAGACTCGCTCTCCCGACTGCACGCACGACAACCCCTTGGAGACTCGGAACATCACCTTCTTTTCCACCAACTGTGTG
E S E P Q T R S P D C T H D N P L E T R N I T F F S T N C V
730 740 750 760 770 780 790 800 810
1 GAAGGTACAGCTAGAGGTGTAGTTGTCGCAACTGGTGATAGAACAGTCATGGGTAGAATTGCCACCTTAGCTTCAGGTTTGGAAGTAGGT
E G T A R G V V V A T G D R T V M G R I A T L A S G L E V G
2 GAAGGCACGGCTCGGGGCGTGGTGGTGGCCACGGGCGACCGCACTGTCATGGGCCGTATCGCCACCCTGGCATCAGGGCTGGAGGTGGGC
E G T A R G V V V A T G D R T V M G R I A T L A S G L E V G
820 830 840 850 860 870 880 890 900
1 AAAACTCCAATTGCAATCGAAATCGAACATTTCATACAATTGATAACCGGTGTCGCCGTATTCTTGGGTGTCTCTTTCTTTATATTGTCA
K T P I A I E I E H F I Q L I T G V A V F L G V S F F I L S
2 AAGACGCCCATCGCCATCGAGATTGAGCACTTCATCCAGCTCATCACCGGCGTGGCTGTCTTCCTGGGTGTCTCCTTCTTCATCCTCTCC
K T P I A I E I E H F I Q L I T G V A V F L G V S F F I L S

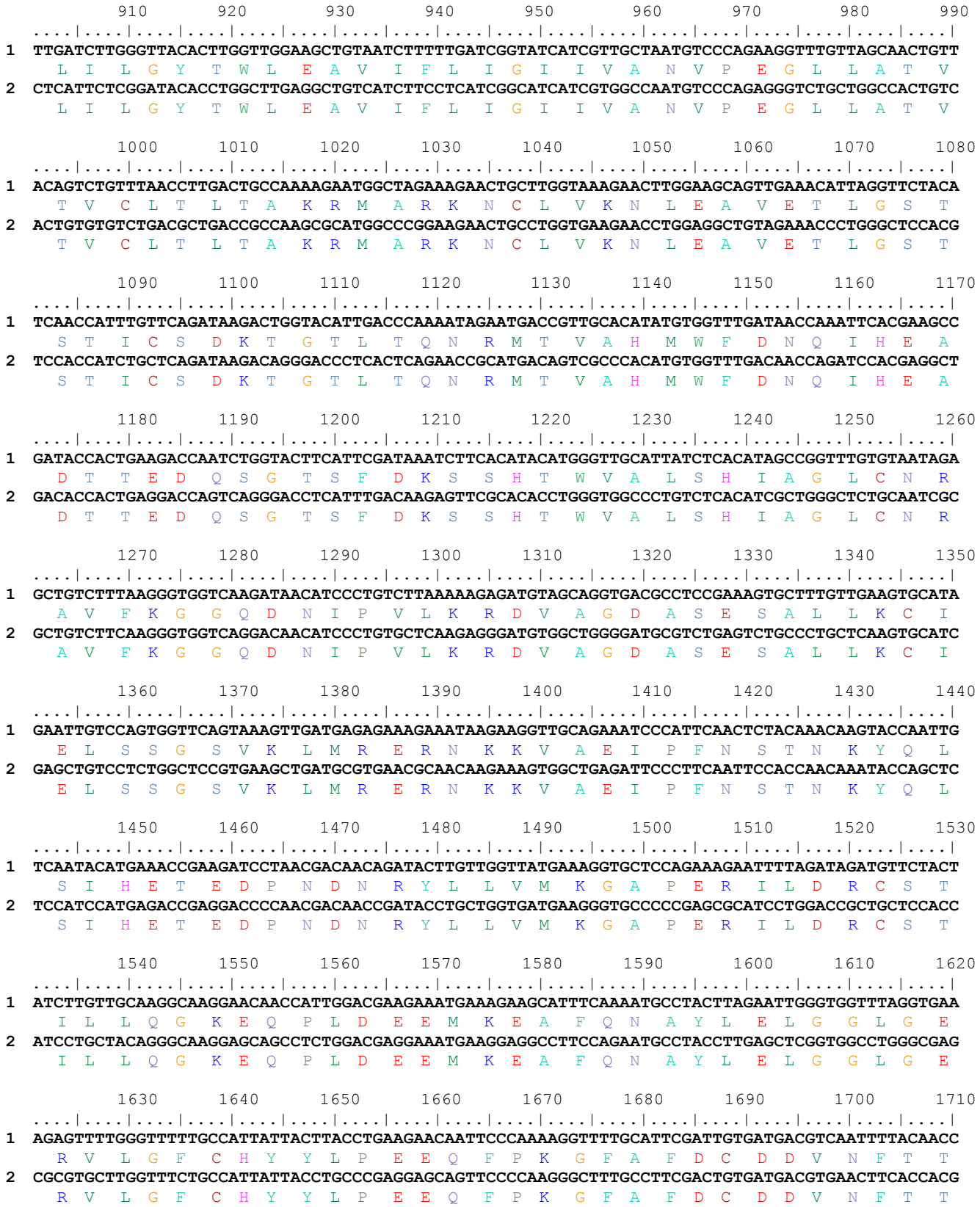
910 920 930 940 950 960 970 980 990
1 TTGATCTTGGGTTACACTTGGTTGGAAGCTGTAATCTTTTTGATCGGTATCATCGTTGCTAATGTCCCAGAAGGTTTGTTAGCAACTGTT
L I L G Y T W L E A V I F L I G I I V A N V P E G L L A T V
2 CTCATTCTCGGATACACCTGGCTTGAGGCTGTCATCTTCCTCATCGGCATCATCGTGGCCAATGTCCCAGAGGGTCTGCTGGCCACTGTC
L I L G Y T W L E A V I F L I G I I V A N V P E G L L A T V
1000 1010 1020 1030 1040 1050 1060 1070 1080
1 ACAGTCTGTTTAACCTTGACTGCCAAAAGAATGGCTAGAAAGAACTGCTTGGTAAAGAACTTGGAAGCAGTTGAAACATTAGGTTCTACA
T V C L T L T A K R M A R K N C L V K N L E A V E T L G S T
2 ACTGTGTGTCTGACGCTGACCGCCAAGCGCATGGCCCGGAAGAACTGCCTGGTGAAGAACCTGGAGGCTGTAGAAACCCTGGGCTCCACG
T V C L T L T A K R M A R K N C L V K N L E A V E T L G S T
1090 1100 1110 1120 1130 1140 1150 1160 1170
1 TCAACCATTTGTTCAGATAAGACTGGTACATTGACCCAAAATAGAATGACCGTTGCACATATGTGGTTTGATAACCAAATTCACGAAGCC
S T I C S D K T G T L T Q N R M T V A H M W F D N Q I H E A
2 TCCACCATCTGCTCAGATAAGACAGGGACCCTCACTCAGAACCGCATGACAGTCGCCCACATGTGGTTTGACAACCAGATCCACGAGGCT
S T I C S D K T G T L T Q N R M T V A H M W F D N Q I H E A
1180 1190 1200 1210 1220 1230 1240 1250 1260
1 GATACCACTGAAGACCAATCTGGTACTTCATTCGATAAATCTTCACATACATGGGTTGCATTATCTCACATAGCCGGTTTGTGTAATAGA
D T T E D Q S G T S F D K S S H T W V A L S H I A G L C N R
2 GACACCACTGAGGACCAGTCAGGGACCTCATTTGACAAGAGTTCGCACACCTGGGTGGCCCTGTCTCACATCGCTGGGCTCTGCAATCGC
D T T E D Q S G T S F D K S S H T W V A L S H I A G L C N R
1270 1280 1290 1300 1310 1320 1330 1340 1350
1 GCTGTCTTTAAGGGTGGTCAAGATAACATCCCTGTCTTAAAAAGAGATGTAGCAGGTGACGCCTCCGAAAGTGCTTTGTTGAAGTGCATA
A V F K G G Q D N I P V L K R D V A G D A S E S A L L K C I
2 GCTGTCTTCAAGGGTGGTCAGGACAACATCCCTGTGCTCAAGAGGGATGTGGCTGGGGATGCGTCTGAGTCTGCCCTGCTCAAGTGCATC
A V F K G G Q D N I P V L K R D V A G D A S E S A L L K C I
1360 1370 1380 1390 1400 1410 1420 1430 1440
1 GAATTGTCCAGTGGTTCAGTAAAGTTGATGAGAGAAAGAAATAAGAAGGTTGCAGAAATCCCATTCAACTCTACAAACAAGTACCAATTG
E L S S G S V K L M R E R N K K V A E I P F N S T N K Y Q L
2 GAGCTGTCCTCTGGCTCCGTGAAGCTGATGCGTGAACGCAACAAGAAAGTGGCTGAGATTCCCTTCAATTCCACCAACAAATACCAGCTC
E L S S G S V K L M R E R N K K V A E I P F N S T N K Y Q L
1450 1460 1470 1480 1490 1500 1510 1520 1530
1 TCAATACATGAAACCGAAGATCCTAACGACAACAGATACTTGTTGGTTATGAAAGGTGCTCCAGAAAGAATTTTAGATAGATGTTCTACT
S I H E T E D P N D N R Y L L V M K G A P E R I L D R C S T
2 TCCATCCATGAGACCGAGGACCCCAACGACAACCGATACCTGCTGGTGATGAAGGGTGCCCCCGAGCGCATCCTGGACCGCTGCTCCACC
S I H E T E D P N D N R Y L L V M K G A P E R I L D R C S T
1540 1550 1560 1570 1580 1590 1600 1610 1620
1 ATCTTGTTGCAAGGCAAGGAACAACCATTGGACGAAGAAATGAAAGAAGCATTTCAAAATGCCTACTTAGAATTGGGTGGTTTAGGTGAA
I L L Q G K E Q P L D E E M K E A F Q N A Y L E L G G L G E
2 ATCCTGCTACAGGGCAAGGAGCAGCCTCTGGACGAGGAAATGAAGGAGGCCTTCCAGAATGCCTACCTTGAGCTCGGTGGCCTGGGCGAG
I L L Q G K E Q P L D E E M K E A F Q N A Y L E L G G L G E
1630 1640 1650 1660 1670 1680 1690 1700 1710
1 AGAGTTTTGGGTTTTTGCCATTATTACTTACCTGAAGAACAATTCCCAAAAGGTTTTGCATTCGATTGTGATGACGTCAATTTTACAACC
R V L G F C H Y Y L P E E Q F P K G F A F D C D D V N F T T
2 CGCGTGCTTGGTTTCTGCCATTATTACCTGCCCGAGGAGCAGTTCCCCAAGGGCTTTGCCTTCGACTGTGATGACGTGAACTTCACCACG
R V L G F C H Y Y L P E E Q F P K G F A F D C D D V N F T T

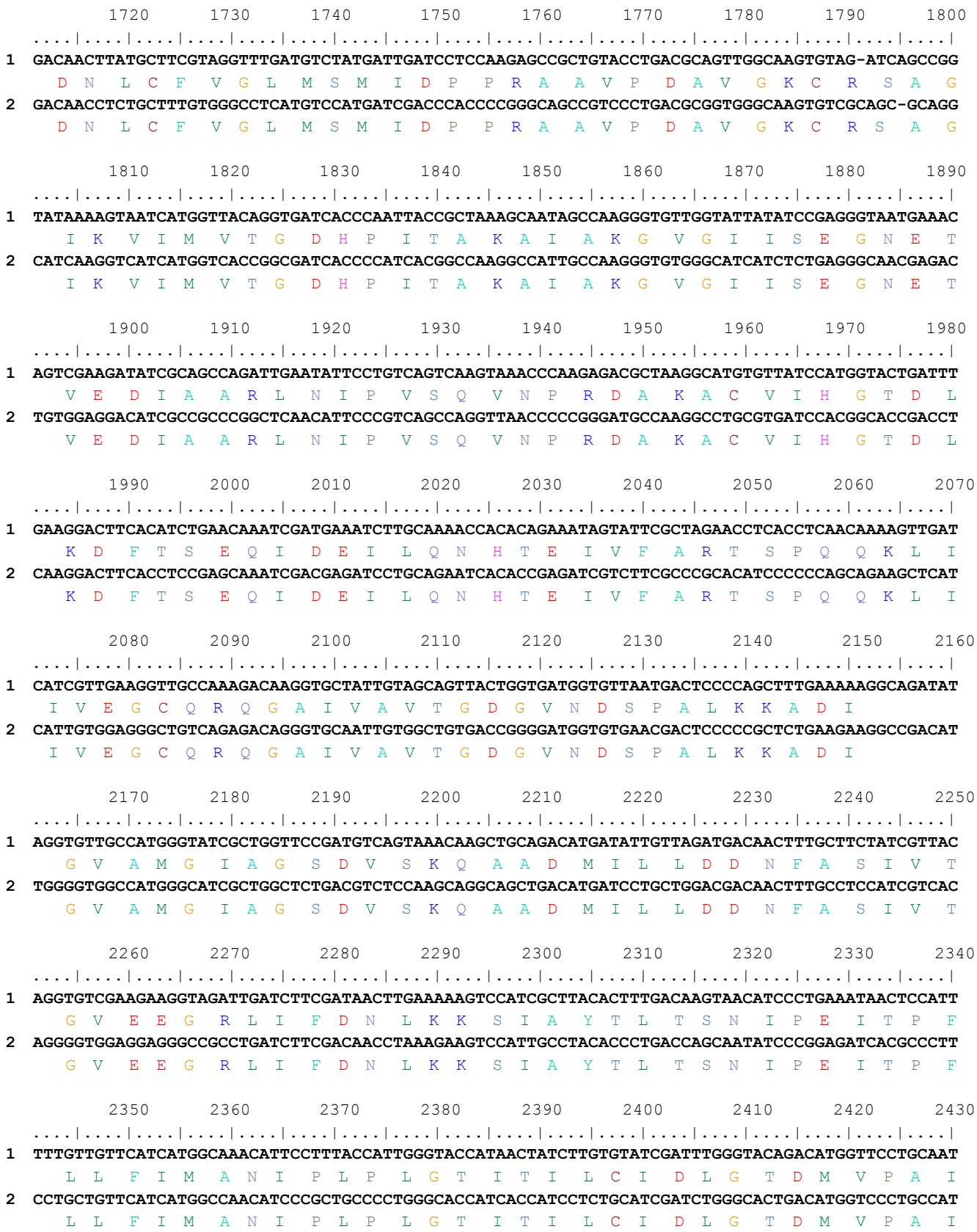
1720 1730 1740 1750 1760 1770 1780 1790 1800
1 GACAACTTATGCTTCGTAGGTTTGATGTCTATGATTGATCCTCCAAGAGCCGCTGTACCTGACGCAGTTGGCAAGTGTAG-ATCAGCCGG
D N L C F V G L M S M I D P P R A A V P D A V G K C R S A G
2 GACAACCTCTGCTTTGTGGGCCTCATGTCCATGATCGACCCACCCCGGGCAGCCGTCCCTGACGCGGTGGGCAAGTGTCGCAGC-GCAGG
D N L C F V G L M S M I D P P R A A V P D A V G K C R S A G
1810 1820 1830 1840 1850 1860 1870 1880 1890
1 TATAAAAGTAATCATGGTTACAGGTGATCACCCAATTACCGCTAAAGCAATAGCCAAGGGTGTTGGTATTATATCCGAGGGTAATGAAAC
I K V I M V T G D H P I T A K A I A K G V G I I S E G N E T
2 CATCAAGGTCATCATGGTCACCGGCGATCACCCCATCACGGCCAAGGCCATTGCCAAGGGTGTGGGCATCATCTCTGAGGGCAACGAGAC
I K V I M V T G D H P I T A K A I A K G V G I I S E G N E T
1900 1910 1920 1930 1940 1950 1960 1970 1980
1 AGTCGAAGATATCGCAGCCAGATTGAATATTCCTGTCAGTCAAGTAAACCCAAGAGACGCTAAGGCATGTGTTATCCATGGTACTGATTT
V E D I A A R L N I P V S Q V N P R D A K A C V I H G T D L
2 TGTGGAGGACATCGCCGCCCGGCTCAACATTCCCGTCAGCCAGGTTAACCCCCGGGATGCCAAGGCCTGCGTGATCCACGGCACCGACCT
V E D I A A R L N I P V S Q V N P R D A K A C V I H G T D L
1990 2000 2010 2020 2030 2040 2050 2060 2070
1 GAAGGACTTCACATCTGAACAAATCGATGAAATCTTGCAAAACCACACAGAAATAGTATTCGCTAGAACCTCACCTCAACAAAAGTTGAT
K D F T S E Q I D E I L Q N H T E I V F A R T S P Q Q K L I
2 CAAGGACTTCACCTCCGAGCAAATCGACGAGATCCTGCAGAATCACACCGAGATCGTCTTCGCCCGCACATCCCCCCAGCAGAAGCTCAT
K D F T S E Q I D E I L Q N H T E I V F A R T S P Q Q K L I
2080 2090 2100 2110 2120 2130 2140 2150 2160
1 CATCGTTGAAGGTTGCCAAAGACAAGGTGCTATTGTAGCAGTTACTGGTGATGGTGTTAATGACTCCCCAGCTTTGAAAAAGGCAGATAT
I V E G C Q R Q G A I V A V T G D G V N D S P A L K K A D I
2 CATTGTGGAGGGCTGTCAGAGACAGGGTGCAATTGTGGCTGTGACCGGGGATGGTGTGAACGACTCCCCCGCTCTGAAGAAGGCCGACAT
I V E G C Q R Q G A I V A V T G D G V N D S P A L K K A D I
2170 2180 2190 2200 2210 2220 2230 2240 2250
1 AGGTGTTGCCATGGGTATCGCTGGTTCCGATGTCAGTAAACAAGCTGCAGACATGATATTGTTAGATGACAACTTTGCTTCTATCGTTAC
G V A M G I A G S D V S K Q A A D M I L L D D N F A S I V T
2 TGGGGTGGCCATGGGCATCGCTGGCTCTGACGTCTCCAAGCAGGCAGCTGACATGATCCTGCTGGACGACAACTTTGCCTCCATCGTCAC
G V A M G I A G S D V S K Q A A D M I L L D D N F A S I V T
2260 2270 2280 2290 2300 2310 2320 2330 2340
1 AGGTGTCGAAGAAGGTAGATTGATCTTCGATAACTTGAAAAAGTCCATCGCTTACACTTTGACAAGTAACATCCCTGAAATAACTCCATT
G V E E G R L I F D N L K K S I A Y T L T S N I P E I T P F
2 AGGGGTGGAGGAGGGCCGCCTGATCTTCGACAACCTAAAGAAGTCCATTGCCTACACCCTGACCAGCAATATCCCGGAGATCACGCCCTT
G V E E G R L I F D N L K K S I A Y T L T S N I P E I T P F
2350 2360 2370 2380 2390 2400 2410 2420 2430
1 TTTGTTGTTCATCATGGCAAACATTCCTTTACCATTGGGTACCATAACTATCTTGTGTATCGATTTGGGTACAGACATGGTTCCTGCAAT
L L F I M A N I P L P L G T I T I L C I D L G T D M V P A I
2 CCTGCTGTTCATCATGGCCAACATCCCGCTGCCCCTGGGCACCATCACCATCCTCTGCATCGATCTGGGCACTGACATGGTCCCTGCCAT
L L F I M A N I P L P L G T I T I L C I D L G T D M V P A I

```
          2440       2450       2460       2470       2480       2490       2500       2510       2520
    ....|....|....|....|....|....|....|....|....|....|....|....|....|....|....|....|....|....|....|....|
1   ATCTTTGGCCTACGAAGCCGCTGAATCAGATATAATGAAGAGACAACCTAGAAACCCAAGAACTGACAAGTTGGTTAACGAAAGATTGAT
       S  L  A  Y  E  A  A  E  S  D  I  M  K  R  Q  P  R  N  P  R  T  D  K  L  V  N  E  R  L  I
2   CTCACTGGCGTACGAGGCTGCCGAAAGCGACATCATGAAGAGACAGCCCAGGAACCCGCGGACGGACAAATTGGTCAATGAGAGACTCAT
       S  L  A  Y  E  A  A  E  S  D  I  M  K  R  Q  P  R  N  P  R  T  D  K  L  V  N  E  R  L  I

          2530       2540       2550       2560       2570       2580       2590       2600       2610
    ....|....|....|....|....|....|....|....|....|....|....|....|....|....|....|....|....|....|....|....|
1   ATCCATGGCCTATGGTCAAATTGGTATGATCCAAGCTTTGGGTGGTTTCTTTTCTTACTTCGTTATCTTGGCTGAAAACGGTTTCTTACC
       S  M  A  Y  G  Q  I  G  M  I  Q  A  L  G  G  F  F  S  Y  F  V  I  L  A  E  N  G  F  L  P
2   CAGCATGGCCTACGGGCAGATTGGAATGATCCAGGCTCTCGGTGGCTTCTTCTCTTACTTTGTGATCCTGGCAGAAAATGGCTTCTTGCC
       S  M  A  Y  G  Q  I  G  M  I  Q  A  L  G  G  F  F  S  Y  F  V  I  L  A  E  N  G  F  L  P

          2620       2630       2640       2650       2660       2670       2680       2690       2700
    ....|....|....|....|....|....|....|....|....|....|....|....|....|....|....|....|....|....|....|....|
1   TGGTAACTTAGTAGGTATCAGATTAAATTGGGATGACAGAACTGTTAACGATTTGGAAGACTCTTATGGTCAACAATGGACATACGAACA
       G  N  L  V  G  I  R  L  N  W  D  D  R  T  V  N  D  L  E  D  S  Y  G  Q  Q  W  T  Y  E  Q
2   CGGCAACCTGGTGGGCATCCGGCTGAACTGGGATGACCGCACCGTCAATGACCTGGAAGACAGTTACGGGCAGCAGTGGACATACGAGCA
       G  N  L  V  G  I  R  L  N  W  D  D  R  T  V  N  D  L  E  D  S  Y  G  Q  Q  W  T  Y  E  Q

          2710       2720       2730       2740       2750       2760       2770       2780       2790
    ....|....|....|....|....|....|....|....|....|....|....|....|....|....|....|....|....|....|....|....|
1   AAGAAAGGTAGTTGAATTTACATGTCATACCGCTTTCTTTGTTTCTATTGTCGTAGTTCAATGGGCAGATTTGATCATCTGCAAGACCAG
       R  K  V  V  E  F  T  C  H  T  A  F  F  V  S  I  V  V  V  Q  W  A  D  L  I  I  C  K  T  R
2   GAGGAAGGTGGTGGAGTTCACCTGCCACACGGCCTTCTTTGTGAGCATCGTTGTCGTCCAGTGGGCCGATCTGATCATCTGCAAGACCCG
       R  K  V  V  E  F  T  C  H  T  A  F  F  V  S  I  V  V  V  Q  W  A  D  L  I  I  C  K  T  R

          2800       2810       2820       2830       2840       2850       2860       2870       2880
    ....|....|....|....|....|....|....|....|....|....|....|....|....|....|....|....|....|....|....|....|
1   AAGAAATTCAGTTTTCCAACAGGGTATGAAGAACAAGATCTTGATCTTCGGTTTGTTCGAAGAAACAGCTTTAGCAGCCTTTTTGTCTTA
     R  N  S  V  F  Q  Q  G  M  K  N  K  I  L  I  F  G  L  F  E  E  T  A  L  A  A  F  L  S  Y
2   GAGGAACTCGGTCTTCCAGCAGGGCATGAAGAACAAGATCCTGATCTTCGGGCTGTTTGAGGAGACGGCCCTGGCTGCCTTCCTGTCCTA
       R  N  S  V  F  Q  Q  G  M  K  N  K  I  L  I  F  G  L  F  E  E  T  A  L  A  A  F  L  S  Y

          2890       2900       2910       2920       2930       2940       2950       2960       2970
    ....|....|....|....|....|....|....|....|....|....|....|....|....|....|....|....|....|....|....|....|
1   TTGTCCTGGTATGGATGTTGCATTAAGAATGTACCCTTTGAAACCATCCTGGTGGTTTTGCGCCTTCCCTTACTCATTTTTGATCTTCGT
       C  P  G  M  D  V  A  L  R  M  Y  P  L  K  P  S  W  W  F  C  A  F  P  Y  S  F  L  I  F  V
2   CTGCCCCGGCATGGACGTGGCCCTGCGCATGTACCCTCTCAAGCCCAGCTGGTGGTTCTGTGCCTTCCCCTACAGTTTCCTCATCTTCGT
       C  P  G  M  D  V  A  L  R  M  Y  P  L  K  P  S  W  W  F  C  A  F  P  Y  S  F  L  I  F  V

          2980       2990       3000       3010       3020       3030       3040
    ....|....|....|....|....|....|....|....|....|....|....|....|....|...
1   TTACGATGAAATCAGAAAGTTGATCTTGAGAAGAAATCCAGGTGGTTGGGTCGAAAAAGAAACTTATTACTGA
       Y  D  E  I  R  K  L  I  L  R  R  N  P  G  G  W  V  E  K  E  T  Y  Y  *
2   CTACGACGAAATCCGCAAACTCATCCTGCGCAGGAACCCAGGGGGTTGGGTGGAGAAGGAAACCTACTACTGA
       Y  D  E  I  R  K  L  I  L  R  R  N  P  G  G  W  V  E  K  E  T  Y  Y  *
```

4.9 Human α_1, α_2, and α_3 Sequences for Expression in the Mammalian Cells

All sequences of human α_1, α_2, and α_3 genes are listed below. Those sequences encode the ouabain resistant isoforms.

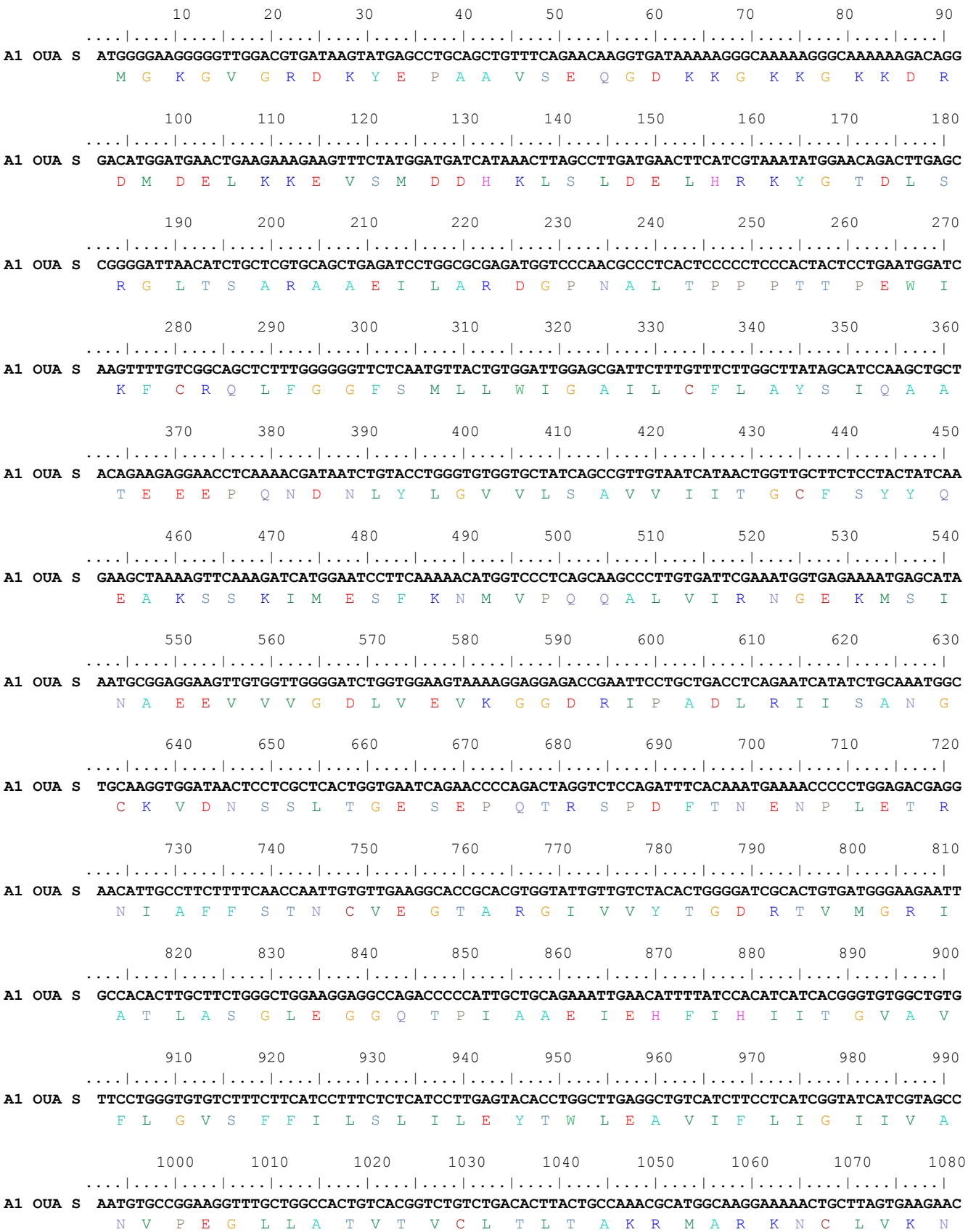
10 20 30 40 50 60 70 80 90
A1 OUA S ATGGGGAAGGGGGTTGGACGTGATAAGTATGAGCCTGCAGCTGTTTCAGAACAAGGTGATAAAAAGGGCAAAAAGGGCAAAAAAGACAGG
M G K G V G R D K Y E P A A V S E Q G D K K G K K G K K D R
100 110 120 130 140 150 160 170 180
A1 OUA S GACATGGATGAACTGAAGAAAGAAGTTTCTATGGATGATCATAAACTTAGCCTTGATGAACTTCATCGTAAATATGGAACAGACTTGAGC
D M D E L K K E V S M D D H K L S L D E L H R K Y G T D L S
190 200 210 220 230 240 250 260 270
A1 OUA S CGGGGATTAACATCTGCTCGTGCAGCTGAGATCCTGGCGCGAGATGGTCCCAACGCCCTCACTCCCCCTCCCACTACTCCTGAATGGATC
R G L T S A R A A E I L A R D G P N A L T P P P T T P E W I
280 290 300 310 320 330 340 350 360
A1 OUA S AAGTTTTGTCGGCAGCTCTTTGGGGGGTTCTCAATGTTACTGTGGATTGGAGCGATTCTTTGTTTCTTGGCTTATAGCATCCAAGCTGCT
K F C R Q L F G G F S M L L W I G A I L C F L A Y S I Q A A
370 380 390 400 410 420 430 440 450
A1 OUA S ACAGAAGAGGAACCTCAAAACGATAATCTGTACCTGGGTGTGGTGCTATCAGCCGTTGTAATCATAACTGGTTGCTTCTCCTACTATCAA
T E E E P Q N D N L Y L G V V L S A V V I I T G C F S Y Y Q
460 470 480 490 500 510 520 530 540
A1 OUA S GAAGCTAAAAGTTCAAAGATCATGGAATCCTTCAAAAACATGGTCCCTCAGCAAGCCCTTGTGATTCGAAATGGTGAGAAAATGAGCATA
E A K S S K I M E S F K N M V P Q Q A L V I R N G E K M S I
550 560 570 580 590 600 610 620 630
A1 OUA S AATGCGGAGGAAGTTGTGGTTGGGGATCTGGTGGAAGTAAAAGGAGGAGACCGAATTCCTGCTGACCTCAGAATCATATCTGCAAATGGC
N A E E V V V G D L V E V K G G D R I P A D L R I I S A N G
640 650 660 670 680 690 700 710 720
A1 OUA S TGCAAGGTGGATAACTCCTCGCTCACTGGTGAATCAGAACCCCAGACTAGGTCTCCAGATTTCACAAATGAAAACCCCCTGGAGACGAGG
C K V D N S S L T G E S E P Q T R S P D F T N E N P L E T R
730 740 750 760 770 780 790 800 810
A1 OUA S AACATTGCCTTCTTTTCAACCAATTGTGTTGAAGGCACCGCACGTGGTATTGTTGTCTACACTGGGGATCGCACTGTGATGGGAAGAATT
N I A F F S T N C V E G T A R G I V V Y T G D R T V M G R I
820 830 840 850 860 870 880 890 900
A1 OUA S GCCACACTTGCTTCTGGGCTGGAAGGAGGCCAGACCCCCATTGCTGCAGAAATTGAACATTTTATCCACATCATCACGGGTGTGGCTGTG
A T L A S G L E G G Q T P I A A E I E H F I H I I T G V A V
910 920 930 940 950 960 970 980 990
A1 OUA S TTCCTGGGTGTGTCTTTCTTCATCCTTTCTCTCATCCTTGAGTACACCTGGCTTGAGGCTGTCATCTTCCTCATCGGTATCATCGTAGCC
F L G V S F F I L S L I L E Y T W L E A V I F L I G I I V A
1000 1010 1020 1030 1040 1050 1060 1070 1080
A1 OUA S AATGTGCCGGAAGGTTTGCTGGCCACTGTCACGGTCTGTCTGACACTTACTGCCAAACGCATGGCAAGGAAAAACTGCTTAGTGAAGAAC
N V P E G L L A T V T V C L T L T A K R M A R K N C L V K N

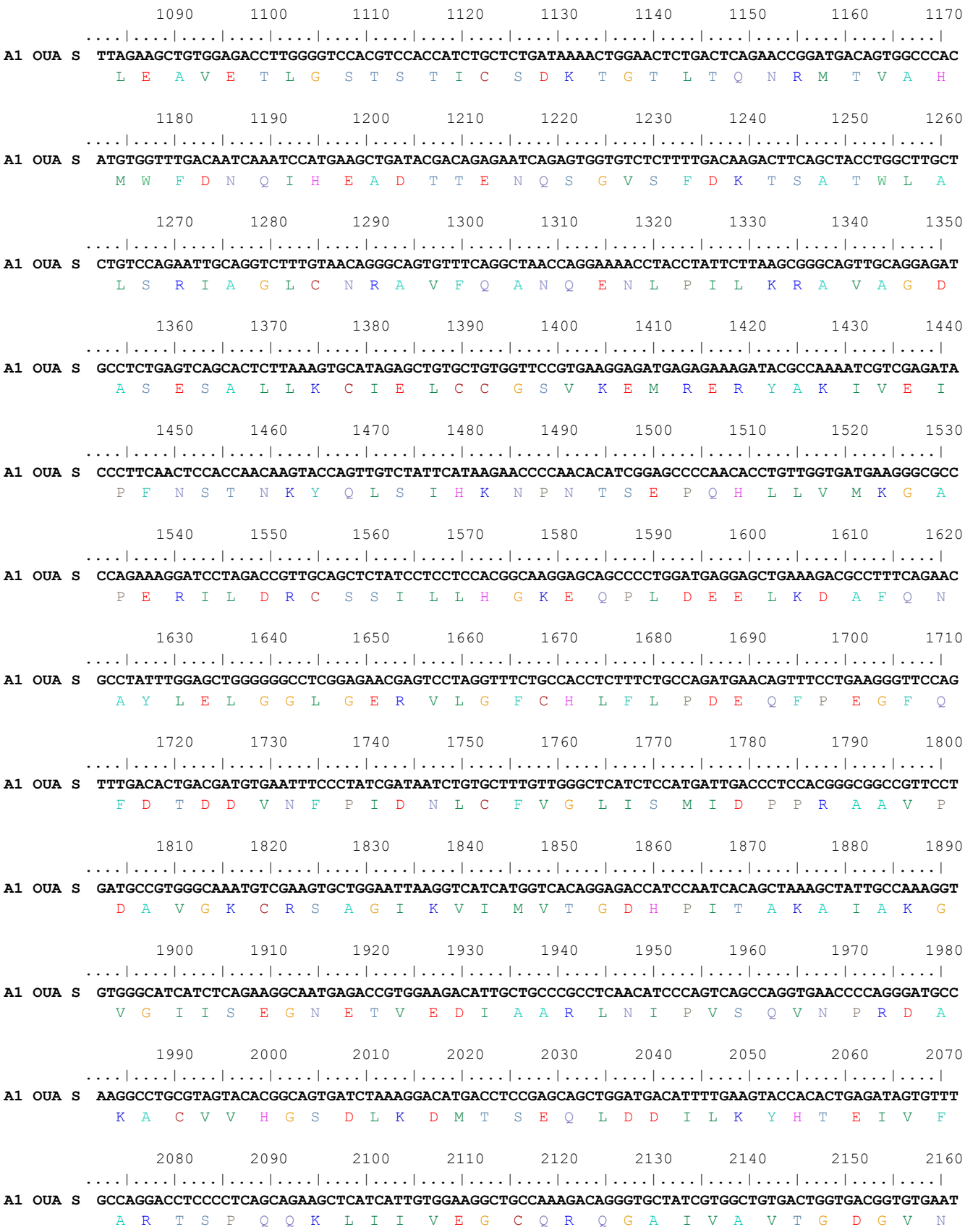
1090 1100 1110 1120 1130 1140 1150 1160 1170
A1 OUA S TTAGAAGCTGTGGAGACCTTGGGGTCCACGTCCACCATCTGCTCTGATAAAACTGGAACTCTGACTCAGAACCGGATGACAGTGGCCCAC
L E A V E T L G S T S T I C S D K T G T L T Q N R M T V A H
1180 1190 1200 1210 1220 1230 1240 1250 1260
A1 OUA S ATGTGGTTTGACAATCAAATCCATGAAGCTGATACGACAGAGAATCAGAGTGGTGTCTCTTTTGACAAGACTTCAGCTACCTGGCTTGCT
M W F D N Q I H E A D T T E N Q S G V S F D K T S A T W L A
1270 1280 1290 1300 1310 1320 1330 1340 1350
A1 OUA S CTGTCCAGAATTGCAGGTCTTTGTAACAGGGCAGTGTTTCAGGCTAACCAGGAAAACCTACCTATTCTTAAGCGGGCAGTTGCAGGAGAT
L S R I A G L C N R A V F Q A N Q E N L P I L K R A V A G D
1360 1370 1380 1390 1400 1410 1420 1430 1440
A1 OUA S GCCTCTGAGTCAGCACTCTTAAAGTGCATAGAGCTGTGCTGTGGTTCCGTGAAGGAGATGAGAGAAAGATACGCCAAAATCGTCGAGATA
A S E S A L L K C I E L C C G S V K E M R E R Y A K I V E I
1450 1460 1470 1480 1490 1500 1510 1520 1530
A1 OUA S CCCTTCAACTCCACCAACAAGTACCAGTTGTCTATTCATAAGAACCCCAACACATCGGAGCCCCAACACCTGTTGGTGATGAAGGGCGCC
P F N S T N K Y Q L S I H K N P N T S E P Q H L L V M K G A
1540 1550 1560 1570 1580 1590 1600 1610 1620
A1 OUA S CCAGAAAGGATCCTAGACCGTTGCAGCTCTATCCTCCTCCACGGCAAGGAGCAGCCCCTGGATGAGGAGCTGAAAGACGCCTTTCAGAAC
P E R I L D R C S S I L L H G K E Q P L D E E L K D A F Q N
1630 1640 1650 1660 1670 1680 1690 1700 1710
A1 OUA S GCCTATTTGGAGCTGGGGGGCCTCGGAGAACGAGTCCTAGGTTTCTGCCACCTCTTTCTGCCAGATGAACAGTTTCCTGAAGGGTTCCAG
A Y L E L G G L G E R V L G F C H L F L P D E Q F P E G F Q
1720 1730 1740 1750 1760 1770 1780 1790 1800
A1 OUA S TTTGACACTGACGATGTGAATTTCCCTATCGATAATCTGTGCTTTGTTGGGCTCATCTCCATGATTGACCCTCCACGGGCGGCCGTTCCT
F D T D D V N F P I D N L C F V G L I S M I D P P R A A V P
1810 1820 1830 1840 1850 1860 1870 1880 1890
A1 OUA S GATGCCGTGGGCAAATGTCGAAGTGCTGGAATTAAGGTCATCATGGTCACAGGAGACCATCCAATCACAGCTAAAGCTATTGCCAAAGGT
D A V G K C R S A G I K V I M V T G D H P I T A K A I A K G
1900 1910 1920 1930 1940 1950 1960 1970 1980
A1 OUA S GTGGGCATCATCTCAGAAGGCAATGAGACCGTGGAAGACATTGCTGCCCGCCTCAACATCCCAGTCAGCCAGGTGAACCCCAGGGATGCC
V G I I S E G N E T V E D I A A R L N I P V S Q V N P R D A
1990 2000 2010 2020 2030 2040 2050 2060 2070
A1 OUA S AAGGCCTGCGTAGTACACGGCAGTGATCTAAAGGACATGACCTCCGAGCAGCTGGATGACATTTTGAAGTACCACACTGAGATAGTGTTT
K A C V V H G S D L K D M T S E Q L D D I L K Y H T E I V F
2080 2090 2100 2110 2120 2130 2140 2150 2160
A1 OUA S GCCAGGACCTCCCCTCAGCAGAAGCTCATCATTGTGGAAGGCTGCCAAAGACAGGGTGCTATCGTGGCTGTGACTGGTGACGGTGTGAAT
A R T S P Q Q K L I I V E G C Q R Q G A I V A V T G D G V N

```
                2170      2180      2190      2200      2210      2220      2230      2240      2250
          ....|....|....|....|....|....|....|....|....|....|....|....|....|....|....|....|....|....|
A1 OUA S  GACTCTCCAGCTTTGAAGAAAGCAGACATTGGGGTTGCTATGGGGATTGCTGGCTCAGATGTGTCCAAGCAAGCTGCTGACATGATTCTT
            D  S  P  A  L  K  K  A  D  I  G  V  A  M  G  I  A  G  S  D  V  S  K  Q  A  A  D  M  I  L

                2260      2270      2280      2290      2300      2310      2320      2330      2340
          ....|....|....|....|....|....|....|....|....|....|....|....|....|....|....|....|....|....|
A1 OUA S  CTGGATGACAACTTTGCCTCAATTGTGACTGGAGTAGAGGAAGGTCGTCTGATCTTTGATAACTTGAAGAAATCCATTGCTTATACCTTA
            L  D  D  N  F  A  S  I  V  T  G  V  E  E  G  R  L  I  F  D  N  L  K  K  S  I  A  Y  T  L

                2350      2360      2370      2380      2390      2400      2410      2420      2430
          ....|....|....|....|....|....|....|....|....|....|....|....|....|....|....|....|....|....|
A1 OUA S  ACCAGTAACATTCCCGAGATCACCCCGTTCCTGATATTTATTATTGCAAACATTCCACTACCACTGGGGACTGTCACCATCCTCTGCATT
            T  S  N  I  P  E  I  T  P  F  L  I  F  I  I  A  N  I  P  L  P  L  G  T  V  T  I  L  C  I

                2440      2450      2460      2470      2480      2490      2500      2510      2520
          ....|....|....|....|....|....|....|....|....|....|....|....|....|....|....|....|....|....|
A1 OUA S  GACTTGGGCACTGACATGGTTCCTGCCATCTCCCTGGCTTATGAGCAGGCTGAGAGTGACATCATGAAGAGACAGCCCAGAAATCCCAAA
            D  L  G  T  D  M  V  P  A  I  S  L  A  Y  E  Q  A  E  S  D  I  M  K  R  Q  P  R  N  P  K

                2530      2540      2550      2560      2570      2580      2590      2600      2610
          ....|....|....|....|....|....|....|....|....|....|....|....|....|....|....|....|....|....|
A1 OUA S  ACAGACAAACTTGTGAATGAGCGGCTGATCAGCATGGCCTATGGGCAGATTGGAATGATCCAGGCCCTGGGAGGCTTCTTTACTTACTTT
            T  D  K  L  V  N  E  R  L  I  S  M  A  Y  G  Q  I  G  M  I  Q  A  L  G  G  F  F  T  Y  F

                2620      2630      2640      2650      2660      2670      2680      2690      2700
          ....|....|....|....|....|....|....|....|....|....|....|....|....|....|....|....|....|....|
A1 OUA S  GTGATTCTGGCTGAGAACGGCTTCCTCCCAATTCACCTGTTGGGCCTCCGAGTGGACTGGGATGACCGCTGGATCAACGATGTGGAAGAC
            V  I  L  A  E  N  G  F  L  P  I  H  L  L  G  L  R  V  D  W  D  D  R  W  I  N  D  V  E  D

                2710      2720      2730      2740      2750      2760      2770      2780      2790
          ....|....|....|....|....|....|....|....|....|....|....|....|....|....|....|....|....|....|
A1 OUA S  AGCTACGGGCAGCAGTGGACCTATGAGCAGAGGAAAATCGTGGAGTTCACCTGCCACACAGCCTTCTTCGTCAGTATCGTGGTGGTGCAG
            S  Y  G  Q  Q  W  T  Y  E  Q  R  K  I  V  E  F  T  C  H  T  A  F  F  V  S  I  V  V  V  Q

                2800      2810      2820      2830      2840      2850      2860      2870      2880
          ....|....|....|....|....|....|....|....|....|....|....|....|....|....|....|....|....|....|
A1 OUA S  TGGGCCGACTTGGTCATCTGTAAGACCAGGAGGAATTCGGTCTTCCAGCAGGGGATGAAGAACAAGATCTTGATATTTGGCCTCTTTGAA
            W  A  D  L  V  I  C  K  T  R  R  N  S  V  F  Q  Q  G  M  K  N  K  I  L  I  F  G  L  F  E

                2890      2900      2910      2920      2930      2940      2950      2960      2970
          ....|....|....|....|....|....|....|....|....|....|....|....|....|....|....|....|....|....|
A1 OUA S  GAGACAGCCCTGGCTGCTTTCCTTTCCTACTGCCCTGGAATGGGTGTTGCTCTTAGGATGTATCCCCTCAAACCTACCTGGTGGTTCTGT
            E  T  A  L  A  A  F  L  S  Y  C  P  G  M  G  V  A  L  R  M  Y  P  L  K  P  T  W  W  F  C

                2980      2990      3000      3010      3020      3030      3040      3050      3060
          ....|....|....|....|....|....|....|....|....|....|....|....|....|....|....|....|....|....|
A1 OUA S  GCCTTCCCCTACTCTCTTCTCATCTTCGTATATGACGAAGTCAGAAAACTCATCATCAGGCGACGCCCTGGCGGCTGGGTGGAGAAGGAA
            A  F  P  Y  S  L  L  I  F  V  Y  D  E  V  R  K  L  I  I  R  R  R  P  G  G  W  V  E  K  E

                3070
          ....|....|..
A1 OUA S  ACCTACTATTAG
            T  Y  Y  *
```


10 20 30 40 50 60 70 80 90 100
A2 OUA S ATGGGCCGTGGGGCTGGCCGTGAGTACTCACCTGCCGCCACCACGGCAGAGAATGGGGGCGGCAAGAAGAAACAGAAGGAGAAGGAACTGGATGAGCTGA
M G R G A G R E Y S P A A T T A E N G G G K K K Q K E K E L D E L
110 120 130 140 150 160 170 180 190 200
A2 OUA S AGAAGGAGGTGGCAATGGATGACCACAAGCTGTCCTTGGATGAGCTGGGCCGCAAATACCAAGTGGACCTGTCCAAGGGCCTCACCAACCAGCGGGCTCA
K K E V A M D D H K L S L D E L G R K Y Q V D L S K G L T N Q R A Q
210 220 230 240 250 260 270 280 290 300
A2 OUA S GGACGTTCTGGCTCGAGATGGGCCCAACGCCCTCACACCACCTCCCACAACCCCTGAGTGGGTCAAGTTCTGCCGTCAGCTTTTCGGGGGGTTCTCCATC
D V L A R D G P N A L T P P P T T P E W V K F C R Q L F G G F S I
310 320 330 340 350 360 370 380 390 400
A2 OUA S CTGCTGTGGATTGGGGCTATCCTCTGCTTCCTGGCCTACGGCATCCAGGCTGCCATGGAGGATGAACCATCCAACGACAATCTATATCTGGGTGTGGTGC
L L W I G A I L C F L A Y G I Q A A M E D E P S N D N L Y L G V V
410 420 430 440 450 460 470 480 490 500
A2 OUA S TGGCAGCTGTGGTCATTGTCACTGGCTGCTTCTCCTACTACCAGGAGGCCAAGAGCTCCAAGATCATGGATTCCTTCAAGAACATGGTACCTCAGCAAGC
L A A V V I V T G C F S Y Y Q E A K S S K I M D S F K N M V P Q Q A
510 520 530 540 550 560 570 580 590 600
A2 OUA S CCTTGTGATCCGGGAGGGAGAGAAGATGCAGATCAACGCAGAGGAAGTGGTGGTGGGAGACCTGGTGGAGGTGAAGGGTGGAGACCGCGTCCCTGCTGAC
L V I R E G E K M Q I N A E E V V V G D L V E V K G G D R V P A D
610 620 630 640 650 660 670 680 690 700
A2 OUA S CTCCGGATCATCTCTTCTCATGGCTGTAAGGTGGATAACTCATCCTTAACAGGAGAGTCGGAGCCCCAGACCCGCTCCCCCGAGTTCACCCATGAGAACC
L R I I S S H G C K V D N S S L T G E S E P Q T R S P E F T H E N
710 720 730 740 750 760 770 780 790 800
A2 OUA S CCCTGGAGACCCGCAATATCTGTTTCTTCTCCACCAACTGTGTTGAAGGCACTGCCAGGGGCATTGTGATTGCCACAGGAGACCGGACGGTGATGGGCCG
P L E T R N I C F F S T N C V E G T A R G I V I A T G D R T V M G R
810 820 830 840 850 860 870 880 890 900
A2 OUA S CATAGCTACTCTCGCCTCAGGCCTGGAGGTTGGGCGGACACCCATAGCAATGGAGATTGAACACTTCATCCAGCTGATCACAGGGGTCGCTGTATTCCTG
I A T L A S G L E V G R T P I A M E I E H F I Q L I T G V A V F L
910 920 930 940 950 960 970 980 990 1000
A2 OUA S GGGGTCTCCTTCTTCGTGCTCTCCCTCATCCTGGGCTACAGCTGGCTGGAGGCAGTCATCTTCCTCATCGGCATCATAGTGGCCAACGTGCCTGAGGGGC
G V S F F V L S L I L G Y S W L E A V I F L I G I I V A N V P E G
1010 1020 1030 1040 1050 1060 1070 1080 1090 1100
A2 OUA S TTCTGGCCACTGTCACTGTGTGCCTGACCCTGACAGCCAAGCGCATGGCACGGAAGAACTGCCTGGTGAAGAACCTGGAGGCGGTGGAGACGCTGGGCTC
L L A T V T V C L T L T A K R M A R K N C L V K N L E A V E T L G S
1110 1120 1130 1140 1150 1160 1170 1180 1190 1200
A2 OUA S CACGTCCACCATCTGCTCGGACAAGACGGGCACCCTCACCCAGAACCGCATGACCGTCGCCCACATGTGGTTCGACAACCAAATCCATGAGGCTGACACC
T S T I C S D K T G T L T Q N R M T V A H M W F D N Q I H E A D T
1210 1220 1230 1240 1250 1260 1270 1280 1290 1300
A2 OUA S ACCGAAGATCAGTCTGGGGCCACTTTTGACAAACGATCCCCTACGTGGACGGCCCTGTCTCGAATTGCTGGTCTCTGCAACCGCGCCGTCTTCAAGGCAG
T E D Q S G A T F D K R S P T W T A L S R I A G L C N R A V F K A
1310 1320 1330 1340 1350 1360 1370 1380 1390 1400
A2 OUA S GACAGGAGAACATCTCCGTGTCTAAGCGGGACACAGCTGGTGATGCCTCTGAGTCAGCTCTGCTCAAGTGCATTGAGCTCTCCTGTGGCTCAGTGAGGAA
G Q E N I S V S K R D T A G D A S E S A L L K C I E L S C G S V R K
1410 1420 1430 1440 1450 1460 1470 1480 1490 1500
A2 OUA S AATGAGAGACAGAAACCCCAAGGTGGCAGAGATTCCTTTCAACTCTACCAACAAGTACCAGCTGTCTATCCACGAGCGAGAAGACAGCCCCCAGAGCCAC
M R D R N P K V A E I P F N S T N K Y Q L S I H E R E D S P Q S H

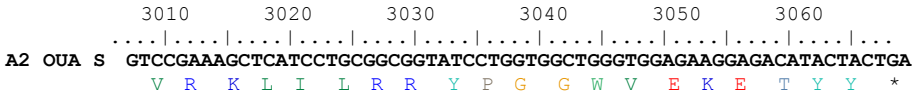
3010 3020 3030 3040 3050 3060
A2 OUA S GTCCGAAAGCTCATCCTGCGGCGGTATCCTGGTGGCTGGGTGGAGAAGGAGACATACTACTGA
V R K L I L R R Y P G G W V E K E T Y Y *


1510 1520 1530 1540 1550 1560 1570 1580 1590 1600
A2 OUA S GTGCTGGTGATGAAGGGGGCCCCAGAGCGCATTCTGGACCGGTGCTCCACCATCCTGGTGCAGGGCAAGGAGATCCCGCTCGACAAGGAGATGCAAGATG
V L V M K G A P E R I L D R C S T I L V Q G K E I P L D K E M Q D
1610 1620 1630 1640 1650 1660 1670 1680 1690 1700
A2 OUA S CCTTTCAAAATGCCTACATGGAGCTGGGGGGACTTGGGGAGCGTGTGCTGGGATTCTGTCAACTGAATCTGCCATCTGGAAAGTTTCCTCGGGGCTTCAA
A F Q N A Y M E L G G L G E R V L G F C Q L N L P S G K F P R G F K
1710 1720 1730 1740 1750 1760 1770 1780 1790 1800
A2 OUA S ATTCGACACGGATGAGCTGAACTTTCCCACGGAGAAGCTTTGCTTTGTGGGGCTCATGTCTATGATTGACCCTCCCCGGGCTGCTGTGCCAGATGCTGTG
F D T D E L N F P T E K L C F V G L M S M I D P P R A A V P D A V
1810 1820 1830 1840 1850 1860 1870 1880 1890 1900
A2 OUA S GGCAAGTGCCGAAGCGCAGGCATCAAGGTGATCATGGTAACCGGGGATCACCCTATCACAGCCAAGGCCATTGCCAAAGGCGTGGGCATCATATCAGAGG
G K C R S A G I K V I M V T G D H P I T A K A I A K G V G I I S E
1910 1920 1930 1940 1950 1960 1970 1980 1990 2000
A2 OUA S GTAACGAGACTGTGGAGGACATTGCAGCCCGGCTCAACATTCCCATGAGTCAAGTCAACCCCAGAGAAGCCAAGGCATGCGTGGTGCACGGCTCTGACCT
G N E T V E D I A A R L N I P M S Q V N P R E A K A C V V H G S D L
2010 2020 2030 2040 2050 2060 2070 2080 2090 2100
A2 OUA S GAAGGACATGACATCGGAGCAGCTCGATGAGATCCTCAAGAACCACACAGAGATCGTCTTTGCTCGAACGTCTCCCCAGCAGAAGCTCATCATTGTGGAG
K D M T S E Q L D E I L K N H T E I V F A R T S P Q Q K L I I V E
2110 2120 2130 2140 2150 2160 2170 2180 2190 2200
A2 OUA S GGATGTCAGAGGCAGGGAGCCATTGTGGCCGTGACGGGTGACGGGGTGAACGACTCCCCTGCATTGAAGAAGGCTGACATTGGCATTGCCATGGGCATCT
G C Q R Q G A I V A V T G D G V N D S P A L K K A D I G I A M G I
2210 2220 2230 2240 2250 2260 2270 2280 2290 2300
A2 OUA S CTGGCTCTGACGTCTCTAAGCAGGCAGCCGACATGATCCTGCTGGATGACAACTTTGCCTCCATCGTCACGGGGGTGGAGGAGGGCCGCCTGATCTTTGA
S G S D V S K Q A A D M I L L D D N F A S I V T G V E E G R L I F D
2310 2320 2330 2340 2350 2360 2370 2380 2390 2400
A2 OUA S CAACTTGAAGAAATCCATCGCCTACACCCTGACCAGCAACATCCCCGAGATCACCCCCTTCCTGCTGTTCATCATTGCCAACATCCCCCTACCTCTGGGC
N L K K S I A Y T L T S N I P E I T P F L L F I I A N I P L P L G
2410 2420 2430 2440 2450 2460 2470 2480 2490 2500
A2 OUA S ACTGTGACCATCCTTTGCATTGACCTGGGCACAGATATGGTCCCTGCCATCTCCTTGGCCTATGAGGCAGCTGAGAGTGATATCATGAAGCGGCAGCCAC
T V T I L C I D L G T D M V P A I S L A Y E A A E S D I M K R Q P
2510 2520 2530 2540 2550 2560 2570 2580 2590 2600
A2 OUA S GAAACTCCCAGACGGACAAGCTGGTGAATGAGAGGCTCATCAGCATGGCCTACGGACAGATCGGGATGATCCAGGCACTGGGTGGCTTCTTCACCTACTT
R N S Q T D K L V N E R L I S M A Y G Q I G M I Q A L G G F F T Y F
2610 2620 2630 2640 2650 2660 2670 2680 2690 2700
A2 OUA S TGTGATCCTGGCAGAGAACGGTTTCCTGCCATCACGGCTACTGGGAATCCGCCTCGACTGGGATGACCGGACCATGAATGATCTGGAGGACAGCTATGGA
V I L A E N G F L P S R L L G I R L D W D D R T M N D L E D S Y G
2710 2720 2730 2740 2750 2760 2770 2780 2790 2800
A2 OUA S CAGGAGTGGACCTATGAGCAGCGGAAGGTGGTGGAGTTCACGTGCCACACGGCATTCTTTGCCAGCATCGTGGTGGTGCAGTGGGCTGACCTCATCATCT
Q E W T Y E Q R K V V E F T C H T A F F A S I V V V Q W A D L I I
2810 2820 2830 2840 2850 2860 2870 2880 2890 2900
A2 OUA S GCAAGACCCGCCGCAACTCAGTCTTCCAGCAGGGCATGAAGAACAAGATCCTGATTTTTGGGCTCCTGGAGGAGACGGCGTTGGCTGCCTTTCTCTCTTA
C K T R R N S V F Q Q G M K N K I L I F G L L E E T A L A A F L S Y
2910 2920 2930 2940 2950 2960 2970 2980 2990 3000
A2 OUA S CTGCCCAGGCATGGGTGTAGCCCTCCGCATGTACCCGCTCAAAGTCACCTGGTGGTTCTGCGCCTTCCCCTACAGCCTCCTCATCTTCATCTATGATGAG
C P G M G V A L R M Y P L K V T W W F C A F P Y S L L I F I Y D E

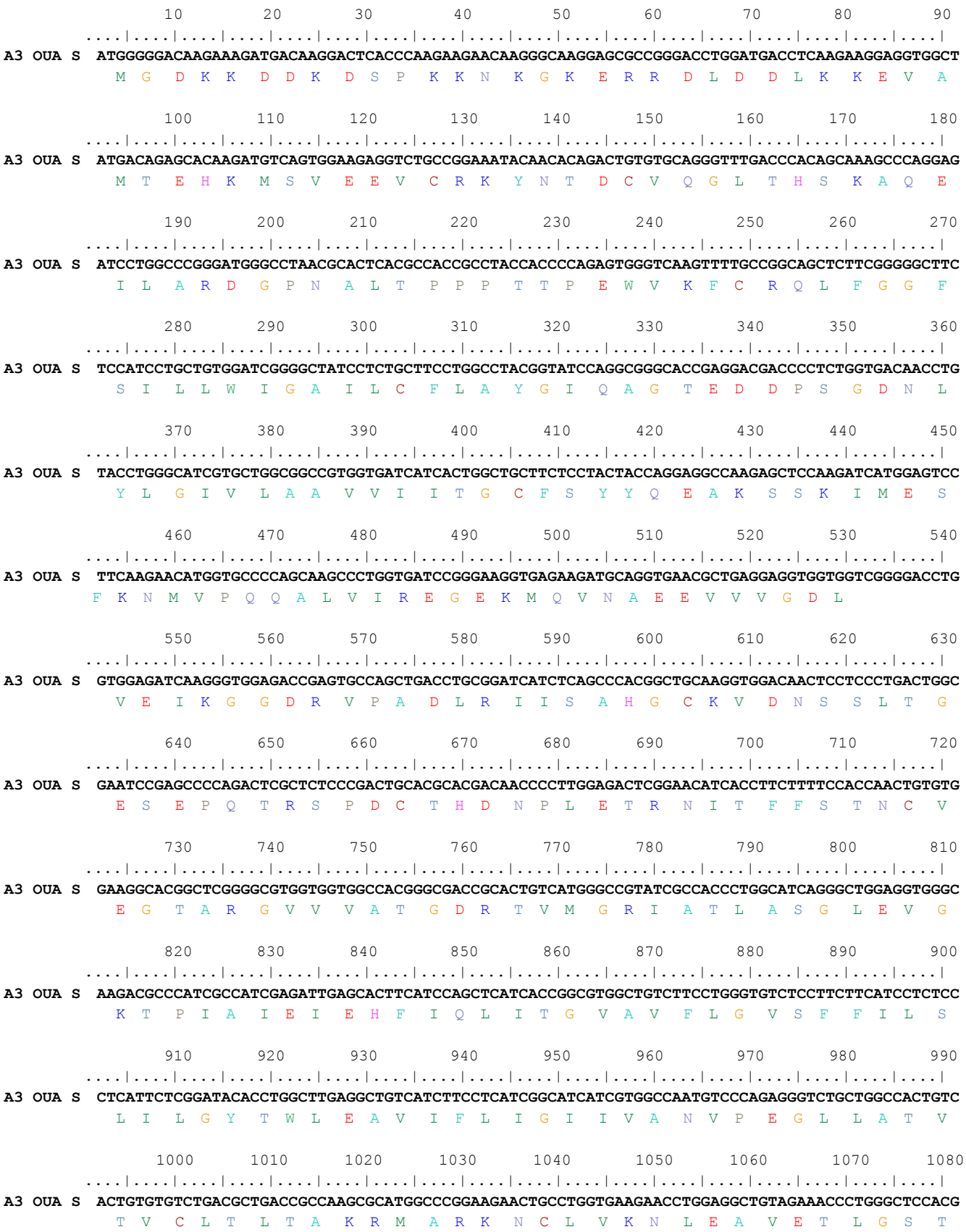
10 20 30 40 50 60 70 80 90
A3 OUA S ATGGGGGACAAGAAAGATGACAAGGACTCACCCAAGAAGAACAAGGGCAAGGAGCGCCGGGACCTGGATGACCTCAAGAAGGAGGTGGCT
M G D K K D D K D S P K K N K G K E R R D L D D L K K E V A
100 110 120 130 140 150 160 170 180
A3 OUA S ATGACAGAGCACAAGATGTCAGTGGAAGAGGTCTGCCGGAAATACAACACAGACTGTGTGCAGGGTTTGACCCACAGCAAAGCCCAGGAG
M T E H K M S V E E V C R K Y N T D C V Q G L T H S K A Q E
190 200 210 220 230 240 250 260 270
A3 OUA S ATCCTGGCCCGGGATGGGCCTAACGCACTCACGCCACCGCCTACCACCCCAGAGTGGGTCAAGTTTTGCCGGCAGCTCTTCGGGGGCTTC
I L A R D G P N A L T P P P T T P E W V K F C R Q L F G G F
280 290 300 310 320 330 340 350 360
A3 OUA S TCCATCCTGCTGTGGATCGGGGCTATCCTCTGCTTCCTGGCCTACGGTATCCAGGCGGGCACCGAGGACGACCCCTCTGGTGACAACCTG
S I L L W I G A I L C F L A Y G I Q A G T E D D P S G D N L
370 380 390 400 410 420 430 440 450
A3 OUA S TACCTGGGCATCGTGCTGGCGGCCGTGGTGATCATCACTGGCTGCTTCTCCTACTACCAGGAGGCCAAGAGCTCCAAGATCATGGAGTCC
Y L G I V L A A V V I I T G C F S Y Y Q E A K S S K I M E S
460 470 480 490 500 510 520 530 540
A3 OUA S TTCAAGAACATGGTGCCCCAGCAAGCCCTGGTGATCCGGGAAGGTGAGAAGATGCAGGTGAACGCTGAGGAGGTGGTGGTCGGGGACCTG
F K N M V P Q Q A L V I R E G E K M Q V N A E E V V V G D L
550 560 570 580 590 600 610 620 630
A3 OUA S GTGGAGATCAAGGGTGGAGACCGAGTGCCAGCTGACCTGCGGATCATCTCAGCCCACGGCTGCAAGGTGGACAACTCCTCCCTGACTGGC
V E I K G G D R V P A D L R I I S A H G C K V D N S S L T G
640 650 660 670 680 690 700 710 720
A3 OUA S GAATCCGAGCCCCAGACTCGCTCTCCCGACTGCACGCACGACAACCCCTTGGAGACTCGGAACATCACCTTCTTTTCCACCAACTGTGTG
E S E P Q T R S P D C T H D N P L E T R N I T F F S T N C V
730 740 750 760 770 780 790 800 810
A3 OUA S GAAGGCACGGCTCGGGGCGTGGTGGTGGCCACGGGCGACCGCACTGTCATGGGCCGTATCGCCACCCTGGCATCAGGGCTGGAGGTGGGC
E G T A R G V V V A T G D R T V M G R I A T L A S G L E V G
820 830 840 850 860 870 880 890 900
A3 OUA S AAGACGCCCATCGCCATCGAGATTGAGCACTTCATCCAGCTCATCACCGGCGTGGCTGTCTTCCTGGGTGTCTCCTTCTTCATCCTCTCC
K T P I A I E I E H F I Q L I T G V A V F L G V S F F I L S
910 920 930 940 950 960 970 980 990
A3 OUA S CTCATTCTCGGATACACCTGGCTTGAGGCTGTCATCTTCCTCATCGGCATCATCGTGGCCAATGTCCCAGAGGGTCTGCTGGCCACTGTC
L I L G Y T W L E A V I F L I G I I V A N V P E G L L A T V
1000 1010 1020 1030 1040 1050 1060 1070 1080
A3 OUA S ACTGTGTGTCTGACGCTGACCGCCAAGCGCATGGCCCGGAAGAACTGCCTGGTGAAGAACCTGGAGGCTGTAGAAACCCTGGGCTCCACG
T V C L T L T A K R M A R K N C L V K N L E A V E T L G S T

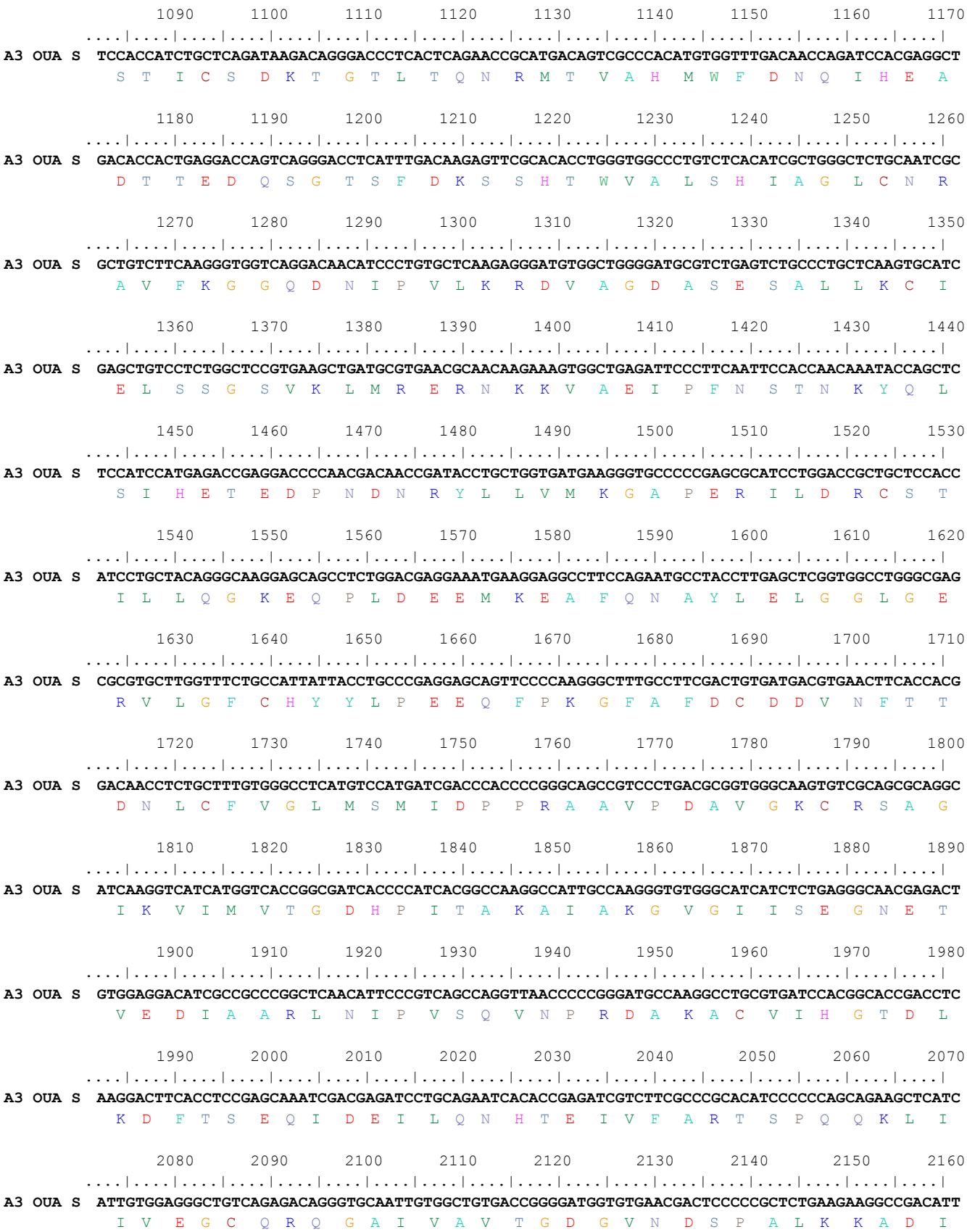
1090 1100 1110 1120 1130 1140 1150 1160 1170
A3 OUA S TCCACCATCTGCTCAGATAAGACAGGGACCCTCACTCAGAACCGCATGACAGTCGCCCACATGTGGTTTGACAACCAGATCCACGAGGCT
S T I C S D K T G T L T Q N R M T V A H M W F D N Q I H E A
1180 1190 1200 1210 1220 1230 1240 1250 1260
A3 OUA S GACACCACTGAGGACCAGTCAGGGACCTCATTTGACAAGAGTTCGCACACCTGGGTGGCCCTGTCTCACATCGCTGGGCTCTGCAATCGC
D T T E D Q S G T S F D K S S H T W V A L S H I A G L C N R
1270 1280 1290 1300 1310 1320 1330 1340 1350
A3 OUA S GCTGTCTTCAAGGGTGGTCAGGACAACATCCCTGTGCTCAAGAGGGATGTGGCTGGGGATGCGTCTGAGTCTGCCCTGCTCAAGTGCATC
A V F K G G Q D N I P V L K R D V A G D A S E S A L L K C I
1360 1370 1380 1390 1400 1410 1420 1430 1440
A3 OUA S GAGCTGTCCTCTGGCTCCGTGAAGCTGATGCGTGAACGCAACAAGAAAGTGGCTGAGATTCCCTTCAATTCCACCAACAAATACCAGCTC
E L S S G S V K L M R E R N K K V A E I P F N S T N K Y Q L
1450 1460 1470 1480 1490 1500 1510 1520 1530
A3 OUA S TCCATCCATGAGACCGAGGACCCCAACGACAACCGATACCTGCTGGTGATGAAGGGTGCCCCCGAGCGCATCCTGGACCGCTGCTCCACC
S I H E T E D P N D N R Y L L V M K G A P E R I L D R C S T
1540 1550 1560 1570 1580 1590 1600 1610 1620
A3 OUA S ATCCTGCTACAGGGCAAGGAGCAGCCTCTGGACGAGGAAATGAAGGAGGCCTTCCAGAATGCCTACCTTGAGCTCGGTGGCCTGGGCGAG
I L L Q G K E Q P L D E E M K E A F Q N A Y L E L G G L G E
1630 1640 1650 1660 1670 1680 1690 1700 1710
A3 OUA S CGCGTGCTTGGTTTCTGCCATTATTACCTGCCCGAGGAGCAGTTCCCCAAGGGCTTTGCCTTCGACTGTGATGACGTGAACTTCACCACG
R V L G F C H Y Y L P E E Q F P K G F A F D C D D V N F T T
1720 1730 1740 1750 1760 1770 1780 1790 1800
A3 OUA S GACAACCTCTGCTTTGTGGGCCTCATGTCCATGATCGACCCACCCCGGGCAGCCGTCCCTGACGCGGTGGGCAAGTGTCGCAGCGCAGGC
D N L C F V G L M S M I D P P R A A V P D A V G K C R S A G
1810 1820 1830 1840 1850 1860 1870 1880 1890
A3 OUA S ATCAAGGTCATCATGGTCACCGGCGATCACCCCATCACGGCCAAGGCCATTGCCAAGGGTGTGGGCATCATCTCTGAGGGCAACGAGACT
I K V I M V T G D H P I T A K A I A K G V G I I S E G N E T
1900 1910 1920 1930 1940 1950 1960 1970 1980
A3 OUA S GTGGAGGACATCGCCGCCCGGCTCAACATTCCCGTCAGCCAGGTTAACCCCCGGGATGCCAAGGCCTGCGTGATCCACGGCACCGACCTC
V E D I A A R L N I P V S Q V N P R D A K A C V I H G T D L
1990 2000 2010 2020 2030 2040 2050 2060 2070
A3 OUA S AAGGACTTCACCTCCGAGCAAATCGACGAGATCCTGCAGAATCACACCGAGATCGTCTTCGCCCGCACATCCCCCCAGCAGAAGCTCATC
K D F T S E Q I D E I L Q N H T E I V F A R T S P Q Q K L I
2080 2090 2100 2110 2120 2130 2140 2150 2160
A3 OUA S ATTGTGGAGGGCTGTCAGAGACAGGGTGCAATTGTGGCTGTGACCGGGGATGGTGTGAACGACTCCCCCGCTCTGAAGAAGGCCGACATT
I V E G C Q R Q G A I V A V T G D G V N D S P A L K K A D I

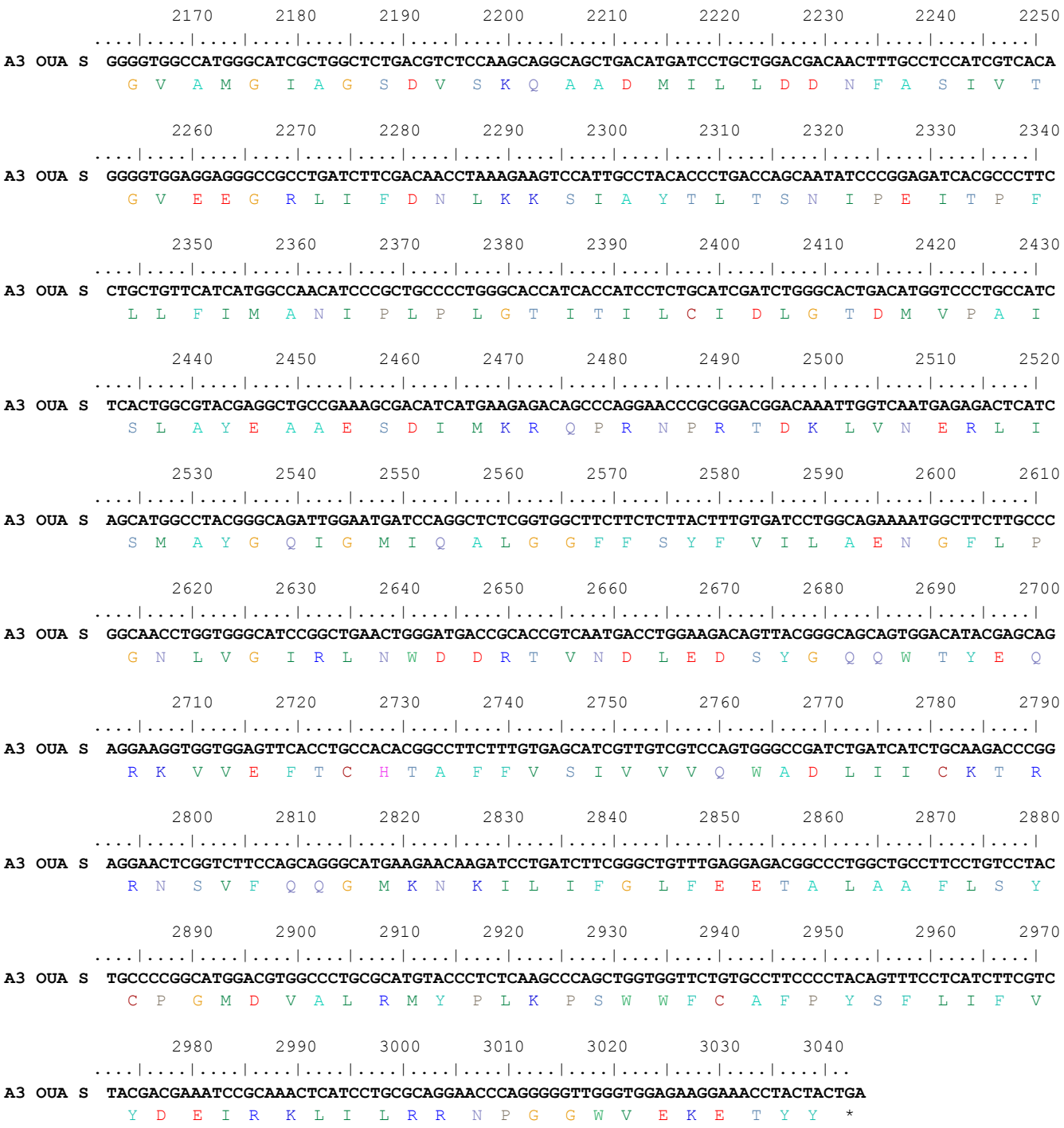
2170 2180 2190 2200 2210 2220 2230 2240 2250
A3 OUA S GGGGTGGCCATGGGCATCGCTGGCTCTGACGTCTCCAAGCAGGCAGCTGACATGATCCTGCTGGACGACAACTTTGCCTCCATCGTCACA
G V A M G I A G S D V S K Q A A D M I L L D D N F A S I V T
2260 2270 2280 2290 2300 2310 2320 2330 2340
A3 OUA S GGGGTGGAGGAGGGCCGCCTGATCTTCGACAACCTAAAGAAGTCCATTGCCTACACCCTGACCAGCAATATCCCGGAGATCACGCCCTTC
G V E E G R L I F D N L K K S I A Y T L T S N I P E I T P F
2350 2360 2370 2380 2390 2400 2410 2420 2430
A3 OUA S CTGCTGTTCATCATGGCCAACATCCCGCTGCCCCTGGGCACCATCACCATCCTCTGCATCGATCTGGGCACTGACATGGTCCCTGCCATC
L L F I M A N I P L P L G T I T I L C I D L G T D M V P A I
2440 2450 2460 2470 2480 2490 2500 2510 2520
A3 OUA S TCACTGGCGTACGAGGCTGCCGAAAGCGACATCATGAAGAGACAGCCCAGGAACCCGCGGACGGACAAATTGGTCAATGAGAGACTCATC
S L A Y E A A E S D I M K R Q P R N P R T D K L V N E R L I
2530 2540 2550 2560 2570 2580 2590 2600 2610
A3 OUA S AGCATGGCCTACGGGCAGATTGGAATGATCCAGGCTCTCGGTGGCTTCTTCTCTTACTTTGTGATCCTGGCAGAAAATGGCTTCTTGCCC
S M A Y G Q I G M I Q A L G G F F S Y F V I L A E N G F L P
2620 2630 2640 2650 2660 2670 2680 2690 2700
A3 OUA S GGCAACCTGGTGGGCATCCGGCTGAACTGGGATGACCGCACCGTCAATGACCTGGAAGACAGTTACGGGCAGCAGTGGACATACGAGCAG
G N L V G I R L N W D D R T V N D L E D S Y G Q Q W T Y E Q
2710 2720 2730 2740 2750 2760 2770 2780 2790
A3 OUA S AGGAAGGTGGTGGAGTTCACCTGCCACACGGCCTTCTTTGTGAGCATCGTTGTCGTCCAGTGGGCCGATCTGATCATCTGCAAGACCCGG
R K V V E F T C H T A F F V S I V V V Q W A D L I I C K T R
2800 2810 2820 2830 2840 2850 2860 2870 2880
A3 OUA S AGGAACTCGGTCTTCCAGCAGGGCATGAAGAACAAGATCCTGATCTTCGGGCTGTTTGAGGAGACGGCCCTGGCTGCCTTCCTGTCCTAC
R N S V F Q Q G M K N K I L I F G L F E E T A L A A F L S Y
2890 2900 2910 2920 2930 2940 2950 2960 2970
A3 OUA S TGCCCCGGCATGGACGTGGCCCTGCGCATGTACCCTCTCAAGCCCAGCTGGTGGTTCTGTGCCTTCCCCTACAGTTTCCTCATCTTCGTC
C P G M D V A L R M Y P L K P S W W F C A F P Y S F L I F V
2980 2990 3000 3010 3020 3030 3040
A3 OUA S TACGACGAAATCCGCAAACTCATCCTGCGCAGGAACCCAGGGGGTTGGGTGGAGAAGGAAACCTACTACTGA
Y D E I R K L I L R R N P G G W V E K E T Y Y *

4.10 Human α_3 Sequence for Expression in Yeast

The sequence for human α_3 genes is listed below. This sequences is a codon optimized sequence for protein expression in yeast *Saccharomyces cerevisiae*.

```
          10        20        30        40        50        60        70        80        90
....|....|....|....|....|....|....|....|....|....|....|....|....|....|....|....|....|
A3  ATGGGTGACAAGAAAGACGATAAGGATAGTCCAAAGAAGAACAAGGGTAAAGAAAGAAGAGATTTAGATGATTTGAAGAAAGAAGTTGCT
      M  G  D  K  K  D  D  K  D  S  P  K  K  N  K  G  K  E  R  R  D  L  D  D  L  K  K  E  V  A

          100       110       120       130       140       150       160       170       180
....|....|....|....|....|....|....|....|....|....|....|....|....|....|....|....|....|
A3  ATGACTGAACATAAGATGTCCGTCGAAGAAGTATGTAGAAAGTACAACACCGATTGCGTTCAAGGTTTAACTCACAGTAAGGCTCAAGAA
      M  T  E  H  K  M  S  V  E  E  V  C  R  K  Y  N  T  D  C  V  Q  G  L  T  H  S  K  A  Q  E

          190       200       210       220       230       240       250       260       270
....|....|....|....|....|....|....|....|....|....|....|....|....|....|....|....|....|
A3  ATTTTAGCAAGAGACGGTCCTAACGCTTTGACACCACCTCCAACTACACCAGAATGGGTTAAGTTCTGTAGACAATTGTTCGGTGGTTTC
      I  L  A  R  D  G  P  N  A  L  T  P  P  P  T  T  P  E  W  V  K  F  C  R  Q  L  F  G  G  F

          280       290       300       310       320       330       340       350       360
....|....|....|....|....|....|....|....|....|....|....|....|....|....|....|....|....|
A3  TCCATTTTGTTATGGATAGGTGCAATCTTATGCTTCTTGGCCTATGGTATACAAGCTGGTACTGAAGATGACCCAAGTGGTGATAACTTG
      S  I  L  L  W  I  G  A  I  L  C  F  L  A  Y  G  I  Q  A  G  T  E  D  D  P  S  G  D  N  L

          370       380       390       400       410       420       430       440       450
....|....|....|....|....|....|....|....|....|....|....|....|....|....|....|....|....|
A3  TACTTGGGTATAGTTTTAGCTGCAGTTGTCATAATCACAGGTTGTTTCTCTTACTACCAAGAGGCTAAGTCTTCAAAGATCATGGAATCA
      Y  L  G  I  V  L  A  A  V  V  I  I  T  G  C  F  S  Y  Y  Q  E  A  K  S  S  K  I  M  E  S

          460       470       480       490       500       510       520       530       540
....|....|....|....|....|....|....|....|....|....|....|....|....|....|....|....|....|
A3  TTCAAGAACATGGTTCCTCAACAAGCCTTGGTCATTAGAGAAGGTGAAAAAATGCAAGTTAACGCTGAAGAAGTAGTTGTCGGTGATTTA
      F  K  N  M  V  P  Q  Q  A  L  V  I  R  E  G  E  K  M  Q  V  N  A  E  E  V  V  V  G  D  L

          550       560       570       580       590       600       610       620       630
....|....|....|....|....|....|....|....|....|....|....|....|....|....|....|....|....|
A3  GTCGAAATTAAGGGTGGTGATAGAGTACCAGCCGACTTGAGAATCATTTCTGCTCATGGTTGTAAGGTTGATAACTCCAGTTTGACTGGT
      V  E  I  K  G  G  D  R  V  P  A  D  L  R  I  I  S  A  H  G  C  K  V  D  N  S  S  L  T  G

          640       650       660       670       680       690       700       710       720
....|....|....|....|....|....|....|....|....|....|....|....|....|....|....|....|....|
A3  GAATCCGAACCTCAAACCAGAAGTCCAGATTGTACTCACGACAACCCTTTGGAAACTAGAAACATCACATTTTTCTCTACCAACTGCGTT
      E  S  E  P  Q  T  R  S  P  D  C  T  H  D  N  P  L  E  T  R  N  I  T  F  F  S  T  N  C  V

          730       740       750       760       770       780       790       800       810
....|....|....|....|....|....|....|....|....|....|....|....|....|....|....|....|....|
A3  GAAGGTACAGCTAGAGGTGTAGTTGTCGCAACTGGTGATAGAACAGTCATGGGTAGAATTGCCACCTTAGCTTCAGGTTTGGAAGTAGGT
      E  G  T  A  R  G  V  V  V  A  T  G  D  R  T  V  M  G  R  I  A  T  L  A  S  G  L  E  V  G

          820       830       840       850       860       870       880       890       900
....|....|....|....|....|....|....|....|....|....|....|....|....|....|....|....|....|
A3  AAAACTCCAATTGCAATCGAAATCGAACATTTCATACAATTGATAACCGGTGTCGCCGTATTCTTGGGTGTCTCTTTCTTTATATTGTCA
      K  T  P  I  A  I  E  I  E  H  F  I  Q  L  I  T  G  V  A  V  F  L  G  V  S  F  F  I  L  S

          910       920       930       940       950       960       970       980       990
....|....|....|....|....|....|....|....|....|....|....|....|....|....|....|....|....|
A3  TTGATCTTGGGTTACACTTGGTTGGAAGCTGTAATCTTTTTGATCGGTATCATCGTTGCTAATGTCCCAGAAGGTTTGTTAGCAACTGTT
      L  I  L  G  Y  T  W  L  E  A  V  I  F  L  I  G  I  I  V  A  N  V  P  E  G  L  L  A  T  V

         1000      1010      1020      1030      1040      1050      1060      1070      1080
....|....|....|....|....|....|....|....|....|....|....|....|....|....|....|....|....|
A3  ACAGTCTGTTTAACCTTGACTGCCAAAAGAATGGCTAGAAAGAACTGCTTGGTAAAGAACTTGGAAGCAGTTGAAACATTAGGTTCTACA
      T  V  C  L  T  L  T  A  K  R  M  A  R  K  N  C  L  V  K  N  L  E  A  V  E  T  L  G  S  T
```


1090 1100 1110 1120 1130 1140 1150 1160 1170
A3 TCAACCATTTGTTCAGATAAGACTGGTACATTGACCCAAAATAGAATGACCGTTGCACATATGTGGTTTGATAACCAAATTCACGAAGCC
S T I C S D K T G T L T Q N R M T V A H M W F D N Q I H E A
1180 1190 1200 1210 1220 1230 1240 1250 1260
A3 GATACCACTGAAGACCAATCTGGTACTTCATTCGATAAATCTTCACATACATGGGTTGCATTATCTCACATAGCCGGTTTGTGTAATAGA
D T T E D Q S G T S F D K S S H T W V A L S H I A G L C N R
1270 1280 1290 1300 1310 1320 1330 1340 1350
A3 GCTGTCTTTAAGGGTGGTCAAGATAACATCCCTGTCTTAAAAAGAGATGTAGCAGGTGACGCCTCCGAAAGTGCTTTGTTGAAGTGCATA
A V F K G G Q D N I P V L K R D V A G D A S E S A L L K C I
1360 1370 1380 1390 1400 1410 1420 1430 1440
A3 GAATTGTCCAGTGGTTCAGTAAAGTTGATGAGAGAAAGAAATAAGAAGGTTGCAGAAATCCCATTCAACTCTACAAACAAGTACCAATTG
E L S S G S V K L M R E R N K K V A E I P F N S T N K Y Q L
1450 1460 1470 1480 1490 1500 1510 1520 1530
A3 TCAATACATGAAACCGAAGATCCTAACGACAACAGATACTTGTTGGTTATGAAAGGTGCTCCAGAAAGAATTTTAGATAGATGTTCTACT
S I H E T E D P N D N R Y L L V M K G A P E R I L D R C S T
1540 1550 1560 1570 1580 1590 1600 1610 1620
A3 ATCTTGTTGCAAGGCAAGGAACAACCATTGGACGAAGAAATGAAAGAAGCATTTCAAAATGCCTACTTAGAATTGGGTGGTTTAGGTGAA
I L L Q G K E Q P L D E E M K E A F Q N A Y L E L G G L G E
1630 1640 1650 1660 1670 1680 1690 1700 1710
A3 AGAGTTTTGGGTTTTTGCCATTATTACTTACCTGAAGAACAATTCCCAAAAGGTTTTGCATTCGATTGTGATGACGTCAATTTTACAACC
R V L G F C H Y Y L P E E Q F P K G F A F D C D D V N F T T
1720 1730 1740 1750 1760 1770 1780 1790 1800
A3 GACAACTTATGCTTCGTAGGTTTGATGTCTATGATTGATCCTCCAAGAGCCGCTGTACCTGACGCAGTTGGCAAGTGTAGATCAGCCGGT
D N L C F V G L M S M I D P P R A A V P D A V G K C R S A G
1810 1820 1830 1840 1850 1860 1870 1880 1890
A3 ATAAAAGTAATCATGGTTACAGGTGATCACCCAATTACCGCTAAAGCAATAGCCAAGGGTGTTGGTATTATATCCGAGGGTAATGAAACA
I K V I M V T G D H P I T A K A I A K G V G I I S E G N E T
1900 1910 1920 1930 1940 1950 1960 1970 1980
A3 GTCGAAGATATCGCAGCCAGATTGAATATTCCTGTCAGTCAAGTAAACCCAAGAGACGCTAAGGCATGTGTTATCCATGGTACTGATTTG
V E D I A A R L N I P V S Q V N P R D A K A C V I H G T D L
1990 2000 2010 2020 2030 2040 2050 2060 2070
A3 AAGGACTTCACATCTGAACAAATCGATGAAATCTTGCAAAACCACACAGAAATAGTATTCGCTAGAACCTCACCTCAACAAAAGTTGATC
K D F T S E Q I D E I L Q N H T E I V F A R T S P Q Q K L I
2080 2090 2100 2110 2120 2130 2140 2150 2160
A3 ATCGTTGAAGGTTGCCAAAGACAAGGTGCTATTGTAGCAGTTACTGGTGATGGTGTTAATGACTCCCCAGCTTTGAAAAAGGCAGATATA
I V E G C Q R Q G A I V A V T G D G V N D S P A L K K A D I

```
          2170      2180      2190      2200      2210      2220      2230      2240      2250
....|....|....|....|....|....|....|....|....|....|....|....|....|....|....|....|....|....|
A3  GGTGTTGCCATGGGTATCGCTGGTTCCGATGTCAGTAAACAAGCTGCAGACATGATATTGTTAGATGACAACTTTGCTTCTATCGTTACA
      G   V   A   M   G   I   A   G   S   D   V   S   K   Q   A   A   D   M   I   L   L   D   D   N   F   A   S   I   V   T

          2260      2270      2280      2290      2300      2310      2320      2330      2340
....|....|....|....|....|....|....|....|....|....|....|....|....|....|....|....|....|....|
A3  GGTGTCGAAGAAGGTAGATTGATCTTCGATAACTTGAAAAAGTCCATCGCTTACACTTTGACAAGTAACATCCCTGAAATAACTCCATTT
      G   V   E   E   G   R   L   I   F   D   N   L   K   K   S   I   A   Y   T   L   T   S   N   I   P   E   I   T   P   F

          2350      2360      2370      2380      2390      2400      2410      2420      2430
....|....|....|....|....|....|....|....|....|....|....|....|....|....|....|....|....|....|
A3  TTGTTGTTCATCATGGCAAACATTCCTTTACCATTGGGTACCATAACTATCTTGTGTATCGATTTGGGTACAGACATGGTTCCTGCAATA
      L   L   F   I   M   A   N   I   P   L   P   L   G   T   I   T   I   L   C   I   D   L   G   T   D   M   V   P   A   I

          2440      2450      2460      2470      2480      2490      2500      2510      2520
....|....|....|....|....|....|....|....|....|....|....|....|....|....|....|....|....|....|
A3  TCTTTGGCCTACGAAGCCGCTGAATCAGATATAATGAAGAGACAACCTAGAAACCCAAGAACTGACAAGTTGGTTAACGAAAGATTGATA
      S   L   A   Y   E   A   A   E   S   D   I   M   K   R   Q   P   R   N   P   R   T   D   K   L   V   N   E   R   L   I

          2530      2540      2550      2560      2570      2580      2590      2600      2610
....|....|....|....|....|....|....|....|....|....|....|....|....|....|....|....|....|....|
A3  TCCATGGCCTATGGTCAAATTGGTATGATCCAAGCTTTGGGTGGTTTCTTTTCTTACTTCGTTATCTTGGCTGAAAACGGTTTCTTACCT
      S   M   A   Y   G   Q   I   G   M   I   Q   A   L   G   G   F   F   S   Y   F   V   I   L   A   E   N   G   F   L   P

          2620      2630      2640      2650      2660      2670      2680      2690      2700
....|....|....|....|....|....|....|....|....|....|....|....|....|....|....|....|....|....|
A3  GGTAACTTAGTAGGTATCAGATTAAATTGGGATGACAGAACTGTTAACGATTTGGAAGACTCTTATGGTCAACAATGGACATACGAACAA
      G   N   L   V   G   I   R   L   N   W   D   D   R   T   V   N   D   L   E   D   S   Y   G   Q   Q   W   T   Y   E   Q

          2710      2720      2730      2740      2750      2760      2770      2780      2790
....|....|....|....|....|....|....|....|....|....|....|....|....|....|....|....|....|....|
A3  AGAAAGGTAGTTGAATTTACATGTCATACCGCTTTCTTTGTTTCTATTGTCGTAGTTCAATGGGCAGATTTGATCATCTGCAAGACCAGA
      R   K   V   V   E   F   T   C   H   T   A   F   F   V   S   I   V   V   V   Q   W   A   D   L   I   I   C   K   T   R

          2800      2810      2820      2830      2840      2850      2860      2870      2880
....|....|....|....|....|....|....|....|....|....|....|....|....|....|....|....|....|....|
A3  AGAAATTCAGTTTTCCAACAGGGTATGAAGAACAAGATCTTGATCTTCGGTTTGTTCGAAGAAACAGCTTTAGCAGCCTTTTTGTCTTAT
      R   N   S   V   F   Q   Q   G   M   K   N   K   I   L   I   F   G   L   F   E   E   T   A   L   A   A   F   L   S   Y

          2890      2900      2910      2920      2930      2940      2950      2960      2970
....|....|....|....|....|....|....|....|....|....|....|....|....|....|....|....|....|....|
A3  TGTCCTGGTATGGATGTTGCATTAAGAATGTACCCTTTGAAACCATCCTGGTGGTTTTGCGCCTTCCCTTACTCATTTTTGATCTTCGTT
      C   P   G   M   D   V   A   L   R   M   Y   P   L   K   P   S   W   W   F   C   A   F   P   Y   S   F   L   I   F   V

          2980      2990      3000      3010      3020      3030      3040
....|....|....|....|....|....|....|....|....|....|....|....|....|..
A3  TACGATGAAATCAGAAAGTTGATCTTGAGAAGAAATCCAGGTGGTTGGGTCGAAAAAGAAACTTATTACTGA
      Y   D   E   I   R   K   L   I   L   R   R   N   P   G   G   W   V   E   K   E   T   Y   Y   *
```

4.11 Human β_1 Sequence for Expression in Yeast

The sequence for human β_1 genes is listed below. This sequences is a codon optimized sequence for protein expression in yeast *Saccharomyces cerevisiae*.

```
          10        20        30        40        50        60        70        80        90
....|....|....|....|....|....|....|....|....|....|....|....|....|....|....|....|....|
B1  ATGGCAAGAGGTAAGGCAAAGGAAGAAGGTAGTTGGAAGAAGTTTATCTGGAATAGTGAAAAGAAGGAATTTTTAGGTAGAACAGGTGGT
      M   A   R   G   K   A   K   E   E   G   S   W   K   K   F   I   W   N   S   E   K   K   E   F   L   G   R   T   G   G

          100       110       120       130       140       150       160       170       180
....|....|....|....|....|....|....|....|....|....|....|....|....|....|....|....|....|
B1  TCCTGGTTCAAGATATTGTTGTTTTATGTAATATTCTACGGTTGTTTGGCAGGTATCTTCATCGGTACTATCCAAGTTATGTTGTTGACA
      S   W   F   K   I   L   L   F   Y   V   I   F   Y   G   C   L   A   G   I   F   I   G   T   I   Q   V   M   L   L   T

          190       200       210       220       230       240       250       260       270
....|....|....|....|....|....|....|....|....|....|....|....|....|....|....|....|....|
B1  ATCAGTGAATTTAAGCCAACCTACCAAGATAGAGTCGCTCCACCTGGTTTGACTCAAATCCCTCAAATCCAAAAGACAGAAATCTCTTTC
      I   S   E   F   K   P   T   Y   Q   D   R   V   A   P   P   G   L   T   Q   I   P   Q   I   Q   K   T   E   I   S   F

          280       290       300       310       320       330       340       350       360
....|....|....|....|....|....|....|....|....|....|....|....|....|....|....|....|....|
B1  AGACCAAACGACCCTAAGTCATATGAAGCTTACGTCTTGAACATAGTAAGATTTTTAGAAAAGTACAAGGATTCCGCACAAAGAGATGAC
      R   P   N   D   P   K   S   Y   E   A   Y   V   L   N   I   V   R   F   L   E   K   Y   K   D   S   A   Q   R   D   D

          370       380       390       400       410       420       430       440       450
....|....|....|....|....|....|....|....|....|....|....|....|....|....|....|....|....|
B1  ATGATTTTCGAAGACTGCGGTGATGTCCCAAGTGAACCTAAAGAACGTGGTGACTTCAACCATGAAAGAGGTGAAAGAAAGGTTTGTAGA
      M   I   F   E   D   C   G   D   V   P   S   E   P   K   E   R   G   D   F   N   H   E   R   G   E   R   K   V   C   R

          460       470       480       490       500       510       520       530       540
....|....|....|....|....|....|....|....|....|....|....|....|....|....|....|....|....|
B1  TTCAAGTTGGAATGGTTGGGTAATTGCTCTGGTTTGAACGATGAAACTTATGGTTACAAGGAAGGCAAGCCATGTATCATCATCAAGTTG
      F   K   L   E   W   L   G   N   C   S   G   L   N   D   E   T   Y   G   Y   K   E   G   K   P   C   I   I   I   K   L

          550       560       570       580       590       600       610       620       630
....|....|....|....|....|....|....|....|....|....|....|....|....|....|....|....|....|
B1  AACAGAGTATTAGGTTTTAAACCAAAGCCACCTAAAAACGAATCATTGGAAACCTATCCTGTTATGAAGTACAATCCAAACGTTTTACCT
      N   R   V   L   G   F   K   P   K   P   P   K   N   E   S   L   E   T   Y   P   V   M   K   Y   N   P   N   V   L   P

          640       650       660       670       680       690       700       710       720
....|....|....|....|....|....|....|....|....|....|....|....|....|....|....|....|....|
B1  GTCCAATGCACAGGTAAAAGAGATGAAGACAAGGATAAAGTTGGTAACGTTGAATACTTCGGTTTGGGTAACTCTCCAGGTTTCCCTTTG
      V   Q   C   T   G   K   R   D   E   D   K   D   K   V   G   N   V   E   Y   F   G   L   G   N   S   P   G   F   P   L

          730       740       750       760       770       780       790       800       810
....|....|....|....|....|....|....|....|....|....|....|....|....|....|....|....|....|
B1  CAATACTACCCATACTACGGCAAGTTGTTGCAACCAAAGTACTTGCAACCTTTGTTGGCCGTTCAATTCACTAACTTGACAATGGATACC
      Q   Y   Y   P   Y   Y   G   K   L   L   Q   P   K   Y   L   Q   P   L   L   A   V   Q   F   T   N   L   T   M   D   T

          820       830       840       850       860       870       880       890       900
....|....|....|....|....|....|....|....|....|....|....|....|....|....|....|....|....|
B1  GAAATCAGAATAGAGTGTAAGGCTTACGGTGAAAACATAGGTTACTCTGAAAAGGACAGATTCCAAGGTAGATTCGATGTTAAGATCGAA
      E   I   R   I   E   C   K   A   Y   G   E   N   I   G   Y   S   E   K   D   R   F   Q   G   R   F   D   V   K   I   E

          910
....|....|..
B1  GTCAAGTCATGA
      V   K   S   *
```

Palacký University in Olomouc
Faculty of Sciences
Department of Biophysics

2017/2018

Mgr. Jaroslava Šeflová

The Sodium-Potassium ATPase - Expression, Purification and its Interactions with Small Molecules

Summary of Doctoral Thesis

Biophysics (P1703)

Supervisor: doc. RNDr. Martin Kubala, Ph.D.

Olomouc 2017

Dizertační práce byla vypracována během prezenčního doktorského studia programu Fyzika, oboru Biofyzika, na Katedře Biofyziky přírodovědecké fakulty Univerzity Palackého v Olomouci v období 2013 – 2017.

Uchazeč: Mgr. Jaroslava Šeflová

Oponenti dizertační práce:

Vedoucí práce: doc. RNDr. Martin Kubala, Ph. D.
Univerzita Palackého v Olomouci
Přírodovědecká fakulta, Katedra Biofyziky
Šlechtitělů 27, Olomouc-Holice, 77146

Autoreferát rozeslán dne:

Obhajoba dizertační práce se koná dne v hod. před komisí pro obhajobu dizertační práce doktorského studia P1703 Biofyzika.

S plným textem dizertační práce a oponentskými posudky je možné se seznámit na studijním oddělení Přírodovědecké Fakulty Univerzity Palackého v Olomouci, tř. 17. listopadu 12, Olomouc, 771 46.

Bibliografická identifikace

Jméno a příjmení autora	Mgr. Jaroslava Šeflová
Název práce	Sodno-Draselná ATPasa - Exprese, Purifikace a její Interakce s Malými Molekulami
Typ práce	Dizertační práce
Pracoviště	Katedra biofyziky
Vedoucí práce	doc. RNDr. Martin Kubala, Ph.D.
Rok obhajoby práce	2017
Abstrakt	Dizertační práce se zaměřuje na studium významného membránového proteinu, sodno-draselné pumpy. Tento enzym svou funkcí vytváří elektrochemický gradient, který je významný pro celou řadu buněčných procesů. V případě nesprávné funkce sodno-draselné ATPasy dochází ke vzniku patologických stavů, poruch a nemocí. Cílem této práce bylo studovat souvislosti mezi strukturou a funkcí toho proteinu s využitím dostupných experimentálních postupů. Příprava celé sodno-draselné pumpy byla provedena dvěma metodami – přímou izolací z tkáně a heterologní expresí v kvasinkách. Enzym izolovaný z prasečích ledvin byl použit pro zkoumání inhibice sodno-draselné pumpy po interakci s flavonolignany, halogenovanými chinolony a platinovými cytostatiky. Změna aktivity enzymu byla detekována pomocí modifikované Baginského metody, která určuje koncentraci fosfátu z hydrolýzy ATP. Dále byly heterologní expresí v bakteriích připraveny izolované cytoplasmatické segmenty proteinu (C45 a C23 kličky). Tyto kličky umožňují zkoumat interakci sodno-draselné pumpy a biologicky významných látek rozpustných ve vodných pufrech. Vybrané aktivní látky byly cílem dalšího výzkumu zaměřeného na odhalení vazebného místa a mechanismu inhibice enzymu.
Klíčová slova	sodno-draselná ATPasa, exprese v bakteriích, exprese v kvasinkách, C45 klička, C23 klička, Baginského metoda určení ATPasové aktivity, flavonolignany, halogenované chinolony, cisplatina
Počet stran	145
Počet stran příloh	32
Jazyk	anglický

Bibliographical identification

Autor's first name and surname	Mgr. Jaroslava Šeflová
Title	The Sodium-Potassium ATPase - Expression, Purification and its Interactions with Small Molecules
Type of thesis	Doctoral
Department	Department of Biohysics
Supervisor	doc. RNDr. Martin Kubala, Ph.D.
The year of presentation	2017
Abstract	The Na^+/K^+-ATPase (NKA) is an essential membrane protein establishing electrochemical gradient used in cell processes. Dysfunction of NKA leads to pathological states and diseases. This thesis is focused on the relations between structure and function using available experimental approaches. Whole protein was prepared by two methods – direct isolation from porcine kidney and by heterologous expression in yeast. NKA isolated from porcine kidney was used for testing of biologically active molecules such as potential drugs (flavonolignans, halogenated hydroquinolones and platinum-based complexes). Furthermore, we studied the interactions of promising molecules inhibiting NKA activity using the modified Baginsky assay. Isolated cytoplasmic parts of the enzyme, represented by C23 and C45 loops, were used for determination of their binding site and for study of inhibitory mechanism.
Keywords	sodium-potassium ATPase, heterologous expression in bacteria, heterologous expression in yeast, C45 loop, C23 loop, Baginsky assay, flavonolignans, halogenated quinolones, cisplatin
Number of pages	145
Number of pages of appendices	32
Language	English

List of Publications

I **Šeflová, J.**, Biler, M., Hradil, P., Kubala, M., and Čechová, P. (2017). Inhibition of Na^+/K^+-ATPase by 5,6,7,8-tetrafluoro-3-hydroxy-2-phenylquinolin-4(1H)-one. *Biochemie*, 4: 30104 – 30109.

II **Šeflová, J.**, Čechová, P., Šišková, K. M., Kapitán, J., Kubala, M., Šebela, M. and Mojzeš, P. (2017) Cisplatin Interacting with Cytoplasmic Loop (C45) of the Na^+/K^+-ATPase: Role of Cysteine Residues. [Manuscript in preparation].

III Kubala, M., Čechová, P., **Geletičová, J.**, Biler, M., Štenclová, T., Trouillas, P., and Biedermann, D. (2016). Flavonolignans as a Novel Class of Sodium Pump Inhibitors. *Frontiers in Physiology*, 7: 1 – 10.

IV Vacek, J., Zatloukalová, M., **Geletičová, J.**, Kubala, M., Modrianský, M., Fekete, L., Mašek, J., Hubatka, F., and Turánek, J. (2016) Electrochemical Platform for the Detection of Transmembrane Proteins Reconstituted into Liposomes. *Analytical Chemistry* 88: 4548 – 4556.

V Kubala, M., **Geletičová, J.**, Huličiak, M., Zatloukalová, M., Vacek, J., and Šebela, M. (2014). Na^+/K^+-ATPase inhibition by cisplatin and consequences for cisplatin nephrotoxicity. *Biomedical Papers*, 158: 194 – 200.

Introduction

This thesis is focused on the enzyme Na^+/K^+-ATPase (sodium-potassium pump, NKA) which is the first described membrane-bound ATPase from the family of P-type ATPases. Since the discovery of NKA in 1957, the significance of this membrane-bound ATPase has increased. NKA is composed of two main subunits denoted as α and β subunits forming functional heterodimer. The $\alpha\beta$ heterodimer is often associated with the tissue specific regulatory protein from FXYD family. The α subunit is formed by 10 transmembrane helices and three cytoplasmic domains (A, P, N).

In the beginning, the NKA was known mainly as a transporter which translocated sodium and potassium ions across the plasma membrane. Later, other roles of NKA were described, such as involvement in the secondary transport, participating in the water reabsorption in the kidney tissues or the signal transduction in neurons. In general, the dysfunction of NKA can result in the pathological states or diseases such as hyperkalemia [1], cataract [2], hypertension [3] and diabetes [4]. The specific mutations in the genes encoding the NKA isoforms are linked with the development of neurological disorders, e. g. Hemiplegic Migraine [5], Rapid-Onset Dystonia Parkinsonism [6] and Alternating Hemiplegia of Childhood [7]. Furthermore, the recently published study have suggested the correlation between the expression of specific isoforms of α subunit of NKA and the cancer development [8], or a potential role of α expression in the treatment of Alzheimer diseases [9].

Although the biological importance of NKA is clear, the research of human variants of NKA remains challenging for many reasons. For example, the whole enzyme can be prepared by two main techniques – the direct isolation from tissue (e. g. porcine kidney, ox brain, duck nasal gland, shark rectal gland) or the heterologous expression (yeast, insect or mammalian cells). Human proteins can not be isolated directly due to ethical issues making the heterologous expression the only way of the protein preparation.

Unfortunately, the use of yeast expression system, which is widely used for membrane protein expression, needs to be optimized mainly due to the different post-translational modification and membrane lipid composition. On the other hand, the mammalian cells are able to produce heterologous NKA, but the naturally expressed NKA is also present. Another disadvantages of mammalian expression system are a high cost and the low heterologous protein yield. Those obstacles might be overcome by using the directly isolated porcine kidney NKA that shows sequence similarity approximatelly 98% with human kidney variant (based on the comparison of human and porcine α_1 sequences obtained from the Uniprot website).

The interactions between water soluble compounds and cytoplasmic domains can

be examined by using isolated the C23 loop (enzyme N-terminus and A domain) and C45 loop (P and N domains). Both loops may be easily overexpressed in bacteria *E. coli*. As was reported earlier, the isolated C45 loop may be separated from the rest of the NKA and it retained its structural and functional properties [10].

As was mentioned above, the proper function of the NKA is essential for the cells. The NKA inhibitors are mainly represented by the group of natural compounds called cardiotonic steroids (CTS) into which belongs specific NKA inhibitor, ouabain. CTS are currently used in medicine as antiarrhythmic and anticancer agents [11]. The significant disadvantage of CTS is their limited useful concentration due to their toxicity. Finding the potential replacements of CTS is important goal of the current research.

In this thesis, the NKA inhibitory effect of 117 compounds was examined, whereas only 5 compounds were active at biologically relevant concentration (10 μM). Active agents can be separated into three separate groups (flavonolignans, halogenated hydroquinolinones, and platinum-based complexes). The first group of compounds was flavonolignans that are natural compounds used in the traditional medicine for centuries. Flavonolignans are well-known mainly for their hepatoprotective properties. Second examined group was halogenated quinolinones that represent synthetic analogues to flavonolignans. Both flavonolignans and halogenated hydroquinolinones bound to the cytoplasmic part of the enzyme and showed different mode of action in comparison to ouabain. The last group of examined compounds was platinum-based complexes.

Those platinum-based complexes (cisplatin, carboplatin and oxaliplatin) are widely used in the treatment of several types of cancer such as testicular, ovarian, bladder, head, neck and small lung cancer [12]. Namely, cisplatin is a dominant agent in the treatment of testicular cancer, where it reaches cure rate over 90% [13]. On the contrary, patients treated by cisplatin may suffer from many side-effects such as nephrotoxicity, neuropathies, or hearing loss [14]. Moreover, during the early stages of cisplatin-based chemotherapy, the kidney damage may occur [15]. The renal NKA might be potentially influenced by the cisplatin binding, which can result in the kidney damage. The substantial cisplatin inhibition of the porcine kidney NKA published by Kubala *et al.* [16] suggested the association of the kidney damage and with the cisplatin treatment.

Cisplatin is a water soluble compound that enters the cells via passive diffusion or by using the active transporters. In the cells, cisplatin is activated without loss of *Cis*-conformation [17] and forms mono- and diaqua complexes [18]. Several papers reported on the cisplatin binding to proteins in the blood and cytosol [19]. This binding is often processed via reactive species within the protein structure such sulfhydryl (-SH) moiety. Additionally, the recently published crystal structure of NKA with bound cisplatin [20] suggested binding to the methionine and cysteine residues on the cytosol-facing part of the enzyme. Here I examined the interaction of cisplatin with the isolated cytoplasmic domain of NKA represented by C45 loop.

The cisplatin binding to the isolated C45 loop was examined using the set of cysteine mutants where each of the 11 naturally occurring cysteine residues was replaced by serine. All mutants were subjected to the cisplatin treatment and their intact masses were determined by using the mass spectrometry (MS). The intact mass differences between the cisplatin treated and untreated samples suggested the binding of approximately

5 cisplatin molecules to the C45 loop. Those results corresponded to the number of cysteine residues detected on the surface of the C45 loop. By using this approach, I identified the hotspot for the cisplatin binding on the C45 loop at positions Cys452, Cys456 and Cys457. This sequence of cysteine residues is unique for the renal isoform of NKA associated with the extending cysteine to serine replacements in the α_2 and α_3 isoforms. The binding of cisplatin to this hotspot was confirmed by the detection of tetra cysteine motif by the TC-FlAsH^{TM} reagent.

The main aims of this thesis were:

- to express α_3 β_1 complex of sodium-potassium ATPase in yeast *Saccharomyces cerevisiae* and optimize this process
- to study the interactions of NKA with the selected group of small molecules (platinum-based anti-cancer drugs, quinolinones and flavonolignans)
- to study the interactions of cisplatin with NKA via cysteine residues on the large cytoplasmic loop connecting transmembrane helices M4 and M5 (C45 loop)
- to prepare C45 and C23 loops derived from the human DNA sequence for α_1, α_2 and α_3 isoforms by the heterologous expression in *Escherichia coli*

Chapter 1

Theoretical Basis

1.1 Membrane-Bound ATPases

The ion pumping ATPases, transporting ions at the expense of ATP, are the major players in ion homeostasis maintenance [21]. ATPases are transporters enabling translocation of specific solutes accros the membranes, which form unique ionic compartments between both inside and outside the cells. Transported solutes are mainly inorganic ions that play vital roles in mammalian physiology, in processes such as neural transduction, energy transformation, and nutrient uptake.

The five main classes of the ion pump ATPase family have been described. They are called P-type ATPase, F-type ATPase, V-type ATPase, A-type ATPase and E-type ATPase. The nomenclatures was derived from phosphorylated intermediate (P-type ATPase), factors of oxidative phosphorylation (F-type ATPase) and a pump found initially in vacuoles (V-type ATPase) [22], a pump found in *Archea* (A-type ATPase), and cell surface pump that hydrolyzes nucleotide triphosphate including extracellular ATP (E-type ATPase).

Na^+/K^+-ATPase (sodium-potassium pump, NKA) was the first P-type ATPase introduced to the field [23], and was shown to translocate two K^+ ions into cell and export three Na^+ ions, coupling these movements with the hydrolysis of one molecule ATP to ADP and phosphate [24]. Similar ion pumps described subsequently include sarcoplasmic (SERCA) or plasma membrane Ca^{2+}-ATPase (PMCA), gastric H^+/K^+-ATPase (HKA), Cu^{2+}-ATPase linked with the Wilsons and Menkes disease [25], plant or fungal plasma membrane H^+-ATPase, etc. This group of pumps forms acyl phosphoenzyme intermediates from ATP (hence the P-type ATPase) prior to ion translocation, and shows two distinct kinetic states named as E1 and E2 conformations. During the reaction cycle of P-type ATPases, pumps alternately expose ion binding sites to the intracellular and extracellular compartments [21].

1.2 Structure of the Sodium-Potassium ATPase

The function of P-type ATPases was illustrated by many crystal structures that have been published so far [26]. Crystal structures illustrating ion transport in SERCA have been already published, but detailed structures illustrating reaction cycle of NKA remains unknown. The X-ray structure of NKA was determined in two main conformations – potassium-bound state (often denoted as E2, open conformation) [27, 28] and sodium-bound state (E1 state, closed conformation) [29, 30]. These structures resolved the structure of separate subunits and helped to understand the reaction cycle.

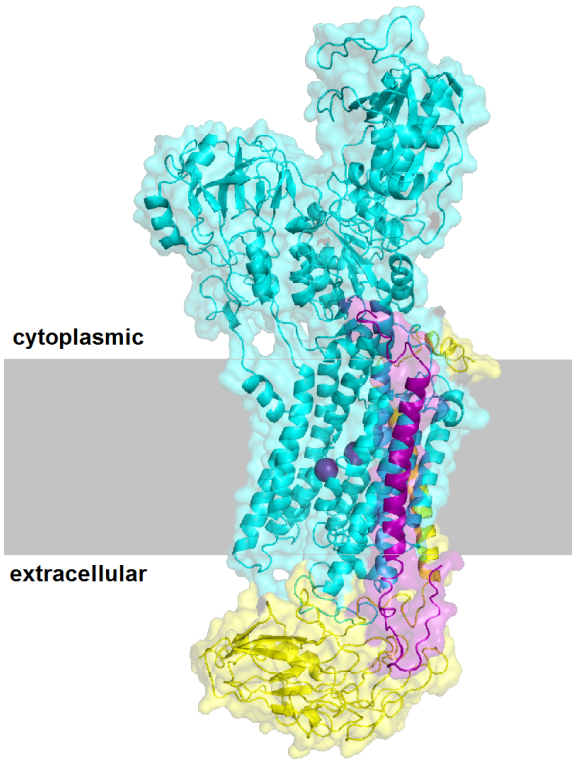

Figure 1: The structure of NKA – the cytoplasmic headpieces of α subunit are widely open towards cytoplasm (upper part of figure). Furthermore, the β (yellow) and α (cyan) subunits form a heterodimer, which is a functional unit of the enzyme. The enzyme is often accompanied by a tissue specific protein from the FXYD family (magenta) which regulates the turnover of the pump. The figure courtesy of Petra Čechová.

Many P-type ATPases (e. g. SERCA) are formed by one transporting subunit, but some P-type ATPases exhibit more complicated structure. Moreover, of all the members in the P-type ATPases family, only Na^+/K^+-ATPase and H^+/K^+-ATPase require two subunits for active transport of ions. Possibly, this two pumps compose a distinct subfamily within the P-type ATPases. The functional NKA is composed of two essential subunits (named as α and β subunit) and is often associated with regulation protein from the FXYD family (see Figure 1). Human body expresses four different isoforms of α subunit, three β subunits and seven isoforms of FXYD protein in a tissue specific manner [31].

The mass of the α subunit is approximately 112 000 Da, and is also called the

catalytic subunit due to its function in the reaction cycle. The β subunit is extensively glycosylated and its molecular weight is approximately 55 kDa depending on the post-translational modification [32]. Moreover, β subunit works as a molecular chaperon that enables folding of alpha subunit into fully functional shape and helps routing an α subunit into the plasma membrane. Finally, the mass of FXYD protein is approximately 10 kDa. The main aim of the FXYD protein is a tissue specific regulation of the pumping carried out by $\alpha\beta$ heterodimer.

1.2.1 α Subunit

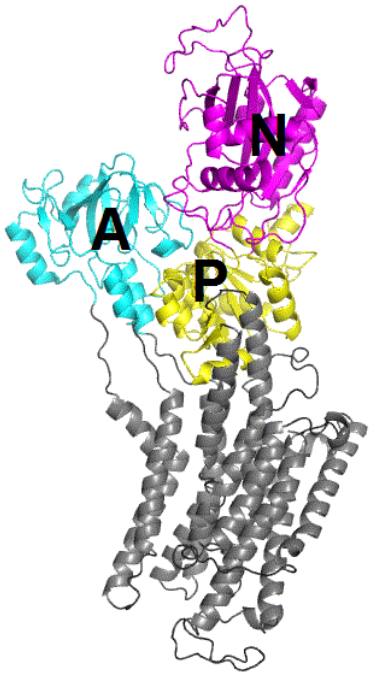

Figure 2: The structure of the α subunit of the NKA. Main domains called A, P and N are highlighted in the structure. The A domain is purple, P domain is yellow and N domain is cyan. The transmembrane part of the enzyme is grey.

The α subunit is composed of three cytoplasmic domains (see Figure 2) named A (actuator), P (phosphorylation), N (nucleotide binding,) and ten transmembrane helices M1 – M10. The α subunit shows very restricted range of divergence in the sequence before a loss of the function (NKA from duck nasal salt gland shows 95.5% similarity and 93.5% identity to that from human kidney). In contrast, similar comparison for the β subunit reveals only 81% similarity and 69% identity between the sequences [33].

The α subunit contains the specific lysine-rich N terminal extension of approximately 40 residues that are able to undergo phosphorylation and serve as platform for protein-protein interaction [34].

The NKA is primarily the pump for sodium ions, however selective filter for potassium ions is less tightly regulated and similar ions can be transported instead. The two binding sites for sodium ions were determined in a good agreement with SERCA

(transports two Ca^{2+} ions). But the third binding site has been described recently [30, 29]. Transported ions bound to NKA are illustrated in the Figure 3.

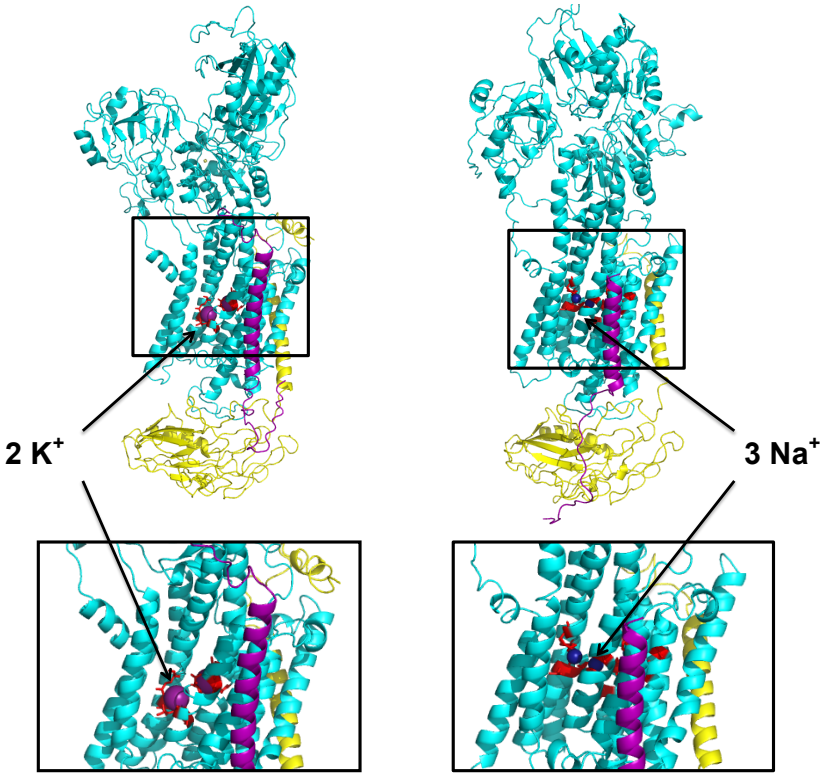

Figure 3: Left: Structure of NKA in open conformation (E2) with bound two K^+ ions. Right: NKA in closed (E1) conformation with bound three Na^+ ions. In the figure are highlighted: α subunit (cyan), β subunit (yellow), FXYD protein (magenta) K^+ ions (purple) and Na^+ ions (dark blue).

Except for the transmembrane domain, the three cytoplasmic domains significantly contribute to the reaction cycle. The N domain recognizes ATP and positions the γ phosphate for nucleophilic attack, whereas a conserved aspartate in the P domain accepts the phosphoryl group and forms a high energy aspartyl-phosphate intermediate [35].

A glutamate in the A domain positions a water molecule for the subsequent hydrolysis which leads to the release of the phosphoryl group. The cytoplasmic domains are connected to the transmembrane segment by five linker regions that form the crucial structural connection between two-steps release of energy on the cytoplasmic side and its conversion into physical translocation of ions through the membrane [36].

1.2.2 β Subunit

This subunit works as a molecular chaperon ensuring proper membrane integration and packing of newly synthesized α subunit in the endoplasmic reticulum (ER) [37]. Most notably, β routes α to the plasma membrane and prevents it from degradation. The overexpression of the β subunit results in integration of β into plasma membrane,

but overexpression of α subunit results in retention of this subunit in the ER [38]. Additionally, β modulates the function of the whole protein by tuning the cation-binding affinity and K^+ occlusion. Furthermore, it was reported that β also modulates the formation of cell-to-cell junctions [32].

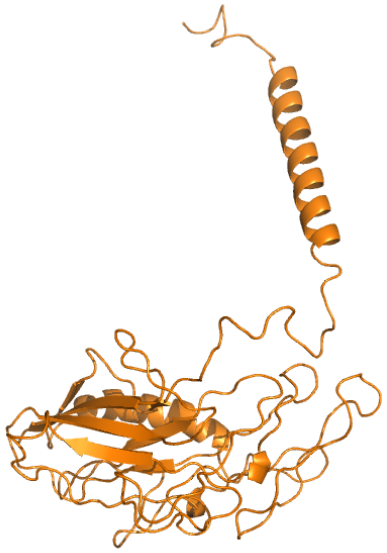

Figure 4: The structure of β subunit of NKA. There is one helical structure associated with the transmembrane part of α subunit, while the protein is anchored in the membrane. The lower part of β subunit works as a lid which opens and closes during the reaction cycle.

The β subunit is extensively glycosylated during the post-translational modification of the protein. From two to four glycosylation sites can be found on the β subunit, but number of these sites depends on the isoform. The glycosylation sites may also regulate the dimer-formation of $\alpha\beta$ complex [34].

1.2.3 FXYD Proteins

The family of FXYD proteins is a group of tissue specific regulators modulating kinetic properties of the whole $\alpha\beta$ heterodimer as well as they are responsible for apparent affinities of transported ions and ATP [32]. FXYD proteins are composed of a single transmembrane helix (adjacent to M7 helix of α subunit), extracellular part containing conserved motif FXYD(Y) and a cytoplasmic part that containing important phosphorylation sites (see Figure 5). The position of conserved motif is just prior to transmembrane helix. Furthermore, the transmembrane domain contains two conserved glycine residues and the most of the functional effect is associated with this part.

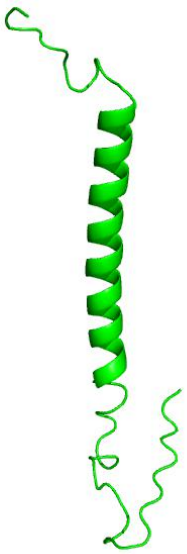

Figure 5: Structure of FXYD protein.

1.2.4 Isoforms of the Structural Subunits

As mentioned previously, the human α subunit exists in four distinct isoforms, human β can be found in three isoforms and human body expresses seven isoforms of FXYD proteins.

Studying the human $\alpha_3\beta_1$ complex of NKA which is expressed by neuronal cells, was one aim of this work. Neurons may express α_1, α_2, α_3 or any combination of these isoforms, and evidence suggests that neuronal type is the determining factor. The function or significance of multiple NKA isoforms and their nonuniform expression between neurons, remain unknown [31]. Neurons express $\alpha_3\beta_1$ and rarely $\alpha_3\beta_2$ complexes of the NKA. However, β_1 and β_2 subunits are also expressed in other tissue and cell types. Different types of central and peripheral glia (astrocytes, oligodentrocytes and Schwann cells) express α_1 or α_1 and α_2, but not α_3 isoform. At least two groups of peripheral neurons were functionally identified expressing α_3, the skeletal muscle stretch receptor afferent neurons and γ-motoneurons [31].

1.2.5 Lipid Enviroment

General lipid-protein interaction depends on the lipid-induced changes with the physiological properties of bilayer [39]. Both chemical and physical properties (hydrophobic thickness, curvature stress, elastic moduli, etc.) of a lipid bilayer affect the final structure and function of the membrane-bound proteins. As reported recently, lipid-protein interactions show strong potential in the distribution of specifically bound lipids at the lipid-protein surface [39]. Moreover, the mutual interaction between lipids and membrane-bound proteins seems to be evolutionarily conserved. Detailed information about membrane architecture can be found in [40].

The effect of annular lipids and specific-bound lipids (see Figure 6) can examine

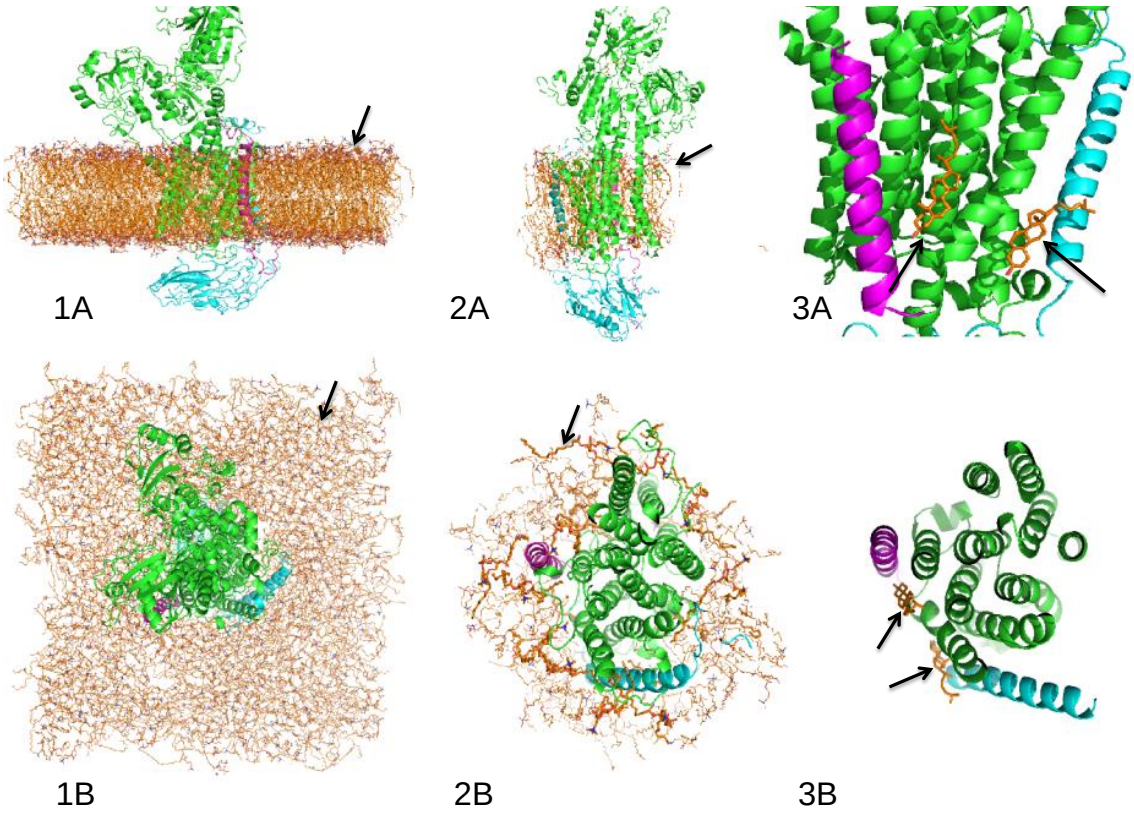

Figure 6: A lipid environment around the NKA – membrane parallel view (A) and membrane perpendicular view (B). Part 1A, B shows free lipids in the membrane, 2A, B illustrate annular lipids which are associated with the protein and 3A, B show specific-bound lipids (non-annular lipids).

the functional effects of phospholipids and cholesterol on the structural stability of the NKA. Annular lipids coat the transmembrane surface of the protein and only the protein structure restricts their free motion. Annular lipids associated with NKA are phosphatidylcholine (PC), phosphatidylserine (PS) and cholesterol (CHS). Any phospholipid or molecule of CHS can serve as specific-bound lipid found within NKA structure [41]. The specific-bound lipids (also called nonannular lipids) are tightly associated with the protein in long-term interactions [42]. The specific-bound lipids are found filling the cavities on the protein, fitting into grooves between the transmembrane helices or they are stacked between the subunits. Such positioning significantly distorts their structure and geometry [43].

1.3 Cytoplasmic Loops C23 and C45

The crystal structures of NKA in closed and open conformation were published by many authors [27, 34, 30, 43]. The crystal structures helped to understand the NKA structure and they are useful for the monitoring of transitions between the main conformational states. The crystal structures represent available information about the natural NKA structure and serve as the basis for the computational methods such as molecular dynamics.

Three large domains (named as A, P, N) could be identified on the cytoplasmic side of the membrane. The A domain consists of the N-terminus and loops between the transmembrane helices M2 a M3 (loop C23). The N and P domains are composed of a large cytoplasmic loop connecting helices M4 and M5 (C45 loop) as shown in Figure 7.

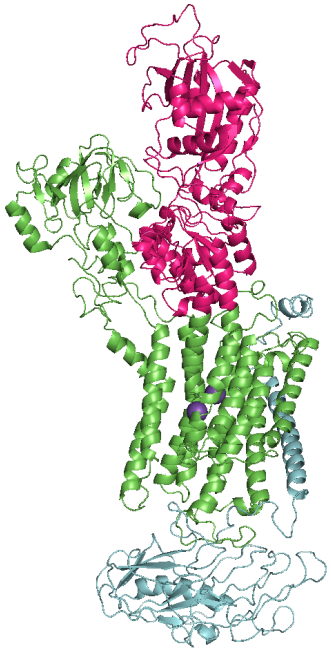

Figure 7: Structure of open NKA with C45 loop. Within green α subunit is C45 loop highlighted in magenta, and β subunit is blue.

Within the conserved sequence of N domain was identified the nucleotide-binding site. Whereas, the central P domain contains the residuum Asp369 that undergoes phosphorylation during the reaction cycle. Many interactions of NKA with the water soluble molecules are limited to the cytoplasmic part of the enzyme. To study interactions of NKA with water soluble molecules, the whole NKA can be represented only by domains which are exposed to the cell exterior such as C23 and C45 loops.

The large cytoplasmic loop C45 connecting transmembrane helices M4 and M5, and smaller loop C23 connecting transmembrane helices M2 and M3 are the most important representatives of the cytoplasmic domains. The structures of both loops are in Figure 8. As published previously, the C45 loop can be isolated from the rest of the enzyme and retains its structural [44] and functional properties [45] including ATP binding [10].

Due to the convenient size of those proteins (C45 – 48 kDa, C23 – 13 kDa), they can be prepared by the heterologous expression in bacteria. The structures of both loops are in Figure 8.

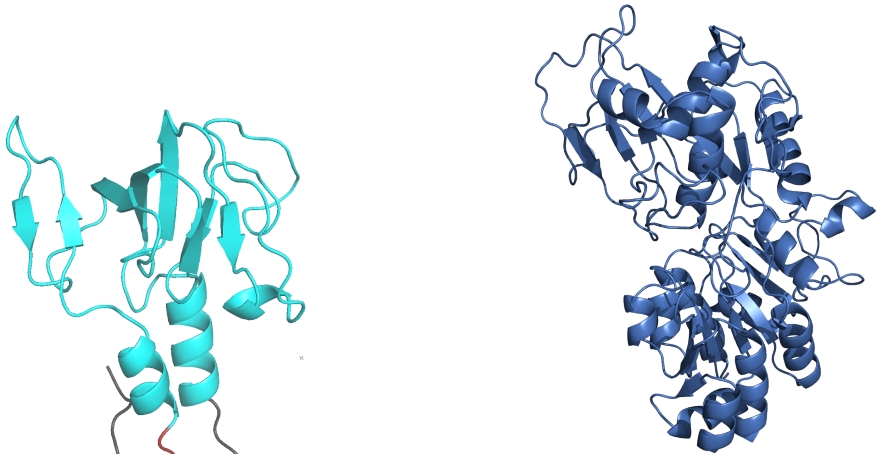

Figure 8: Left: The structure of the C23 loop. Right: The structure of C45 loop. The figure courtesy of Petra Čechová.

1.4 Isolation of the NKA from a Porcine Kidney

Although, NKA is present in most animal cells, it is particularly abundant in secretory and excitatory tissues. The most common sources for purification are kidney, brain, nasal glands, and electric organs [46]. The enzyme can be isolated from various source animals e. g. pig [47], mouse [48], ox [49], shark [50], duck [51] and electric eel [52]. The study of the human variant is challenging due to ethical issues and inability of mammalian expression systems to provide sufficient amount of the protein for the research.

1.5 Determination of the Na^+/K^+-ATPase Activity

Two basic methods are available for the determination of NKA activity: Enzyme-coupled assay and Baginsky assay. In principle, both methods detect inorganic phosphate, but they use different approach. Following sections introduce these methods.

1.5.1 Baginsky assay

The ATPase activity can be determined by a direct colourimetric detection of inorganic phosphate, called Baginsky assay [53]. The principle of the Baginsky assay is a monitoring the interaction of ammonium molybdate with a product of ATP hydrolysis (inorganic phosphate), which leads to a colour change measured at 710 nm. The main advantages of this method are its effectivity, low time consumption and the ability to automate the process using an automatic pipetting workstation.

The Baginsky assay is a simple and sensitive procedure for phosphate determination that eliminates error caused by a nonenzymatic phosphate hydrolysis. A unique feature of the method concerns the fact that the reagents form the stable coloured complex

with the inorganic phosphate present, but any additional phosphate cannot react with reagents involved in complex formation.

1.5.2 Enzyme-Coupled Method

This method is an alternative to Baginsky assay enabling the determination of the NKA activity. The coupled ATPase assay is used for the determination of mitochondrial Ca^{2+} and Na^+/K^+-ATPase. This method was described by Norby [54], and is based on the following linked reactions:

$$\text{ATP} \xrightarrow{\text{Na}^+/\text{K}^+ - \text{ATPase}} \text{P}_\text{i} + \text{ADP} \quad (1)$$

$$\text{P}_\text{i} + \text{phosphoenolpyruvate} \xrightarrow{\text{pyruvate kinase}} \text{ATP} + \text{pyruvate} \quad (2)$$

$$\text{pyruvate} + \text{NADH} \xrightarrow{\text{lactate dehydrogenase}} \text{lactate} + \text{NAD}^+ \quad (3)$$

All reactions have reaction equilibrium shifted toward products (proceed to the right side of the reaction). The first step of detection (1) requires NKA cofactor Mg^{2+}, and transported ions (Na^+, and K^+). The rate of the last reaction (3) is determined as a change in absorbance, which is monitored at 340 nm (NADH). The steady-state absorbance measures the uninhibited rate of reaction (1) since the steady state concentration of ADP is always significantly lower than the inhibitory concentrations, and the auxiliary enzymes and their reactants exhibit no influence on the reaction catalyzed by NKA [54].

1.6 Small Molecules Influencing NKA Activity

1.6.1 Cardiotonic Steroids and Their Analogues

Cardiotonic glycosides (also known as cardiotonic steroids, CTS) and ouabain (specific inhibitor of NKA) undergo extensive research for decades due to their remarkable biological effects (congestive heart failure treatment, arrhythmia treatment, anticancer drugs, diuretics, emetics, and abortificants) [11]. These compounds are often isolated from natural sources (plants and animals), but many of CTS display high toxicity (IC_{50} in range of nanomoles) which also limits their use in the drug development. Englishman William Withering used extract from foxglove (*Digitalis purpurea L.*) and oleander (*Nerium oleander L.*) for treatment of congestive heart failure 250 years ago. This extract contained CTS such as digitalis, digoxin and oleandrin [11].

Nowadays, CTS are used in the prevention and/or treatment of proliferative diseases such as cancer. CTS inhibit cell proliferation and exhibit favorable cytotoxic activity against several cell lines. Their action is mostly based on the induction of apoptosis [55]. More specifically, the inhibition of NKA by CTS leads to the accumulation of sodium and calcium ions in the cells and this reduce the membrane potential and intracellular potassium concentration [56]. Although, CTS are known as antiarrythmic agents, they also increase the level of reactive oxygen species [2] which contributes to mentioned effect through the redox modification of cardiac ryanodine receptors [57, 58].

In hearth, the mechanism of CTS action arises from the inhibition of NKA. Interaction between CTS and NKA results in the NKA inhibition, which leads to increasing sodium concentration in the intracellular space [59]. This elevated sodium level affects the plasma membrane Na^+/Ca^{2+}-exchanger, leading to a significant increase in the intracellular calcium concentration, and heart contraction [60]. This positive ionotropic effect of CTS enables their use as a major therapeutic agent in the management of congestive heart failure [60]. But for this to occur, sufficient number of NKA must be inhibited to significantly increase intracellular sodium concentration, even if this occurs in a limited space in the cytoplasm [61]. Additionally, current research have revealed anticancer properties of CTS. However, their role in the anticancer treatment is still not well established.

It is no surprise that binding site for ouabain is a highly conserved sequence across evolutionary spectrum excluding parasites of *Acokanthera schimperi* and *Strophantus gratus* – plants from which the inhibitor is extracted. The highly conserved binding site for ouabain suggests existence of natural ouabain-like compound which has role of NKA regulator [61].

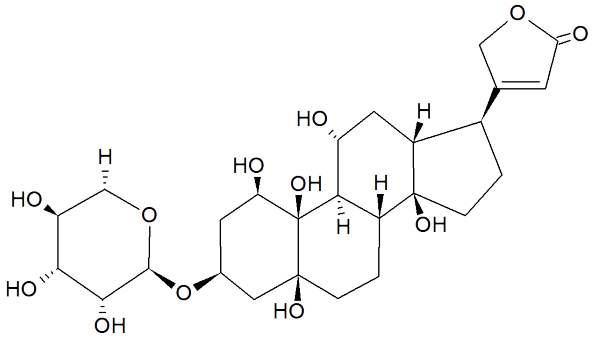

Figure 9: Structure of typical member of cardiotonic steroids family – ouabain.

Binding site for CTS is highly conserved region within animals [62], insects [63] and human [64], but some exceptions exist. For example monarch butterflies [63] and leaf beetles [63] developed a resistance to ouabain since they consume the plant materials containing CTS. The detailed study of their NKA revealed two binding sites for CTS within α subunit [61].

The potential involvement of CTS compounds in the cancer treatment was discussed 40 years ago [65]. This research was abandoned due to high toxicity of the compounds. In the 1970s, only murine cell lines were available for testing the potential drugs, and those cell lines were less sensitive to CTS action. Some CTS inhibit cell proliferation of human and monkey cell lines [66] at non-toxic nanomolar concentrations, where

they are [67]. Nowadays, CTS should be considered for skin cancer treatment, or they should be investigated for possible adjuvant therapy for malignant diseases [11].

1.6.2 Flavonolignans

The scope of our research was included the series of phenolic compounds, called flavonoids, which had been known since ancient times (approximately 4^{th}. century B. C.). In general, flavonoids are a broad class of a secondary metabolites contained in plants, and they are responsible for yellow, red or blue pigmentation of the flowers [68]. Major dietary sources of flavonolignans are tea, red wine, apple, tomato, onion, thyme, parsley, soy beans, legumes, grapefruit, lemon and several vegetables, fruits, and trees such as Ginkgo or neem [69].

Flavonoids can be isolated from *Silybum marianum* as a mixture called silymarin. This extract is currently included in many commercial products. Silymarin is a standardized active extract from plant seeds containing approximately 70 – 80% of the silymarin flavonolignans, and 20 – 30% of a chemically undefined fraction comprising mostly polymeric and oxidized polyphenolic compounds (called phenolic fraction – PP) [70]. By now, 23 flavonolignans have been identified in *Silybum marianum* [71].

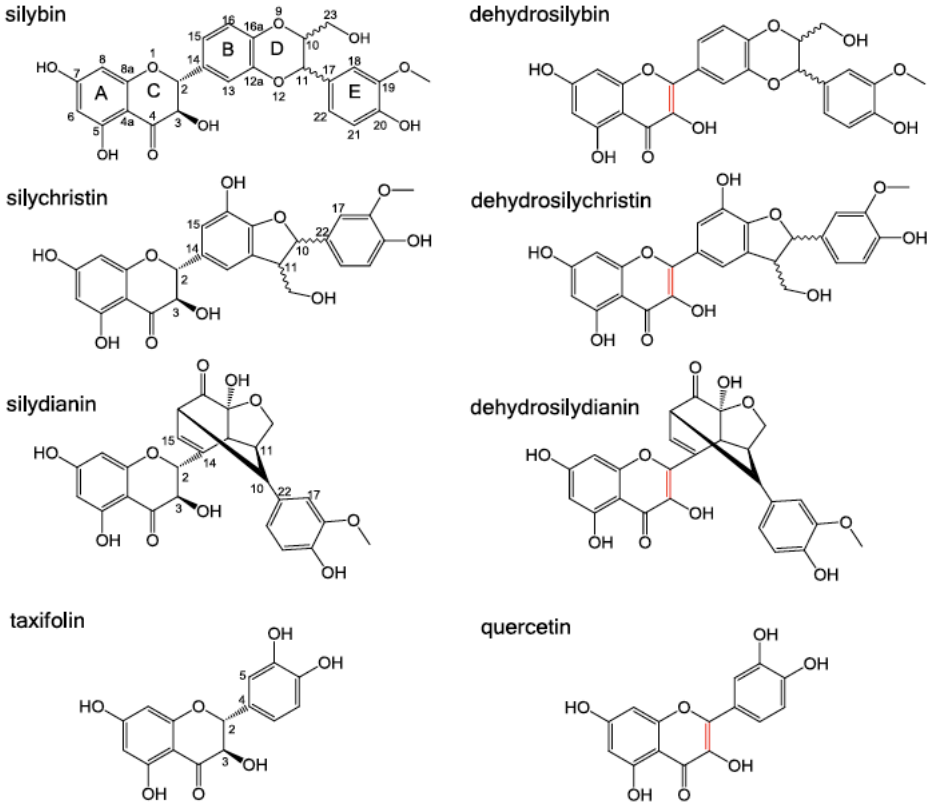

Figure 10: Structures of silybin (SB), silychristin (SCH), silydianin (SD), and their dehydroderivatives (DHSB, DHSCH, DHSD), taxifolin (TAX), and quercetin (QUE). The 2,3-double bond in dehydroderivatives is highlighted in red [72]. The figure courtesy of Michal Biler.

The main component of silymarin is silybin. Silybin is a mixture of two distinct

diastereomers, denoted as silybin A and silybin B. Despite the 1:1 proportion of those diastereomers, the isomers were finally separated in 2003 [73]. Other flavonolignans present in silymarin are isosilybin, dehydrosilybin, silychristin, silydianin, and few flavonoids such as taxifolin [74]. Only silybin (A and B), isosilybin (A and B), silychristin and silydianin are the most important constituents of seed extracts.

Unfortunately, the positive effects of flavonolignans suffers from some controversy. The main controversy of effects is the variability of the silymarin composition caused by the different methods of extract preparation used in published studies. It has been documented previously that the properties of respective compounds in various silymarines depend on the source of seeds (cultivar and planting conditions), processing conditions, and extraction method [70].

Natural flavonoids are antioxidative [75], free-radical scavenging [76], hepatoprotective [77], and cytotoxic agents [78]. The main disadvantage of flavonolignans is their limited bioavailibility [79] due to low water-solubility of these compounds. Several approaches were applied to improve the biovailibility of the flavonoids such as the preparation of silybin bis-hemisuccinate [80], the preparation of phosphatidylcholine complex of silybin [80], or the addition of a sugar moiety to silybin scaffold [80]. More information on effects and applications of the flavonolignans can be found in the literature [81].

1.6.3 Halogenated Quinolinones

The synthetic analogues of natural flavonoids based on the 3-hydroxyquinolinone scaffold called quinolinones represent other biologically relevant compounds. They are isosteric to flavoniods – they contain three-member-ring skeleton. The group of pyrrolo-[3, 4-h]quinolin-2-ones was synthetized from furocumarines, and was applied in the skin disease treatment. They compounds can act as photo-induced cell killers after irradiation by long-wave UV light [82]. Quinolinones exhibit the cytostatic and antileukemic activity [83]. Moreover, 2-heptyl-3-hydroxyquinolin-4-one is a bacterial signal molecule that can act as strong antiprotozoal agent due to its role in the cell-to-cell communication system [84]. Copper(II) quinolinonato-7-carboxamido complexes were prepared as analogues to platinum complexes [85]. Finally, the novel structural analogues of quinolinones are being currently prepared to obtain higher activity, low toxicity, and more specific selectivity.

The low solubility of quinolinones limits their bioavailability. Respecting their limited water solubility, current research is focused on the improvement of the bioavailability of selected compounds [86]. Moreover, the delivery system based on the silica nanoparticals was established recently [87]. The therapeutic properties of quinolones can might be further altered by the chemical modification of the quinolone scaffold, e. g. chloro- and dichloro- derivatives of 3-hydroxy-2-phenylquinolin-4(1*H*)-ones, but biological activity of halogenated quinolinones is unknown.

Monochloro- and dichloro-3-phenyl-3-hydroxyqiunolin-4(*1H*)-ones were evaluated as potential anticancer drugs in the National Cancer Institute Bethesda [83]. All tested compounds were subjected to three distinct cell lines, but only three compounds passed

Acronym	R_1	R_2	R_3	R_4
TFHPQ	F	F	F	F
DFHPQ	H	F	F	H
8CHPQ	H	H	H	Cl
6CHPQ	H	Cl	H	H
DCHPQ	Cl	Cl	H	H

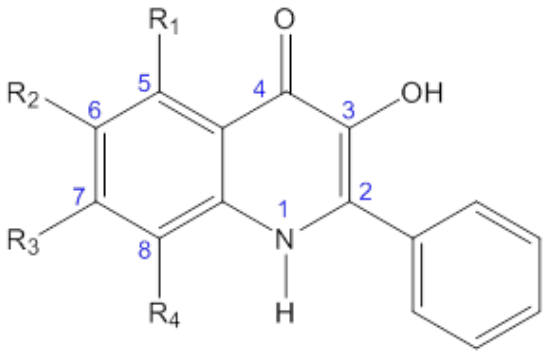

Figure 11: Structure and acronyms of 3-hydroxy-2-phenylquinolin-4(*1H*)-one derivatives [88].

NCI's criteria, and were evaluated against the 60 tumor cell lines. Furthermore, 5,6-dichloro-, 5,7-dichloro-, and 7,8-dichloro-3-phenyl-3-hydroxyqiunolin-4(*1H*)-ones inhibited the growth of the cell lines derived from colon and breast cancer [83]. Structures and positions of halogen atoms within the 3-hydroxy-2-phenylquinolin-4(*1H*)-one derivatives are summed in Figure 11.

1.6.4 Platinum-Based Drugs

Cisplatin (*Cis*-diamminedichloroplatinum(II)) was approved for the treatment of the both ovarian [12] and testicular cancer [13] in 1978 [89], and it was also administrated for many other types of cancer, e. g. bladder, head and neck, oeasopheral, small cell lung cancer [12] and lymphomas [15]. The first characterization and synthesis of cisplatin was performed by Peyrone in 1845 [90].

Nowadays, the cisplatin treats testicular cancer with cure rate more than 90% efficiency [91]. But some tumors such as colorectal, and non small cell lung cancers [92] exhibit an intrinsic resistance for cisplatin treatment. Furthermore, ovarian and small cell lung cancers were found to acquire the resistance during the early stages of the cisplatin treatment [93].

Oxaliplatin (1,2-diamminocyclohexaneplatinum(II) oxalate), the only one registered platinum-based agent demonstrating activity against cisplatin-resistant tumors [94]. Another platinum-based drug – carboplatin (*Cis*-diammine(1,1-cyclobutanedicarboxylato)platinum(II) shows similar action in the cancer treatment as cisplatin with lower toxicity [18].

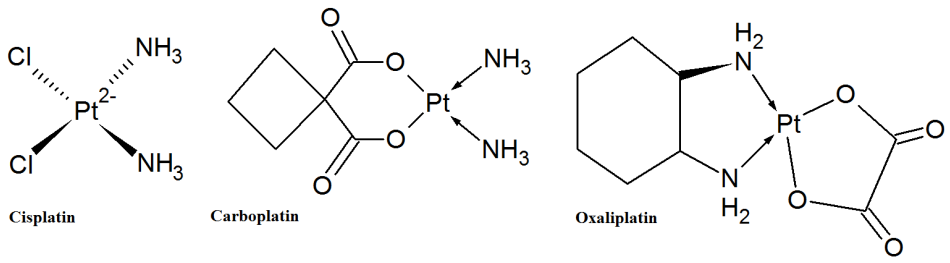

Figure 12: The most widely used platinum-based anticancer drugs – cisplatin, carboplatin, and oxaliplatin.

Selective toxicity to tumor cells is a complex machinery involving the drug uptake, transport to the cell nucleus, formation of adducts with target DNA, and recognition by damage-response proteins [95]. The formation of these adducts and cross-links with target DNA in the cell nucleus inhibits the DNA replication, thus, interfering with the cell division by mitosis. Subsequently, the signal transduction pathway is transactivated and other nuclear proteins contribute to cell-cycle arrest, attempt to repair damaged DNA, apoptosis and necrosis [18].

After the cisplatin activation, the cisplatin can covalently bind to DNA. As a result, the DNA double helix is slightly unwound and bent [96]. More specifically, the monoaqua cisplatine complex readily forms monofunctional adducts with the N^7 atom of purine bases [95]. Eventually, bifunctional adducts can be formed [97], but adducts were found between two guanines on the opposite strands at d(GpC).d(GpC) sites [98]. Intrastrand adducts are rather rare due to steric inaccessibility [14]. Moreover, cisplatin-carbonato complexes have been reported to form monofunctional [99, 100] and difunctional [100] adducts with target DNA. The study of DNA of cisplatin-treated patients confirmed the presence of approximately 65% 1,2d(GpG), 25% 1,2d(ApG), and 5 – 10% 1,3d(GpNpG) adducts [101]. Oxaliplatin and carboplatin exhibit different DNA-binding kinetics and form disparate adduct profiles [102].

Cisplatin causes many dose-limiting side effects (e. g. severe nausea, myelosupression, neurotoxicity, nephrotoxicity, emetogenesis or ototoxicity [103]). Cisplatin also bind to many blood and cytoplasmic proteins [19]. Moreover, the crystal structure of NKA with bound cisplatin was published in 2012 [104].

Chapter 2

Material and Methods

2.1 Isolation of NKA from Porcine Kidney

2.1.1 Materials

The purification was performed according to [46] with some modifications. All solutions were prepared using ultrapure water and analytical grade reagents. The pH adjustments were carried out using HCl. All solutions, instruments and equipment were cooled down in advance. The isolation was performed in the cold room temperated to 4°C.

2.2 Expression of NKA in Yeast

2.2.1 Strains and Media

P. A. Pedersen, University of Copenhagen, Denmark kindly provided *Saccharomyces cerevisiae* strain BJ 5457 [105, 106]. This yeast strain was employed as a host organism for the expression of the α_3 β_1 human NKA. The transformed cells were selected on the synthetic minimal medium containing 0.5% glucose and supplemented with leucine (30 mg·l^{-1}) and lysine (20 mg·l^{-1}).

The *Escherichia coli* cells XL1 ([107]) were used as a host organism for the construction of recombinant DNA vector. *E. coli* cells were grown in the Luria-Bertani medium [108] with the appropriate antibiotics.

2.2.2 Transformation of *Saccharomyces cerevisiae* and *Escherichia coli*

This project was solved under the supervision of professor Poul Nissen, Aarhus University, Denmark (yeast expression, HPLC purification) and Per Amstrup Pedersen, University of Copenhagen, Denmark (expression vector construction, detergent screening and optimization of protein expression).

Yeast cells were transformed by homologous recombination according to [109, 110] and the plates were incubated at 30°C for 72 hours at least.

E. coli strains were transformed by the heat-shock according to [111] where the plates were incubated at 37°C for approximately 17 hours.

2.2.3 Plasmid Construction for Expression in Yeast

P. A. Pedersen, University of Copenhagen, Denmark kindly provided the *S. cerevisiae-E. coli* shuffle vector pEMBLyex4 (2259) [106]. The pUC57 vector containing gene for α_3 (PUC57-α_3) or β_1 (pUC57-β_1) were synthetized by GenScript. The *S. cerevisiae-E. coli* shuffle vector was digested by BamHI, HindIII and PstI endonucleases (all from Thermo Fisher) for gene insertion. All selected genes were amplified by PCR using synthetized pUC57-α_3 or pUC57-$beta_1$ vector as a template.

The α_3 gene was mutated by the site-directed mutagenesis to produce mutant proteins Asp811Asn, Glu825Lys, Asp933Asn, Asp933Tyr, and Gly957Arg. The PCR products were inserted into vector by homologous recombination. DNA from yeast was purified by the lyticase method, and *E.coli* XL1 cells were transformed to select the constructs. The pEMBLyex4 vector containing the α_3 wild-type (WT) or mutant gene was purified from *E.coli* by GeneJET Plasmid Miniprep Kit (Thermo), and digested by endonuclease NruI (Thermo). The shuffle vector with the inserted β_1 was used as a template for PCR. The PCR product with the β_1 gene was incorporated into the digested pEMBLyex4 vector containing α_3 gene by the homologous recombination. The sequences of final constructs were verified by DNA sequencing.

2.2.4 Site-Directed Mutagenesis

Specific mutations (Asp811Asn, Glu825Lys, Asp933Tyr and Gly957Arg) in the α_3 gene were performed using QuikChange Lightning Site-Directed Mutagenesis Kit (Agilent Technologies). All mutated residues were verified by DNA sequencing (GATC Biotech AG, Germany).

2.2.5 Heterologous Expression in Yeast

The proteins were expressed using galactose-regulated promoters. The yeast cells were grown in shake flasks in synthetic minimal medium containing 0.5% glucose, 3% glyc-

erol as a carbon source, and supplemented with all amino acids except lysine, isoleucine, leucine, glutamine, asparagine, glycine. A single colony of transformed yeast was selectively propagated into 5 ml of synthetic minimal media supplemented with leucine until saturation (according to [105]). An aliquot of 100 µl of the culture was transferred into 5 ml of synthetic minimal media supplemented with lysine but without leucine. The culture was grown until saturation. Then, 500 µl of the culture was transferred into 50 ml of the same media. For the large scale protein preparation 2.0 liters of minimal media with lysine was inoculated. All selected cultures were grown at 30°C until they reached optical density OD_{450} 1.0 and then induced with 2% galactose. The cultures were separated into aliquot containing 1.5 liter, and the other aliquot with 0.5 liter of culture and they were incubated at 15°C and 30°C, respectively. The cultures were harvested by centrifugation after 48 h cultivation. During the cultivation period, 50 ml of the culture were harvested for monitoring of the protein expression.

2.2.6 Isolation of the Yeast Membranes

The isolation of yeast membranes was performed according to Pedersen *et al.* [105]. Galactose-induced yeast cells were harvested at 5800 g for 5 minutes, and washed with ice-cold water. The yeast cells were resuspended in an ice-cold lysis buffer composed of 25 mM imidazole, 1 mM EDTA, 1 mM EGTA, 10% sucrose (w/v), 1 mM PMSF, 1 µg/mg chymostatin, 1 µg/mg leupeptin a 1 µg/ml pepstatin and pH was adjusted to 7.5. The cells were homogenized in an ice-cold Bead Beater (Biospec) three times for 1 minute. The homogenate was centrifuged at 1100 g for 20 minutes. The supernatant was further centrifuged at 3000 g for 20 minutes. The final supernatant was centrifuged at 164600 g for 1.5 h. The resulting crude membrane fraction was homogenized in a Teflon-glass Braun homogenizer in an ice-cold lysis buffer. All centrifugation steps were hold at 4°C. The membranes were stored at −80°C.

2.2.7 Purification of NKA from Crude Membranes

The prepared membranes were thawed and diluted to the final concentration of 2 $mg^{-1}{\cdot}ml^{-1}$ in lysis buffer containing 2 mg/ml of detergent (n-dodecyl-β-D-maltoside, DDM or octaethylene glycol monodecyl ether, $C_{12}E_8$) and supplemented with 1.2 mg/ml cholesteryl hemisuccinate. The solubilisation of membranes was performed at 4°C for 1 h. The solubilized membranes were further centrifuged at 164300 g, at 4°C for 30 minutes. The supernatant was diluted with the ice-cold buffer (25 mM Tris, 10 mM imidazole, 500 mM NaCl and 10% glycerol, pH 7.6) to 1.5 CMC (critical micelle concentration) of detergent. Ni-NTA beads (Qiagen) were added into membranes solution in the ratio of 0.5 ml of beads to 1 ml of supernatant. The solution was incubated at 4°C overnight. The protein was eluted by the series of elution buffers (25 mM Tris, 500 mM NaCl, 10% glycerol, 0.75 $mg{\cdot}ml^{-1}$ detergent, 0.15 $mg{\cdot}ml^{-1}$ cholesteryl hemisuccinate and 10 – 500 mM imidazole) with increasing imidazole concentration.

2.2.8 Size-Exclusion Chromatography (SEC)

All samples prepared using Gal4ΔPep4 strain were analyzed by SEC. Running buffer based on [112] was composed of 100 mM NaCl, 20 mM Tris-HCl, 10% glycerol, 0.2 mg·ml^{-1} DDM or 0.1 mg·ml^{-1} C_12E_8, 0.05 mg·ml^{-1} DOPS or SOPS, and 0.01 mg·ml^{-1} CHS; pH 7.4. The buffer was filtered using 0.22 μm syringe filter. The running buffer for [113] based protocol was composed of 20 mM KCl, 5 mM KF, 5 mM $MgCl_2$, 100 mM NMNG, 40 mM MOPS-Tris; pH 7.0. The running buffer was filtered as described above.

The SEC was performed using instrument Akta Micro (GE Healthcare, Sweden) and Superdex 200 Increase 3.2/300 column (GE Healthcare, Sweden). The separation was performed at room temperature with cooled column (4°C). Flow rate was set to 0.05 ml·min^{-1} and 100 μl fractions were collected into microwell plate.

2.3 Preparation of the Large Cytoplasmic Loop of NKA (C45 Loop)

The large cytoplasmic segment connecting the transmembrane helices 4 and 5 (C45 loop, residues Leu354 – Ile777 of the mouse brain sequence) with a $(His)_{10}$-tag at N terminus was expressed in *E. coli* Rosetta DE3 cells (Promega, USA) and purified using Co^{2+}-based affinity resin (TALON resin, Clontech, USA) as described by Grycova *et al.* [10]. The protein concentration was determined using the Bradford assay [114] with BSA as a standard.

2.3.1 The Set of Cysteine Mutants of the C45 Loop

The cDNA sequence of mouse brain C45 loop was digested at restriction sites of NheI and HindIII for cloning into final vector. The template, 1275 bp DNA of mouse brain C45 loop, was commercially synthetized and cloned using the restriction enzymes NheI, HindIII and sealed by T4 ligase (NEB) into pET28b plasmid. The construct was multiplied by Top 10 *Escherichia coli* bacteria (Thermo Fisher, USA) and isolated using Wizzard Plus SV Minipreps DNA Purification System (Promega). A set of eleven recombinant proteins (Figure **??**) containing one point mutation in codon TGC→ AGC or TGT→ AGT (amino acid replacement Cys→ Ser) and one protein containing double replacement of cysteine residues. The primers used for cloning are listed in Table **??**. The sequences were verified by DNA-sequencing using primers T7-terminator (GCTAGTTATTGCTCAGCGG) and T7-promoter (TAATACGACTCACTATAGGG). Heterologous expression in *E. coli* using similar expression and purification of isolated C45 was described in detail by others (e. g. [10]).

2.3.2 C45 Loops Intact Mass Determination

MALDI-TOF analysis for the intact mass determination of the C45 loop was performed on the Microflex LRF20 instrument. Samples of the untreated C45 loop and its derivatives were incubated with cisplatin (molar ratio of 1:20) for 24 h at 4°C, whereas the control samples were mixed with water. The cisplatin-treated and control samples were dialyzed against 2 l of dialysis buffer (20 mM Tris-HCl; pH 7.5) for 72 h at 4°C. The 1 µl of each sample was placed onto the target plate (MSP BigAnchor Chip TM 96, microScript Target), immediately mixed with 1 µl of matrix (20 $mg \cdot ml^{-1}$ Sinapic acid in 0.1% TFA/acetonitrile, 1:1, v/v) and allowed to dry on air. At least 500 single-pulse spectra were acquired in the linear mode for positive ions. The instrument parameters were as follows: acceleration voltage 20 kV, extraction voltage 18 kV, lens voltage 9.5 kV and delayed extraction time 1000 ns. Then the mass spectrum of each sample was obtained by summing over all these subspectra. The final molecular weight of the protein was averaged from 10 replicates and plotted by Matlab2017a software. The external calibration was performed using a mixture of Protein Calibration Standard II (Bruker Daltonics, Germany, 1:1, v/v).

2.3.3 Chemical Modification of Cysteine Residues

The chemical modification was performed according to [115, 116, 117]. The C45 WT proteins were diluted to the final concentration of 1 $mg \cdot ml^{-1}$ and alkylated by 330 mM iodoacetate in 100 mM ammonium bicarbonate (final concentration of iodoacetate was 55 mM) at room temperature for 30 minutes. The reaction was stopped by adding 10 mM β-mercaptoethanol. The modified C45 WT was dialyzed against 2 l of dialysis buffer (20 mM Tris-HCl, pH 7.5) at 4°C overnight. The intact masses of modified C45 WT before and after cisplatin treatment were detected using the same set up as described in the section 2.3.2.

2.4 Preparation of Human C23 and C45 Loops

Thomas Friedrich from Institute of Chemistry, Technical University of Berlin, Germany kindly provided the DNA sequences encoding human α_1, α_2 and α_3 subunits in 3.1x DNA vector. Each sequence of C45 and C23 was multiplied using standard PCR and digested by NdeI a XhoI (New England Biolabs) endonucleases. DNA fragment was selected by standard 1% agarose electrophoresis, and isolated from gel using Wizard SV Gel and PCR Clean-Up System (Promega) mixed with linearized pET28b (New England Biolabs) vector. The vector with C45 gene was sealed using T4-DNA Ligase (New England Biolabs) and inserted into TOP 10 *E. coli* cells (Invitrogene). The construct DNA was isolated with GeneJET Plasmid Miniprep Kit (Thermo). The sequences of all constructs were verified by the DNA sequencing (Seqme s. r. o., Czech Republic).

2.4.1 Purification of Human C23 Loops

The C23 loop connecting the transmembrane helices 2 and 3 with a $(His)_{10}$-tag at N terminus was expressed in *E. coli* Rosetta DE3 cells (Promega, USA) and purified using Co^{2+}-based affinity resin (Clontech, USA). The cell cultures were grown until OD_{600} 0.6 and consequently, the induction was performed using 500 μM IPTG. Induced cultures were incubated on shaker at 17°C for 20 h. The cultures were harvested, resuspended in lysis buffer (10 mM Tris-HCl, 10 mM NaCl; pH 7.5) containing protease inhibitors (2 $\mu g \cdot ml^{-1}$ leupeptin, 2 $\mu g \cdot ml^{-1}$ pepstatin and 1 mM PMSF) and directly subjected to cell disruption by ultrasound homogenizator model 3000 (BioLogics, USA). The cell lysate was centrifuged (15000 g, 25 minutes at 4°C), pellet was removed and supernatant was left to interact with TALON resin. TALON affinity resin was washed with set of wash buffers (wash buffer 1: 20 mM Tris-HCl, 20 mM imidazole, 100 mM NaCl; wash buffer 2: 20 mM Tris-HCl, 20 mM imidazole, 500 mM NaCl; and wash buffer 3: 20 mM Tris-HCl, 30 mM imidazole, 100 mM NaCl. pH of all wash buffers was adjusted to 7.4.). The elution was carried out using elution buffer (500 mM imidazole, 20 mM Tris-HCl, 140 mM NaCl; pH 7.4). Immediately after the elution, the protein was dialyzed into dialysis buffer (20 mM Tris-HCl; pH 7.4) and stored at −20°C. Protein concentration was determined using the Bradford assay [114] with BSA as a standard.

2.4.2 Purification of Human C45 Loops

All C45 loops were expressed and purified using the same protocol as described in Section 2.3.

2.5 Determination of NKA Activity

2.5.1 Enzyme-Coupled Assay

The measurements of NKA activity were performed at Department of Biophysics (Aarhus University, Denmark) in collaboration with Natalya Fedosova.

The reaction was started by adding of the NKA (2 μl at concentration 6.78 $mg \cdot ml^{-1}$) into reaction buffer (30 mM L-histidine, 130 mM NaCl, 20 mM KCl, 4 mM $MgCl_2$, 1 mM PEP, 3 mM Na-ATP, 0.22 mM NADH, 12.5 $U \cdot ml^{-1}$ PK, and 30 $U \cdot ml^{-1}$ LDH; pH 7.4). After the initialization of the reaction, the absorbance was monitored for 300 s. The reaction stopped by the addition of 500 μM ouabain, and residual absorbance was determined by absorbance at 340 nm measurement for 300 s.

2.5.2 Baginsky Assay

The NKA activity was measured using modified Baginsky assay protocol by Baginsky *et al.* [118] with some modifications [53]. Baginsky assay demands relatively low

amount of samples and provides a wide range of reproducible results in comparison with other methods. This colourimetric method relies on the detection of inorganic phosphate which interacts with ammonium molybdate. The reaction results in a colour change which can be monitored as a change of absorbance at 710 nm measurable using microplate reader Synergy Mx (BioTek, USA). Baginsky assay was easily automatized using the automated pipetting station Freedom EVO (Tecan, Switzerland).

The ATPase activity of untreated NKA decreases to approximately 10 % in the presence of ouabain, which serves as a specific inhibitor of Na^+/K^+-ATPase. 10 mM ouabain was used to reveal residual activity of ATPases. The residual activity in presence of ouabain has been subtracted from the total estimated ATPase activity.

I have tested using the Baginsky assay several compounds belonging into group of flavonolignans. Namely silybin (SB), silydianin (SD), silychristin (SCH) a taxifolin (TAX), and their dehydro- derivatives dehydrosilybin (DHSB), dehydrosilydianin (DHSD), dehydrosilychristin (DHSCH), and quercetin (QUE) were examinated in the paper III [72]. We have also tested the group of halogenated quinolinones and platinum-based complexes (cisplatin, oxaliplatin, and carboplatin).

Chapter 3

Results and Discussion

3.1 Isolation of NKA from Porcine Kidney

The 234 g of the outer medulla tissue was dissected from 3.6 kg of whole porcine kidneys. The centrifugation 3 yielded 23.52 g of pellet, which was subjected to ultracentrifugation. Series of ultracentrifugation and pellet resuspendation enabling to reach high purity of the final protein. The protein yield and activity is summarized in Table 3.1

Sample	Concentration ($mg \cdot ml^{-1}$)	Specific ATPase activity ($\mu mol \cdot mg^{-1} \cdot h^{-1}$)	Unspecific ATPase activity ($\mu mol \cdot mg^{-1} \cdot h^{-1}$)
Microsomes	4.0	9.9	41.0
NKA+0.8 $mg \cdot ml^{-1}$ SDS	4.0	30.1	64.3
NKA+2.0 $mg \cdot ml^{-1}$ SDS	4.0	36.3	76.5
Pure NKA	1.0	109.8	164.9

Table 3.1: Summary of the NKA preparation from the porcine kidney. The specific ATPase activity is ouabain-sensitive activity, and the unspecific activity is overall activity of all ATPases present in the sample.

The microsomes, which were treated by higher SDS concentration (2.0 $mg \cdot ml^{-1}$) yielded lower specific and unspecific activity. Activities of the samples from the most important steps of the purification process are presented in Table 3.1.

One purification from 25 kidneys yielded approximately 87.0 mg of pure NKA with specific activity approximately 164.9 $\mu mol \cdot mg^{-1} \cdot h^{-1}$. The concentration and purity of the final pure protein was estimated using Bradford assay and SDS-PAGE (see Figure 13) We used centrifugal filters to increase the protein concentration and for removal of contaminants with small molecular weight. The concentrated protein exhibited improved purity, but the loss of ATPase activity appeared within days. I assume that this loss of the protein function could be linked with free lipids from solubilized

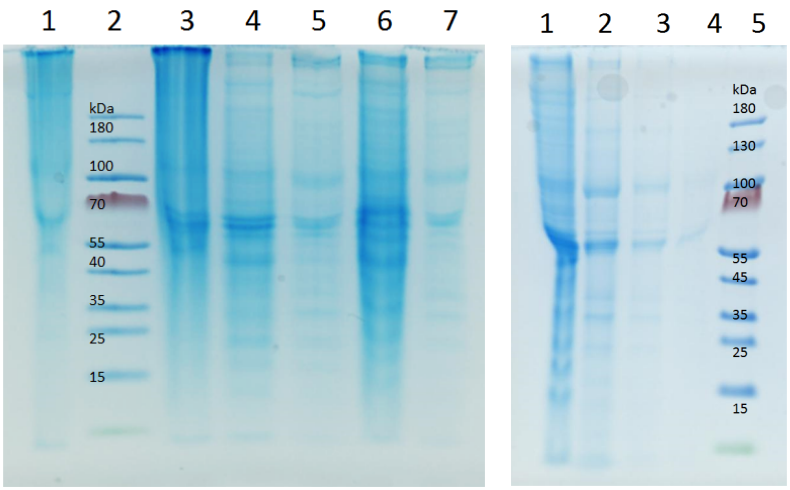

Figure 13: Left: SDS-PAGE of the purified NKA without homogenization with the ice-packed Buffer 2. The samples were loaded as follows: 1 – porcine kidney NKA isolated using the differential ultracentrifugation on the sucrose gradient, 2 – marker, 3 – crude membranes 4 mg·ml^{-1}, 4 – membranes solubilized by 0.8 mg·ml^{-1} SDS, 5 – pure protein solubilized by 0.8 mg·ml^{-1} SDS (final concentration of 1.0 mg·ml^{-1}), 6 – membranes solubilized by 2.0 mg·ml^{-1} SDS, 7 – pure protein solubilized by 2.0 mg·ml^{-1} SDS (final concentration of 0.7 mg·ml^{-1}). Right: SDS-PAGE of the purified NKA without homogenization with the ice-packed Buffer 2. The samples were following 1 – microsomes 4.6 mg·ml^{-1}, 2 – pure protein 1 mg·ml^{-1}, 3 – pure protein 0.2 mg·ml^{-1}, 4 – pure protein 0.1 mg·ml^{-1}, and 5 – marker.

membrane. The use of centrifugal filters may removed some free lipids that caused loss of the NKA function.

3.2 Expression of NKA in Yeast Strain BJ5457

In general, some useful expression strategies for the integral membrane protein expression were published previously [119]. Unfortunately, the expression of NKA excludes the use of the GFP fusion protein expression due to protein misfolding caused by GFP fusion. NKA cannot be GFP-tagged neither within α subunit (both N- and C-termini), nor within β subunit without significant change of the complex association (according to personal communication with Per Amstrup Pedersen). However, the whole NKA complex can be expressed in yeast with high yield (according to [109]).

The effective purification can be performed using N-terminal $(His)_{10}$-tag placed on the β subunit. Similar approach using BJ5457 yeast strain was previously used for purification of the porcine $\alpha_1\beta_1$ complex [105]. Furthermore, [120] developed simple protocol for the increase of yield produced membrane proteins using yeast expression system.

I prepared the expression vector for co-expression of human complex of $\alpha_3\beta_1$ in yeast *Saccharomyces cerevisiae* (strain BJ5457). I also expressed a set of mutant proteins (D811N, E825K and G957 in human α_1 numbering). These mutations are often

mentioned as a possible causative mutations for AHC and RDP [121]. I would like to note that for easier understanding I will keep using the human α_1 numbering.

The both genes (encoding α_3 and β_1 subunit) were placed into expression vector pEMBLye4 under control of the same promoter sequence which was positively regulated by galactose and negatively regulated by glucose. The yeast strain BJ5457 also contained cyclic galactose promoter enabling a high yield protein expression under selected conditions. Moreover, we monitored the time-dependent protein expression and we tested two distinct cultivation temperatures (15°C, 30°C) after the induction of protein expression. For the optimization of membrane solubilization, αDDM and $C_{12}E_8$ detergents were used. Obtained results are presented in the following section.

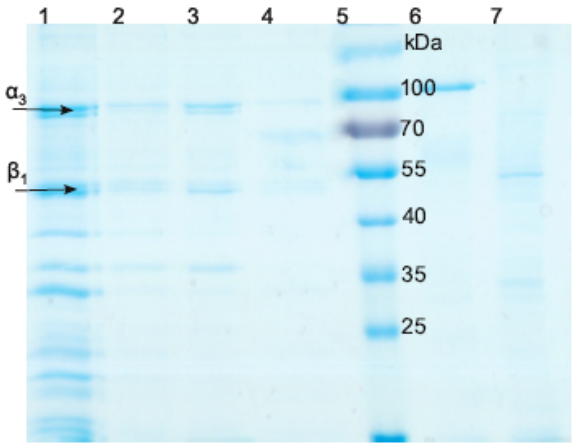

Figure 14: The pure NKA protein analyzed by SDS-PAGE. Positive control is represented by NKA isolated from porcine kidney and plasma membrane Ca^{2+}-ATPase (PMCA) expressed in yeast as negative control. Samples were loaded in the following order: 1 – α_3Gly957Arg+β_1WT, 2 – α_3Glu825Lys+β_1WT, 3 – α_3Asp811Asn+β_1WT, 4 – α_3WT+β_1WT, 5 – marker, 6 – porcine kidney NKA, and 7 – PMCA as a negative control.

Yeast strain BJ5457 expressed NKA complex as illustrated in Figure 14. The molecular weight of the prepared complex is in good agreement with the control sample (porcine kidney NKA).

The size of the β subunit expressed in yeast exhibited lower molecular weight (approx. 40 kDa) than β subunit from porcine kidney NKA complex (approx. 50 kDa), as can be seen in Figure 15. For example, the methylotrophic yeast *Pichia pastoris* expresses the β subunit as two strains with molecular weight 44 and 47 kDa [122]. I assume that the molecular weight difference was linked with the post-translational modifications more specifically with glycosylation. The β is highly glycosylated in the animal cells and those glycosylations may be chemically removed. β subunit without glycosylations then exhibited the same molecular weight for both, heterologous and porcine protein [112].

Furthermore, several bands for β subunit were observed. Those results agreed with the results obtained for heterologously expressed NKA [123]. The presence of multiple bands for β subunits were considered as different levels of glycosylations.

The α subunit was expressed as a full size protein with molecular weight approx-

imately 110 kDa which correlated with expected weight (the porcine kidney NKA α subunit). In contrast to β subunit, the α subunit is not glycosylated and was expressed as a single peptide without differences in the molecular weight.

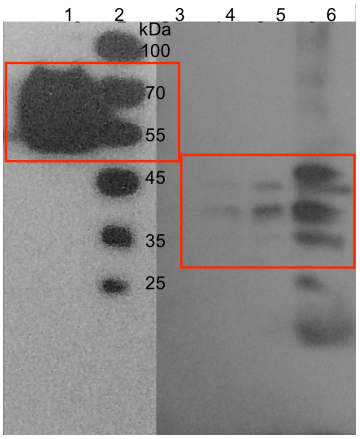

Figure 15: Pure proteins analyzed by Western blotting. The specific antibodies for β_1 subunit were used for the protein detection. In the figure is highlighted the position of β subunit. The samples were loaded in the following order: 1 – porcine kidney NKA, 2 – marker, 3 – α_3WT+β_1WT, 4 – α_3Asp811Asn+β_1WT, 5 – α_3Glu825Lys+β_1WT, and 6 – α_3Gly957Arg+β_1WT.

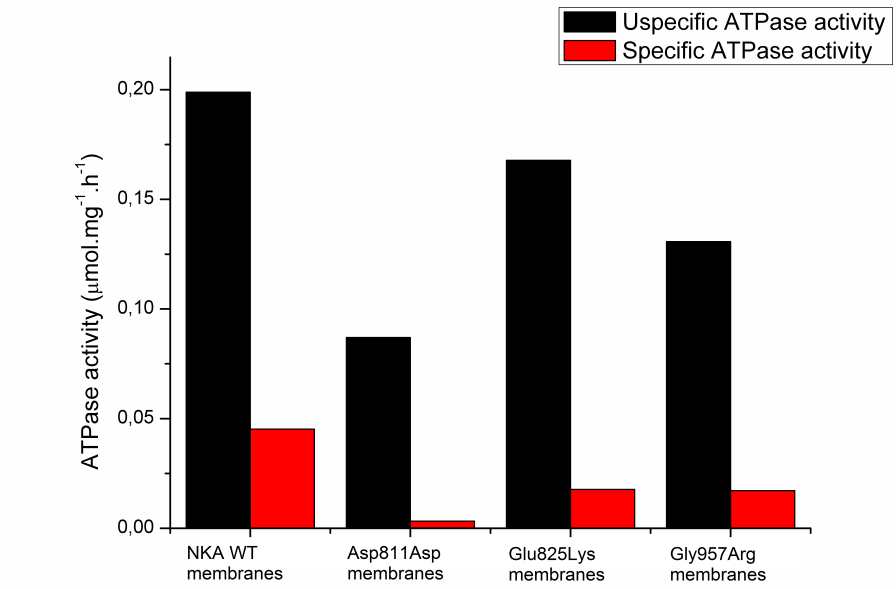

Figure 16: Activity of NKA expressed in yeast strain BJ5457 detected by Baginsky assay. The NKA expressed in yeast exhibited activity only if incorporated in the membranes. After the membrane solubilization NKA lost its function.

The temperature and glucose concentration at the time of induction plays a major role in the α subunit expression. For example, if the induction was performed at higher temperature than 15°C, a truncated product was observed. In the presence of residual glucose, the level of expression was suppressed decreasing the total complex yield. The induction temperature and residual glucose concentration had an dramatic influence on the quality and quantity of prepared protein.

Furthermore, the highest expression level is detected using 48 hours long cultivation time at 15°C. Thus, a large scale preparation of NKA was conducted at 15°C for 48 hours.

Moreover, two detergents at 1.5 CMC were also used for the solubilization of yeast membranes prepared under mentioned conditions. The better solubilization was observed for αDDM detergent than for $C_{12}E_8$. The use of detergent depends on the composition of the membrane that should be solubilized. For the NKA purification from porcine kidney I used SDS detergent due to its low prize and high efficiency. This detergent may be too drastic for the mild solubilization of yeast membranes.

The Baginsky assay was used for the determination of specific ATPase activity with NKA isolated from porcine kidney as a standard (see Figure 17). The expressed proteins seemed deactivated after their isolation from membranes. These results were in good agreement with the ATPase activity measured by the enzyme coupled method (see Figure 16).

Finally, the local environment is a crucial parameter ensuring the protein function [39]. Although, the protein preparations described above were carried out only in the presence of CHS, the ATPase activity of membrane samples was detected. Nevertheless, the lipid composition of a reconstituted membrane around the expressed protein should be optimized in the future.

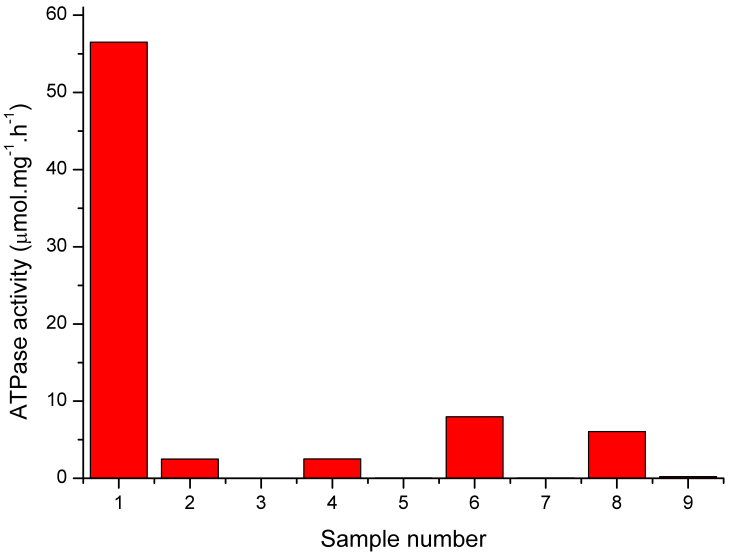

Figure 17: Activity of NKA expressed in yeast strain BJ5457. The detected activities were determined using enzyme-coupled of ATPase activity determination. The samples numbering corresponds to 1 – porcine kidney NKA, 2 – α_3WT+β_1WT membranes, 3 – α_3WT+β_1WT pure protein, 4 – α_3Asp811Asn+β_1WT membranes, 5 – α_3Asp811Asn+β_1WT pure protein, 6 – α_3Glu825Lys+β_1WT membranes, 7 – α_3Glu825Lys+β_1WT pure protein, 8 – α_3Gly957Arg+β_1WT membranes, 9 – α_3Gly957Arg+β_1WT pure protein. The tested membrane samples exhibit ATPase activity, yet the activity of purified proteins was below the detection limits of this method.

3.3 Expression of NKA in Yeast Strains Gal4ΔPep4 and ΔPep4

3.3.1 Gal4ΔPep4 and ΔPep4 Strains

The yeast strains Gal4ΔPep4 and ΔPep4 [124] were also used for NKA production. These strains were kindly provided by Poul Nissen and the optimization of the protein isolation was performed in the collaboration of student of mine, Veronika Kolomazníková. Selected strains varied mainly in the post-translational modifications – specifically in glycosylations. In comparison to BJ5457 strain, the cultivation was shortened due to the absence of the cyclic galactose promoter. This cyclic promoter enables to cultivate yeast to high optical densities without decreasing the galactose concentration after induction (galactose is not consumed by yeast). Therefore Gal4ΔPep4 strain was used for the consequent preparations.

3.3.2 Optimization of Preparation Protocol

The protocol of the pure protein preparation used for BJ5457 strain exhibited low yield when applied to Gal4ΔPep4 and ΔPep4 strains. The optimization of the protein expression was based on the protocol published by [112] for the NKA preparation from methylotrophic yeast *Pichia pastoris*. The second protocol used for optimization was based on the potassium-bound state of NKA published by Morth *et al.* [113]. Unfortunately, the second mentioned protocol yielded protein, which was not able to retain its activity. This loss of the enzyme activity was caused by the presence of potassium in the buffers [112, 125]. The proteins prepared using both protocols were subjected to HPLC analysis, Western blotting and activity determination.

Before the separation of the prepared protein using compact fast protein liquid chromatography (FPLC) we tested the separation method using large aggregates to detect the void peak elution time. Solution containing ribosomes was used for this purpose. The position of the void containing aggregates was eluted at retention time of 20 minutes after separation initialization.

Then the same conditions were applied to samples prepared according to Cohen *et al.* [112] and Morth *et al.* [113], respectively (Figure 18).

From the elution profile (see Figure 19), I assume that conditions of preparation resulted in the protein denaturation. Haviv *et al.* [126] published the protocol derived from Cohen *et al.* [112], where the protein after elution is stored at -20°C in the presence of a high concentration of imidazole. However, my results suggest that protein was denatured under these conditions (see elution profile in the Figure 18). Due to the protein denaturation, I added a dialysis step just after the protein elution. Dialyzed proteins exhibited different elution profile when separated by HPLC (see Figure 19).

The elution profile showed a typical double peak which suggested the presence of a dimer and monomer form of NKA. Furthermore, similar elution profiles were obtained for other P-type ATPases (personal communication with Joseph Lyons). I also

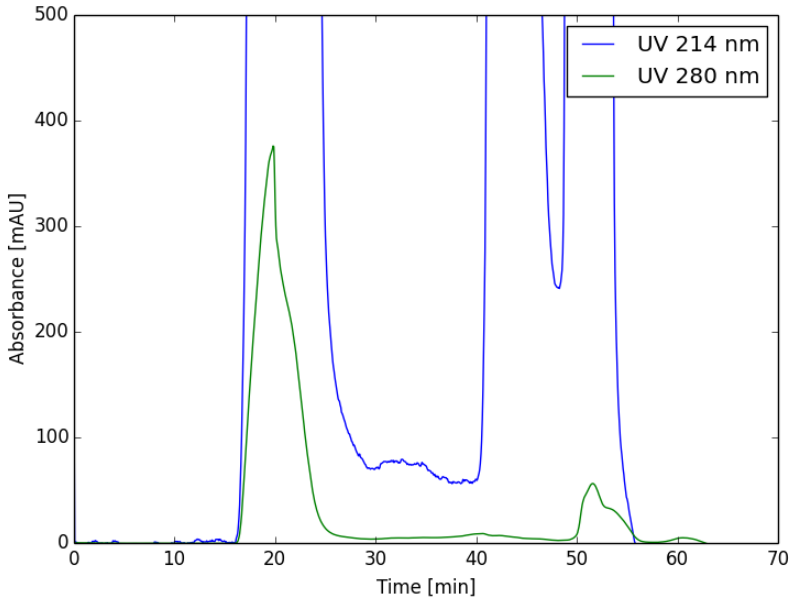

Figure 18: Elution profile of pure protein prepared using Cohen *et al.* [112] protocol. Absorbances at 214 nm and 280 nm are highlighted in blue and green, respectively. The peak-shape suggested an immediate elution of the aggregated NKA just after the void peak at retention time of 20 minutes.

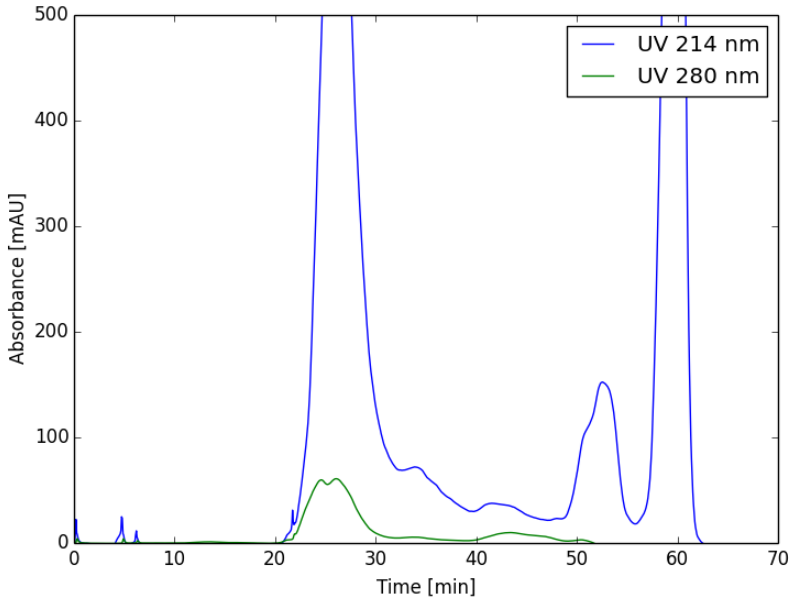

Figure 19: Elution profile of the dialyzed pure protein prepared according to Cohen *et al.* [112] protocol with added dialysis step (dialysis overnight against 2 l of the dialysis buffer). absorbances at 214 nm and 280 nm are highlighted in blue and green, respectively. The double peak was detected at time retention time of approximately 25 minutes after separation initialization. The peak can be interpreted as elution of NKA in the dimeric and monomeric form.

observed multiple bands for β subunit due to presence of several forms with different glycosylation levels. I significantly reduced the presence of those forms using urea treatment during crude membranes preparation. The cell lysate was centrifuged (1000 g, 10 minutes) and immediately mixed with 2M urea and 100 mM KCl. The cell lysate was incubated for 25 minutes at 4°C. Then, the urea-treated lysate was subjected to centrifugation (20 000 g, 20 minutes) and preparation continued standardly. Urea treated samples showed approximately 2 main bands for β subunit instead of 4 or more bands.

Despite the promising elution profile and western-blots, the pure protein completely lost its function. Due to the loss of a function we optimized detergent solubilization (time of solubilization and detergent type) and artificial membrane reconstitution.

I tested 6 distinct detergents (namely SDS, LMNG, $C_{12}E_8$, αDDM, βDDM, and DM), two solubilization times (2 or 17 hours) and 6 different lipid solutions based on [112, 127], which are listed in Table 3.2.

Mixture No.	Composition	Concentration ($mg \cdot ml^{-1}$)
1.	60% DOPS 20% PC 20% CHS	0.25 0.25 0.10
2.	80% DOPS 20% CHS	0.25 0.10
3.	60% DOPS 40% CHS	0.25 0.10
4.	100% DOPS	0.25
5.	100% Brain PS	0.25
6.	100% Brain polar extract	0.25

Table 3.2: Used lipid solutions for artificial membrane reconstitution. All lipids were dissolved in the chloroform, dried out in stream of nitrogen and dissolved in the detergent solution.

Unfortunately, any lipid composition used for an artificial membrane reconstitution did not improve the function of the purified enzyme. Due to the loss of NKA function and due to losing a considerable amount of the α subunit caused by IMAC, we decided to prepare the protein using analogous approach to isolation from porcine kidney. The crude membranes were subjected to a series of centrifugations to obtain the pure protein. I screened the same set of detergents as in the previous protocol.

I determined the NKA activity of the prepared crude membranes and of the pure proteins using standard Baginsky assay. The crude membrane samples showed high background possibly caused by other ATPases and the activity of the pure proteins was below the detection limit of used method. Therefore, on that account, I optimized the protocol for Baginsky assay by adding other nonspecific ATPases inhibitors such as KNO_3, NaN_3 and Na_2MO_4 at final concentrations of 50 mM, 5 mM, and 0.25 mM, respectively. Despite this optimization we did not improve obtained results. I assume that the NKA activity was not detected due to the low concentration of ex-

pressed protein, insufficient glycosylation or inappropriate composition of the artificial membrane.

3.4 Interaction of NKA With Small Molecules

3.4.1 Flavonolignans

My findings of the interaction between porcine kidney NKA and flavonoids were published in Frontiers in Physiology [72]. In this study I examined the inhibitory effect of SB, SD, SCH, TAX, DHSB, DHSD, DHSCH and QUE on the NKA activity. In the beginning, all compounds were tested in the initial screening at the final concentration of 10 μM, and the most active compounds were selected for the molecular modelling performed by Petra Čechová.

The ouabain-sensitive ATPase activity was measured for the increasing concentration of all selected compounds (see Figure 20). Substantial inhibition caused by the compound at final concentration of 10 μM was observed only for SCH, DHSCH and DHSD. IC_{50} values calculated for those compounds were 110 ± 40 μM, 138 ± 8 μM and 36 ± 14 μM, respectively.

The determined Hill coefficients exceeded 1 indicating the presence of multiple binding sites and negative cooperativity. The active compounds (SCH, DHSCH, DHSD) were subjected to deeper analysis of their inhibitory mechanism. Furthermore, there was no change in IC_{50} for ouabain or in K^+/ouabain antagonism in the presence of active compounds (Figure 21 A). In contrast to ouabain, which elevates $K_{0.5}(K^+)$, none of the tested flavonolignans altered the K^+-dependence of the NKA activity (Figure 21 B).

We used molecular docking tools for the prediction of the potential binding sites for selected compounds (see Figure 22). All five major binding sites were localized mostly on the large cytoplasmic loop connecting transmembrane helices M4 and M5 (C45 loop). Furthermore, all compounds exhibited similar affinities (-11 to -9 kcal.mol^{-1}) to all predicted binding sites in both major enzyme conformations. We identified five major binding sites, but only three of them were conserved in open and closed conformations. The binding site in the close proximity of residue Asn733 was observed only in the open conformation, and binding to Arg248 was limited to close conformation.

The C45 represents more than 40% of the mass of the whole α subunit of NKA, and serves as a target for interaction with soluble molecules due to its position. Consequently, an isolated C45 loop was prepared in bacteria *E. coli* to verify the binding of flavonolignans to cytoplasm-facing part of NKA. The relative changes in the absorption spectra for SCH, DHSCH and SD confirmed the interaction with C45 (performed by Martin Kubala) as suggested by the molecular modelling (performed by Petra Čechová).

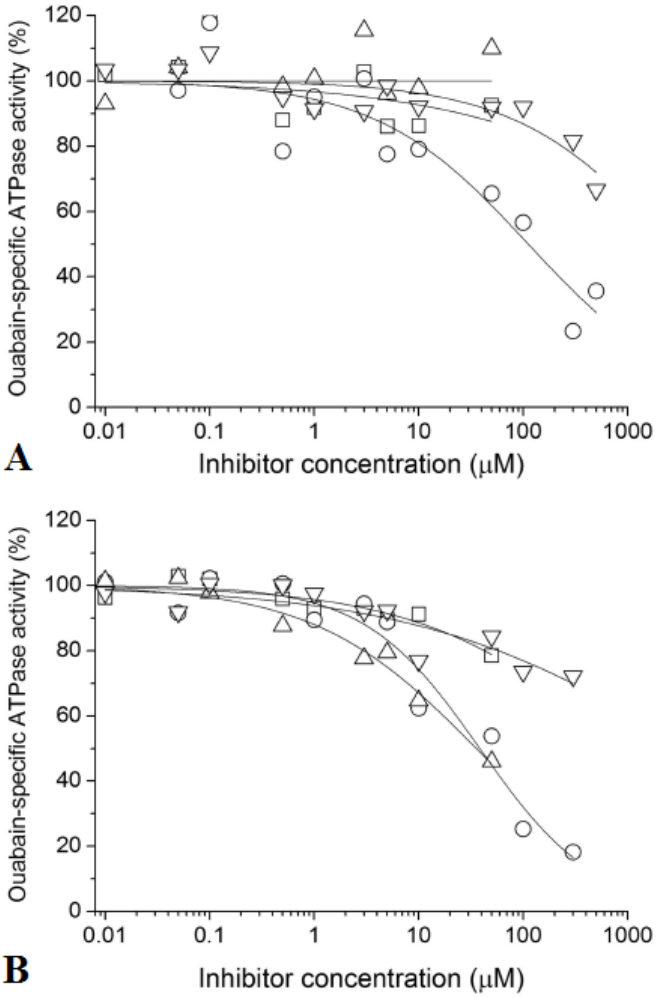

Figure 20: A: Inhibition of NKA by SB (squares □), SCH (circles ○), SD (up triangles △), TAX (down triangles ▽). B: Inhibition of NKA by corresponding dehydroderivatives DHSB, DHSD, DHSCH and QUE, respectively. The reference value (100%) represents ouabain-specific activity of untreated NKA, and each point is represented as the mean ± S. E. M.

3.4.2 Halogenated Hydroquinolinones

In paper I [88], we described the NKA inhibitory effect of selected halogenated hydroquinones.

I tested halogenated hydroquinolinones as potential NKA inhibitors. The initial screening of quinolinones (31 compounds) at final concentration of 10 μM revealed only one significantly active molecule – 5,6,7,8-tetrafluoro-3-hydroxy-2-phenylquinolin-4(1H)-one (TFHPQ). In contrast to dichlor- or difluor- derivatives, this compound decreased the NKA activity to ca. 45% of its initial activity (see Figure 23). The observed inhibitory effect of TFHPQ depended on concentration – increasing concentration of inhibitor decreased the NKA activity. However, the limited water solubility of TFHPQ significantly limited the IC_{50} determination. The determination of IC_{50} or Hill coefficient requires estimated value of the minimal activity in the presence of inhibitor, which was out of available concentration range. Indeed, at concentration higher

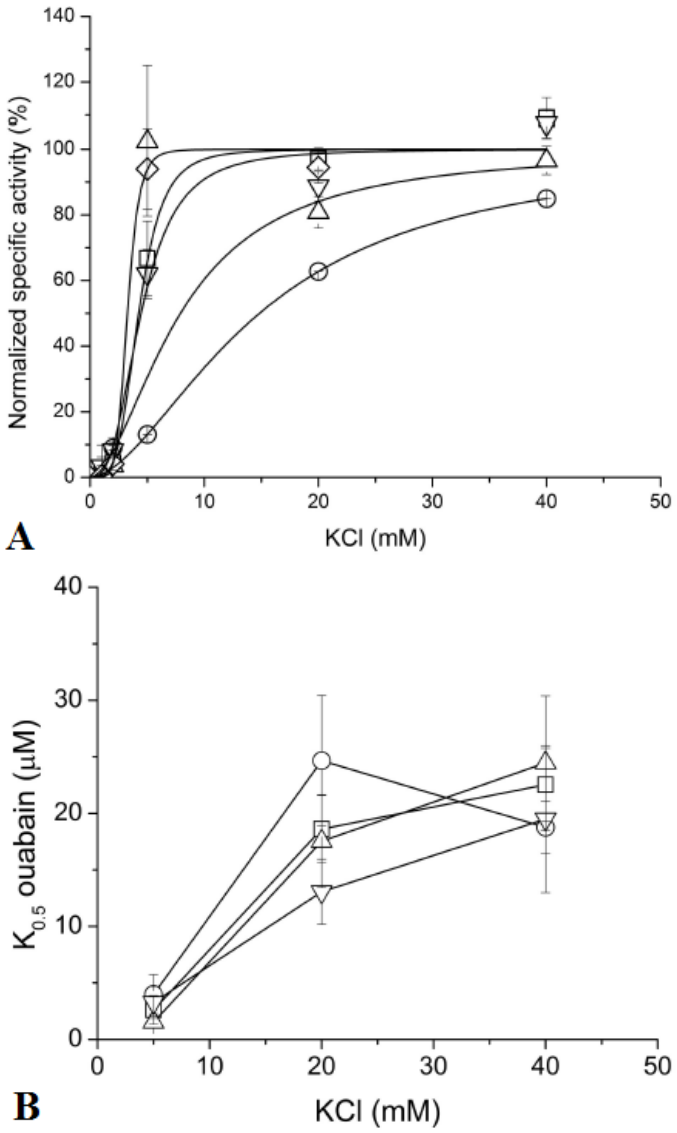

Figure 21: A: the K^+-dependence of the NKA activity in the absence of any ligand (squares □) or in the presence of ouabain (circles ○), SCH (up triangles △), DHSCH (down triangles ▽) or DHSD (diamonds ◇). B: the K^+/ouabain antagonism in the absence or in the presence of 40 μM SCH (circles ○), DHSCH (up triangles △) or DHSD (down triangles ▽) [72]. Each data point is represented as the mean ± S. E. M. of four replicates.

than 15 μM, the aggregates appeared. Due to the poor control of the real aggregated and non-aggregated TFHPQ concentration in solution, these data were excluded from quantitative analysis. Therefore, the NKA activity in the presence of 10 μM yielded 45% of the initial NKA activity, from which I assumed that the IC_{50} value was near 10 μM.

TFHPQ was subjected to molecular docking to predict the potential binding sites. Molecular modelling suggested the position of the potential binding site for TFHPQ in the open conformation in the close proximity of the C-terminal end of the protein (residuum αTyr1022 and βTrp12) as showed in Figure 11. One of the proposed binding sites corresponds to binding site for flavonolignans. The closed structure determined

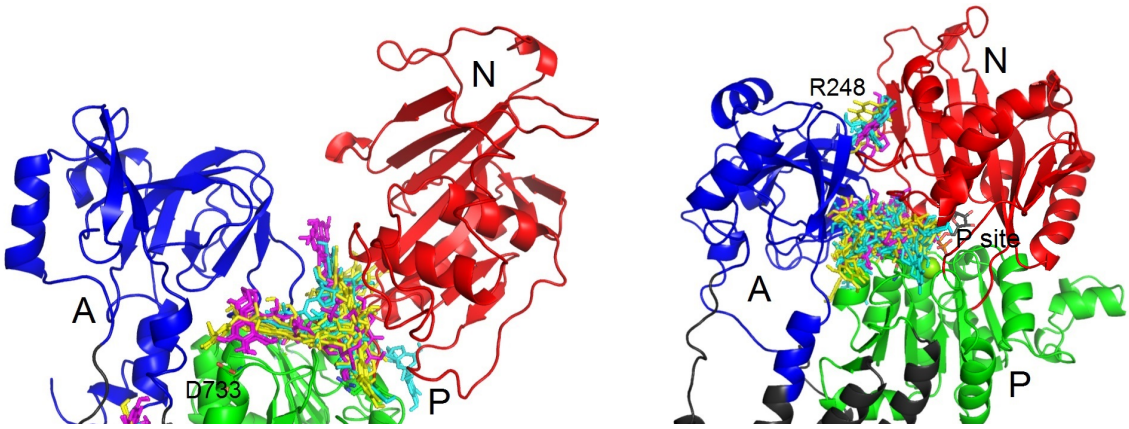

Figure 22: Zoom to the binding sites of SCH (yellow), DHSCH (cyan) and DHSD (magenta) on cytoplasmic loop in the open (left) and close (right) structure. The α is composed of A domain (blue), P domain (green) and N domain (red) [72]. The figure courtesy of Petra Čechová.

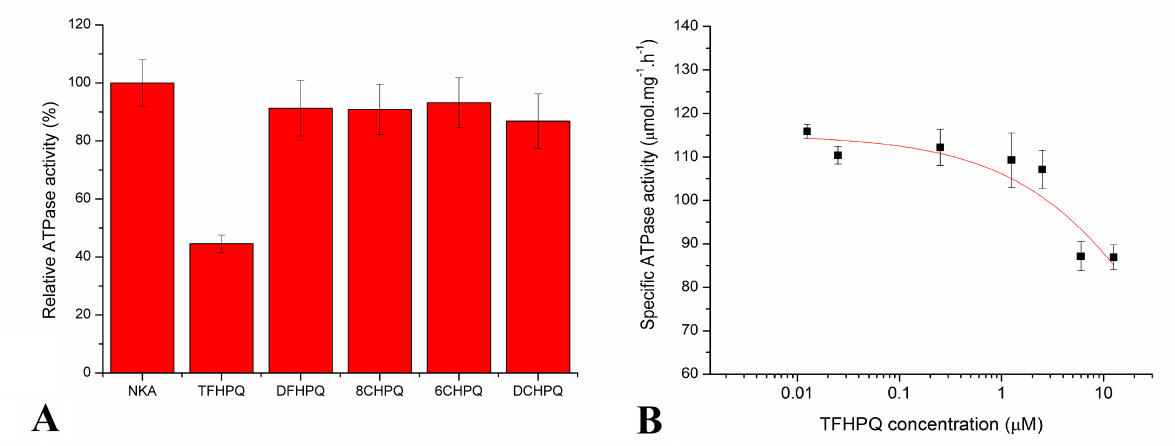

Figure 23: A: The changes of the relative ATPase activity caused by the halogenated quinolinones at final concentration of 10 μM. B: The relative ATPase activities were obtained by normalizing the ATPase activity of the quinolinone-treated enzyme by the activity of the enzyme incubated without inhibitor. The inhibitory effect caused by TFHPQ at increasing concentration. Each data point represents average of four replicates [88].

TFHPQ binding to αTyr970, αTrp988 and γPhe33 which was localized in the transmembrane domain.

Nevertheless, our model was based on the closed crystal structure containing the cholesterol molecule bound in the same position. Unfortunately, the authors of the crystal structure [30] claimed that cholesterol molecule is the crystallographic artifact. The other compounds could bind to the C-terminal binding site in the open structure, but with lower affinities than TFHPQ. Moreover, they occupied several other binding poses on the protein that were not available for TFHPQ. In the closed conformation, they bound to the similar sites as TFHPQ, but again, with lower affinities.

In order to better understand the TFHPQ inhibition, I evaluated its effect on NKA activation by Na^+, K^+ or ATP (Figure 25). TFHPQ exhibited an effect on the

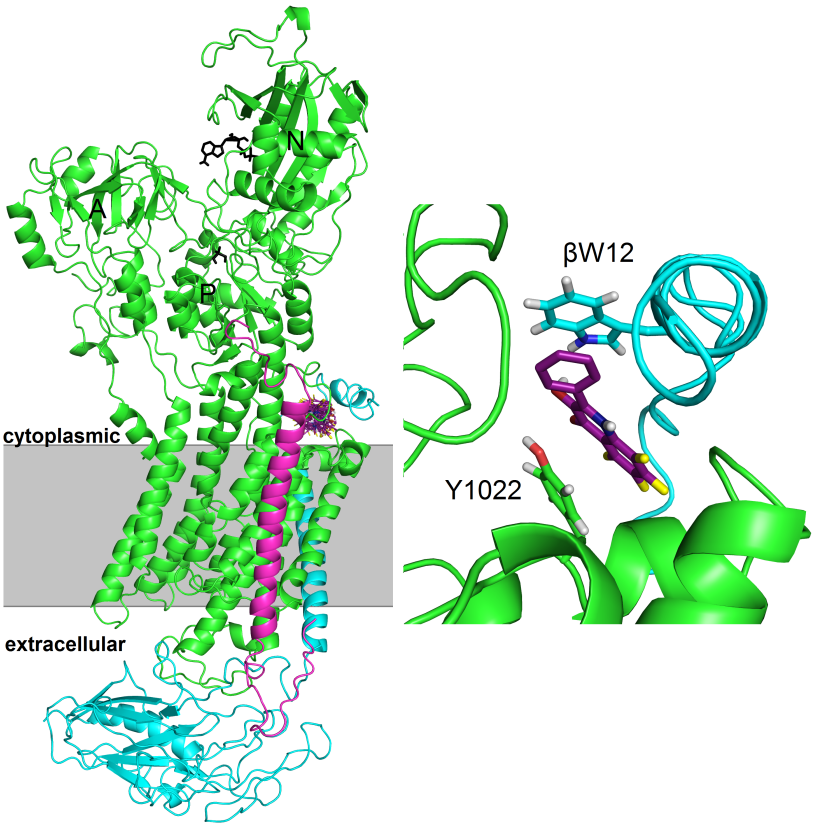

Figure 24: Localization of TFHPQ binding site in the open conformation of the protein (left), and zoom (right). The docked TFHPQ is highlighted in purple, α subunit is in green, β subunit is in cyan, and the FXYD protein is in magenta [88]. The figure courtesy of Petra Čechová.

Na^+ dependent NKA activation, altering the enzyme affinity for Na^+. The activity at high NaCl concentration was decreased only to 45% of maximal activity in the presence of THFPQ (Figure 25 A). Similarly, the NKA activity was insignificantly decreased by TFHPQ at high K^+ concentrations, reaching only 45% of the control (Figure 25 B). The shape of the curve was not substantially affected by the presence of TFHPQ (Figure 25 C). Again, the affinity for K^+ slightly decreased suggesting that the TFHPQ inhibition leads to the decrease of the enzyme affinity for transported cations. The ATP-dependence of NKA activity follows the well-known bell-shaped curve [128], which suggests unchanged mechanism of ATP binding.

3.4.3 Platinum-Based Drugs

In the paper V [16], we determined inhibition of NKA by selected platinum-based anticancer drugs (cisplatin, oxaliplatin and carboplatin). In the recent study [129], paper II, we have described binding to the cysteines on the cytoplasmic domain (C45 loop) of NKA.

Interactions of cisplatin and other platinum-based anticancer drugs with NKA were reported recently [16]. Understanding of this interaction on the molecular level could be

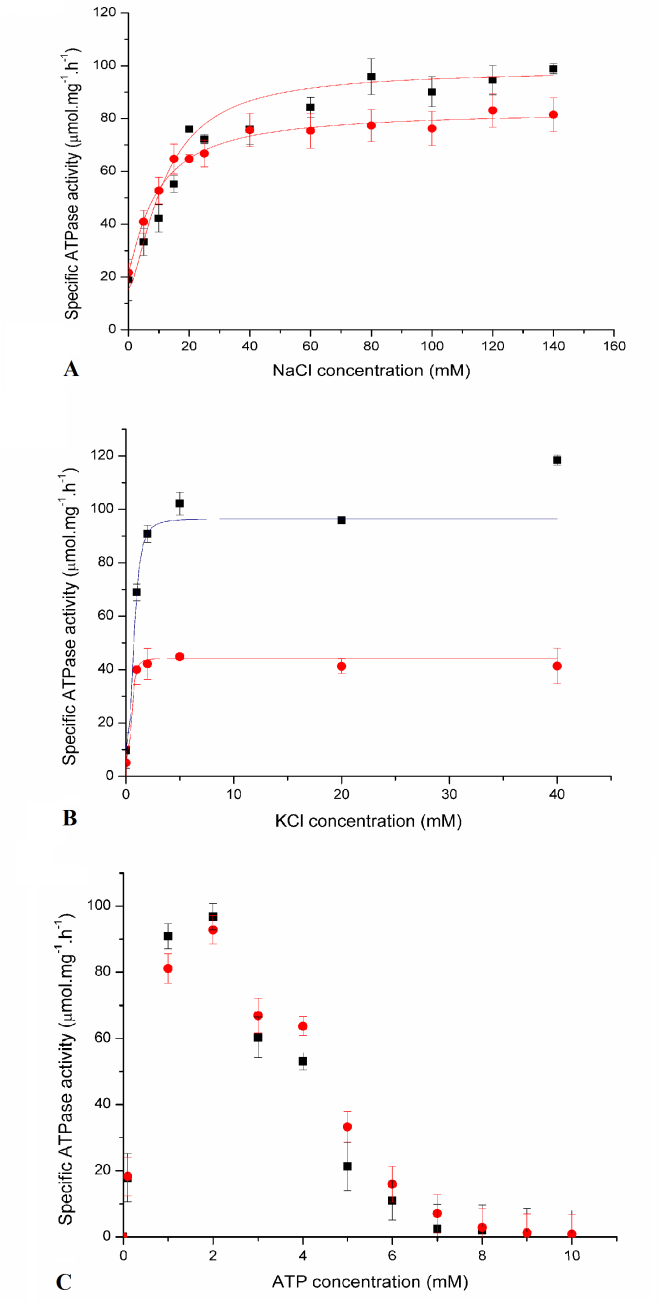

Figure 25: The Na^+-dependence (A), K^+-dependence (B) and ATP-dependence of the NKA activity in the absence of any inhibitor (■) and in the presence of 12.5 μM TFHPQ (●). Each data point represents average of four replicates [88].

the first step in elimination of inevitable side-effects. More specifically, nephrotoxicity of cisplatin is limiting its use as a drug [13, 130, 131].

The most reactive species within the protein structures are cysteine residues, which are involved in interactions of various proteins with cisplatin [132]. I assumed that the interaction between NKA and cisplatin is taking place within the cytosol-facing domain of NKA (C23 and C45 loop). Thus, the isolated large cytoplasmic loop C45 (soluble

in buffered aqueous solutions) presents a useful system for examining the cisplatin interactions with NKA [10].

Small water-soluble molecules and the protein and/or its cytoplasmic parts can interact through cysteine residues, more specifically the sulfhydryl moiety [133]. Although, whole C45 loop contains 11 cysteine residues we assume that binding of cisplatin is restricted to only few residues. The C45 loop contains segment with cysteines Cys452, Cys456 and Cys457 that lay in the close proximity of the protein surface. This segment is accessible from solvent and can be hypothetically involved in many processes.

Protein	Intact mass (m/z) Without Cisplatin	Standard Deviation (m/z)	Intact mass (m/z) With Cisplatin	Standard Deviation (m/z)	Mass Difference (m/z)
C45 WT	48316	31	49491	20	1175
Cys367Ser	48243	15	48580	62	1337
Cys421Ser	48330	16	49607	31	1277
Cys452Ser	48319	15	49274	36	955
Cys456Ser	48321	20	49337	19	1016
Cys457Ser	48321	72	49252	23	931
Cys456Ser+ Cys457Ser	48181	41	48803	33	623
Cys511Ser	48522	25	49831	31	1575
Cys549Ser	48310	10	49449	36	1139
Cys577Ser	48427	22	49421	21	994
Cys599Ser	48632	17	49835	26	1203
Cys656Ser	48317	18	49265	34	948

Table 3.3: The intact masses detected for C45 WT and mutant proteins in the presence and absence of cisplatin.

Therefore, the sequential single amino acid replacement (cysteine to serine) of all cysteine residues could be helpful in the identification of the cisplatin binding site. The Cys456Ser+Cys457Ser mutant (with two adjacent cysteines) was also prepared and its interaction with cisplatin tested. Moreover, the single amino-acid replacements did not alter overall protein yield and purity.

Unfortunately, the solvation of cisplatin is solute-dependent [135], moreover, the changes in ligands of the platinum complex can be observed depending on the media [20]. This fact could largely influence the measured total mass of the protein-cisplatin systems.

detected intact masses for a complete set of C45 proteins (WT and mutants with replaced cysteine residues) in the presence and absence of cisplatin. For C45 WT, I determined intact mass in the presence of two other platinum complexes (carboplatin and oxaliplatin). Carboplatin and oxaliplatin were excluded from detailed study of binding to the C45 loop due to their negligible effects on the overall NKA activity. The

detected intact masses for cisplatin untreated and treated proteins are summarized in Table 3.3.

The intact masses of the C45 loops were detected using MALDI-TOF mass spectrometry that provided a molecular mass value of 48316 ± 31 Da, which is in good agreement with mass detected by SDS-PAGE and with previously published data [104]. The intact mass of cisplatin-treated C45 WT protein was determined as 49490 ± 20 Da (see Figure 26). The molecular mass difference between the treated and untreated C45 WT was approximately 1170 Da which suggested the formation of five adducts with cisplatin (see Figure 26).

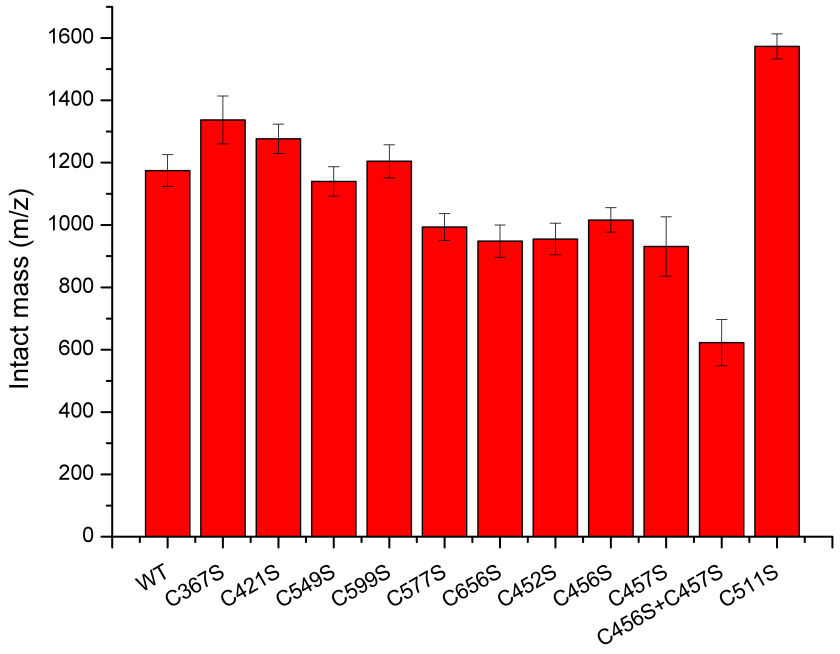

Figure 26: Relative changes in the intact mass of cisplatin untreated C45 WT and cisplatin treated C45 loops.

The similar differences between treated and untreated proteins were observed for residues Cys367Ser, Cys421Ser, Cys549Ser and Cys599Ser. The lower value of molecular mass difference was detected for the residues Cys452Ser, Cys456Ser, Cys457Ser, Cys456Ser+Cys457Ser, Cys577Ser and Cys656Ser (Figure 26, Table 3.3) and was accounted for approximately 250 Da. I assume that named residues interacts with cisplatin. For double mutant Cys456Ser+Cys457Ser the molecular weight of cisplatin untreated protein was 48181 ± 41 Da and cisplatin treated sample was 48803 ± 33 Da. The molecular weight difference detected for double mutant was only 620 Da which suggested the loss of binding of two cisplatin molecules (see Figure 26).

On the other hand, the abnormal mass difference was detected only for Cys511Ser mutant which exhibited mass difference 1573 ± 40 Da. This abnormal difference may be caused by the interaction between C45 loop and Tris buffer.

Furthermore, the localization of cysteine residues were detected by the chemical modification using iodoacetate. The chemical modification increases the intact mass

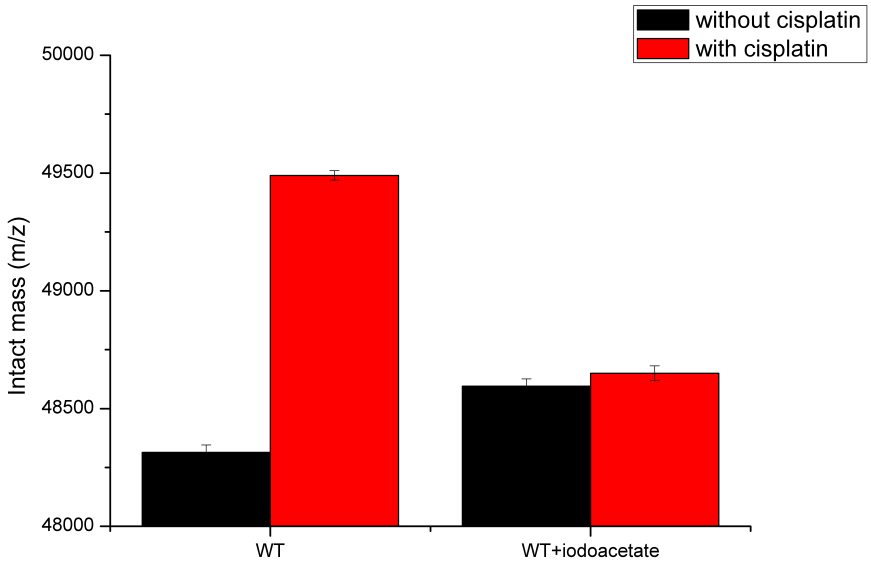

Figure 27: The changes in the intact mass of C45 WT proteins after chemical modification of cysteine residues. One aliquot of C45 WT protein without any modification was used as a control (WT) and two aliquots of C45 WT were subjected to chemical modification of cysteine residues (WT+iodoacetate). The intact mass was detected after the chemical modification (black) and after cisplatin treatment (red).

of the protein in ratio 57 Da per one modified residue. For C45 WT was detected intact mass of 48428 ± 31 Da that suggested the modification of five cysteine residues. This difference remained constant after the cisplatin treatment which supported the hypothesis that cisplatin was not able to bind to the modified cysteine residues (see Figure 27).

The only controversy was observed for Cys511Ser mutant for which was not detected using the fluorescence signal. For Cys511Ser we also observed abnormal intact mass difference between cisplatin treated and untreated proteins. This protein is possibly misfolded and the observed abnormalities may be result of a conformational change.

Nevertheless, [104] suggested involvement of cysteine Cys367, which is only two residues apart from phosphorylation site at position Asp369 [136]. We detected negligible difference between molecular mass shifts of Cys367Ser mutant and C45 WT suggesting that impairment of NKA function is not caused by impairment of the phosphorylation.

3.5 Expression and Purification of Human C23 and C45 Loops

The expression and purification of α_1 C45 and α_3 C45 is illustrated in Figure **??**. Expression and purification of both proteins was optimized in collaboration with student under my supervision Martina Jamečná. We identified both proteins α_1 C45 and α_3

C45 in the elution. For efficient protein expression was used the low concentration of IPTG as well as the low cell density. Under those conditions we were able to prepare sufficient amount of the protein which was used for study of platinum-based complexes. Nonetheless, the α_2 C45 struggles to express as full size protein (see Figure **??**). The human α_2 C45 possibly acquires the construct reclonning for the stable protein expression. None of the tested conditions (IPTG concentration, cell density, time and temperature of cultivation after induction) improved significantly the full size protein expression. Based on the analysis of the protocol used for the protein expression optimization, I assume that the difficulties occurs on the expression level.

Consequently, the C23 loops seems to be more complicated to prepare due to its small size and its interaction with the membrane. My construct missed the helices which are normally near the membrane. I decided to prepare the truncated form of the loop due to aggregation of full-size construct. Unfortunately, it seemed that the protein preparation was not significantly improved, because no C23 was detected in elution when IMAC was used for protein purification. The loss of the protein during IMAC might have been caused by the incorrect protein folding that resulted in the inaccessibility of the His-tag. I was able to obtain the protein using the centrifugal filters with two distinct MWCO (30 kDa and 3 kDa, respectively). Nonetheless, the yield and purity of the final protein remained low.

The prepared α_1 C45 and α_3 C45 loops were treated by the platinum-based complexes (cisplatin, carboplatin and oxaliplatin) that exhibited the toxicity to different cells and their intact mass was determined by mass spectroscopy.

For mouse brain C45, I detected approximately two molecules of carboplatin and three molecules of oxaliplatin interacting with C45. Unfortunately, I was not able to detect a complete set of intact masses for human α_1 and α_3 C45 loops treated by all three platinum complexes due to low signal detection. Obtained results revealed variable number of bound cisplatin molecules which can be the starting point for the future research.

Chapter 4

Conclusions

4.1 Expression of NKA in Yeast

NKA is an essential membrane protein establishing the membrane potential by actively pumping sodium and potassium ions across the plasma membrane. I used and optimized two basic methods of NKA preparation – direct isolation from tissue and heterologous expression.

I prepared the cloning vector for the expression of human $\alpha_3\beta_1$ complex of NKA in the yeast, and I tested three distinct yeast strains (BJ5457, Gal4ΔPep4 and ΔPep4) for protein expression. I verified the presence of both (α and β) subunits in the membrane fraction, and in the final pure protein sample for all tested strains. The protocol for cultivation and purification was subjected to detailed optimization (in collaboration with my Bc. student Veronika Kolomazníková).

Furthermore, I prepared a set of single amino acid mutants linked with the neurological disorders (Asp811Asn, Glu825Lys and Gly957Arg mutants). All proteins (WT and mutants) exhibited similar expression level suggesting no influence of the protein expression caused by mutation.

4.2 Isolation of NKA From Porcine Kidney

Our laboratory standardly prepares the NKA from porcine kidney using the protocol based on procedure reported by Fedosova *et al.* [46] with some modifications. Namely, I introduced the step of the rough homogenization of dissected tissue (in the kitchen blender) before the homogenization in the teflon homogenizer. This step significantly improved the protein yield, purity and stability.

The enzyme prepared using this method may be used for the ATPase activity determination using both Baginsky assay and Enzyme coupled method. In this thesis, I preferably used the Baginsky assay for its experimental convenience, low time and

financial consumptions. Moreover, the Baginsky assay was automated using the pipetting station and used for the testing of a large number of the potential NKA inhibitors.

4.3 Interaction of NKA With Small Molecules

All compounds were tested on the porcine kidney NKA isolated by the above mentioned method, and the final concentration of tested compounds was 10 μM.

In this thesis, I examined the interactions of NKA with selected small molecules (flavonolignans, halogenated quinolinones, and platinum-based complexes). I evaluated the inhibitory effect of these small molecules and determined the mechanism of their inhibition.

4.3.1 Flavonolignans

I tested eight flavonolignans (SB, SD, SCH, QUE, DHSB, DHSD, DHSCH, and TAX) from which only three (DHSD, SCH, and DHSCH) exhibited the substantial NKA inhibition. Flavonolignans showed the limited water solubility which is their main disadvantage. Despite the limited range of useful concentrations, the IC_{50} values for DHSD, SCH, and DHSCH were determined and were accounted for 36 ± 14 μM, 110 ± 40 μM, and 38 ± 8 μM, respectively.

I determined the Na^+, K^+, and ATP-dependent NKA activation in the presence or absence of flavonolignans or ouabain. My results suggested that the inhibitory mechanism of flavonolignans differ from ouabain, the specific inhibitor of NKA and typical representative of the cardiotonic steroid family.

I prepared the isolated cytoplasmic loop C45, and verified that flavonolignans bind there as predicted by molecular docking.

4.3.2 Halogenated Hydroquinolinones

Halogenated hydroquinolinones are chemical analogues of flavonolignans. From the large group of tested halogenated hydroquinolinones only one compound, called TFHPQ, significantly inhibited the NKA activity. By contrast, the monochloro- and dichloro-derivatives did not exhibit substantial NKA inhibition.

Similarly to flavolignans, halogenated hydroquinolinones showed limited solubility, therefore the determination of the IC_{50} value was proceeded with low precision. At 10 μM concentration, TFHPQ decreased the NKA activity to approximately 45% suggesting the IC_{50} value to be slightly below 10 μM. For future use, the solubility should be improved by the chemical modification, or by the encapsulation which might increase the bioavaibility of TFHPQ.

The predicted binding site for TFHPQ was found in the close proximity of C-

terminal pathway. The binding of TFHPQ into this site may cause the steric impairment of the ion transport. This mechanism of the inhibition varied from the mechanism described for ouabain.

4.3.3 Platinum-Based Drugs

I tested the influence of anti-cancer agents – cisplatin, carboplatin and oxaliplatin – on the porcine kidney NKA. Carboplatin and oxaliplatin did not seem to inhibit the NKA. By contrast, cisplatin completely supressed the NKA activity. The inhibition by cisplatin was studied in detail.

I identified 5 cysteine residues (Cys452Ser, Cys456Ser, Cys457Ser, Cys577Ser, and Cys656Ser) on the C45 loop interacting with cisplatin. They represents the binding sites of cisplatin on the C45 loop as unambiguously determined and confirmed by mass spectrometry.

4.4 Human C23 and C45 Loops

I prepared a set of C23 and C45 loops derived from the human α_1, α_2, and $\alpha 3$ sequences. All those loops were overexpressed in bacteria cells. The isolated human α_1 and α_3 C45 loops were successfully prepared using the heterologous protein expression method. The protocol for this preparation was optimized (in the collaboration with my Bc. student Martina Jamečná). Unfortunately, human α_2 C45 was prepared in the truncated form. The used vector for the protein expression should be improved in order to obtain the natural structure of the human α_2 C45 protein. Current results may be the starting point for investigation of the isoform-related NKA inhibition.

Bibliography

[1] Hana R Pohl, John S Wheeler, and H Edward Murray. Interrelations between Essential Metal Ions and Human Diseases. In *Metal Ions in Life Sciences*, volume 13, pages 29–47. Springer, 2013.

[2] P. Babula, M. Masarik, V. Adam, I. Provaznik, and R. Kizek. From $Na^+[K^+$-ATPase and Cardiac Glycosides to Cytotoxicity and Cancer Treatment. *Anti-Cancer Agents in Medicinal Chemistry*, 13(March):1069–87, 2013.

[3] Vladimir V. Matchkov and Igor I. Krivoi. Specialized Functional Diversity and Interactions of the Na^+/K^+-ATPase. *Frontiers in Physiology*, 7(MAY), 2016.

[4] a G Therien and R Blostein. Mechanisms of Sodium Pump Regulation. *American journal of physiology. Cell physiology*, 279(3):C541–66, 2000.

[5] H. Poulsen, H. Khandelia, J. P. Morth, M. Bublitz, O. G. Mouritsen, J. Egebjerg, and P. Nissen. Neurological Disease Mutations Compromise a C-Terminal Ion Pathway in the $Na^+[K^+$-ATPase. *Nature*, 467(7311):99–102, 2010.

[6] Erin L Heinzen, Kathryn J Swoboda, Yuki Hitomi, Fiorella Gurrieri, Boukje De Vries, F Danilo Tiziano, Bertrand Fontaine, Nicole M Walley, Matthew T Sweney, Tara M Newcomb, Louis Viollet, Chad Huff, B Lynn, Sandra P Reyna, Kelley J Murphy, Kevin V Shianna, and Curtis E Gumbs. *De novo* Mutations in *ATP1A3* Cause Alternating Hemiplegia of Childhood. *Nature Genetics*, 44(9):1030–1034, 2013.

[7] K. M. Weigand, M. Messchaert, H. G. P. Swarts, F. G. M. Russel, and J. B. Koenderink. Alternating Hemiplegia of Childhood Mutations Have a Differential Effect on $Na^+[K^+$-ATPase Activity and Ouabain Binding. *Biochimica et Biophysica Acta - Molecular Basis of Disease*, 1842(7):1010–1016, 2014.

[8] Alexey Bogdanov, Fedor Moiseenko, and Michael Dubina. Abnormal expression of *ATP1A1* and *ATP1A2* in breast cancer. *F1000 Research*, 6:10, 2017.

[9] Li Nan Zhang, Yong Jun Sun, Shuo Pan, Jun Xia Li, Yin E. Qu, Yao Li, Yong Li Wang, and Zi Bin Gao. Na^+/K^+-ATPase, a Potent Neuroprotective Modulator Against Alzheimer Disease. *Fundamental and Clinical Pharmacology*, 27(1):96–103, 2013.

[10] Lenka Grycova, Petr Sklenovsky, Zdenek Lansky, Marika Janovska, Michal Otyepka, Evzen Amler, Jan Teisinger, and Martin Kubala. ATP and Magnesium Drive Conformational Changes of the Na^+/K^+-ATPase Cytoplasmic Headpiece. *Biochimica et Biophysica Acta - Biomembranes*, 1788(5):1081–1091, 2009.

[11] R. A. Newman, P. Yang, A. D. Pawlus, and K. I. Block. Cardiac Glycosides as Novel Cancer Therapeutic Agents. *Molecular Interventions*, 8:36–49, 2008.

[12] G. Giaccone. Clinical Perspectives on Platinum Resistance. *Drugs*, Suppl 4:9–17, 2000.

[13] Victoria Cepeda, Miguel Fuertes, Josefina Castilla, Carlos Alonso, Celia Quevedo, and Jose Perez. Biochemical Mechanisms of Cisplatin Cytotoxicity. *Anti-Cancer Agents in Medicinal Chemistry*, 7(1):3–18, 2007.

[14] K. Barabas, R. Milner, D. Lurie, and C. Adin. Cisplatin: a Review of Toxicities and Therapeutic Applications. *Veterinary and Comparative Oncology*, 6:1–18, 2008.

[15] R. P. Miller, R. K. Tadagavadi, G. Ramesh, and W. B. Reeves. Mechanisms of cisplatin nephrotoxicity. *Toxins*, 2:2490–2518, 2010.

[16] Martin Kubala, Jaroslava Geleticova, Miroslav Huliciak, Martina Zatloukalova, Jan Vacek, and Marek Sebela. Na^+/K^+-ATPase inhibition by cisplatin and consequences for cisplatin nephrotoxicity. *Biomedical Papers*, 158(2):194–200, 2014.

[17] M. F. Howe-Grant and S. J. Lippard. *Metals Ions in Biochemical Systems*. Marcel Dekker, New York, USA, 1980.

[18] Yongwon Jung and Stephen J Lippard. Direct Cellular Responses to Platinum-Induced DNA Damage Direct Cellular Responses to Platinum-Induced DNA Damage. *Chemical reviews*, 107(5):1387–1407, 2007.

[19] C. G. Hartinger, Y. O. Tsybin, J. Fuchser, and P. J. Dyson. Characterization of Platinum Anti-Cancer Drug Protein-Binding Sites Using a Top-Down Mass Spectrometric Approach. *Inorganic Chemistry*, 47:17–19, 2008.

[20] Miroslav Huliciak, Linda Reinhard, Mette Laursen, Natalya Fedosova, Poul Nissen, and Martin Kubala. Crystals of Na^+/K^+-ATPase with Bound Cisplatin. *Biochemical Pharmacology*, 92:494–498, 2014.

[21] M. Futai, Y. Wada, and J. H. Kaplan, editors. *Handbook of ATPases*. WILEY-VCH, Weinheim, Germany, 1. st edition, 2004.

[22] P. L. Pedersen and E. Carafoli. Ion Motive ATPases. I. Ubiquity, Properties, and Significance to Cell Function. *Trends in Biochemical Sciences*, 12:146–150, 1987.

[23] J. C. Skou. The Influence of Some Cations on an Adenosin Triphosphatase From Peripheral Nerves. *Biochimica et Biophysica Acta (BBA)*, 23:394–401, 1957.

[24] A. K. Sen and R. L. Post. Stoichiometry and Localization of Adenosine Triphosphoate-Dependent Sodium and Potassium Transport in the Erythrocyte. *The Journal of biological chemistry*, 239(1):345–52, 1964.

[25] S Lutsenko and J Kaplan. Organization of P-type ATPases Significance of Structural Diversity. *Biochemistry*, 34(48):6003–6013, 1995.

[26] C. Toyoshima and F. Cornelius. New crystal structures of PII-type ATPases: excitement continues. *Current Opinion in Structural Biology*, 23:507–514, 2013.

[27] T. Shinoda, H Ogawa, F. Cornelius, and C. Toyoshima. Crystal Structure of the Sodium-Potassium Pump at 2.4 ÅResolution. *Nature*, 459(7245):446–50, may 2009.

[28] H. Ogawa, T. Shinoda, F. Cornelius, and C. Toyoshima. Crystal Structure of the Sodium-Potassium Pump ($Na^+[K^+$-ATPase) with Bound Potassium and Ouabain. *Proceedings of the National Academy of Sciences of the United States of America*, 106(33):13742–7, aug 2009.

[29] R. Kanai, H. Ogawa, B. Vilsen, F. Cornelius, and C. Toyoshima. Crystal Structure of a Na^+-bound $Na^+[K^+$-ATPase Preceding the E1P State. *Nature*, 502(7470):201–6, 2013.

[30] M. Nyblom, L. Reinhard, M. Andersson, E. Lindahl, N. Fedosova, and P. Nissen. Crystal Structure of $Na^+[K^+$-ATPase in the Na^+-Bound State. *Science*, 342(2013):123–127, 2013.

[31] Maxim Dobretsov and JR R Joseph R Stimers. Neuronal Function and α_3 Isoform of the $Na^+[K^+$-ATPase. *Front iers in Bioscience*, 10:2373–2396, 2005.

[32] K. Geering. Functional Roles of $Na^+[K^+$-ATPase Subunits. *Current Opinion in Nephrology and Hypertension*, 17(5):526–532, 2008.

[33] D. W. Martin. Structure-Function Relationships in $Na^+[K^+$-pump. *Seminars in Nephrology*, 25(5):282–91, sep 2005.

[34] C. Toyoshima, R. Kanai, and F. Cornelius. First Crystal Structures of $Na^+[K^+$-ATPase: New Light on the Oldest Ion Pump. *Structure*, 19(12):1732–1738, 2011.

[35] M. Hilge, G. Siegal, G. W. Vuister, P. Güntert, S. M. Gloor, and J. P. Abrahams. ATP-induced conformational changes of the nucleotide-binding domain of Na^+,K^+-ATPase. *Nature Structural and Molecular Biology*, 10:469–474, 2003.

[36] Maike Bublitz, Hanne Poulsen, J. Preben Morth, and Poul Nissen. In and Out of the Cation Pumps: P-type ATPase Structure Revisited. *Current Opinion in Structural Biology*, 20(4):431–9, aug 2010.

[37] C Gatto, S M McLoud, and J H Kaplan. Heterologous Expression of Na^+/K^+-ATPase in Insect Cells: Intracellular Distribution of Pump Subunits. *American journal of physiology. Cell physiology*, 281(3):C982–C992, 2001.

[38] Melissa D. Laughery, Matthew L. Todd, and Jack H. Kaplan. Mutational Analysis of α-β Subunit Interactions in the Delivery of Na^+/K^+-ATPase Heterodimers to the Plasma Membrane. *Journal of Biological Chemistry*, 278(37):34794–34803, 2003.

[39] F. Cornelius, M. Habeck, R. Kanai, C. Toyoshima, and S. J. D. Karlish. General and Specific Lipid-Protein Interactions in $Na^+[K^+$-ATPase. *Biochimica et Biophysica Acta - Biomembranes*, 1848(9):1729–1743, 2015.

[40] B. Alberts, A. Johnson, J. Lewis, and M. Raff. *Molecular Biology of the Cell*. Garland Science, New York, USA, fifth eddi edition, 2008.

[41] M. Esmann, D. Watt, and D. Marsh. Spin-label studies of lipid-protein interactions in Na, K-ATPase membranes from Squalus acanthias. *Biochemistry*, 24:1386–1393, 1985.

[42] Nelson P. Barrera, Min Zhou, and Carol V. Robinson. The Role of Lipids in Defining Membrane Protein Interactions: Insights from Mass Spectrometry. *Trends in Cell Biology*, 23(1):1–8, 2013.

[43] M. Laursen, L. Yatime, P. Nissen, and N. Fedosova. Crystal Structure of the High-Affinity $Na^+[K^+$-ATPase-Ouabain Complex with Mg^{2+} Bound in the Cation Binding Site. *Proceedings of the National Academy of Sciences of the United States of America*, 110(27):10958–63, 2013.

[44] M. Kubala, R. Krumscheid, and W. Schoner. Phe 475 and Glu 446 but not Ser 445 participate in ATP-binding to the α subunit of $Na^+[K^+$-ATPase. *Biochemical and Biophysical Research Communications*, 297(2002):154–159, 2002.

[45] M. Kubala, J. Teisinger, R. Krumscheid, and W. Schoner. Eight Amino Acids Form the ATP Recognition Site of $Na^+[K^+$-ATPase. *Biochemistry*, 42:6446–6452, 2003.

[46] Natalya Fedosova. P-Type ATPases: Methods and Protocols. In Maike Bublitz, editor, *Springer Protocols - Methods in Molecular Biology: Purification of Na, K-ATPase from Pig Kidney*, pages 5–10. Springer, 2016.

[47] P. L. Jorgensen. Purification of $Na^+[K^+$-ATPase: Enzyme Sources, Preparative Problems, and Preparation from Mammalian Kidney. *Methods in Enzymology*, 156(1982):29–43, 1988.

[48] Satvinder Kaur, Manoj Panchal, Mohd Faisal, Vibha Madan, Parul Nangia, and Birendra N. Mallick. Long Term Blocking of GABA-A Receptor in *Locus Coeruleus* by Bilateral Microinfusion of Picrotoxin Reduced Rapid Eye Movement Sleep and Increased Brain $Na^+[K^+$-ATPase Activity in Freely Moving Normally Behaving Rats. *Behavioural Brain Research*, 151(1-2):185–190, 2004.

[49] I. Klodos. Large-Scale Preparation of $Na^+[K^+$-ATPase from Ox Brain. *Analytical Biochemistry*, 403:397–403, 1975.

[50] P Silva, J Stoff, M Field, L Fine, J N Forrest, and F H Epstein. Mechanism of active chloride secretion by shark rectal gland: role of Na^+/K^+-ATPase in chloride transport. *The American journal of physiology*, 233(4):F298–306, 1977.

[51] Dwight W. Martin and John R. Sachs. Preparation of $Na^+[K^+$-ATPase with Near Maximal Specific Activity and Phosphorylation Capacity: Evidence That the Reaction Mechanism Involves All of the Sites. *Biochemistry*, 38(23):7485–7497, 1999.

[52] Atsunobu Yoda and Shizuko Yoda. A New Simple Preparation Method for $Na^+[K^+$-ATPase-Rich Membrane Fragments. *Analytical Biochemistry*, 110(1):82–88, 1981.

[53] L. Cariani, L. Thomas, J. Brito, and J. R. Del Castillo. Bismuth citrate in the quantification of inorganic phosphate and its utility in the determination of membrane-bound phosphatases. *Analytical Biochemistry*, 324(1):79–83, 2004.

[54] Jens G. Nørby. Coupled Assay of Na^+/K^+-ATPase Activity. *Biochemistry*, 324(1984):116–119, 1988.

[55] J. M. Rovinsky, G. L. Tewalt, and A. T. Sneden. Maquiroside A, a New Cytotoxic Cardiac Glycoside from *Maquira calophylla*. *Journal of Natural Products*, 50:211_216, 1987.

[56] Z. W. Xu, F. M. Wang, M. J. Gao, X. Y. Chen, W. L. Hu, and R. C. Xu. Targeting the Na^+/K^+-ATPase α_1 Subunit of Hepatoma HepG2 Cell Line to Induce Apoptosis and Cell Cycle Arresting. *Biological and Pharmaceutical Bulletin*, 33:743–751, 2010.

[57] T. Sagawa, K. Sagawa, J. E. Kelly, R. G. Tsushima, and J. A. Wasserstrom. Activation of Cardiac Ryanodine Receptors by Cardiac Glycosides. *American journal of physiology. Heart and Circulatory Physiology*, 282:H1118–1126, 2002.

[58] H. T. Ho, S. C. W. Stevens, R. Terentyeva, C. A. Carnes, D. Terentyev, and S. Gyorke. Arrhythmogenic Adverse Effects of Cardiac Glycosides are Mediated by Redox Modification of Rhyanodine Receptors. *Journal of Physiology (London)*, 589:4697–4708, 2011.

[59] J. Liu, J. Tian, M. Haas, J. I. Shapiro, A. Askari, and Z. Xie. Ouabain Interaction with Cardiac $Na^+[K^+$-ATPase Initiates Signal Cascades Independent of Changes in Intracellular Na^+ and Ca^{2+} Concentrations. *Journal of Biological Chemistry*, 275(36):27838–27844, 2000.

[60] T. Akera and T. M. Brody. Ionotropic Action of Digitalis and Ion Transport. *Life Sciences*, 18:135–142, 1976.

[61] J. B. Lingrel. The Physiological Significance of the Cardiotonic Steroid/Ouabain-Binding Site of the Na^+/K^+-ATPase. *Annual Review of Physiology*, 72:395–412, 2010.

[62] T. Akera, F. S. Larsen, and T. M. Brody. The Effect of Ouabain on Sodium-and Potassium-Activated Adenosine Triphosphatase form Hearts of Several Mammalian Species. *Journal of Pharmacology and Experimental Therapeutics*, 170:17–26, 1969.

[63] R. M. Lebovitz, K. Takeyasu, and D. Fambrough. Molecular Characterization and Expression of the (Na^+/K^+)-ATPase α-Subunit in *Drosophila melanogaster*. *EMBO Journal*, 8:193–202, 1989.

[64] G. Crambert, U. Hasler, A. Beggah, N. Yu, N. N. Modyanov, J. D. Horisberger, L. G. Lelievre, and K. Geering. Transport and Pharmacological Properties of Nine Different Human Na^+/K^+-ATPases Isozymes. *Journal of Biological Chemistry*, 275:1976–1986, 2000.

[65] O. Shiratori. Growth Inhibitory Effects of Cardiac Glycosides and Aglycones on Neoplastic Cells: *In vitro* and *in vivo* studies. *Gann*, 58:521–528, 1967.

[66] J. Haux. Digitoxin is a Potent Anticancer Agent for Several Types of Cancer. *Medical Hypotheses*, 53:543–548, 1999.

[67] E. Erdmann and W. Schoner. Ouabain-Receptor Interactions in (Na^+/K^+)-ATPase Preparations from Different Tissues and Species. *Biochimica et Biophysica Acta (BBA)*, 307:386–398, 1973.

[68] D. Biedermann, E. Vavříková, L. Cvak, and V. Křen. Chemistry of Silybin. *Natural Product Report*, 31(9):1138–1157, 2014.

[69] D. K. Sharma. Pharmacological Properties of Flavonoids Including Flavonolignans - Integration of Petrocrops with Drug Development from Plants. *Journal of Scientific and Industrial Research*, 65(6):477–484, 2006.

[70] Radek Gažák, Daniela Walterová, and Vladimír Křen. Silybin and Silymarin – New and Emerging Applications in Medicine. *Current medicinal chemistry*, 14(3):315–338, 2007.

[71] Dezső Csupor, Attila Csorba, and Judit Hohmann. Recent Advances in the Analysis of Flavonolignans of *Silybum marianum*. *Journal of Pharmaceutical and Biomedical Analysis*, 130:301–317, 2016.

[72] M. Kubala, P. Čechová, J. Geletičová, M. Biler, T. Štenclová, P. Trouillas, and D. Biedermann. Flavonolignans as a Novel Class of Sodium Pump Inhibitors. *Frontiers in Physiology*, 7(March):1–10, 2016.

[73] N.-C. Kim, T. N. Graf, C. M. Sparacino, M. C. Wani, and M. E. Wall. Complete Isolation and Structure Identification of Silybins and Isosilybins from the Milk Thistle (*Silybum marianum*). *Organic Biomolecules Chemistry*, 1:1684–1689, 2003.

[74] V. Šimánek, V. Křen, J. Ulrichová, J. Vičar, and L. Cvak. Silymarin: What is in the Name...? An Appeal for a Change of Editorial Policy. *Hepatology*, 32:442, 2000.

[75] J. Vacek, M. Zatloukalová, T. Desmier, V. Nezhodová, J. Hrbáč, M. Kubala, and Et Al. Antioxidant, Metal-Binding and DNA-Damaging Properties of Flavonolignans a Joint Experimental and Computational Highlight Based on 7-Galloylsilybin. *Chemico-Biological Interactons*, 205:173–180, 2013.

[76] L. Mira, M. Silva, and C. F. Manso. Scavenging of Reactive Oxygen Species by Silibinin Dihemisuccinate. *Biochemical Pharmacology*, 17:753–759, 1994.

[77] C. Longuercio and D. Pesci. Silybin and the Liver: from Basic Research to Clinical Practice. *World Journal of Gastroenterology*, 17:2288, 2011.

[78] R. Agarwal, C. Agarwal, H. Ichikawa, R. P. Singh, and B. B Aggarwal. Anticancer Potential of Silymarin: From Bench to Bed Side. *Anticancer Research*, 26:4457–4498, 2006.

[79] R. Weyhenmeyer, H. Mascher, and J. Birkmayer. Study on Dose-Linearity of the Pharmacokinetics of Silibinin Diastereomers Using a New Stereospecific Assay. *International Journal of Clinical Pharmacology and Theoretical Toxicology*, 30:134–138, 1992.

[80] V. Křen, J. Kubisch, Petr Sedmera, Petr Halada, V. Přikrylová, Alexandr Jegorov, Ladislav Cvak, Rolf Gebhardt, J. Ulrichová, and V. Šimánek. Glycosylation of Silybin. *Optimization*, pages 2467–2474, 1997.

[81] Vladimir Kren and Daniela Walterova. Silybin and Silymarin - New Effects and Applications. *Biomedical Papers*, 149(1):29–41, 2005.

[82] P. Barraja, P. Diana, A. Montalbano, A. Carbone, G. Viola, G. Basso, A. Salvador, D. Vedaldi, F. Dall'Acqua, and G. Cirrincione. Pyrrolo-[3,4-h]-quinolinones a New Class of Photochemotherapeutics Agents. *Bioorganic and Medicinal Chemistry*, 19:2326–2341, 2011.

[83] P. Hradil, P. Krejci, J. Hlavac, I. Wiedermannova, A. Lycka, and V. Bertolasi. Synthesis, NMR Spectra and X-Ray Data of Chloro and Dichloro Derivatives of 3-Hydroxy-2-Phenylquinolin-4(*1H*)-Ones and Their Cytostatic Activity. *Journal of Heterocyclic Chemistry*, 41(3):375–379, 2004.

[84] E. C. Pesci, J. B. J. Milbank, J. P. Pearson, S. McKnight, A. S. Kende, E. P. Greenberg, and B. H. Iglewski. Quinolone Signaling in the Cell-to-Cell Communication System of *Pseudomonas aeruginosa*. *Proceedings of the National Academy of Sciences*, 96(20):11229–11234, 1999.

[85] R. Krikavova, J. Vanco, Z. Travnicek, R. Buchtik, and Z. Dvorak. Copper(II)quinolinonato-7-carboxamido Complexes as Potent Anti-tumor Agents with Broad Spectra and Selective Effects. *Royal Society of Chemistry*, 6:3899–3899, 2015.

[86] M. di Cagno, J. Styskala, J. Hlaváč, M. Brandi, A. Bauer-Brandl, and N. Skalko-Basnet. Liposomal Solubilization of New 3-hydroxy-quinolinone Derivatives with Promising Anti-Cancer Activity: A Screening Method to Identify Maximum Incorporation Capacity. *Journal ofo Liposome Research*, 21:272–278, 2011.

[87] K. Bürglová, J. Hlaváč, and J. R. Bartlett. Synthesis of Silica Nanoparticals for Encapsulation of Oncology Drugs with Low Water Solubility: Effect of Processing Parameters in Structural Evolution. *Journal of Nanoparticle Research*, 17:123, 2015.

[88] Jaroslava Šeflová, Michal Biler, Pavel Hradil, Martin Kubala, Petra Čechová, Michal Biler, Pavel Hradil, and Martin Kubala. Inhibition of Na^+/K^+-ATPase by 5,6,7,8-tetrafluoro-3-hydroxy-2-phenylquinolin-4(1H)-one. *Biochemie*, 138:56–61, 2017.

[89] C. Monneret. Platinum Anti-Cancer Drugs. From Serendipity to Rational Design. *Annales Pharmaceutiques Francaises*, 69:286–295, 2011.

[90] M. Peyrone. Über die Einwirkung des Ammoniaks auf Platinchlorür [On the Influence of Ammonia on Platinum Chloride]. *Annals of Chemical Pharmacy*, 51:1, 1844.

[91] G. J. Bosl, D. F. Bajorin, J. Sheinfeld, and R. Motzer. *Cancer of the Testis*. Lippincott Wiliams and Wilkins, Phialdeplhia, Pennsylvania, 6. edditio edition, 2001.

[92] T. Boulikas and M. Vougiouka. Recent Clinical Trials Using Cisplatin, Carboplatin and Their Combination Chemotherapy Drugs. *Oncology Reports*, 11:559–595, 2004.

[93] M. A. Fuertes, C. Alonso, and J. M. Perez. Biochemical Modulation of Cisplatin Mechanisms of Action: Enhancement of Antitumor Activity and Circumvention of Drug Resistance. *Chemical Reviews*, 103:645–662, 2003.

[94] E. Cvitkovic. A Historical Perspective on Oxaliplatin: Rethinking the Role of Platinum Compounds and Learning from Near Misses. *Seminars in Oncology*, 25:1_3, 1998.

[95] E. R. Jamieson and S. J. Lippard. Structure, Recognition, and Processing of Cisplatin-DNA Adducts. *Chemical Reviews*, 99:2467–2498, 1999.

[96] G. L. Cohen, W. R. Bauer, J. K. Barton, and S. J. Lippard. Binding of Cis- and Trans-Dichlorodiammineplatinum(II) to DNA: Evidence for Unwinding and Shortening of the Double Helix. *Science*, 203:1014–1060, 1979.

[97] D. P. Bancroft, C. A. Lepre, and S. J. Lippard. Platinum-^{195}NMR Kinetic and Mechanistic Studies of Cis- and Trans-Diamminedichloroplatinum(II) Binding to DNA. *Journal of American Chemical Society*, 112:6860–6871, 1990.

[98] M. A. Lemaire, A. Schwertz, A. R. Rahmouni, and M. Leng. Interstrand Cross-Links are Preferentially Formed at the d(GC) Sites in the Reaction Between Cis-Diamminedichloroplatinum (II) and DNA. *Proceedings of the National Academy of Sciences of the United States of America*, 88:1982–1985, 1991.

[99] A. Binter, J. Goodisman, and J. C. Dabrowiak. Formation of Monofunctional Cisplatin-DNA Adducts in Carbonate Buffer. *Journal of Inorganic Biochemistry*, 100:1219, 2006.

[100] A. J. di Pasqua, J. Goodisman, D. J. Kerwood, B. B. Toms, R. L. Dubowy, and J. C. Dabrowiak. Activation of Carboplatin by Carbonate. *Chemical Research in Toxicology*, 19:139–149, 2006.

[101] M. Kartalou and J. M. Essigmann. Mechanisms of Resistance to Cisplatin. *Mutation Research*, 478:23–43, 2001.

[102] C.P. Saris, PJ.M. van de Vaart, R.C. Rietbroek, and FA. Bloramaert. *In vitro* Formation of DNA Adducts by Cisplatin, Lobaplatin and Oxaliplatin in Calf Thymus DNA in Solution and in Cultured Human Cells. *Carcinogenesis*, 17(12):2763–2769, 1996.

[103] S. R. McWhinney, R. M. Goldberg, and H. L. McLeod. Platinum Neurotoxicity Pharmacogenetics. *Molecular Cancer Therapy*, 8:10–16, 2009.

[104] M. Huličiak, J. Vacek, M. Šebela, E. Orolinová, J. Znaleziona, M. Havlíková, and M. Kubala. Covalent Binding of Cisplatin Impairs the Function of $Na^+[K^+$-ATPase by Binding to its Cytoplasmic Part. *Biochemical Pharmacology*, 83(11):1507–1513, 2012.

[105] P. A. Pedersen, J. H. Rasmussen, and P. L. Jørgensen. Expression in High Yield of Pig $\alpha_1\beta_1$ $Na^+[K^+$-ATPase and Inactive Mutants D369N and D807N in *Saccharomyces cerevisiae*. *The Journal of Biological Chemistry*, 271(5):2514–2522, 1996.

[106] L. Steffensen and P. A. Pedersen. Heterologous Expression of Membrane and Soluble Proteins Derepresses *GCN4* mRNA Translation in the Yeast *Saccharomyces cerevisiae*. *Eukaryotic Cell*, 5(2):248–261, 2006.

[107] W. O. Bullock, J. M. Fernandez, and J. M. Short. XL1-Blue: A High Efficiency Plasmid Transforming recA *Escherichia coli* Strain with β-Galactosidase Selection. *Biotechniques*, 5:376–389, 1987.

[108] G. Bertani. Studies on Lysogenesis. I. The Mode of Phage Liberation by Lysogenic *Escherichia coli*. *Journal of bacteriology*, 62(3):293–300, 1951.

[109] David Drew, Simon Newstead, Y. Yo Sonoda, Hyun Kim, and Gunnar Von Heijne. GFP-Based Optimization Scheme for the Overexpression and Purification of Eukaryotic Membrane Proteins in *Saccharomyces cerevisiae*. *Nature Protocols*, 3(5):784–798, 2009.

[110] F. Sherman. Getting Started with Yeast. *Methods in Enzymology*, 350(2002):3–41, 2002.

[111] A. Nishimura, M. Morita, Y. Nishimura, and Y. Sugino. A Rapid and Highly Efficient Method for Preparation of Competent *Escherichia coli* Cells. *Nucleic Acids Research*, 18(20):6169, 1990.

[112] E. Cohen, R. Goldshleger, A. Shainskaya, D. M. Tal, C. Ebel, M. le Maire, and S. J. D. Karlish. Purification of Na^+/K^+-ATPase Expressed in *Pichia pastroris* Revealed an Essential Role of Phospholipid-Protein Interaction. *Journal of Biological Chemistry*, 280:16610–16618, 2005.

[113] J. P. Morth, B. P. Pedersen, M. S. Toustrup-Jensen, T. L. M. Sørensen, J. Petersen, J. P. Andersen, B. Vilsen, and P. Nissen. Crystal Structure of the Sodium-Potassium Pump. *Nature*, 450(7172):1043–9, dec 2007.

[114] M. M. Bradford. Rapid and Sensitive Method for the Quantitation of Microgram Quantities of Protein Utilizing the Principle of Protein-Dye Binding. *Analytical Biochemistry*, 72:248–254, 1976.

[115] R. L. Lundblad and C. M. Noyes. *Chemical Reagents for Protein Modification*. CRC Press, Boca Ralton, Florida, 1. edition, 1984.

[116] M. Kalimi and K. Love. Role of Chemical Reagents in the Activation of Rat Hepatic Glucocoticoid-Receptor Complex. *Journal of Biological Chemistry*, 255:4687–4690, 1980.

[117] J. Beinhauer, R. Lenobel, D. Loginov, I. Chamrád, P. Řehulka, M. Sedlářová, M. Marchetti-Deschmann, G. Allmaier, and M. Šebela. Identification of *Brenia lactucae* and *Oidium neolycopersici* proteins extracted for intact spore MALDI mass spectrometric biotyping. *Electrophoresis*, 37:2940–2952, 2016.

[118] E. Baginski, L. M. Weiner, and B. Zak. The Simple Determination of Nucleotide Phosphorus. *Clinica Chimica Acta*, 10:378–379, 1964.

[119] P. Scharff-Poulsen and Per Amstrup Pedersen. *Saccharomyces cerevisiae*-Based Platform for Rapid Production and Evaluation of Eukaryotic Nutrient Transporters and Transceptors for Biochemical Studies and Crystallography. *PLoS ONE*, 8:e76851, 2013.

[120] J. L. Parker and S. Newstead. Method to Increase the Yield of Eukaryotic Membrane Protein Expression in *Saccharomyces cerevisiae* for Structural and Functional Studies. *Protein Science*, 23:1309–1314, 2014.

[121] E. L. Heinzen, A. Arzimanoglou, A. Brashear, S. J. Clapcote, F. Gurrieri, D. B. Goldstein, S. H. Jóhannesson, M. A. Mikati, B. Neville, S. Nicole, L. J. Ozelius, H. Poulsen, T. Schyns, K. J. Sweadner, A. van den Maagdenberg, B. Vilsen, and H. Sigurður. Distinct neurological disorders with *ATP1A3* mutations. *Lancet Neurology*, 13(5):503–514, 2015.

[122] D. Strugatsky, R. Goldshleger, E. Bibi, and S. J. D. Karlish. Expression of Na^+/K^+-ATPase in *P. pastoris*: Fe^{2+}-Catalyzed Cleavage of the Recombinant Enzyme. *Annals of the New York Academy of Sciences*, 986:247–248, 2003.

[123] J. B. Koenderink and H. G. P. Swarts. Expression of Na^+/K^+-ATPase and H^+/K^+-ATPase Isoforms with the *Baculovirus* Expression System. In M. Bublitz, editor, *P-Type ATPases: Methods and Protocols*, pages 71–78. Springer, 1. edditio edition, 2016.

[124] Guillaume Lenoir, Thierry Menguy, Fabienne Corre, Pierre Falson, Per A Pedersen, and Denyse Thine. Overproduction in Yeast and Rapid and Efficient Purification of the Rabbit SERCA1a Ca^{2+}-ATPase. *Culture*, 1560:67–83, 2002.

[125] C. Toyoshima, M. Nakasako, H. Nomura, and H. Ogawa. Crystal Structure of the Calcium Pump of Sarcoplasmic Reticulum at 2.6 ÅResolution. *Nature*, 405:647–655, 2000.

[126] H. Haviv, E. Cohen, Y. Lifshitz, D. M. Tal, R. Goldshleger, and S. J. D. Karlish. Stabilization of Na^+/K^+-ATPase Purified from *Pichia pastoris* Membranes by Specific Interactions with Lipids. *Biochemistry*, 46:12855–12867, 2007.

[127] H. Haviv, M. Habeck, R. Kanai, C. Toyoshima, and S. J. D. Karlish. Neutral Phospholipids Stimulate Na^+/K^+-ATPase Activity: A Specific Lipid-Protein Interaction. *Journal of Biological Chemistry*, 288:10073–10081, 2013.

[128] J. C. Skou. Further Investigations on a Mg^{++} + Na^+-Activated Adenosinetriphosphatase, Possibly Related to the Active, Linked Transport of Na^+ and K^+ Across the Nerve Membrane. *Biochimica et biophysica acta*, 42:6–23, 1960.

[129] J. Šeflová, P. Čechová, K. M. Šišková, J. Kapitán, M. Kubala, M. Šebela, and P. Mojzeš. Cisplatin Interacting with Cytoplasmic Loop (C45) of the Na^+/K^+-ATPase: Role of Cysteine Residues. *X*, X:X, 2017.

[130] R. Safaei. Role of Copper Transporters in the Uptake and Efflux of Platinum Containing Drugs. *Cancer Letters*, 234:34–39, 2006.

[131] M. C. Lim and R. B. Martin. The Nature of Cis-Amine Pd(II) and Anti-tumor Cis-Amine Pt(II) Complexes in Aqueous Solutions. *Journal of Inorganic and Nuclear Chemistry*, 38:1911–1914, 1976.

[132] J. C. Dabrowiak. *Metals in Medicine*. Wiley-VCH, Weinheim, Germany, first edition, 2009.

[133] Elena A. Dergousova, Irina Yu Petrushanko, Elizaveta A. Klimanova, Vladimir A. Mitkevich, Rustam H. Ziganshin, Olga D. Lopina, and Alexander A. Makarov. Effect of Reduction of Redox Modifications of Cys-residues in the Na^+,K^+-ATPase α_1-subunit on its Activity. *Biomolecules*, 7(1):1–11, 2017.

[134] George L. Ellman. Tissue Sulfhydryl Groups, 1959.

[135] Viktor Brabec, Ondrej Hrabina, and Jana Kasparkova. Cytotoxic platinum coordination compounds . DNA binding agents. *Coordination Chemistry Reviews*, (May):1–30, 2017.

[136] P. A. Pedersen. Importance of Conserved α Subunit Segment 709GDGVND for Mg^{2+} Binding, Phosphorylation, and Energy Transduction in Na^+[K^+-ATPase. *Journal of Biological Chemistry*, 275(48):37588–37595, sep 2000.